THE UNIVERSITY
of EDINBURGH

Consequences of dissipative dynamics in the early universe

Rafael Hernández Jiménez

A thesis submitted in fulfilment of the requirements
for the degree of Doctor of Philosophy
to the
University of Edinburgh
August 2019

Abstract

Warm inflation presents an exceptional description of the early universe cosmology. It is a scenario of an inflationary dynamics in which the state of the universe during inflation is not the vacuum state, but rather an excited statistical thermal state. It introduces dissipation into the inflationary dynamics which can be well explained by first principles of a quantum multi-field theory. Besides, this approach has several attractive features. For instance, the additional friction may ease the required flatness of the inflaton potential. Besides, even if radiation is subdominant during inflation, may smoothly become the leading component if the ratio of dissipation $Q \gtrsim 1$ at the end of inflation ($\epsilon_{eff} \sim 1 + Q$), with no need for a separate reheating period. It also may explain the nature of the classical inhomogeneities observed in the CMB, since for WI the fluctuations of the inflaton are thermally induced; hence there is no need to explain the troublesome quantum-to-classical transition problem of the standard inflation picture, cold inflation, due to the purely quantum origin of the density perturbations. Furthermore, one well established key aspect is the prediction for a low tensor-to-scalar ratio, which now we see is consistent with Planck legacy.

Taking into account above encouraging warm inflation characteristics, in this thesis we will describe both warm inflation model building and the confrontation of theory with observation. We will examine two basic models: The *Warm Little Inflaton* scenario and the *distributed mass* model. In each case, we determine the parametric regimes in which the dynamical evolution is consistent for 50-60 e-folds of inflation, taking into account thermal corrections to the scalar potential (if necessary). In the first model we consider three distinct types of scalar potentials for the inflaton, namely chaotic inflation with a quartic monomial potential, a Higgs-like symmetry breaking potential and a non-renormalizable plateau-like potential. On the other hand, the distributed mass model is examined for various mass distributions considering a chaotic quartic potential. Both scenarios are theoretically and observationally successful for a broad range of parameter values. Indeed, they agree remarkably with the Planck legacy data.

The Warm Little Inflaton is undoubtedly the simplest realisation of warm inflation within a concrete quantum field theory construction, since it requires only a small number of fields; in particular, the inflaton is directly coupled to just two light fields. Distributed mass models can be viewed as realisations of the landscape property of string theory, with the mass distributions coming from the underlying spectra of the theory, which themselves would be affected by the vacuum of the theory.

Lay Summary

The purpose of this thesis is to describe the consequences of dissipative dynamics in the early universe. Moreover, the objective of early universe cosmology is to quantify the observed features of the universe and to develop a physical model to account for them. The most recent cosmological observations highly suggest that the early universe went through a period of rapid exponential growth. This inflationary epoch can successfully describe an expanding universe that is spatially flat, homogeneous and isotropic on large scales, and where the large scale structure originated from primordial fluctuations with a nearly scale-invariant, adiabatic, and gaussian spectrum. However, in the standard inflationary picture, cold inflation (CI), depicted by a homogeneous scalar "inflaton" field, the short period of quasi-de Sitter accelerated expansion phase quickly dilutes away all traces of any pre-inflationary matter or radiation density, so that the state of the universe is the vacuum state. However, this generates a supercooled universe and leaves indeterminate a reasonable description of the transition from inflation to the "hot Big Bang" scenario, required by Big Bang Nucleosynthesis, and the physics of recombination leading to the Cosmic Microwave Background (CMB) that we observe today. This necessarily requires the conversion of inflaton energy density into ordinary matter and radiation and thus to its interactions with other fields. Thereby the inflaton field could be coupled to other components and might dissipate its vacuum energy and warm up the universe. This alternative scenario is known as the *warm inflation* (WI) paradigm, where dissipative effects and associated particle production can, in fact, sustain a thermal bath concurrently with the accelerated expansion of the universe during inflation.

In the first project we explore the dynamics and observational predictions of the Warm Little Inflaton scenario, presently the simplest realisation of warm inflation within a concrete quantum field theory construction. We consider three distinct types of scalar potentials for the inflaton, namely chaotic inflation with a quartic monomial potential, a Higgs-like symmetry breaking potential and a non-renormalizable plateau-

like potential. In each case, we determine the parametric regimes in which the dynamical evolution is consistent for 50-60 e-folds of inflation, taking into account thermal corrections to the scalar potential and requiring, in particular, that the two fermions coupled directly to the inflaton remain relativistic and close to thermal equilibrium throughout the slow-roll regime and that the temperature is always below the underlying gauge symmetry breaking scale. We then compute the properties of the primordial spectrum of scalar curvature perturbations and the tensor-to-scalar ratio in the allowed parametric regions and compare them with Planck data, showing that this scenario is theoretically and observationally successful for a broad range of parameter values.

In the second project we study the dynamics and observational predictions of warm inflation within a supersymmetric distributed mass model. This dissipative mechanism is well described by the interactions between the inflaton and a tower of chiral multiplets with a mass gap, such that different bosonic and fermionic fields become light as the inflaton scans the tower during inflation. We examine inflation for various mass distributions, analysing in detail the dynamics and observational predictions. We show, in particular, that warm inflation can be consistently realised in this scenario for a broad parametric range and in excellent agreement with the Planck legacy data. Distributed mass models can be viewed as realisations of the landscape property of string theory, with the mass distributions coming from the underlying spectra of the theory, which themselves would be affected by the vacuum of the theory. We discuss the recently proposed swampland criteria for inflation models on the landscape and analyse the conditions under which they can be met within the distributed mass warm inflation scenario. We demonstrate mass distribution models with a range of consistency with the swampland criteria including cases in excellent consistency.

To sum up, I wish to describe the state of the art, with respect to both warm inflation model building and the confrontation of theory with observation.

Declaration

I declare that this thesis was composed by myself, that the work contained herein is my own except where explicitly stated otherwise in the text. Where the work was done in collaboration with others, a significant contribution was made by the author. And that this work has not been submitted for any other degree or professional qualification except as specified.

(*Rafael Hernández Jiménez, August 2019*)

To my father Rafael Hernández Lupercio ...

... ¡achicale! ...

... and to Yinyin and Sebastián

Acknowledgements

Arjun Berera, thank you for giving me this wonderful opportunity to be my supervisor, but most importantly for being so patient and supportive throughout my PhD. I am deeply grateful for encouraging me during difficult times.

Mar Bastero-Gil, you were the whole time guiding me with a lot of patient and encouragement, I am deeply grateful. João G. Rosa, thank you for all the knowledge which you have passed on to me. Rafael Cerezo, you helped me a lot during my first year of the PhD. Thank you very much to you three.

Paulina, there is not enough text in the world to describe my deepest gratitude I have for you, even so, I have few words to say to you. You have supported me wholeheartedly in every way possible. I love you with all my being.

My friends, Joscha Reichel, Delia Murguia, Felix Wiesner, Christian Brønnum-Hansen, Marco Garofalo, Francesco Buciuni, Andries Waelkens, Ava Khamseh, Oscar Ramírez, Esperanza Farieta, James Cockburn, Jorge Zavala, Antonio Herrera, Marco D'oleire, Leonardo de la Cruz. My mexican friends, José Socorro García, Omar Soltero and Alexis Torres, and the great mexican community in Edinburgh, Samuel Casasola, Efraín Zarazúa, Germán Pérez, Ricardo López, Selina Aragón, Rodrigo García, Alejandra Schiavon, and more. Remarkably, Patrick Levy and Vanessa Smer, you helped me and Paulina with open arms, we owe you a lot; and I hope we can do the same for you one day. Thank you all.

Mary Moffet, thank you for sharing your lovely house and exquisite food. I am deeply grateful.

I deeply thank my family: my parents, my siblings, my brothers in law and my sister in law, who were a great support to meet my goals. Thank you very much indeed.

My examiners, Roger Horsley and Antonio Padilla, thanks for taking your time to examine my thesis.

To everyone else who has helped in some way, you should know who you are and that I am grateful.

Finally, I want to thank CONACyT for funding my PhD.

Publications

The work in this thesis is based on the following publications completed during the course of my PhD:

M. Bastero-Gil, A. Berera, R. Hernández-Jiménez and J. G. Rosa, *Dynamical and observational constraints on the Warm Little Inflaton scenario*, Phys. Rev. D **98**, no. 8, 083502 (2018) [arXiv:1805.07186 [astro-ph.CO]].

M. Bastero-Gil, A. Berera, R. Hernández-Jiménez and J. G. Rosa, *Warm inflation within a supersymmetric distributed mass model*, Phys. Rev. D **99**, no. 10, 103520 (2019) [arXiv:1812.07296 [hep-ph]].

Contents

List of Figures

List of Tables

Chapter 1

Introduction

> "I saw the Aleph from every point and angle, and in the Aleph I saw the earth and in the earth the Aleph and in the Aleph the earth; I saw my own face and my own bowels; I saw your face; and I felt dizzy and wept, for my eyes had seen that secret and conjectured object whose name is common to all men but which no man has looked upon the unimaginable universe."
>
> —Jorge Luis Borges, The Aleph

For centuries humankind has observed the vast night sky and wondered which would be its right place in this immense cosmos. Such desire for knowledge has shaped numerous civilisations. Through culture they have given birth to several transcendental interpretations of how our universe came to be what we observe. Among many explanations, the scientific ones remain the most relevant since they endure the test of time and stand exhaustive rational assessments. In western society, greek philosophy is considered the most influential worldview. Philosophers such as Leucippus, Democritus, Pythagoras and Ptolemy have helped to conceive a feasible description of the universe. The geocentric model (also known as geocentrism, or the Ptolemaic system) illustrates such relevance of those great greek thinkers.

In 1543, Nicolaus Copernicus challenged the geocentric system with the publications of his famous book "On the Revolutions of the Heavenly Spheres", in which states that the Earth and the other planets instead revolved around the Sun. The Copernican scheme was not actually more accurate than Ptolemy's model, since it still used circular orbits. With the invention of the telescope, later on, Johannes Kepler's work (published between 1609 and 1619) improved the heliocentric theory of Nicolaus Copernicus, explaining how the planets' speeds varied, and using elliptical orbits rather than circular

orbits with epicycles [1]. It was Kepler's exceptional theoretical interpretation of the voluminous data, left by Tycho Brahe, that culminated in Isaac Newton's "Principia Mathematica" (1687), in which Newton derived Kepler's laws of planetary motion from a force-based theory of universal gravitation [2].

However, newtonian theory of reality yields inexplicable upshot, such as Bentley's paradox: "If all bodies attracted each other as Newton's theory implies, Bentley thought that each star and planet should, over time, be pulled towards its neighbours; eventually the whole universe would come crashing in upon itself" [3]. Nonetheless, Newton's description, until today, remains as a sufficient explanation of gravity, since it can explain adequately this interaction as long as, roughly speaking, the mass M of a system is small compared to the size, $R : M/R \ll 1$ (weak gravitational field). Conversely, what paradigm may be expected to be important where either R becomes small faster than M or M becomes large faster than R? The answer is General Relativity (GR), Einstein's awe-inspiring theory.

The equivalence principle is the cornerstone of Einstein GR, since it supports the equality of gravitational and inertial mass. Einstein's basic intuition was to postulate that at a certain point in space-time one cannot distinguish experimentally between a uniformly accelerated body and a uniform gravitational field. The equivalence principle says that the cancelation of gravitational constituent by the inertial one, and hence their equivalence, correspond to freely falling systems. Although for freely falling systems in an inhomogeneous or time-dependant gravitational field, the inertial component is not exactly equivalent to the gravitational one, we can still expect an approximate cancellation if we restrict or attention to such a small region of space-time that the field changes very little over the region. Therefore the equivalence principle is formulated as the statement that "at every space-time point in an arbitrary gravitational field it is possible to chose a "locally inertial coordinate system" such that, within a sufficiently small region of the point in question, the laws of nature take the same form as in unaccelerated Cartesian coordinate system in the absence of gravitation" [4]. Based on the aforementioned principles Einstein formulated the gravity field equation:

$$R_{\mu\nu} - \frac{1}{2} g_{\mu\nu} R - g_{\mu\nu}\Lambda = 8\pi G\, T_{\mu\nu}\,. \tag{1.1}$$

From the Einstein's gravitational field equations we can say that the left-hand side of the equality describes the geometry of spacetime, and the right-hand side represents the matter (energy) contained in such geometrical configuration; hence one can say that the interaction of the material content modifies the geometry of spacetime. I will explain in detail the above expression in the next chapter.

When considering the universe as a whole [5], it includes all matter that exists in our spacetime. *Cosmology* is the study of the universe considering a large-scale structure and intrinsic physical behaviour. The formal study of cosmology as a discipline of physics has been developed since the early twentieth century to today; it started with the theory of Friedmann-Lemaître-Robertson-Walker (FLRW) of a universe that came from a great explosion (Big Bang), through the inflationary theory [6] (one that tells us that the cosmos at an early age must have gone through a dynamic phase of extremely rapid growth) to the current stage of accelerated expansion [7]. It should be noted that the introduction of a scalar field theory in FLRW can successfully reproduce inflation, and in addition to accelerated expansion at late times [8, 9].

Nevertheless, scientific ideas must be proved by logic and well conducted experiments; being the latter that demand the most overwhelming efforts. Without any doubt, we are currently in the era of precision cosmology. As such, we have been able to test, with high accuracy, the observable universe. According to the standard cosmology, which I will introduce in detail later, light decoupled from the rest of the energy components at temperatures about $T_{dec} \approx 0.3\text{eV}$ at a time $t_{dec} \approx 3.8 \times 10^5$ years after the Big Bang, from this time on photons (primordial photons) free-streamed and travelled basically uninterrupted until they have reached us, giving rise the *cosmic microwave background* (CMB); also known as *the surface of last scattering*. Before that, photons were highly interacting leaving the universe effectively opaque. Therefore, the CMB remains the most ancient piece of knowledge we have from the early universe. However, other sources of information, such as neutrinos and gravitational waves could have travelled from further.

The most recent cosmological observations of the CMB once again confirm a universe that is expanding, spatially flat, homogeneous, and isotropic on large scales, and where the large scale structure originated from primordial fluctuations with a nearly scale-invariant, adiabatic, and gaussian spectrum [10].

Despite the fact that the standard "hot Big Bang" (SBB) cosmology is quite remarkably simple, and it can explain successfully the basic characteristics of the observed universe, such as the CMB, the Big Bang Nucleosynthesis (BBN), etc.; this presents imperfections, or more accurately: it is not without its shortcomings. Indeed, it cannot elucidate the primordial spectrum of rather small, but extremely important density fluctuations imprinted in the CMB, and it requires incredibly precise initial conditions to allow the universe to evolve into the one we observe today.

Originally the inflationary scenario was introduced in order to solve the shortcomings

of the SBB [6], however, nowadays is considered as the most elegant process so far proposed to understand for what reasons the universe is remarkably in agreement with the standard cosmology, albeit there are still unanswered enigmas, such as the dark sector. Hence inflation does not replace the SBB cosmology, but rather it is considered as a "supplement" which occurred at the early stages of the universe.

Inflationary cosmology is based on the hypothesis that the early universe expanded exponentially quickly for a fraction of a second. For an inflationary expansion of about a factor of 10^{26} [a] the problems of the SBB can be overcome. During this inflationary regime the universe was dominated by a very peculiar form of energy [b], which is often modelled by a scalar field ϕ: the "inflaton", with potential energy density $V(\phi)$.

Accelerated expansion occurs when the potential energy of the field, $V(\phi)$, dominates over its kinetic counterpart, $\dot{\phi}^2/2$. This mechanism to explain acceleration in the early universe is called *slow-roll inflation*, since the field evolves slowly "enough", so that the potential energy dominates over its kinetic equivalent. Inflation ends at ϕ_{end} when the kinetic energy has grown to become comparable to the potential one, i.e. $\dot{\phi}^2/2 \approx V(\phi)$. Moreover, inflation has the ability to correlate scales in such a way that otherwise they would be disconnected, i.e. this paradigm offers an explanation on the primordial spectrum imprinted on the CMB. The basic picture is that quantum fluctuations, that were in causal contact with themselves, during inflation are stretched beyond the horizon by inflation, where we see them as classical fluctuations on scales larger than the horizon at the end of it. Indeed, inflation can successfully explain the recent measurements of the temperature anisotropies of the CMB; in particular models based on the dynamics of a slowly rolling scalar field are in outstanding agreement with observations, since they can generate a primordial spectrum of density perturbations that is essentially adiabatic, gaussian and nearly scale-invariant. Ultimately, inflation provides an explanation for the initial conditions observed throughout the large-scale structure of the universe

However, by itself, this solution creates additional problems. For instance, the universe is not currently in an exponential inflationary phase; therefore, a viable model must provide a way to end such a period of inflation. Besides, if the solution was applied to anything, it should leave us with no matter and radiation in this universe. So there should be a way to regenerate the content material after enough inflation has happened. Also, since density perturbations produced during inflation evolve into the

[a] This factor means that inflation lasted for at least 60 e-folds, since $\ln 10^{26} \simeq 60$. I will introduce later the concept of e-folding, but essentially is the amount by which the universe inflates.

[b] Essentially for a quasi-de Sitter accelerated expansion the universe must be dominated by an energy content with negative pressure.

classical inhomogeneities observed in the CMB, there must be an explanation of the troublesome quantum-to-classical transition problem. There are more issues that are relevant to tackle, besides the aforementioned shortcomings, but I will discuss them later.

In the standard inflation picture, cold inflation (CI), depicted by a homogeneous scalar "inflaton" field, the short period of quasi-de Sitter accelerated expansion phase quickly dilutes away all traces of any pre-inflationary matter or radiation density, so that the state of the universe is the vacuum state. However, this generates a supercooled universe and leaves indeterminate a reasonable description of the transition from inflation to the SBB scenario, required by BBN, and the physics of recombination leading to the CMB that we observe today. This necessarily requires the conversion of inflaton energy density into ordinary matter and radiation and thus to its interactions with other fields.

Besides, in CI the inflaton decay can only play a significant role at the end of the slow-roll regime, since particle production is not pictured to occur within the inflationary expansion phase. This leads to cold inflation ending through the standard "(p)reheating" [c] paradigm [11]. The reasoning behind this phase lies in the fact that the perturbative decay width of a particle is generically smaller than its mass, which in turn lies below the Hubble expansion rate for a slowly rolling scalar field. Consequently such interplay between the inflaton and other constituents may perform a negligible role during the slow-roll phase of inflationary models. Nonetheless, it is relevant to note that the perturbative decay width only describes the decay of a field close to the minimum of its potential [12], which is evidently not the case during slow-roll dynamics, and that finite temperature effects can further significantly enhance the rate at which the inflaton dissipates its energy into other degrees of freedom. Thereby the inflaton field could be coupled to other components and might dissipate its vacuum energy and warm up the universe. This alternative scenario is known as the *warm inflation* (WI) paradigm [13, 14], where dissipative effects and associated particle production can, in fact, sustain a thermal bath concurrently with the accelerated expansion of the universe during inflation.

Essentially warm inflation is a more profound realisation of inflation. It is not an exhaustive reformulation but rather a deeper rethinking. Recall that throughout the inflationary regime, the dynamics is governed by a scalar field, which during inflation carries most of the energy of the universe and which interacts with other counterparts

[c] Briefly, reheating is a hypothetical process that occurred right after inflation ended but before the radiation domination era or the SBB scenario. This scenario intends to explain that most of the energy density of the inflaton field at the end of inflation, in the CI scenario, may be available for conversion into thermalised form.

(radiation, matter, etc.). On the one hand, the CI scenario assumes explicitly that these interactions have no other effect except to modify the scalar field effective potential through quantum corrections. On the other hand, the WI scenario poses that interactions not only modify the scalar field potential but also lead to fluctuation and dissipation effects. Moreover, dissipative effects can be well explained by first principles of a quantum multi-field theory, and they are important during the inflation period so that radiation production occurs simultaneously with inflationary expansion.

The idea of inflationary expansion and particle production occurring concurrently was suggested by L.Z. Fang, Moss, Yokoyama and Maeda [15] and then independently rediscovered almost a decade later by Berera and Fang [13]. At first the main insight was to introduce a dissipative term $\Upsilon\dot{\phi}$ in the inflaton evolution equation, as a source of radiation production; but later was not only included the dissipative contribution but also a noise force term that would drive the inflaton fluctuations, with a fluctuation-dissipation theorem uniquely specifying the inflaton fluctuations.

WI has other several attractive features. For instance, the additional friction may ease the required flatness of the inflaton potential. Also, even if radiation is subdominant during inflation, it may smoothly become the leading component at the end of inflation, with no need for a separate reheating period. It also may explain the nature of the classical inhomogeneities observed in the CMB, since for WI the fluctuations of the inflaton are thermally induced, as such, these initial seeds of density perturbation already are classical upon definition; hence there is no need to explain the troublesome quantum-to-classical transition problem of CI, due to the purely quantum origin of the CI density perturbations.

Realising warm inflation within a consistent quantum field theory framework has, however, proved to be a challenging endeavour. Non-equilibrium dissipative effects are Boltzmann suppressed unless the particles in the radiation bath are relativistic, while the inflaton typically gives a large mass to the fields it couples directly to. In addition, relativistic particles change the form of the inflaton potential at finite temperature, typically inducing large thermal corrections to the inflaton's mass that may prevent slow-roll unless the associated inflaton couplings are very suppressed, therefore rendering dissipative effects ineffective in sustaining a thermal bath during inflation [16, 17]. For several years, the leading solution to these problems was to consider models where the inflaton only couples directly to heavy fields, which in turn decay into light particles in the thermal bath [18]. In these scenarios thermal corrections to the inflaton potential become Boltzmann-suppressed, while dissipative effects can nevertheless be significant if one considers a large number of fields coupled to the

inflaton[d]. While such scenarios may find natural realisations in specific constructions within e.g. string theory [22] where field multiplicities can be large during inflation, they cannot provide a simple and sufficiently generic realisation of warm inflation.

A more promising scenario was proposed recently [23] where the above-mentioned problems were addressed using symmetries rather than large field multiplicities. This *Warm Little Inflaton* (WLI) scenario, so-called due to its similarities with Little Higgs models of electroweak symmetry breaking [24, 25], considers an inflaton field that corresponds to the relative phase between two complex Higgs scalars that collectively break a local U(1) symmetry. These complex scalars interact with fermions through Yukawa interactions that, in addition, satisfy a discrete interchange symmetry, essentially leading to an effective theory below the symmetry breaking scale M involving the inflaton field and two Dirac fermions.

On the other hand, one of the earliest warm inflation models [26] suggested the idea that parameters in an inflation model could be randomly distributed. The distributed-mass-model (DM model) [27–30] was subsequently proposed and built on this idea in the context of string theory. It observed [30] that models from string theory have states at many energy levels and the distribution of these levels is ultimately dictated by the string vacuum. This proposal was highly criticised at that time, for instance in [31] authors remarked how difficult is to realise the idea of WI in realistic models of elementary particles, due to its large number of fields. Nevertheless, the model was intended to illustrate a scheme developed by first principles inspired by string theories exhibiting $\mathcal{N} = 1$ global supersymmetry, with the inflaton coupled to massive modes of the string [32]. Within this context, as a natural consequence of the modification of short-distance physics, required by string theory, a large number of fields is necessary to accomplish sufficient inflation [27–29]. Although, this model may be regarded as discouraging from any realistic inflation physics, such methodology is a good constructive tool for studying WI dynamics. Moreover, this scheme is evidence that combining theoretical implementation with observations, inflation paradigm can be examined as multi-field problem.

The purpose of this thesis is to describe the consequences of dissipative dynamics in the early universe. I will start this thesis with a brief review of some fundamental cosmology since it will be necessary to set the scene for the subsequent segments of this thesis. In Chapter 2 I will present the The Standard "hot Big Bang" (SBB) cosmology. In Chapter 3 I will present the inflationary paradigm, and how this (at some degree) solves

[d] In this case dissipative effects are the result of heavy virtual modes that are not Boltzmann-suppressed [19–21].

the problems associated with the standard cosmological. Moreover, I will describe how the most recent cosmological observations of the CMB can be well explained by density perturbations due to the inflaton. In Chapter 4 I will introduce briefly warm inflation and fluctuation-dissipation dynamics, in particular I will show how these effects play an important role during inflation. In Chapter 5 I will present my original contribution. We explore the dynamics and observational predictions of the Warm Little Inflaton scenario. In Chapter 6 I will present another original contribution. We study the dynamics and observational predictions of warm inflation within a supersymmetric distributed mass model. In Chapter 7 I conclude this work and offer an outlook of what needs to be done for further research in this attractive field.

Chapter 2

The Standard "hot Big Bang" (SBB) cosmology

> "It is part of the martyrdom which I endure for the cause of the Truth that there are seasons of mental weakness, when Cubes and Spheres flit away into the background of scarce-possible existences; when the Land of Three Dimensions seems almost as visionary as the Land of One or None; nay, when even this hard wall that bars me from my freedom, these very tablets on which I am writing, and all the substantial realities of Flatland itself, appear no better than the offspring of a diseased imagination, or the baseless fabric of a dream."
>
> —Edwin A. Abbott, Flatland: A romance of many dimensions

The standard model of cosmology, also known as the Standard "hot Big Bang" (SBB) model, explains successfully the origin and evolution of the universe, due to two essential astronomical observations that support its acceptance:

- The current expansion of the universe and
- The background radiation of almost three Kelvin (electromagnetic radiation observed in all directions of the universe, which is associated with its temperature).

Fundamentally this paradigm is established on *the cosmological principle*, introduced first by Albert Einstein based on the ideas of Ernst Mach [33]. It can be summarised as follows: in every epoch, the universe presents the same aspect in each point[a], except

[a] Almost any contemporary model of cosmology is based on the idea that the universe is very much the same everywhere, a statement that is sometimes known as the "Copernicus principle".

for local irregularities, that is to say that the universe on large scales[b] is homogeneous and isotropic.

Before I introduce more technical details, we must revise Edwin Powell Hubble's tremendous astronomical discovery, as well as the concept of redshift.

2.1 Redshift

Cosmology is a science where the source of data is astronomical observations. However, distances and cosmological times are not directly evident, since we are anchored on the earth. Instead, we have to use what we can actually measure, which is the properties of objects that we can see, i.e. objects on our past light cone. Moreover, if the universe is expanding, these objects, such as galaxies, should move away from each other, meaning that the wavelength of light emitted by a retreating galaxy stretches out. Hence, this stretching factor is defined as the redshift z:

$$1 + z \equiv \frac{\lambda_{obs}}{\lambda_{emit}} = \frac{\nu_{emit}}{\nu_{obs}}\,, \tag{2.1}$$

where $\nu = c/\lambda$ is the frequency of the emitted or observed object. For non-relativistic recession velocity $v_z \ll c$ or low redshifts, the redshift is simply given by $z = v_z/c$, where c is the speed of light in the vacuum. We shall see that higher redshift in general means further away and older. Since astronomical observations from distant galaxies exhibit a red shifted spectra, we conclude that the universe is expanding.

2.2 Hubble's Law

In the 1920's Edwin Powell Hubble was studying cosmic objects from Mount Wilson, which were known at the time as nebulae. He determined, by stars of variable brightness known as Cepheids, that the distance of the Andromeda galaxy was about 700,000 light-years [34]. Likewise, using a method known as cosmic distance scale [35], found the distances to different nebulae that turned out to be extragalactic. He concluded that the *island universes* are located very far from our galaxy.

Moreover, Hubble established that the speed of the galaxies and their distances were correlated in such a way that the farther they were from the earth, the faster they

[b] To greater scales than 100 megaparsec. The parsec (pc symbol) is a unit of length used in astronomy. Its name is derived from the parallax of one arc second. 1 parsec = 206 265 UA = 3.26 light-years = 3.0857×10^{16} m.

moved away from us, this result is known as Hubble's law [36]. This realisation is a law of cosmology that states that the redshift z, which is related to the distance to the location of a galaxy, is proportional to the speed v_z with which the galaxy moves away from us. This law in terms of the redshift states:

$$v_z = zc = Hd\,, \tag{2.2}$$

where v_z is the speed of separation among the galaxies (recession speed), d is the distance among them and H is the Hubble parameter. Hubble obtained a value for the constant H equal to $500\,\mathrm{km\,s^{-1}\,Mpc^{-1}}$, i.e. for each megaparsec of distance its recession speed increases at a rate $500\,\mathrm{km\,s^{-1}}$. The implementation of different methods of measuring distances and speeds has led to this parameter is changing. The most current value was provided by Planck satellite: $H_0 = 67.36 \pm 0.54\,\mathrm{km\,s^{-1}\,Mpc^{-1}}$, where the subscript 0 represents the present outcome [10].

A decade before Hubble made his observations, several physicists and mathematicians had established a consistent theory of the relationship between space and time using Einstein's field equations of general relativity. Applying the general principles to the nature of the universe produced a dynamical solution that contrasted with the then prevailing notion of a static universe, but thanks to these studies, Hubble made his greatest discovery, and certainly one of the most important in the history of humanity: the universe is expanding[c].

2.3 Friedmann equations of motion: FLRW universes

The most general metric that represents a homogeneous and isotropic spacetime with constant curvature is given by the FLRW metric, that is:

$$ds^2 = c^2dt^2 - a^2(t)\left[\frac{dr^2}{1-kr^2} + r^2\left(d\theta^2 + \sin^2\theta d\phi^2\right)\right]\,, \tag{2.3}$$

where t is the cosmological time, $a(t)$ is the scale factor (magnitude that yields a measurement of the evolution of the distances between two fixed points in a given spatial section), k is the curvature of a prescribed spatial region and takes values among

[c]However, this statement comes with controversy. A few years before Hubble published his discoveries, George Lemaître studied the cosmos on theoretical grounds, by implementing GR, and he reported that the universe is expanding. Yet, it was not until 1931 that Lemaître published in english an article in Nature setting out his theory of the "primeval atom" [37]. In it, he enunciated: "If we go back in the course of time we must find fewer and fewer quanta, until we find all the energy of the universe packed in a few or even in a unique quantum". Arguably this can be the birth of the hot Big Bang model.

0,1, and -1 (space of zero, positive, and negative curvature); r is the radial coordinate, θ is the polar angle, and ϕ is the azimuthal angle. Seen in this way, space-time is *sliced* in space cuts perpendicular to the direction of cosmological time t, where k is the curvature of each spatial slice, homogeneous and isotropic. The form of $a(t)$ depends on the properties of the matter of the universe, as we will see next.

To derive the equations of motion, we must use Einstein's gravitational field equations:

$$R_{\mu\nu} - \frac{1}{2}g_{\mu\nu}R - g_{\mu\nu}\Lambda = \kappa^2 T_{\mu\nu}\,, \tag{2.4}$$

where we have taken $c = 1$, then $\kappa^2 = 8\pi G$, $G = 6.674 \times 10^{-11} m^3 kg^{-1} s^{-2}$ is the Newtonian constant of gravitation, $g_{\mu\nu}$ is the metric tensor (eq. (2.3)), which signature is $(+,-,-,-)$, $R_{\mu\nu}$ and $R = g^{\mu\nu}R_{\mu\nu}$ are the Ricci curvature tensor and scalar curvature, respectively. The greek indices run from 0 to 3, additionally if latin indices i, j, etc. appear, they go from 1 to 3. Also Λ is the cosmological constant[d], and the stress-energy tensor:

$$T_{\mu\nu} = (\rho + p)U_\mu U_\nu - p g_{\mu\nu}\,, \tag{2.5}$$

note that we have considered a stress-energy tensor corresponding to a perfect fluid, of which the universe is full. Hence ρ is the energy density and $p = p(\rho)$ is the isotropic pressure; both expressions are functions that depend on t. Also, the local 4-velocity of the fluid $U^\mu = (1, 0, 0, 0)$, that must be a temporal vector, i.e. $U^\mu U_\mu = 1$. Perfect fluids, also called Pascal's fluids, are those that are described only by their distribution of mass (mass-energy density) and pressure (which is isotropic); neither viscosity nor thermodynamics are involved.

Implementing the FLRW metric eq. (2.3) into the field eq. (2.4) and the perfect fluid stress-energy tensor eq. (2.4), the Einstein equations for this fluid are:

$$H^2 \equiv \left(\frac{\dot{a}}{a}\right)^2 = \frac{\kappa^2\rho}{3} - \frac{k}{a^2} + \frac{\Lambda}{3}\,, \tag{2.6}$$

and

$$\frac{\ddot{a}}{a} = -\frac{\kappa^2}{6}(\rho + 3p) + \frac{\Lambda}{3}\,, \tag{2.7}$$

where we have defined the Hubble parameter as the ratio of expansion; the upperdot $\dot{\bullet}$ represents the derivate with respect to time t, and the cosmological constant is related

[d]Nowadays Λ may refer as the energy density of space, or vacuum energy, that arises in Albert Einstein's field equations of general relativity. It is closely associated to the concepts of dark energy and quintessence [38].

to the energy density of the vacuum as $\rho_{vac} = \Lambda/\kappa^2$. The expression (2.6) is called Friedmann equation, while eq. (3.12) is the Raychaudhuri one.

The formula that describes how the material content of the universe changes over time, i.e. the energy density ρ and the pressure p, is obtained by taking the covariant derivative of the energy-momentum tensor $\nabla_\mu T^{\mu\nu} = 0$; whose expression, by considering the metric eq. (2.3), yields:

$$\dot{\rho} + 3H\,(\rho + p) = 0\,. \tag{2.8}$$

It is important to note that the above expression represents the conservation of energy. In order to describe in more detail how distinct matter configurations affect dynamically the geometry, let us define the cosmological density:

$$\Omega_i \equiv \frac{\rho_i}{\rho_{crit}}\,, \tag{2.9}$$

this parameter helps us to describe the dynamical effects of the density of total matter in the universe, and ρ_{crit} is called the critical density:

$$\rho_{crit} = \frac{3H^2}{\kappa^2}\,. \tag{2.10}$$

Due to special relativity, we know that energy and matter represent the same physical entity, only that each one shows its different face; hence, we must add all the contributions of the different energy constituents of the cosmos. One can parametrise the various species of components by employing the density parameter Ω_i, then the Friedmann equation (2.6) can be written as:

$$\Omega = \Omega_m + \Omega_\Lambda = \Omega_k + 1\,, \tag{2.11}$$

where $\Omega_\Lambda = \Lambda/3H^2$ corresponds to the energy density of the cosmological constant, $\Omega_k = k/(a^2H^2)$ parameterises curvature, and $\Omega_m = \kappa^2\rho/3H^2$ is the total density of matter, which can be divided into $\Omega_m = \Omega_{dm} + \Omega_b$, where Ω_{dm} and Ω_b constitute the density of dark and baryonic[e] matter, respectively. The sign of k is, therefore,

[e]Practically all matter that we may experience or encounter in everyday life is baryonic matter, which includes atoms of any sort.

determined by Ω in the following way:

$$\begin{aligned} &\text{if} \quad \rho \;<\; \rho_{crit} \Rightarrow \Omega < 1 \Rightarrow k < 0 \Rightarrow \text{open universe}\,, \\ &\text{if} \quad \rho \;=\; \rho_{crit} \Rightarrow \Omega = 1 \Rightarrow k = 0 \Rightarrow \text{flat universe}\,, \\ &\text{if} \quad \rho \;>\; \rho_{crit} \Rightarrow \Omega > 1 \Rightarrow k > 0 \Rightarrow \text{closed universe}\,. \end{aligned} \tag{2.12}$$

Hence, the cosmological density parameter tells us which of the three FLRW geometries describes our cosmos. Currently, observations of the CMB and the large-scale structure: baryon acoustic oscillations (BAO) and supernovae (SNe), find that the universe is nearly flat, with $\Omega_k \ll 1$ as seen in fig. 2.1. Note that the evidence for flatness cannot be obtained from CMB observations alone.

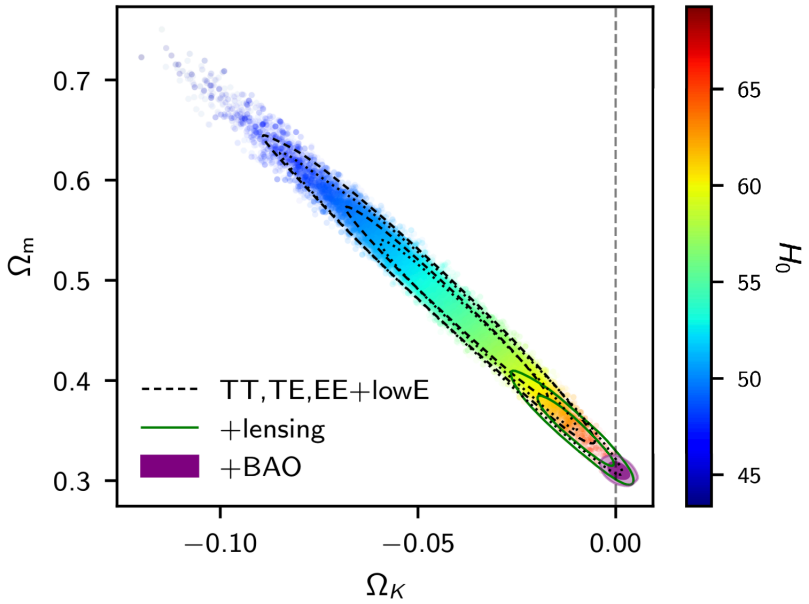

Figure 2.1: Plot of the total density of matter Ω_m versus the spatial curvature Ω_k from Planck alone or in combination with BAO data. This plot constraints the spatial curvature, where the vertical dashed line indicates a spatially flat universe. Indeed, this upshot is quite consistent with the combination of all of the observations (solid, purple filled contour). Also, points are coloured by the value of the Hubble constant (colour bar), dashed lines show the 68 and 95 % confidence contours from the fiducial likelihood, while dotted lines show those from the alternative (CamSpec) likelihood as an indication of the systematic uncertainty. Source Planck Legacy [10].

2.4 Solutions to Einstein's equations

In this section I present some solutions for the evolution equations of a FLRW cosmology. First of all, note from the eqs. (2.6), (2.7), and (2.8), that two of these expressions are linearly independent, and since we have the following set of variables

to be determined: $\{a(t)\,,\rho(t)\,,p(t)\}$, we need another equation to close the system. Hence we must specify a state equation for the perfect fluid, in this case we will use a barotropic fluid, whose equation of state is given by:

$$p = \omega\rho\,, \tag{2.13}$$

where ω is a constant, $-1 \leq \omega \leq 1$, called the barotropic parameter. It can described radiation $\omega = 1/3$, non-relativistic matter (or dust) $\omega = 0$, or vacuum energy $\omega = -1$.

The first cosmological models were very useful to understand the dynamics of the universe, however, the cosmological constant was not considered, since at that time it was not known exactly what it represented physically; therefore it is taken as $\Lambda = 0$ for the models in which non-relativistic matter and radiation dominate.

Then, in order to solve the equations of motion, we substitute eq. (2.13) into eq. (2.8), so we obtain:

$$\dot{\rho} + 3H(\omega + 1)\rho = 0\,, \tag{2.14}$$

having as a solution:

$$\rho \propto a^{-3(\omega+1)}\,. \tag{2.15}$$

Now, we must find the dependency of a with respect to t, so we employ eq. (2.15) into eq. (2.6), yielding:

$$\left(\frac{\dot{a}}{a}\right)^2 = \frac{\kappa^2}{3a^{3(\omega+1)}} - \frac{k}{a^2}\,. \tag{2.16}$$

Finally, by taking $k = 0$, the solution to the previous equation is:

$$a \propto t^{\frac{2}{3(\omega+1)}}\,. \tag{2.17}$$

Note that with eq. (2.17) one can find basically any solution, once the barotropic parameter is fixed, however, for the vacuum energy case ($\omega = -1$) see that the power of t becomes infinity, yielding a mathematical inconsistency; so one has to pursue another approach in order to find $a(t)$.

For the case $\omega = -1$ we have a negative pressure, i.e. $p = -\rho$, so we have to examine $\Lambda \neq 0$. But before proceeding, it is interesting to note that once Einstein published GR, he devoted himself to make cosmological considerations using it, hence all work in the cosmological context from that moment has employed such theory as the fundamental tool. He discovered that it was impossible to construct a mathematical model of a static universe consistent with GR [39], however, Einstein was convinced that the universe was static, for this reason he introduced a constant: the cosmological constant

Λ. The implementation of this expression was to offer a force of attraction against the expansive solution that he had found, and by that time was not favoured by the observations. Currently, this term is elucidated somewhat different, since now it can be seen as a negative pressure that counteracts the force of attraction, and can also explain the "present" accelerated expansion that is observed [7]; moreover, this constant has rather similar characteristics to the vacuum energy. Then, let us consider $\Lambda \neq 0$, by considering $\rho = 0$ hence $p = 0$, then eq. (2.6) with $k = 0$ yields:

$$\frac{\dot{a}}{a} = \sqrt{\frac{\Lambda}{3}}\,, \tag{2.18}$$

and as a result we have

$$a \propto \exp(Ht)\,, \tag{2.19}$$

where the Hubble parameter is $H = (\Lambda/3)^{1/2}$. This scenario is known as *de-Sitter* solution; this represent the model of an empty universe ($\rho = p = 0$) and null curvature ($k = 0$). In this empty framework, test particles move away from each other due to the gravitational repulsion effect caused by the cosmological constant. It is obvious that if we lived in a universe dominated by the cosmological constant, a would grow exponentially, that is, spacetime would be expanding at an incredibly huge rate. Notice here that given $\Omega_\Lambda = 0.6847 \pm 0.0073$ [10] and due to total Ω is equal to 1 (in a flat universe), an interesting question arises: are we living in a time when the vacuum energy (cosmological constant) dominates? Current measurements tend to an affirmative response [10].

Several epochs can be distinguished via different dominated forms of matter within the cosmos (when $k = 0$), the main ones that intersect with the astrophysical observations are the following [f]:

$$\begin{aligned}
p = \frac{1}{3}\rho: &\quad \text{radiation} \Rightarrow \rho \propto a^{-4} \Rightarrow a \propto t^{1/2} \Rightarrow H \propto \frac{1}{2t} \\
p = 0: &\quad \text{non-relativistic matter} \Rightarrow \rho \propto a^{-3} \Rightarrow a \propto t^{2/3} \Rightarrow H \propto \frac{2}{3t} \\
p = -\rho: &\quad \text{vacuum energy} \Rightarrow \rho \propto \text{constant} \Rightarrow a \propto \exp(Ht) \Rightarrow H \propto \text{constant}
\end{aligned} \tag{2.20}$$

The early universe was dominated by radiation, the adolescent one by matter, and the present universe is being dominated by vacuum energy. Indeed, observations of the CMB and the large-scale structure find that the late universe is being dominated by dark energy Λ (see fig. 2.2). Once again, note that the evidence for dark energy

[f] The real world is a messy place, consisting of different sort of energy densities. Since distinct kind of constituents involve different ranges, in any way, for long periods of time, the energy density can be clearly dominated by only one type of source.

becomes noticeable by the blending of various data sources.

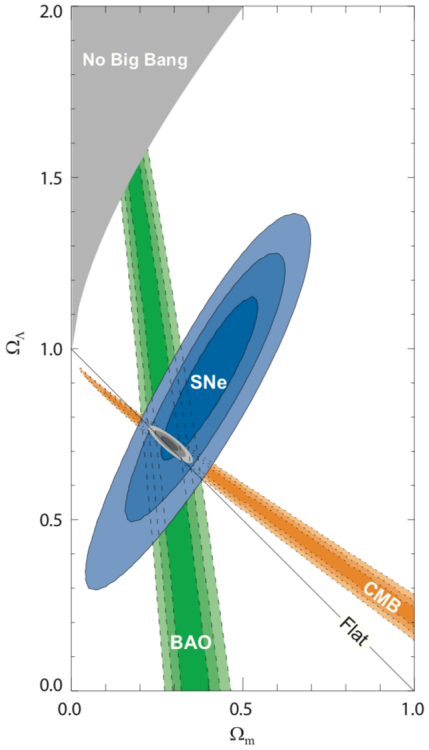

Figure 2.2: Plot of the 68.3%, 95.4% and 99.7% confidence level contours on Ω_Λ and Ω_m obtained from CMB, BAO and the Union SN set, as well as their combination (assuming $\omega = -1$). This plot represents a distinct evidence for dark energy. Source M. Kowalski *et al.* [40]

2.5 Distance-redshift relation

Measuring distances in an expanding universe requires subtle considerations. Moreover, the cosmological principle implies that the expansion should be the same everywhere at any given time. By means of the scale factor $a(t)$ we can measure cosmological distances. Also, we can imagine space as a lattice which expands uniformly as time evolve. Then, the *comoving distance* between two points is the measurement of the difference between coordinates, so if points in the grid maintain their coordinate, this remains constant. On the other hand, the *physical distance* is proportional to the scale factor, so in fact this does change with time. In a flat universe in the absence of interactions [g], light travels a comoving distance $d\tau = dt/a(t)$ (*conformal time*), which corresponds to null rays $ds^2 = 0$ (see eq. (2.3)). Hence the total comoving distance

[g]Due to the homogeneity and isotropy of space one may select $r_0 = 0$, hence geodesics passing through r_0 are lines of constant θ and ϕ, so $d\theta = d\phi = 0$.

light could have traveled since $t = 0$ is:

$$\tau = \int_0^t \frac{dt'}{a(t')} \,. \tag{2.21}$$

Such integral is simple to calculate for any given $a(t)$, provided a particular model, but the distance is not itself directly measurable. Moreover, this distance becomes very relevant because no information could have propagated further than τ since the beginning of time. Therefore, regions separated by distance greater than τ are not causally connected. Often $a(t)$ is normalised so that $a(t_0) = 1$ today, so that for instance, $a = 1/2$ corresponds when the universe was half as expanded as it is today. Then the redshift can be written as:

$$1 + z = \frac{a(t_{obs})}{a(t_{emit})} = \frac{1}{a(t)} \,, \tag{2.22}$$

since $a(t_{obs}) = a(t_0) = 1$. Any increase (decrease) in $a(t)$ leads to a red-shift (blue-shift) of the light from distant sources. Note that $dz/dt = -\dot{a}/a^2 = -H/a$, hence the distance travelled by light between redshift z and the present is:

$$\tau = \int_0^z \frac{dz'}{H(z')} \,. \tag{2.23}$$

We can think of τ as the *comoving particle horizon*, which is the maximum distance from which light can have reached us, starting out at the Big Bang when $z = \infty$. For instance, the photons from the CMB last scattered off electrons at $z_{dec} \simeq 1100$; indeed, this is the furthest distance light can have travelled from decoupling, since then photons have gone through a free journey throughout space. Before that, photons were interacting leaving the universe, in that epoch, effectively opaque. Additionally, the distance of the last-scattering surface is often considered the boundary of our observable universe, however, in principle both neutrinos and gravitational waves could have travelled from further.

On the other hand the *event horizon* designates the limit of how far we can see in the infinite future (which corresponds to redshift $z = -1$). If the universe is accelerating, the integral will converge, meaning there is a limit to how far we can see in the universe ever, while if the deceleration were to cease in the future there may be no event horizon.

2.6 Equilibrium thermodynamics in the expanding universe

Through most of the early universe the density of material within it was at high densities, hence reactions proceeded fast enough to keep particles in equilibrium. Different species shared a common temperature T, and they can be considered to behave as perfect gaseous fluids. The properties of such a gas come from considering a volume $V = L^3$ and expanding the fields inside it into periodic waves; the density of states in k-space is:

$$dN = g_i \frac{V}{(2\pi)^3} d^3k \,, \tag{2.24}$$

where g_i is the degeneracy of the species that accounts for the number of spin or other quantum states (e.g., equal to 2 for the photon for its polarisations) and as usual the momentum is given by $P = k$ [h]. For a species in *kinetic equilibrium* the phase space occupancy f is given by the familiar Fermi-Dirac or Bose-Einstein distributions:

$$f = \left[e^{(E-\mu)/T} \pm 1 \right]^{-1} \,, \tag{2.25}$$

with a minus (plus) sign for bosons (fermions), which takes into account their difference as indistinguishable (distinguishable) particles; and μ is the chemical potential. The energy is $E(P) = \sqrt{P^2 + m^2}$. Note that the occupation number depends on both the ambient temperature T and the chemical potential μ. Full thermal stability requires both chemical and kinetic equilibrium, i.e. the particles have both the correct overall number density and the correct energy distribution, and then μ is zero. This follows directly from the first law of thermodynamics associated with a change in particle number, which states:

$$dE = TdS - pdV + \mu dN \,. \tag{2.26}$$

Hence, as N regulates to its equilibrium value, we expect that the system will be stationary with respect to small changes in N. In a thermal equilibrium background, the number density of particles is then given by:

$$n = \frac{1}{V} \int dN f = \frac{g_i}{(2\pi)^3} \int \frac{d^3P}{e^{(E-\mu)/T} \pm 1} = \frac{g_i 4\pi}{(2\pi)^3} \int_0^\infty \frac{dP P^2}{e^{(E-\mu)/T} \pm 1} \,. \tag{2.27}$$

On the other hand, to compute the energy density of the background, we multiply the occupation of each mode by its energy $E(P)$ and integrate over all modes:

$$\rho = \frac{g_i}{(2\pi)^3} \int \frac{d^3P}{e^{(E-\mu)/T} \pm 1} E(P) = \frac{g_i 4\pi}{(2\pi)^3} \int_0^\infty \frac{dP P^2}{e^{(E-\mu)/T} \pm 1} E(P) \,, \tag{2.28}$$

[h] Note that in fact $P = \hbar k$, but since I considered $c = 1$ so $\hbar = 1$; also the Boltzmann constant $k_B = 1$ as well.

and the pressure p is computed by:

$$p = \frac{g_i}{(2\pi)^3}\int \frac{d^3P}{e^{(E-\mu)/T}\pm 1}\frac{P^2}{3E(P)} = \frac{g_i 4\pi}{(2\pi)^3}\int_0^\infty \frac{dPP^2}{e^{(E-\mu)/T}\pm 1}\frac{P^2}{3E(P)}\,. \tag{2.29}$$

In the relativistic limit ($T \gg m$), for $T \gg \mu$,

$$\rho = \begin{cases} g_i\frac{\pi^2}{30}T^4 & \text{Bosons} \\ \frac{7}{8}\left(g_i\frac{\pi^2}{30}T^4\right) & \text{Fermions} \end{cases} \tag{2.30}$$

$$n = \begin{cases} g_i\frac{\zeta(3)}{\pi^2}T^3 & \text{Bosons} \\ \frac{3}{4}\left(g_i\frac{\zeta(3)}{\pi^2}T^3\right) & \text{Fermions} \end{cases} \tag{2.31}$$

$$p = \frac{\rho}{3}\,, \tag{2.32}$$

where $\zeta(3) = 1.202\ldots$ is the Riemann zeta function of 3. In the non-relativistic limit ($m \gg T$) the number density, energy density and pressure are the same for Bose and Fermi species:

$$n = g_i\left(\frac{mT}{2\pi}\right)^{3/2}\exp\left[-(m-\mu)/T\right] \tag{2.33}$$

$$\rho = nm \tag{2.34}$$

$$p = nT \ll \rho\,, \tag{2.35}$$

note that the number density is suppressed by the exponential "Boltzmann" factor, which in turn restrains ρ and p. For a nondegenerate ($T \gg \mu$), relativistic species, the average energy per type is:

$$\langle E\rangle \equiv \frac{\rho}{n} = \frac{\pi^4}{30\zeta(3)}T \simeq 2.701\,T \qquad \text{Bosons} \tag{2.36}$$

$$= \frac{7\pi^4}{180\zeta(3)}T \simeq 3.151\,T \quad \text{Fermions} \tag{2.37}$$

By taking the chemical potential much smaller than the temperature, the distribution function depends only on E/T and the pressure satisfies[i]:

$$\frac{dp}{dT} = \frac{\rho + p}{T}\,, \tag{2.38}$$

moreover, since the early universe was to a robust approximation in thermal equilibrium, energy and entropy are extensive quantities for a thermal background. Thus,

[i] One can prove this by making a change of integration variable: $P = \sqrt{E^2 - m^2}$ so $dP = EdE/\sqrt{E^2-m^2}$, then one takes the derivative d/dT of p (eq. (2.29)), noting that $f = f(E/T)$ so this leads to $\partial f/\partial T$, however, one can rewrite $\partial f/\partial T$ in the integral as $-(E/T)\partial f/\partial E$, then one can integrate eq. (2.29) by parts, and from there its is straightforward to find $dp/dT = (\rho + p)/T$.

writing the first law of thermodynamics for $\mu = 0$ and using $E = \rho V$ we have:

$$TdS = d(\rho V) + pdV = d\left[(\rho + p)V\right] - Vdp\,, \tag{2.39}$$

so we substitute eq. (2.38) into eq. (2.39), it yields:

$$dS = \frac{1}{T} d\left[(\rho + p)V\right] - \frac{(\rho + p)V}{T}\frac{dT}{T} = d\left[\frac{(\rho + p)V}{T} + \text{constant}\right], \tag{2.40}$$

hence the entropy per comoving volume is:

$$S = a^3 \frac{\rho + p}{T}\,, \tag{2.41}$$

up to an additive constant. Recall that the energy conservation law (first law of thermodynamics) can be written as:

$$d\left[(\rho + p)V\right] = Vdp\,, \tag{2.42}$$

then substituting eq. (2.38) into eq. (2.42), it yields:

$$d\left[\frac{(\rho + p)V}{T}\right] = 0\,, \tag{2.43}$$

this result indicates that the entropy per comoving volume is conserved [j]. Additionally, in the relativistic limit the energy density obeys the usual black-body scaling $\rho \propto T^4$. We also know that the pressure is $p = \rho/3$, so that the entropy density takes an interesting and simple form:

$$s \equiv \frac{S}{V} = \frac{4}{3}\frac{\rho}{T} = \frac{2\pi^2}{45} g_i T^3 \qquad \text{Bosons} \tag{2.44}$$

$$= \frac{7}{8}\left(\frac{2\pi^2}{45} g_i T^3\right) \qquad \text{Fermions} \tag{2.45}$$

Recall that the number density also scales as T^3 (eq. (2.31)), we have that the resulting entropy just counts the number of particles. Indeed, this result is usually called the entropy per baryon, which is the ratio of the number density of photons in the universe to the number density of baryons (protons plus neutrons).

Collecting the above together, the total density of relativistic species at a temperature

[j] The expansion of the universe takes place at constant entropy, since there is no heat flow in a homogeneous cosmos.

T can be written as:

$$\rho = \frac{\pi^2}{30} g_{eff} T^4 \,, \qquad g_{eff} \equiv \sum_{bosons} g_i + \frac{7}{8} \sum_{fermions} g_i \,, \tag{2.46}$$

where g_{eff} counts the total number of effectively massless degrees of freedom for energy density and pressure, which expresses the fermion contribution as an effective number of bosons, where the relative factor 7/8 accounts for the difference in Fermi-Dirac and Bose-Einstein statistics. Additionally, a similar relation holds for entropy density:

$$s = \frac{2\pi^2}{45} h_{eff} T^3 \,, \tag{2.47}$$

where now h_{eff} is the total number of effectively massless degrees of freedom for entropy density. The general relations at background temperature T, by taking into account the possibility that species i may have a different temperature than the surroundings, are:

$$g_{eff} \equiv \sum_{bosons} g_i \left(\frac{T_i}{T}\right)^4 + \frac{7}{8} \sum_{fermions} g_i \left(\frac{T_i}{T}\right)^4 \,, \tag{2.48}$$

$$h_{eff} \equiv \sum_{bosons} g_i \left(\frac{T_i}{T}\right)^3 + \frac{7}{8} \sum_{fermions} g_i \left(\frac{T_i}{T}\right)^3 \,. \tag{2.49}$$

In the early universe all particles species shared a common temperature, since they were in thermal equilibrium, hence $h_{eff} = g_{eff}$; however, this ceases to be true at late times, when the neutrinos and photons have different temperatures. In the relativistic limit, at high temperature, all the particles of the Standard Model are present: 28 bosonic and 90 fermionic degrees of freedom, therefore $g_{eff} = h_{eff} = 28 + (7/8)90 = 106.75$. These parameters fall and separate each other as the temperature drops and more species of particles become non-relativistic.

As mentioned before, throughout the early universe, and particularly during the radiation dominated era, the reaction rates of particles in the thermal bath, Γ_{int}, were much greater than the expansion rate, H, thus a local thermal equilibrium should have been maintained. Beside the conservation of S implies that $s \propto a^{-3}$, and hence that $h_{eff} T^3 a^3$ remains constant as the universe expands. Therefore, the temperature evolves as

$$T^3 h_{eff} \propto a^{-3} \,. \tag{2.50}$$

Note that while h_{eff} is constant (T-independent), we obtain just $T \propto a^{-1}$, where this is outcome can be recognised by other means: by noting that for radiation $\rho \propto a^{-4}$ and while $\rho \propto T^4$ the conventional relation $T \propto a^{-1}$ is informally justified.

2.7 Early universe puzzles

The SBB paradigm explains successfully the basic characteristics of the observed universe, such as the CMB, the BBN, etc.. However, for a deeper understanding of the early universe, there remain key conceptual riddles. From a more observational perspective, there are the astounding flatness and homogeneity of the universe; where the latter is also refer as the horizon problem; as well as the absence of monopoles and other topological defects produced during phase transitions in the early universe. I will briefly introduce some of them, for a more detailed discussion however, consult, for instance [41–44].

2.7.1 The horizon problem (or how is that the universe is very homogenous and isotropic on large scales)

The comoving spacetime region in which one point could affect or have been affected by other points, i.e. the comoving particle horizon (eq. (2.21)), is time-dependent:

$$\tau = \int_0^t \frac{dt'}{a(t')} = \int_0^a \frac{d\ln a'}{a'H(a')}\,, \tag{2.51}$$

where the factor $(aH)^{-1}$ is called the *comoving Hubble radius*; this represents the distance beyond which particles cannot communicate at a given time. Additionally, observations of the CMB indicate the existence of temperature correlations across distances throughout the sky; these photons randomly distributed have nearly the same temperature $T = 2.7255 \pm 0.00057\,\mathrm{K}$ [45]. Hence, at the time light decoupled from the rest of the energy components the observed near-homogeneity of the CMB tells us that the universe was quasi-homogeneous, which is a property of thermal equilibrium. However, if we think in simple terms, in a universe dominated by radiation or non-relativistic matter, the comoving particle horizon grows monotonically: $\tau \propto a\,(a^{1/2})$ for radiation (non-relativistic matter). Thus the evolution of the comoving particle horizon, on either matter content, suggests that structures on length scales entering the horizon today have never been in causal contact before, which contradicts the CMB quasi-homogeneity. Hence one must assume an extremely fine-tuned initial condition.

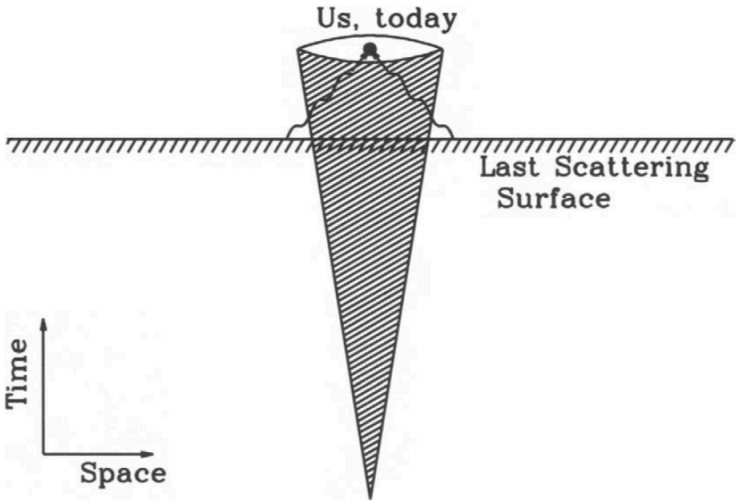

Figure 2.3: A sketch of the horizon problem. The region inside the cone at any time is causally connected to us (at the centre). Photons emitted from the last scattering surface (at redshift $z \sim 1000$) started outside of this region. Therefore, at the last scattering surface, they were not in causal contact with us and certainly not with each other. Yet their temperatures are almost identical. Source S. Dodelson [44]

2.7.2 The flatness problem (or why the total energy density of the universe is "critical")

As mentioned before, in GR the description of the geometry of the cosmos is related to its matter content; and if the total energy density of the universe takes the critical value ρ_c (eq. (2.10)) then the spatial geometry is flat (see eq. (2.12)). Indeed, observations show that the present universe is very nearly flat $\Omega(t_0) \sim \mathcal{O}(1)$ [10]. Hence, if the early universe was indeed flat, then it must remain so for all time. However, since the factor aH is a decreasing function of time during radiation or matter domination epochs, as given by eq. (2.20), therefore a flat curvature is an unstable circumstance:

$$|\Omega - 1| \propto t \qquad \text{radiation epoch} \tag{2.52}$$

$$|\Omega - 1| \propto t^{2/3} \qquad \text{non-relativistic matter epoch} \tag{2.53}$$

Indeed, even a tiny deviation from curvature zero would cause that Ω evolved quite differently and very quickly the universe would have become more curved. To explain the geometric flatness of space today therefore once again requires an extreme fine-tuning in the SBB.

2.7.3 The relic problem

This problem arises from the fact that many Grand Unified Theories[k] (GUTs) predict the existence of stable exotic particles and topological defects, that would have theoretically formed at very early stages of the universe under hot and highly energetic conditions. These particles would have been produced, in great abundance, due to the breaking of a number of fundamental symmetries, such as GUT symmetries. Thus, whilst the universe cooled below the corresponding critical temperatures these anomalies would persist until today. However, none of these peculiar relic has been detected. Moreover, among some cosmological anomalies, such as heavy strings or gravitinos, the most disseminated must be the production of a large number of magnetic monopoles. This multitude of monopoles would have yielded a substantial energy density, so the early universe would have been overloaded collapsing long before the present time; or else it would be dominated by magnetic monopoles, however, none has been found any yet whatsoever.

Even though the aforementioned shortcomings do not seem to have a satisfactory answer, but a rather extreme fine-tuning justification, there is an alternative solution to these issues that could well explain these puzzles of the early universe. Moreover, it provides a new framework with new and interesting predictions that have to be compared with observational data. Inflation raises its hand to answer these conundrums.

[k] To find a simple theory to describe the universe, several models in particle physics were suggested in order to unified three of the four forces presented in the Standard Model of Particle Physics (SM): strong force, weak and electro-magnetic force. These classes of theories are called Grand Unified Theories (GUTs) [46].

Chapter 3

Inflationary universe

> "Si Dios y la Humanidad son poderosos con lo que contienen, hasta el punto de que para ellos mismos todo está en todo, yo advierto que me falta a mí mucho menos todavía, y que no tengo que quejarme de mi "futilidad". Yo no soy nada en el sentido de vacío, pero soy la nada creadora, la nada de la que saco todo."
>
> —Max Stirner, El único y su propiedad

Some of the problems of the SBB cosmology require for their solution, a period of exceptionally rapid expansion or, equivalently, a dissolution of its contents. Brout et al. [47] showed that the horizon problem does not exist in the early stages of expanding de-Sitter space. In 1981 Alan Guth [48] pointed out that the early universe must have gone through a phase where the dynamic was the same as in an empty universe, but with large positive cosmological constant. Guth assumed an inflationary regime, in the early universe, which is well approximately by a de-Sitter solution and expands very quickly. If this happened so, the causal horizon in the universe today is much higher than that calculated by extrapolating FLRW back in time to the Big Bang. Interposing such expansion between us and the beginning of the universe, it reduces the curvature (flatness problem), and expansion of the region of space that could arise from a region causally connected (horizon problem and the problem of structure formation). Moreover, during this dramatic expansion, the density of the unwanted relics was diluted away; then with enough inflation this dilution guaranteed the particles stayed completely out of the observable scope, making quite difficult to localise even a single monopole (relic problem). Thus an inflationary scenario will be the one that period of exceptionally abrupt expansion of the early universe.

Inflationary cosmology [6] in any way does not replace the SBB cosmology, but rather it

is considered as a "supplement" which occurred at the early stages. Moreover, inflation is not forever, since the greatest achievements of the SBB cosmology, such as the BBN and the CMB require the standard progressive evolution of the era that mastered the radiation up to matter domination, then it is assumed that inflation must have finalised some considerable time before admitting the generation of the observed properties such as baryon-antibaryon asymmetry in the universe [49]. For an inflationary expansion of about a factor of 10^{26} the problems of the SBB cosmology can be overcome. Inflationary models easily manage this amount of expansion. Even as this paradigm solves the problems SBB cosmology has, one must ask if this is the true guideline for the origin and evolution of the universe. Therefore, we should turn the problem of defining the characteristics and the appropriate circumstances to the early universe, hoping to find under these conditions the components that lead to an inflationary scenario.

3.1 Solution of the SBB cosmology shortcomings

As mentioned before, inflationary cosmology is based on the hypothesis that the early universe expanded exponentially quickly for a fraction of a second. Let us see how this brief period of accelerated expansion solves the problems of the SBB cosmology.

First of all, to understand how inflation explains the near-homogeneity present in the CMB and the flatness problem, let us implement the concept of particle horizon τ and the comoving Hubble radius $(aH)^{-1}$. At a given time τ could have been much greater than $(aH)^{-1}$, hence the scales that are out of causal contact today may have been able to communicate in the past. Indeed, this could have happened if the comoving Hubble radius $(aH)^{-1}$ were decreasing, therefore it would have contributed more to the integral in τ. We can think that such a period is the early universe; then $(aH)^{-1}$ shrank drastically in early times contributing more to τ than late times. Thus, if thermal equilibrium was achieved throughout some small portion of the early universe before the comoving Hubble radius contracted far below the size of that domain, the whole observable universe would then be contained within one such region, explaining the remarkably homogeneity we observe today. Moreover, the flatness and relic problems are also settled down by a shrinking comoving Hubble radius. On one hand, note that the factor $|\Omega - 1| \propto (aH)^{-2}$, then if $(aH)^{-1}$ becomes small quite fast therefore Ω is driven towards the unity rather than away from it, hence the former shortcoming is explained. On the other hand, the density of the exotic particles was diluted away by the same contraction mechanism. Thus, the immense reduction of the comoving Hubble radius drives the universe towards flatness and dilutes the unwanted vestiges,

and also provides a very reasonable elucidation on the horizon problem (see fig. 3.1).

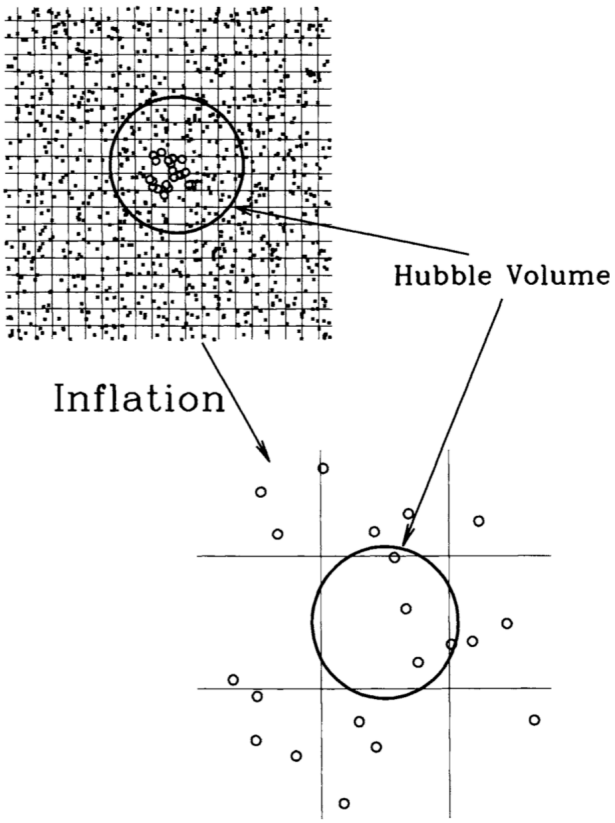

Figure 3.1: A sketch of the inflation mechanism solving the horizon problem. Particles on the comoving grid before (top) and after (bottom) inflation. Open circles are the same particles on top and bottom. Before inflation, the comoving Hubble radius was quite large, encompassing dozens of cells on the grid. After inflation, the comoving Hubble radius has shrunk to just one cell. (In this caricature, the scale factor has grown by a factor of order 7; during inflation the scale factor increases by greater than e^{60}.) The shrinkage of the comoving Hubble radius means that particles which were initially in causal contact with one another (within the large circle at top) can now no longer communicate. Note that the physical Hubble radius, depicted by large circles on the top and bottom grids, remains roughly constant during inflation. Source S. Dodelson [44]

In summary, in order to solve the aforementioned problems we must satisfy that:

$$\frac{d}{dt}(aH)^{-1} < 0 \quad \Longleftrightarrow \quad \frac{d^2a(t)}{dt^2} > 0 \quad \Longleftrightarrow \quad \rho + 3p < 0\,. \tag{3.1}$$

Demanding a shrinking comoving Hubble radius (see fig. 3.1) is therefore equivalent to accelerated expansion produced by a fluid with negative pressure $p < -\rho/3$. I will present in more detail above conditions. For now, inflation is precisely defined as the epoch of accelerated expansion in the early universe.

3.2 Cold inflation (CI)

In the standard inflation picture (CI), depicted by a homogeneous scalar "inflaton" field ϕ. Accelerated expansion occurs when the potential energy of the field, $V(\phi)$, dominates over its kinetic counterpart, $\dot{\phi}^2/2$. This mechanism to explain acceleration in the early universe is called single-field slow-roll (SFSR), since the field evolves slowly "enough", so that the potential energy dominates over its kinetic equivalent. In the following segments I will present the characteristics and the appropriate circumstances to the early universe, hoping to find under these conditions the components that lead to an inflationary scenario.

3.2.1 Single field inflation

In particle physics, a scalar field is used to represent particles with zero spin. In a homogeneous universe, the scalar field is only a function of time. The traditional starting point is the action, which is an integral of the Lagrangian density over space and time and which one can obtain the equations of motion. For a universe described by Einstein field equations whose material content consists of a scalar field and ordinary matter, the action is:

$$S = \int d^4x\sqrt{-g}\left(-\frac{R}{16\pi G} + g^{\mu\nu}\partial_\mu\phi\partial_\nu\phi - V(\phi) + \mathcal{L}_m\right), \tag{3.2}$$

where g is the determinant of the metric tensor, R is the curvature scalar (Ricci scalar), $\phi = \phi(x^\mu)$ is the scalar field, $V(\phi)$ is a potential and $\mathcal{L}_m$ is the Lagrangian density for any matter field. This is consistent because the Euler-Lagrange equations for this action give the Einstein equations:

$$G^{\mu\nu} \equiv R^{\mu\nu} - \frac{1}{2}g^{\mu\nu}R = 8\pi G T^{\mu\nu}, \tag{3.3}$$

where the stress-energy tensor is given in terms of the Lagrangian density by:

$$T^{\mu\nu} = -\frac{2}{\sqrt{-g}}\frac{\partial(\mathcal{L}_m\sqrt{-g})}{\partial g_{\mu\nu}} = -2\frac{\partial\mathcal{L}_m}{\partial g_{\mu\nu}} - g^{\mu\nu}\mathcal{L}_m\,. \tag{3.4}$$

The Lagrangian density of a minimally-coupled scalar field is given by:

$$\mathcal{L}_\phi = \frac{1}{2}\partial_\mu\phi\partial^\mu\phi - V(\phi)\,. \tag{3.5}$$

This is the usual *kinetic energy-potential energy* form in a homogeneous universe, and generalise the kinetic term to include gradient energy when there are perturbations. We can calculate the stress-energy tensor from eq. (3.4) as:

$$T^{\mu\nu} = -2\frac{\partial \mathcal{L}_m}{\partial g_{\mu\nu}} - g^{\mu\nu}\mathcal{L}_m = \partial^\mu\phi\partial^\nu\phi - g^{\mu\nu}\left(\frac{1}{2}\partial_\sigma\phi\partial^\sigma\phi - V\right), \tag{3.6}$$

or lowering an index yields:

$$T^\mu{}_\nu = g^{\mu\rho}\partial_\rho\phi\partial_\nu\phi - \delta^\mu{}_\nu\left(\frac{1}{2}\partial_\rho\phi\partial^\rho\phi - V\right), \tag{3.7}$$

In general $T^i{}_j$ can have off-diagonal components, corresponding to anisotropic stresses; T^0_i measures the heat flux, in the fluid context proportional to the fluid velocity. If we consider this scalar field behaves like a perfect fluid, then we can associate an energy density $\rho_\phi = T^0_0$ and pressure $T^i{}_j = -p_\phi\delta^i{}_j$ given as follows:

$$\rho_\phi = \frac{1}{2}\dot{\phi}^2 + V(\phi), \tag{3.8}$$

$$p_\phi = \frac{1}{2}\dot{\phi}^2 - V(\phi), \tag{3.9}$$

where $\dot{\phi}$ represents the derivative of the scalar field with respect to t. One may represent the first term as the kinetic energy and the second as the potential energy. The potential $V(\phi)$ can be thought in turn, as the configurational energy or binding energy, it measures how much energy is associated with a particular field value. Typically, as in all systems, scalar fields try to minimise these energies; however, an important factor allowing inflation to occur is that these scalar fields are not always very efficient to achieve this state of minimum energy.

In a given model one would specify the form for the potential $V(\phi)$, at least for some parameters that one would expect to measure (such as the effective mass, the force of interaction of the scalar field, etc.). However, we will see later how single field inflation models are indeed constrained by CMB data.

3.2.2 Equations of motion

The dynamic equations for a model described by a perfect fluid with a homogeneous and isotropic metric considering eqs. (3.8) and (3.9) are:

$$H^2 = \frac{1}{3M_P^2}\left[\rho + \frac{1}{2}\dot{\phi}^2 + V(\phi)\right], \tag{3.10}$$

$$\ddot{\phi} + 3H\dot{\phi} = -V_\phi\,. \tag{3.11}$$

where V_ϕ is the derivative of the potential energy with respect to the field, $M_P = 1/\sqrt{8\pi G}$ is the reduced Plank mass and the expansion rate $H = \dot{a}/a$. We have ignored the term of curvature k, since it is known that will quickly become negligible once inflation starts. The first one is called Friedmann constraint, and the second is the scalar field equation Klein-Gordon or the energy-momentum conservation equation, $\dot{\rho} = -3H(\rho + p)$. This is just the equation for a damped harmonic oscillator, with H being the damping term due to the expansion of the universe and the force given by $-V_\phi$. An analogous system would be a ball rolling on a hill with some friction, an analogy that is often used when describing inflation models. The shape of the hill is determined by the potential and the friction is determined by the expansion rate H. What generically happens is that if the field (ball) starts somewhere away from the minimum of the potential (up the hill) it will roll down towards the minimum.

Since general relativity ties the expansion of the universe to the energy in it, we now need to ask what type of energy can produce acceleration. We can get immediate answer if we appeal to the time-time and space-space components of the Einstein equations:

$$\frac{\ddot{a}}{a} = -\frac{1}{6M_P^2}(\rho + 3p)\,. \tag{3.12}$$

Acceleration is defined to mean that $\ddot{a}$ is positive. For this to happen, the terms in the parentheses on the right must be negative. Thus inflations requires:

$$p < -\frac{\rho}{3}\,. \tag{3.13}$$

Since the energy density is always positive, the pressure must be negative. Moreover, the scalar field carries most of the energy of the universe hence any other matter content must be subdominant, therefore inflation requires that $\rho \ll \rho_\phi$. Then in the cosmological case the universe inflates as the field (alone) is rolling down the hill. The

Friedmann equation becomes:

$$H^2 = \frac{1}{3M_P^2}\left[\frac{1}{2}\dot{\phi}^2 + V(\phi)\right], \tag{3.14}$$

which is nearly constant if the field is slowly rolling (so $\dot{\phi}^2 \ll V(\phi)$), corresponding to SFSR. Specifically we need to achieve $p < -\rho/3$. The potential energy therefore has to dominate the kinetic energy, and we can neglect $\dot{\phi}^2/2$ in the Friedmann eq. (3.14). Additionally, as $\dot{\phi}^2 \ll V(\phi)$ by differentiating this suggests the further condition $|\ \ddot{\phi}\ | \ll |\ V_\phi\ |$, however, note that derivatives of approximations need not themselves be valid approximations, and so this is an additional condition. Then we also neglect the $\ddot{\phi}$ term in the equation of motion eq. (3.11). Thus, these approximations are called the *slow-roll approximations*. They are not strictly required for inflation to take place, but they are consistent and simple. In summary we have in the SFSR scenario:

$$H^2 \simeq \frac{1}{3M_P^2}V\,, \tag{3.15}$$

$$3H\dot{\phi} \simeq -V_\phi\,. \tag{3.16}$$

An inflationary model is sometimes parametrised by expanding the potential in a Taylor series, i.e. in higher and higher derivatives of V. The first two so called slow-roll parameters:

$$\epsilon_\phi \equiv \frac{M_P^2}{2}\left(\frac{V_\phi}{V}\right)^2, \tag{3.17}$$

$$\eta_\phi \equiv M_P^2\frac{V_{\phi\phi}}{V}\,. \tag{3.18}$$

The first one measures the slope of the potential and the second one the curvature. In order for slow-roll to be self-consistent we therefore need that

$$\epsilon_\phi \ll 1 \qquad \text{and} \qquad |\eta_\phi| \ll 1\,. \tag{3.19}$$

In other words: the inflation potential needs to be very flat. To get a potential that is flat enough can be difficult in particle physics models. Unfortunately, although these are necessary are not sufficient, i.e., even if the potential is very flat, it may be that the scalar field has a great speed. Additionally, the slow-roll condition amounts to $|\eta_\phi| \lesssim 1$, which equivalently means the potential cannot have mass terms bigger than $\sim H^2\phi^2$. The "eta problem" arises when it becomes very difficult for a particular potential to preserve flatness at the level of $|\eta_\phi| \lesssim 1$, ruining the main requirement of particle physics, arising from the density perturbation (it will be well explained in the

section 3.3) and slow-roll conditions of inflation: a very flat potential. There is a more elaborate version of the slow-roll parameters, based on Hamilton-Jacobi formulation of inflation [50]. Essentially, this other scheme is governed by the evolution of the Hubble parameter rather than the potential energy density. If $H(\phi)$ is taken as the primary quantity, then there is a better choice of slow-roll parameters. The slow-roll parameters, ϵ_H and η_H, are [50]:

$$\epsilon_H = 2M_P^2 \left(\frac{H_\phi}{H}\right)^2 , \tag{3.20}$$

$$\eta_H = 2M_P^2 \frac{H_{\phi\phi}}{H} , \tag{3.21}$$

where $H_\phi = dH(\phi)/d\phi$. Above expression have a very useful set of properties which make them better choices to ϵ_ϕ and η_ϕ as descriptors of inflation, namely:

- They are exactly

$$\epsilon_H = 3\frac{\dot\phi^2/2}{\dot\phi^2/2 + V} \quad \left(= -\frac{d\ln H}{d\ln a} = -\frac{\dot H}{H^2}\right) , \tag{3.22}$$

$$\eta_H = -3\frac{\ddot\phi}{3H\dot\phi} \quad \left(= -\frac{d\ln \dot\phi}{d\ln a} = -\frac{d\ln H_\phi}{d\ln a}\right) . \tag{3.23}$$

- The condition for inflation to occur is precisely

$$\ddot a > 0 \Longleftrightarrow \epsilon_H < 1 . \tag{3.24}$$

  Hence the true endpoint of inflation occurs exactly at $\epsilon_H = 1$.

At least these two attributes illustrate the benefit of implementing the slow-roll parameters ϵ_H and η_H as an alternative description of inflation, contrary to the parameters V-dependant (eqs. (3.17,3.18)). However, in practice numerical calculations show the parameters ϵ_ϕ and η_ϕ to work well, and given a potential we can immediately identify regions upon it that can drive inflation. Henceforth, we will be using both versions of the slow-roll parameters, emphasising in the condition for inflation $\epsilon_H < 1$, and the termination of inflation exactly at $\epsilon_H = 1$.

3.2.3 Number of e-foldings

The amount by which the universe inflates is measured as the number of e-foldings N_e, and since the size of the expansion is expected to be an enormous quantity, it is useful

to compute it in terms of the logarithm of the ratio of the scale factor between the end of inflation and a time t during inflation defined by:

$$N_e \equiv \ln\left(\frac{a(t_{end})}{a(t)}\right) = \int_t^{t_{end}} dtH \simeq -\frac{1}{M_P^2}\int_\phi^{\phi_{end}} d\phi \frac{V}{V_\phi}\,, \tag{3.25}$$

where in the last step we have used the slow-roll eqs. (3.15) and (3.16). Typically between 40 and 60 e-foldings of observable inflation[a] are large enough to solve the horizon and flatness problems.

3.3 Cosmological perturbation theory: a brief description

Inflation has the ability to correlate scales in such a way that otherwise they would be disconnected. Previously, the zero-order scheme was introduced to ensure that the universe will be uniform on all scales of interest today. However, there are perturbations about this background scheme, and these fluctuations, created early on when the scales were causally connected, remain long after inflation has finalised.

First of all, perturbations around the FLRW universe can be described using GR, and they can be classified according to their transformation properties as *scalar*, *vector*, and *tensor*. Scalar perturbations correspond to variations in the density from point to point, and are often called density perturbations. Moreover, these scalar perturbations to the metric couple to energy density fluctuations, such as the density of matter and radiation, and ultimately they both are responsible for most of the inhomogeneities and anisotropies in the universe, thus they are the ones responsible for structure formation. Note that coordinate invariance in GR means that the same physical situation can be described in different ways, known as "gauges". For instance, we may consider curvature perturbations on surfaces of constant density, or density perturbations with respect to hypersurfaces of constant curvature. It is possible to work entirely with "gauge-invariant" quantities, but this is rather algebraically complicated, hence more commonly a fixed gauge (or combination of gauges) is used. Inflationary perturbations are commonly expressed in terms of the curvature perturbation in the flat slicing (uniform curvature) gauge. Then, there are vector perturbations, which are usually thought to be unimportant as they are not sourced in inflation models driven by a scalar field and would decay even if they were. In addition to scalar perturbations, though, inflation also generates tensor fluctuations in the gravitational metric, so-called

[a] CMB fluctuations, from the size of the observable universe down to the size of galaxies, were generated during ∼10 e-folds about 60 e-folds before the end of inflation.

gravity waves. These are not coupled to the density and so are not responsible for the large-scale structure of the universe, but they do induce fluctuations in the CMB. In fact, these fluctuations turn out to be a unique signature of inflation and offer the best window on the physics driving inflation, so they are clearly worthy of our study [b].

The basic picture is that quantum fluctuations during inflation are stretched beyond the horizon [c] (in causal contact with itself) by inflation, where we see them as classical fluctuations on scales larger than the horizon at the end of inflation. Hence, in order to compute the quantum fluctuations, we need to quantise the field. For both tensor and scalar perturbations, we have to devise an strategy so the problem (quantum fluctuations equations) resembles a simple harmonic oscillator. Once we achieve the aforementioned we move to a Fourier space since it is a powerful tool for analysing the stochastic properties of the perturbations. So we need to study the inflaton field at the quantum level to calculate the fluctuations produced and their power spectrum, which is a function of wavenumber k and indicates the typical size of perturbations on scale k, and then the subsequent evolution. For good reviews see for instance [42, 44, 52] .

3.3.1 Sub- and super-horizon perturbations

First of all, density perturbations can be described by linear perturbation theory, as long as these have low amplitude, and fluctuations on each comoving wavenumber evolve independently, i.e. perturbations are carried along with the expansion. Then, when dealing with these linear variations, one has to compare a perturbation's comoving wavenumber $k = 2\pi a/\lambda$, where λ is its physical wavelength, with the characteristic scale of an expanding universe, the horizon aH. Thus a comoving wavenumber k is at the Hubble scale if $k = aH$. Modes with k greater (smaller) than this are said to be inside (outside) the horizon.

Recall that for inflation to happen the precise condition is that the comoving Hubble radius $(aH)^{-1}$ is decreasing with time (see eq. (3.1)). Hence the typical history of a comoving scale during inflation is that it starts well inside the horizon, $k \gg aH$, and ends up far outside the horizon $k \ll aH$. The largest comoving scales exit the horizon first during inflation, and they are the last to come back to the horizon later during matter or radiation domination. Thus this process allows inflation to generate

[b] I will not discuss in much detail this point, since primordial gravity waves need a more exhaustive and formal study than I pretend to implement here. However, for a concise and well explained review of this matter see for instance [51]

[c] To save space and time (ba dum chhh!), in the cosmological jargon horizon refers to the inverse of the comoving Hubble radius.

fluctuations which appear to be on length scales much larger than the horizon size inferred from merely SBB cosmology. Habitually, one can study the behaviour in the two extreme regimes:

- Sub-horizon $k \gg aH$: if a perturbation is on scales much less than the Hubble ones, its behaviour should be independent of how the universe is expanding, since it will behave as if in flat space-time.
- Super-horizon $k \ll aH$: if a perturbation with a wavelength much larger than the horizon scale and causality prevents it from evolving, hence the behaviour is again independent of how the universe is expanding.

Hence in both limits the evolution of a perturbations is independent of how the universe expands, one can therefore deduce that any fluctuation should depend only on the way the universe is evolving during a brief epoch when $k_* \simeq a_* H_*$, known as *horizon crossing*. Hence we should expect that the ultimate amplitude of density perturbations can be written in terms of quantities evaluated at horizon crossing.

In summary, during inflation the universe expands exponentially and physical wavelengths grow faster than the horizon. Fluctuations are hence stretched outside of the horizon during inflation and re-enter the horizon in the late universe. Scales that are outside of the horizon at CMB decoupling were in fact inside the horizon before inflation. The region of space corresponding to the observable universe therefore was in thermal equilibrium before inflation and the uniformity of the CMB is given a causal explanation.

3.3.2 Scalar and tensorial (briefly) cosmological perturbations and observables

During inflation, the universe primarily is described by a smooth background metric and contains a uniform scalar field. Against this background, the fields fluctuate quantum mechanically. Moreover, scalar perturbations to the metric couple to energy density fluctuations, and these blended fields fluctuate together, so we have to implement a framework in order to compute how do the perturbations get transferred from the inflaton field ϕ to the scalar perturbations to the metric. Even though this correlation requires a bit of work to understand, the most important idea is that quantum mechanical fluctuations during inflation are responsible for the variations around the smooth background.

At any given time, the average fluctuation is zero, because there are regions in which the field is slightly larger than its nonzero vacuum expectation value and regions in which it is smaller. The average of the square of the fluctuations (the variance), however, is not zero. Looking ahead, once we know this variance, we can draw from a distribution with this variance to set the initial conditions.

We may split the inflaton field as:

$$\phi(\mathbf{x}, t) = \phi(t) + \delta\phi(\mathbf{x}, t)\,, \tag{3.26}$$

where ϕ is a classical field, that is, is the nonzero vacuum expectation value of the inflaton on the homogeneous and isotropic state, whereas $\delta\phi$ describes the quantum fluctuation around ϕ. Provided that inflation produces an exponential expansion, the horizon remains essentially constant while all other scales grow up, so we can focus on the evolution of the scalar quantum fluctuations in a small region compared to the horizon. Thus one can assume the space is locally flat and ignore the metric perturbations.

The evolution of the inflaton fluctuations $\delta\phi$ [d] by substituting into equation eq. (3.11), yielding:

$$\ddot{\delta\phi} + 3H\dot{\delta\phi} + V_{\phi\phi}\delta\phi - \frac{\nabla^2}{a^2}\delta\phi = 0\,. \tag{3.27}$$

Now, working in the Fourier space, above equation becomes:

$$\ddot{\delta\phi}_k + 3H\dot{\delta\phi}_k + \frac{k^2}{a^2}\delta\phi_k = 0\,, \tag{3.28}$$

note that $V_{\phi\phi}\delta\phi$ term is dropped since the scalar field is overdamped and slow rolling, therefore $V_{\phi\phi}^{1/2} \simeq m_\phi \ll H$. Eq. (3.28) represents the equation of motion for a simple harmonic oscillator with a time-dependent frequency k/a [e] and a friction term $3H$ due to the expansion. Moreover, in Fourier space the modes evolve independently, this essentially implies that perturbations generated by vacuum fluctuations have uncorrelated Fourier modes, i.e. the signature of *Gaussian perturbations*. We introduce the comoving variable $\psi_k(t) = a(t)\delta\phi_k(t)$, hence eq. (3.28) becomes:

$$\ddot{\psi}_k + H\dot{\psi}_k + \frac{k^2}{a^2}\left(1 - \frac{2a^2H^2}{k^2}\right)\psi_k = 0\,, \tag{3.29}$$

[d] Note that we assumed that $\delta\phi$ is linear, this hypothesis is equivalent to the neglect of any interaction between $\delta\phi$ and other field.

[e] The time dependence arises because of the stretching of the wavelength of a comoving Fourier mode.

where we have taken H as constant[f] since in slow-roll regime this varies slowly. A more helpful form will be implementing the conformal time or proper time τ (eq. (2.51)) or $dt = ad\tau$, moreover, a simple relation between the conformal time τ and the expansion rate holds. In particular, during inflation:

$$\tau = \int_0^a \frac{da}{Ha^2} \simeq \frac{1}{H}\int_0^a \frac{da}{a^2} \simeq -\frac{1}{aH}\,, \tag{3.30}$$

the evolution of Fourier modes ψ_k in conformal time reduces to:

$$\psi_k'' + k^2\left(1 - \frac{2}{k^2\tau^2}\right)\psi_k = 0\,, \tag{3.31}$$

where prime is the derivative with respect to τ. As mentioned before, we want to quantise the fluctuations, so we move to the quantum world and make the corresponding associations of operators to classical variables, we implement the annihilation $\hat{a}$ and creation $\hat{a}^\dagger$ operators. Analogous to the prescription upon quantisation of a simple harmonic oscillator, the quantum dynamics will be determined by [42, 52]:

$$\hat{\psi}_k(\tau) = \psi_k(\tau)\hat{a}(k) + \psi^*_{-k}(\tau)a^\dagger(-k)\,, \qquad \psi_k(\tau) = \frac{e^{-ik\tau}}{\sqrt{2k}}\left(1 - \frac{i}{k\tau}\right)\,, \tag{3.32}$$

where $\psi_k(\tau)$ is precisely the solution of eq. (3.31) called Bunch-Davies mode function. Note that in fact eq. (3.31) must have two independent solutions, however, by considering particular boundary conditions that I will enunciate in the next sentences, these yield a unique expression eq. (3.32). First, the inflationary regime dilutes all possible particles existing before this period, hence the ground state of the system is given by the vacuum; in other words, we must have:

$$\hat{a}_k|0\rangle = 0\,, \tag{3.33}$$

hence this corresponds to specifying the first boundary conditions for $\psi_k(\tau)$. Additionally, the (complex) mode function $\psi_k(\tau)$ at very early times before inflation has done most of its work, hence all comoving scales were deep inside the horizon ($k \gg aH$); therefore one can select the Minkowski vacuum of a comoving observer in the far past $\tau \to -\infty$ or equivalently $|k\tau| \gg 1$. Thus the initial amplitude of the mode function is:

$$\lim_{\tau\to-\infty}\psi_k(\tau) = \frac{e^{-ik\tau}}{\sqrt{2k}}\,. \tag{3.34}$$

We come back to our original variable but already quantised $\delta\hat{\phi}_k$, then compute the

[f] Recall previous chapter the solution de-Sitter, which corresponds to an exponential scale factor, i.e. an appropriate candidate for an accelerated expansion.

two point correlation function (variance):

$$\begin{aligned}\langle\hat{\delta\phi}_k^\dagger\hat{\delta\phi}_{k'}\rangle &= (2\pi)^3\delta(\mathbf{k}-\mathbf{k}')\frac{|\psi_k(\tau)|^2}{a^2} \\ &\equiv (2\pi)^3\delta(\mathbf{k}-\mathbf{k}')\Delta_\phi^2\frac{2\pi^2}{k^3}\,, \qquad\qquad \Delta_\phi^2 \equiv \frac{|\psi_k(\tau)|^2}{a^2}\frac{k^3}{2\pi^2}\,, \end{aligned} \tag{3.35}$$

where the second line defines the *scalar field power spectrum*, Δ_ϕ^2; moreover, the Dirac's delta distribution guarantees that modes relative to different wave-numbers are uncorrelated in order to preserve homogeneity. Note that the factors k^{-3} is added so that the power spectrum is dimensionless and $2\pi^2$ so to be in concordance with the most popular one in the early universe community. As I mentioned before, the typical history of a comoving scale during inflation is that it starts well inside the horizon and ends up far outside the horizon ($|k\tau| \ll 1$), hence from eq. (3.34) we have at leading order:

$$\begin{aligned}|\psi_k(\tau)|^2 &\simeq \frac{1}{2k}\left[\left(1-\frac{i}{k\tau}\right)\left(1+\frac{i}{k\tau}\right)\right] = \frac{k^2\tau^2+1}{2k^3\tau^2} \simeq \frac{1}{2k^3\tau^2} \\ &\simeq \frac{a^2H^2}{2k^3}\,, \end{aligned} \tag{3.36}$$

therefore the scalar field power spectrum becomes:

$$\Delta_\phi^2 = \left(\frac{H}{2\pi}\right)^2\,. \tag{3.37}$$

As we mentioned previously the dynamics of the spacetime metric are related, by the Einstein equations, to the energy content of the universe, quantum fluctuations of the inflaton induce perturbations in the metric. Following the gauge-ready formalism for cosmological perturbations by Hwang and Noh [53], the spacetime metric for a scalar-type of perturbation is given by:

$$ds^2 = -a^2(1+2\alpha)d\eta^2 - 2a^2\beta_{,i}\,d\eta\,dx^i + a^2\left[\delta_{ij}(1+2\varphi) + 2\gamma_{,i|j}\right]dx^i dx^j\,, \tag{3.38}$$

where α, β, γ and φ are spacetime-dependent perturbed-order variables. Also a vertical bar | indicates a covariant derivative based on the 3-dimensional spatial background metric δ_{ij}. Although, at first sight both sources of fluctuations are indeed mixed, we can use a gauge-invariant variable in which these perturbations decouple. We work in the gauge-invariant comoving curvature perturbation (*primordial curvature perturbation*) at linear order:

$$\mathcal{R} \equiv \varphi + \frac{H}{\dot{\phi}}\delta\phi\,, \tag{3.39}$$

which is related to the scalar field perturbation $\delta\phi$, and it has the property to be

constant within few Hubble times after the horizon crossing ($k_* = a_* H_*$), therefore we can compute it at horizon exit and remain ignorant about the subhorizon physics during and after reheating until horizon re-entry of a given $\mathcal{R}$-mode [g]. Consider a gauge with spatially flat slicing $\varphi = 0$, then the curvature perturbation becomes:

$$\mathcal{R} = \frac{H}{\dot{\phi}} \delta\phi \,. \tag{3.40}$$

The power spectrum of $\mathcal{R}$ and the power spectrum of inflaton fluctuations are related as follows:

$$\begin{aligned} \langle \mathcal{R}_k \mathcal{R}_{k'} \rangle &= \left(\frac{H}{\dot{\phi}}\right)^2 \langle \hat{\delta\phi}_k^\dagger \hat{\delta\phi}_{k'} \rangle \\ &= (2\pi)^3 \delta(\mathbf{k} - \mathbf{k}') \Delta_\phi^2 \frac{2\pi^2}{k^3} \left(\frac{H}{\dot{\phi}}\right)^2 \\ &= (2\pi)^3 \delta(\mathbf{k} - \mathbf{k}') \Delta_{\mathcal{R}}^2 \frac{2\pi^2}{k^3} \,, \qquad \Delta_{\mathcal{R}}^2 \equiv \Delta_\phi^2 \left(\frac{H}{\dot{\phi}}\right)^2 \,, \end{aligned} \tag{3.41}$$

therefore the *primordial curvature power spectrum* is:

$$\Delta_{\mathcal{R}}^2 = \left(\frac{H_*}{\dot{\phi}_*}\right)^2 \left(\frac{H_*}{2\pi}\right)^2 \,, \tag{3.42}$$

where the relevant scales are evaluated at horizon crossing $k_* = a_* H_*$. Before I proceed, let me discuss an important characteristic of inflaton fluctuations. Single field inflation produces purely *adiabatic* primordial density perturbations characterised by an overall curvature perturbations, $\mathcal{R}$, if the inflaton field then upon decay its fluctuations are transferred evenly to all the degrees of freedom it decays into with $\delta(n_m/n_r) = 0$, or

$$\frac{\delta\rho_r}{\rho_r} = \frac{4}{3} \frac{\delta\rho_m}{\rho_m} \,, \tag{3.43}$$

where the index m collectively stands for non-relativistic species (baryons or cold dark matter (CDM)) and r for relativistic components (photons or neutrinos); and the relative factor 4/3 takes into account the different scaling behaviours of relativistic and non-relativistic matter. Thus the adiabaticity property implies that all perturbations of the cosmological fluid (photons, neutrinos, baryons and CDM particles) originate from the same curvature perturbation $\mathcal{R}$. Remarkably the latest observational data shows no violation of the adiabaticity condition (eq. (3.43)) [10]. The power spectrum of the adiabatic perturbations is measured from CMB observations and Planck Legacy provides the value $\Delta_{\mathcal{R}}^2 \simeq 2.2 \times 10^{-9}$ [10].

[g] $\mathcal{R}$ becomes constant on super-horizon scales; perturbations with comoving wave number k are said to "freeze in" as soon as the comoving Hubble horizon shrinks so far that $k^{-1} > (aH)^{-1}$.

On the other hand, the creation of primordial gravitational waves corresponds to the tensor part of the metric perturbation (for more details see [42, 44, 52]). Essentially in Fourier space, tensor perturbations can be expressed as the superposition of two polarisation modes: h_+ and $h_\times$, where $+$, $\times$ represent the longitudinal and transverse modes respectively. Taking the results of the scalar perturbations, each $h_{+,\times}$ has a *tensor power spectrum* Δ_h^2, which corresponds for h_+ and $h_\times$ separately; these are uncorrelated, so the power spectrum for all modes must be multiplied by a factor of 2, yielding:

$$\Delta_t^2 = 2\Delta_h^2 = \frac{2}{\pi^2}\frac{H_*^2}{M_P^2}\,, \tag{3.44}$$

In summary, adiabatic perturbations "freeze out" once they exit the horizon, they become super-horizon scales remaining unaltered until horizon re-entry. Fluctuations which were super-horizon now return within the horizon and commence to evolve once again under by the influence of causal processes (see fig. 3.2).

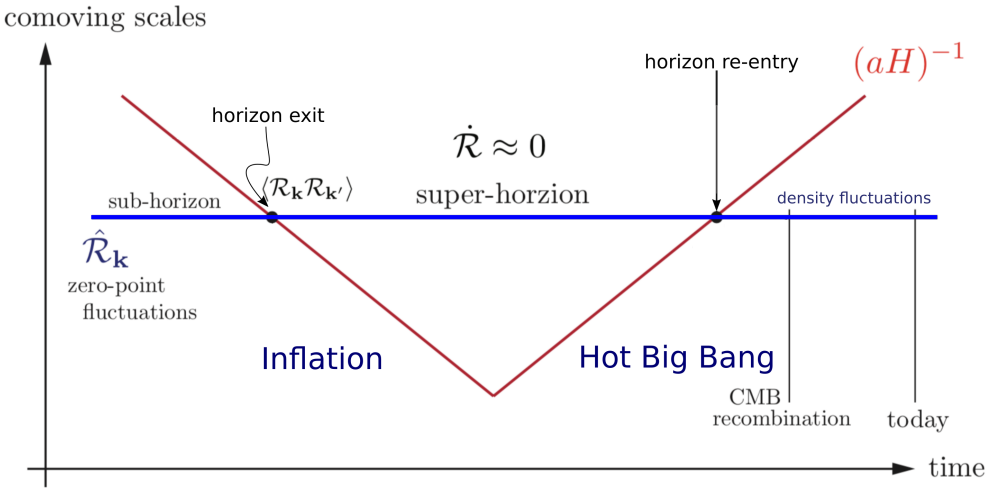

Figure 3.2: Creation and evolution of perturbations in the inflationary universe. Fluctuations are created quantum mechanically on sub-horizon scales. While comoving scales, k^{-1}, remain constant the comoving Hubble radius during inflation, $(aH)^{-1}$, shrinks and the perturbations exit the horizon. Causal physics cannot act on super-horizon perturbations and they freeze until horizon re-entry at late times. Source D. Baumann [42]

Even though we have taken the Hubble parameter as constant for the whole inflationary evolution, roughly speaking it is not entirely constant but slowly decreasing with the evolution of the inflaton. Hence this yields a mild deviation from scale-invariance. This slight departure from invariability of scale can be parametrised by:

$$\Delta_{\mathcal{R}}^2 = A_s(k_\star)\left(\frac{k}{k_\star}\right)^{n_s-1}\,, \qquad \Delta_t^2 = A_t(k_\star)\left(\frac{k}{k_\star}\right)^{n_t}\,, \tag{3.45}$$

where A_s, A_t are the scalar and tensor amplitudes measured at some pivot scale $k_\star$ [h] and the *spectral indices* n_s and n_t contain the scale dependency:

$$n_s - 1 \equiv \frac{d \ln \Delta^2_{\mathcal{R}}}{d \ln k} \,, \qquad n_t \equiv \frac{d \ln \Delta^2_t}{d \ln k} \,. \tag{3.46}$$

A scale-invariant spectrum, called Harrison-Zel'dovich (HZ), has constant variance on all length scales and it is characterised by $n_s = 1$. Subsequent evolution will modify the spectrum from its initial form. A small deviation from scale-invariance may also consider as a representative signature of the inflationary scenarios. In simple terms the spectral indices n_s and n_t can be expressed by means of the slow-roll parameters ϵ_V and η_V, to leading order, as:

$$n_s - 1 \simeq 2\eta_{\phi_*} - 6\epsilon_{\phi_*} \,, \qquad n_t \simeq -2\epsilon_{\phi_*} \,. \tag{3.47}$$

A convenient quantity for differentiating between inflationary models is the *tensor-to-scalar ratio* r; where in the slow-roll approximation yields:

$$r \equiv \frac{\Delta^2_t}{\Delta^2_{\mathcal{R}}} \simeq 16\epsilon_{\phi_*} \,. \tag{3.48}$$

An important immediate outcome arises since $\Delta^2_{\mathcal{R}}$ and $\Delta^2_t \propto H^2 \approx V$, hence r is a direct measure of the energy scale of inflation:

$$V^{1/4} \sim \Big(\frac{r}{0.01}\Big)^{1/4} 10^{16} GeV \,, \tag{3.49}$$

hence for values of the tensor-to-scalar ratio $r \geq 0.01$, inflation may occur at GUT scale energies.

3.4 Study of different inflaton potentials

The dynamics of the inflaton field, from the time when CMB fluctuations were created at ϕ_* to the end of inflation at ϕ_{end}, is determined by the shape of the inflationary driven potential $V(\phi)$. Distinct $V(\phi)$'s profiles can be categorised by determining whether they allow the inflaton field to move over a large or small distance $\Delta\phi = \phi_* - \phi_{end}$, as measured in Planck units. In *large-field* models the inflaton field starts at a large field values and then evolves to a minimum at the origin $\phi = 0$. Additionally, if the field evolution is super-Planckian, $\Delta\phi > M_P$, the gravitational waves produced by inflation

[h] For instance, the pivot scale for Planck survey is $k_\star = 0.05 \mathrm{Mpc}^{-1}$ [10], which is a specific physical scale in the present universe.

should be observed in the near future. The archetypal large-field scenario is chaotic inflation where a single monomial term dominates the potential (see fig. 3.3):

$$V(\phi) = \lambda_p \phi^p \,, \tag{3.50}$$

We will see next that for such a potential the slow-roll parameters are small, although, the coupling constant λ_p is independent of them. However, to arrange for a small amplitude of density fluctuations, Δ_R^2, the inflaton self-coupling has to be very small. This condition automatically guarantees that the potential energy (density) is sub-Planckian, $V \ll M_P^4$, and quantum gravity effects are not necessarily important. We will illustrate this fact subsequently.

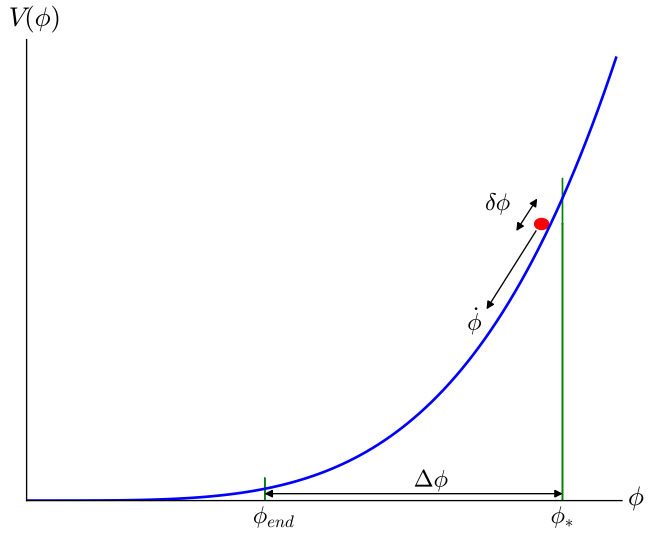

Figure 3.3: Large-field inflation. In an important class of inflationary models the inflationary dynamics is motivated by a mass-like potential, which can be illustrated as a monomial term in the potential, $V(\phi) \propto \phi^p$. In these models the inflaton field evolves over a super-Planckian range during inflation, $\Delta\phi > M_P$, and a large amplitude of gravitational waves is produced by quantum mechanical fluctuations.

On the other hand in *small-field* models the field evolution is sub-Planckian, $\Delta\phi < M_P$. The potentials that give rise to such small-field evolution often arise in mechanisms of spontaneous symmetry breaking, where the field rolls off an unstable equilibrium toward a displaced vacuum. A simple example is the Higgs-like potential (see fig. 3.4):

$$V(\phi) = \frac{\lambda}{4}\left(\phi^2 - v^2\right)^2 \,. \tag{3.51}$$

Generally, small-field models can be locally approximated by the expansion:

$$V(\phi) = \frac{\lambda v^4}{4}\left(1 - \left(\frac{\phi}{v}\right)^2\right)^2 + \cdots , \tag{3.52}$$

where the dots represent higher-order terms that may become important near the end of inflation and during reheating. Historically, a famous inflationary potential is the Coleman-Weinberg potential [54, 55]:

$$V(\phi) = V_0\left[\left(\frac{\phi}{v}\right)^2\left(\ln\left(\frac{\phi}{v}\right) - \frac{1}{4}\right) + \frac{1}{4}\right] , \tag{3.53}$$

which arises as the potential for radiatively-induced symmetry breaking in electroweak and grand unified theories. I will present later the current observational status of inflation.

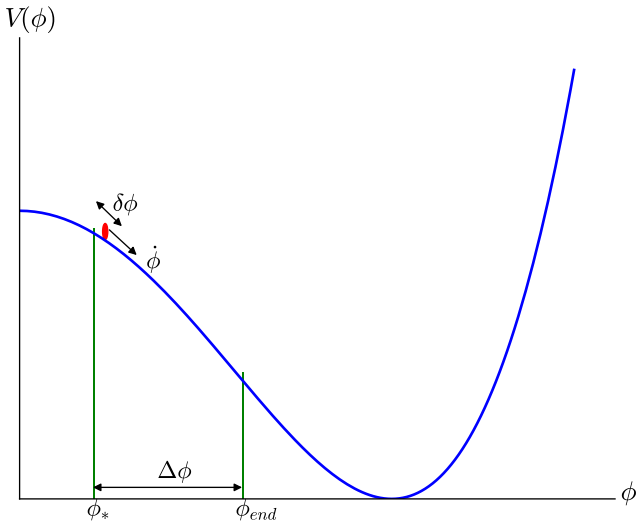

Figure 3.4: Small-field inflation. Inflation occurs in the "hilltop" part of the potential. In small-field models the field moves over a small (sub-Planckian) distance: $\Delta\phi < M_P$. This is relevant for future observations because small-field models predict that the amplitude of the gravitational waves produced during inflation is too small to be detected.

3.4.1 Inflation with a chaotic quartic potential

In this section I analyse the inflationary dynamics of a large field value monomial potential of the form:

$$V(\phi) = \frac{\lambda}{4}\phi^4 . \tag{3.54}$$

For this potential, the slow-roll parameters are given by:

$$\epsilon_\phi = 8\frac{M_P^2}{\phi^2}\,, \quad \eta_\phi = 12\frac{M_P^2}{\phi^2}\,. \tag{3.55}$$

Then the number of e-folds of inflation after the present CMB scales become super-horizon at a field value ϕ_* is given by:

$$N_e = \frac{\phi_*^2 - \phi_{end}^2}{8M_P^2}\,, \tag{3.56}$$

where ϕ_{end} is the final field value that corresponds to the smallest field value for which $\epsilon_\phi = 1$. So at the end of inflation we have $\phi_{end} = 2\sqrt{2}M_P$. Moreover, we can compute the inflaton value at horizon crossing:

$$\phi_* = 2\sqrt{2(N_e+1)}M_P\,, \tag{3.57}$$

we have that at 50-60 e-folds before the end of inflation we have $\phi_*/M_P \simeq \{20, 22\}$, respectively. Note that these large field values yield super-Planckian outcome. To satisfy the normalisation of scalar fluctuations, $\Delta_R^2 \simeq 2.2\times10^{-9}$ [10], we need to fix the self-coupling λ at 50-60 e-folds before the end of inflation. Then λ can be computed by:

$$\lambda = \frac{3\pi^2}{2}\frac{\Delta_R^2}{(N_e+1)^3}\,, \tag{3.58}$$

hence the coupling $\lambda \sim 10^{-13}$. Although the inflaton field is super-Planckian, the inflation driven potential is much smaller than the Planck mass at horizon crossing: $9.6\times10^{-3} \lesssim V^{1/4}/M_P \lesssim 1.0\times10^{-2}$, where the minimum and the maximum values correspond to 60 and 50 e-folds. The scalar spectral index n_s and the tensor-to-scalar ratio r evaluated at CMB scales are:

$$n_s = 1 - \frac{3}{N_e+1}\,, \quad r = \frac{16}{N_e+1}\,, \tag{3.59}$$

hence at 50 e-folds $n_s \simeq 0.9412$ and $r \simeq 0.3137$, and at 60 e-folds $n_s \simeq 0.9508$ and $r \simeq 0.2623$. We will see next that these upshot are not consistent with present observational constraints.

3.4.2 Inflation with a Higgs-like potential

In this section I analyse the inflationary dynamics of a small field value Higgs-like "mexican hat" inflaton potential of the form:

$$V(\phi) = \frac{\lambda}{4}\left(\phi^2 - v^2\right)^2 , \tag{3.60}$$

with inflation occurring in the "hilltop" part of the potential. For this potential, the slow-roll parameters are given by:

$$\epsilon_\phi = 8\left(\frac{M_P}{v}\right)^2 \frac{x^2}{(1-x^2)^2} , \quad \eta_\phi = -4\left(\frac{M_P}{v}\right)^2 \frac{1-3x^2}{(1-x^2)^2} , \tag{3.61}$$

where $x = \phi/v$. From above expression we immediately see that this potential suffers from an "eta problem" and cannot sustain a sufficiently long period of inflation for $v < 2M_P$ even if the field is initially very close to the origin. We thus expect a successful period of inflation to occur only for super-planckian values of v. This is similar to chaotic inflation models, where the slow- roll conditions are only satisfied for super-planckian field values, but in this case inflation may actually occur for sub-planckian field values, the condition $v \gtrsim 2M_P$ being essentially a condition on the curvature of the potential near the origin [56].

Then the number of e-folds of inflation after the present CMB scales become super-horizon at a field value ϕ_* is given by:

$$N_e = \frac{v^2}{8M_P^2}\left[\ln\left(\frac{x_{end}^2}{x_*^2}\right) + x_*^2 - x_{end}^2\right] , \tag{3.62}$$

where $x_{end}(\phi_{end})$ corresponds to field value for which $\epsilon_\phi = 1$. So at the end of inflation we have:

$$x_{end} = -\frac{\sqrt{2}M_P}{v} \pm \sqrt{\frac{2M_P^2}{v^2} + 1} . \tag{3.63}$$

From above expression one can find (numerically) the inflaton value at horizon crossing $x_*(\phi_*)$. Then, the scalar spectral index n_s and the tensor-to-scalar ratio r evaluated at CMB scales are:

$$n_s = 1 - 8\left(\frac{M_P}{v}\right)^2 \frac{1+3x_*^2}{(1-x_*^2)^2} , \quad r = 128\left(\frac{M_P}{v}\right)^2 \frac{x_*^2}{(1-x_*^2)^2} . \tag{3.64}$$

Typically the model is only in agreement with observations for $15M_P \lesssim v \lesssim 40M_P$, which corresponds to the regime where the observable e-folds of inflation occur for super-planckian field values [56]. For instance, for $v = 20M_P$ at 60 (50) e-folds we have

$x_* = 0.34(0.38)$, hence $n_s = 0.9655(0.9610)$ and $r = 0.047(0.064)$. As expected these outcome agree remarkably with Planck Legacy [10].

In summary, the dynamics of the inflaton field is determined by the shape of the inflationary driven potential $V(\phi)$. Distinct $V(\phi)$'s profiles can be categorised by determining whether they allow the inflaton field to move over a large or small distance $\Delta\phi = \phi_* - \phi_{end}$, as measured in Planck units. However, large-field models are more disfavoured by observations; on the other hand small-field values are in better agreement with most recent Planck data [10]. I will present the current $n_s - r$ constraints in fig. 3.5.

3.5 Observational Status of Inflation

The CMB remains as the main source of observational evidence for early cosmology. If inflation were to be true, the temperature fluctuations we observe in the CMB were seeded by the density perturbations created during this short but remarkably important period; therefore their properties are a pivotal tool for scrutinising the distant physics of inflation. Hence, inflation has the ability to drive quantum fluctuations outside the Hubble radius, where they become classical perturbations in the gravitational potentials and density of the universe [52]. Planck has dramatically improved upon this early legacy by firmly establishing essentially all of the major predictions of inflation (amongst others): a spatially flat universe $\Omega_k = 0.0007 \pm 0.0037$, with a nearly scale-invariant (red) spectrum of density perturbations $n_s = 0.9649 \pm 0.0042$, which is almost a power law $dn_s/d\ln k = -0.0045 \pm 0.0067$, dominated by scalar perturbations $r_{0.002} < 0.064$ [10].

Overall Planck provides very strong support for the inflationary paradigm, and at the same time tightly constrains the space of allowed inflationary models (fig. 3.5). The consistency of these predictions with all current cosmological data suggests that inflation is an idea that should be taken seriously and studied further.

Even though, CI offers a sufficient explanation for most of the current observational data, this paradigm is highly enhanced by including dissipation into it. For instance, in warm inflation scalar perturbations are predominantly produced by thermal, not quantum nature, and their spectrum is measurably different, as I will describe in section 4.2. This indeed may explain the nature of the classical inhomogeneities observed in the CMB, since fluctuations are thermally induced, hence classical by definition, therefore there is no need to explain the quantum-to-classical transition process, due to the purely quantum origin of the CI density perturbations. Although, thermal

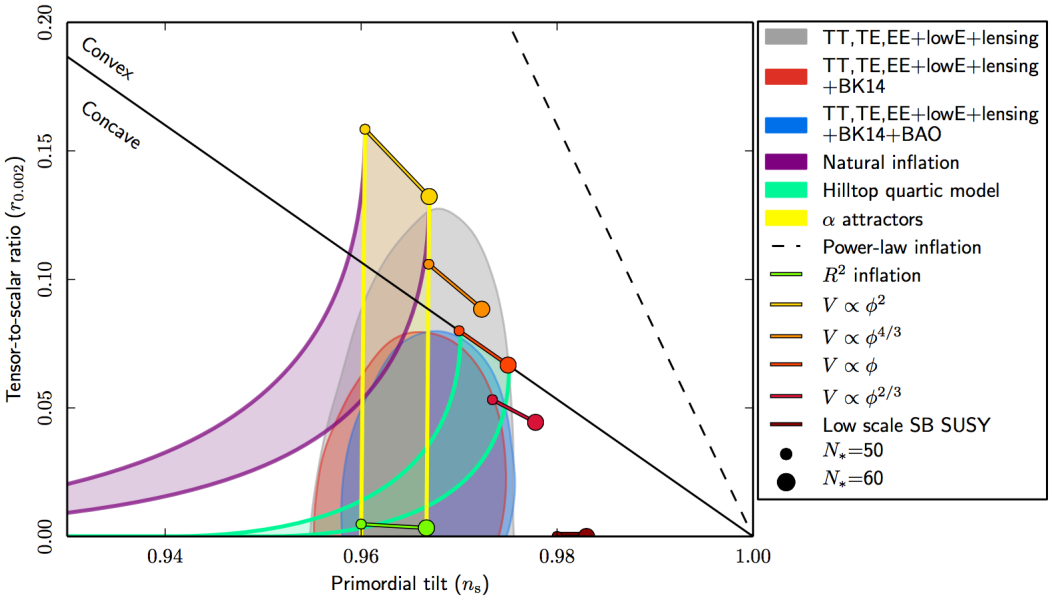

Figure 3.5: Limits on the tensor-to-scalar ratio, $r_{0.002}$ as a function of n_s at 95% CL, from Planck alone (grey area) or including BICEP2/Keck data 2014 (red) and BAO (blue). Constraints assume negligible running of the inflationary consistency relation ($dn_s/d\ln k = 0$) and the lines show the predictions of a number of models as a function of the number of e-folds, $N_* = N_{e*}$, till the end of inflation. Source Planck Legacy [57].

fluctuations generically increase the amplitude of scalar perturbations compared to quantum fluctuations alone, the tensor contribution remains unchanged. As a result, the tensor-to-scalar ratio is suppressed. These new features can bring some of the models that are already ruled out by $n_s - r$ constraints in the CI paradigm back into agreement with the data. For instance, inflation with a quartic chaotic is in good agreement with Planck data if one includes a dissipation mechanism [23, 58].

3.6 An unfinished story: the cold inflationary universe has to reheat

The quasi-exponential expansion driven by a scalar field brought the inflationary universe to a very cold and empty place, and during this period any other energy content was completely subdominant. However, once inflation ended, the cosmos needed to reheat and "repopulated" with at least the Standard Model (SM) degrees of freedom. Thus there must have existed a mechanism able of transfer the vacuum energy of the inflaton into the SM constituents. Hence this procedure may require the inflaton to couple with other degrees of freedom, in order to the decay of the inflaton condensate

can act as the *reheating* mechanism. Therefore, any efficient model of inflation needs to explain this transition from the vacuum- to the radiation-dominated universe. Indeed, this reheating machinery is an important application of the quantum theory of particle creation [59, 60]. Essentially, at the end of inflation the inflaton began to oscillate near the minimum of its effective potential. This generated two effects[i]: first the inflaton decayed into relativistic particles [59–63] and second the early universe returned to a radiation-dominated phase. The second stage is characterised by thermal equilibrium with some temperature T_{reh}, which was called the *reheating temperature*.

The first models of reheating are based on the assumption that after inflation ends the inflaton ϕ may decay into bosons χ and fermions ψ due to the interactions $-g^2\sigma\phi\chi^2$ and $-h\bar{\psi}\psi\phi$, where g and h are small coupling constants and σ has dimensions of mass [60]. This classical oscillating scalar field ϕ can be represented as a collection of these scalar (fermion) particles at rest, in which individual inflaton particles were assumed to decay independently of each other, and reheating was studied as a perturbative process [62]. Moreover, it is assumed for simplicity that the bare masses of the fields χ and ψ are very small, so that one can write $m_\chi = g\phi\,, m_\psi = |h\phi|$. Then, the decay rates of the processes $\phi \to \chi\chi$ and $\phi \to \bar{\psi}\psi$ (for $m_\phi \gg 2m_\chi, 2m_\psi$) are given by [60]:

$$\Gamma(\phi \to \chi\chi) = \frac{g^4\sigma^2}{8\pi m_\phi}\,, \qquad \Gamma(\phi \to \bar{\psi}\psi) = \frac{h^2 m_\phi}{8\pi}\,. \tag{3.65}$$

As mentioned before, once inflation ends the inflaton field becomes underdamped with $m_\phi \gg H$ and begins to oscillate about the minimum of its potential with a frequency $\omega^2 = V_{\phi\phi} = m_\phi^2$. This perturbative process is usually modelled by including a phenomenological reheating term, $\Gamma\dot{\phi}$ (a friction term), into the background equation of motion:

$$\ddot{\phi} + 3H\dot{\phi} + \Gamma_{tot}\dot{\phi} + V_\phi = 0\,, \tag{3.66}$$

where total decay rate is $\Gamma_{tot} = \Gamma(\phi \to \chi\chi) + \Gamma(\phi \to \bar{\psi}\psi)$. This extra term in the equation of motion essentially describes the loss of the vacuum energy due to the oscillating inflaton field and the creation of relativistic particles at this reheating stage. Reheating finalises when the Hubble parameter becomes smaller than the total decay rate Γ_{tot}, i.e. as soon as $\Gamma_{tot} \simeq H$ the decay products from these processes can reach thermal equilibrium. At this point, the energy density is dominated by relativistic constituents, hence $H^2 \simeq \rho/(3M_P^2)$ and $\rho = g_*\pi^2 T^4/30$, where g_* is the effective number

[i] In fact authors in [60] described the process of reheating in three different stages, the first one they called it *pre-heating*, which is essentially an extremely rapidly (explosively) process where the classical coherently oscillating inflaton field ϕ decays into massive bosons (in particular, into ϕ-particles) due to parametric resonance. They did this differentiation in order to distinguish this stage from the stage of particle decay and thermalisation.

of relativistic degrees of freedom, of order 10^2 for the SM; one can estimate the reheating temperature at the end of the thermalisation process, yielding:

$$T_{reh} \simeq \left(\frac{90}{\pi^2 g_*}\right)^{1/4} \sqrt{\Gamma_{tot} M_P}\,. \tag{3.67}$$

Note that T_{reh} does not depend on the initial value of the field ϕ, it is completely determined by the parameters of the underlying elementary particle theory via the decay rate Γ_{tot}. However, in order to get numerical estimates for the decay rate of the inflaton field and for the reheating temperature T_{reh}, one should know the mass of the inflaton field and the coupling constants. Since this reheating framework is based from perturbation theory [62], the coupling constants cannot be too large, otherwise the radiative corrections alter the shape of the inflaton potential. Besides, one has to consider the condition for the decay of inflaton oscillations is $\omega \gg 2m_\chi, 2m_\psi$ ($m_\phi \gg 2m_\chi, 2m_\psi$). And the parameters of the inflaton potential are restricted from the constraints on amplitude of the cosmological fluctuations (eq. (3.42)). Hence, by considering all the aforementioned conditions the largest possible total decay rate in perturbation theory is $\Gamma_{tot} < 10^{-20} M_P$ [64]. At the relativistic limit $g_* = 106.75$ and by taking $\Gamma_{tot} \simeq 9.9 \times 10^{-19} M_P$, from eq. (3.67) one can obtain the general bound on the reheating temperature, yielding:

$$T_{reh} < 5.38 \times 10^{-10} M_P \simeq 1.31 \times 10^9 \text{GeV}\,. \tag{3.68}$$

This is a very small temperature, due to the weak interaction of the field ϕ with itself and with other fields. Fortunately, at such a temperature no cosmologically anomalies, such as heavy strings, monopoles and textures can be produced, because the generation of the GUT (10^{16}GeV) topological defects require the high temperature phase transitions at $T_{GUT} \sim 10^{16}$GeV [64].

In summary, the reheating mechanism, except for the preheating epoch [63–65], is considered as a perturbative process once inflation has finalised. The classical oscillating scalar field ϕ decayed into other light degrees of freedom. Nonetheless, to sustain the exponential expansion one requires that $m_\phi \ll H$ [j] hence $\Gamma \ll H$. Thus the inflaton is essentially stable on Hubble time scales and the interactions should have a negligible impact on the dynamics. However, if the inflaton was interacting with other fields (with non trivial distributions), then this interplay can indeed have a remarkable effect on the dynamics, beyond the quantum corrections to the effective potential. Thereby if the inflaton was interacting with other particles, which can be described as thermal bath at

[j] This conditions is essentially $|\eta_\phi| < 1$.

ambient temperature T, and they were (including the inflaton) in thermal equilibrium or close to it, then the decay rate of the inflaton is $\Gamma \propto T$. Moreover, if $T > H$ then the timescale for this decay is shorter than the timescale characterising the expansion and thus the inflaton can decay. Indeed, this is still compatible with a slow-roll regime $m_\phi \ll H < T$. We shall see that the presence of this new scale, T, during inflation can allow for significant energy transfer between the inflaton and a radiation bath through interactions without violating slow-roll. This very simple picture in essence (to some extent) is the idea behind warm inflation.

Chapter 4

Warm Inflation

> "Vine a Comala porque me dijeron que acá vivía mi padre, un tal Pedro Páramo. Mi madre me lo dijo. Y yo le prometí que vendría a verlo en cuanto ella muriera. Le apreté sus manos en señal de que lo haría; pues ella estaba por morirse y yo en plan de prometerlo todo. ≪No dejes de ir a visitarlo-me recomendó-. Se llama de otro modo y de este otro. Estoy segura de que le dará gusto conocerte≫. Entonces no pude hacer otra cosa sino decirle que así lo haría, y de tanto decírselo se lo seguí diciendo aun después que a mis manos les costó trabajo zafarse de sus manos muertas."
>
> —Juan Rulfo, Pedro Páramo.

Any efficient model of inflation needs to explain the transition from the vacuum- to the radiation-dominated universe. Indeed, in CI this mechanism is called reheating. The first model of reheating are based on the assumption that after inflation ends the inflaton ϕ may decay into light constituents, either boson of fermion fields, which in turn gave birth to at least the SM degrees of freedom so that BBN could have taken place. However, reheating was studied as a perturbative process, where the classical oscillating scalar field ϕ can be represented as a collection of these scalar (fermion) particles at rest [62]. Wherein the decay width can be calculated perturbatively through Quantum Field Theory (QFT) [59, 60]. Moreover, one can go beyond this simple perturbative picture to consider preheating, which takes into account the time dependent mass of the decay products, and it results in a extremely rapidly process where the classical coherently oscillating inflaton field ϕ decays within the first few oscillations of the inflaton field [63–65].

As I mentioned before, the inflaton field is inevitably coupled to other degrees of freedom

in order to dissipate its vacuum energy and reheat the universe. Hence, one may conceive scenarios where dissipative effects become important during and not only after the slow-roll phase (opposite to the reheating mechanism). The idea of inflationary expansion and particle production occurring concurrently was suggested by L.Z. Fang, Moss, Yokoyama and Maeda [15] and then independently rediscovered almost a decade later by Berera and Fang [13]. At first the main insight was to introduce a dissipative term $\Upsilon\dot{\phi}$ in the inflaton evolution equation, as a source of radiation production; but later was not only included the dissipative contribution but also a noise force term that would drive the inflaton fluctuations, with a fluctuation-dissipation theorem uniquely specifying the inflaton fluctuations. The later framework is generically known as *warm inflation* (WI) scenario [13, 14]. Hence, the inflationary universe is not in a perfect vacuum state, even though vacuum energy is the dominant component responsible for the accelerated expansion.

Simply, as the inflaton, embedded in a thermal bath, rolls down its potential, it loses its vacuum energy due to the interaction with additional fields, and it deposits it in the radiation bath. Thus the early universe experiences a smooth transition from inflation to radiation domination as the radiation density starts predominating at the end of inflation, see fig. 4.1. Nonetheless, in the same way as the traditional reheating, there exist a risk of overproducing cosmological anomalies, such as gravitinos (relic problem), which may potentially damage BBN. Indeed, this issue has been studied, for instance, by Bueno Sanchez et al. [66] and Bartrum et al. [67]. However, I will not consider it further here.

In the next section, I will present very briefly the fluctuation-dissipation dynamics. Basically, in WI the interactions between the inflaton and other constituents modify the field evolution and lead to the production of a thermal bath in the background dynamics. Hence such interactions introduce a stochastic source and a non-local dissipation-like term in the inflaton field equation, turning it into a Langevin-type stochastic equation. Although, the main dissipative calculations are done either in chapters 5 and 6.

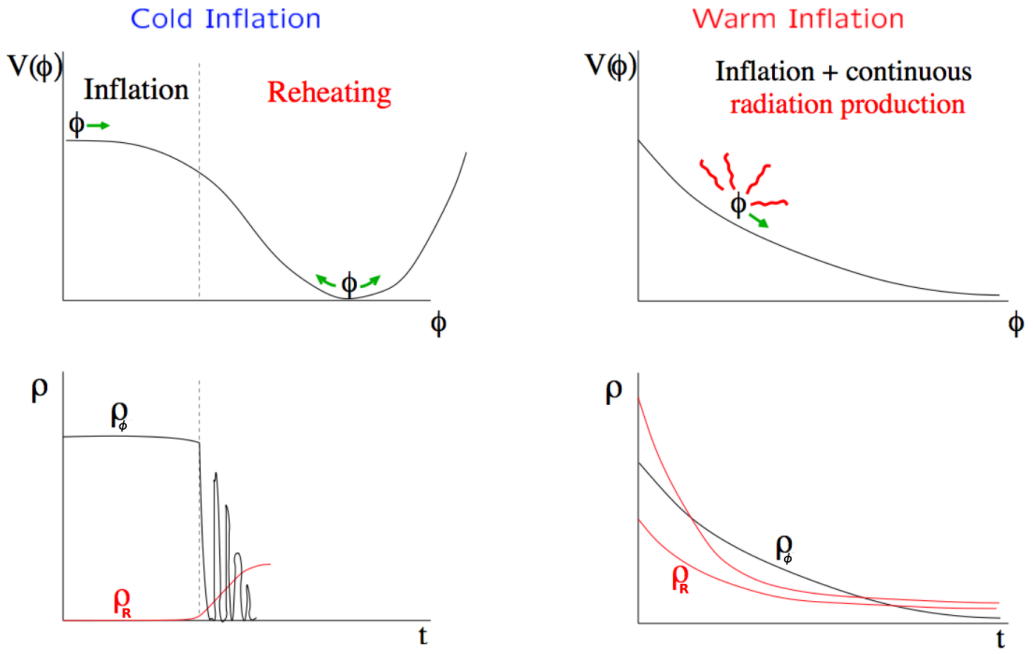

Figure 4.1: Comparison of the cold and warm inflationary pictures, top graphs show the scalar field ϕ evolution and the bottom graphs show the vacuum and radiation energy density evolution, ρ_ϕ and ρ_R respectively. Source, A. Berera *The warm inflationary universe*, Contemp. Phys. **47**, 33 (2006) [68].

4.1 Fluctuation-dissipation dynamics. A brief description

Non-equilibrium effects[a] in the dynamics of a scalar field are generically produced due to interactions with an ambient thermal bath. The leading non-equilibrium effect, for a field evolving slowly compared to the characteristic time scale of the thermal bath, is a dissipative friction term $\Upsilon\dot{\phi}$ in its equation of motion [69], where $\Upsilon = \Upsilon(\phi, T)$ can be computed from first principles given the form of the interactions between the scalar field and the thermalised degrees of freedom [b].

In warm inflation, particle production during inflation provides a damping effect on the inflaton. The ultimate destination of the vacuum energy from the inflationary phase is into excitations of the light sector fields. Moreover, one has to consider the possibility that these excitations enhance the loop corrections to the inflaton potential and violate the flatness conditions that inflation requires. Due to this concern, we will compute the loop corrections to the potential under the assumption that the

[a] Although, the black-body spectrum of the CMB and the successful predictions of BBN exhibit a universe in a state very close to local thermal equilibrium for a great part of its early history, one can assume that all relevant particle states always remain near this configuration.

[b] Indeed, in the next two chapters I will show all the details regarding the computation of the dissipative coefficient Υ.

light fields thermalise. From the finite temperature effective potential one can derive the thermodynamic properties of the cosmological fields, such as their energy density, entropy and pressure, as well as thermal mass corrections.

4.2 Warm inflation dynamics and primordial perturbation spectrum

For a homogeneous field, this implies the continuity equation:

$$\dot{\rho}_\phi + 3H(\rho_\phi + p_\phi) = -\Upsilon\dot{\phi}^2\,, \tag{4.1}$$

such that overall energy-momentum conservation implies the existence of an identical term with opposite sign in the continuity equation for the thermal fluid. It can be proved that dissipative effects in the inflaton's equation of motion lead to particle production in the thermal bath, so it prevents the exponential dilution of the latter in a quasi-de Sitter background. Therefore the temperature does not drop abruptly and the universe is able to smoothly cross to the radiation epoch. Taking into account dissipative effects, the evolution equation for the background inflaton field is given by:

$$\ddot{\phi} + (3H + \Upsilon)\,\dot{\phi} + V_{eff,\phi}(\phi, T) = 0\,, \tag{4.2}$$

where $V_{eff,\phi} = dV_{eff}/d\phi = V_{eff,\phi} = V(\phi)_{,\phi} + V_{T,\phi}$ includes the effective thermal potential $V_{eff} = V(\phi) + V_T$, where $V(\phi)$ is the zero temperature potential, and V_T is the finite temperature effective potential, also it refers to the radiative corrections of the potential due to any light component (fermion or scalar fields); Υ is the dissipative coefficient and H is the Hubble parameter, given by the Friedmann equation for a flat FRW universe:

$$H^2 = \frac{\rho_T}{3M_p^2}\,, \tag{4.3}$$

where

$$\rho_T = \frac{\dot{\phi}^2}{2} + V_{eff} + Ts_R\,, \tag{4.4}$$

is the total energy density of the system, which includes the contribution of the scalar field and the radiation,

$$s_R = -\frac{\partial V_{eff}}{\partial T} \tag{4.5}$$

is the entropy density, and and M_p is the reduced Planck mass, as well as the total pressure p_T:

$$p_T = \frac{\dot{\phi}^2}{2} - V_{eff}\,. \tag{4.6}$$

Note that $\rho_T + p_T = \dot{\phi}^2 + Ts$, having $\rho_T + p_T = (\rho_\phi + p_\phi) + (\rho_R + p_R) = \dot{\phi}^2 + Ts$, where $\rho_R + p_R$ is the energy density and pressure of a relativistic fluid, respectively; and the thermodynamic relation $\rho_R + p_R = Ts_R$ is exactly eq. (2.41). Indeed, energy momentum conservation now implies entropy production. Then, since WI scenario assumes the presence of a thermal bath, at temperature T; the evolution of such dissipative mechanism can be obtained from the evolution equation for the entropy density, given by:

$$T\left(\dot{s}_R + 3Hs_R\right) = \Upsilon\dot{\phi}^2\,. \tag{4.7}$$

Without including the T-dependent corrections in the inflaton potential, we would have the standard relation $Ts_R = 4\rho_R/3 = 4C_RT^4/3$, where $C_R = \pi^2 g_{eff}(T)/30$, $g_{eff}(T)$ is the effective T-dependent degrees of freedom. All relativistic light fields contribute to the effective degrees of freedom, having:

$$g_{eff}(T) = -\frac{90}{4\pi^2}\frac{1}{T^3}\frac{\partial V_{eff}}{\partial T}\,. \tag{4.8}$$

We can recover an alternative equation in the case when the temperature corrections to the potential are negligible. From $\rho_R = 3Ts_R/4$, then eq. (4.7) becomes:

$$\dot{\rho}_R + 4H\rho_R = \Upsilon\dot{\phi}^2\,. \tag{4.9}$$

One parameter that quantifies dissipation during WI is defined as dissipative ratio:

$$Q \equiv \frac{\Upsilon}{3H}\,. \tag{4.10}$$

Depending on the ratio Q we can have different kind of regimes: when $Q < 1$, this is called *weak dissipative warm inflation*; and when $Q \gtrsim 1$ we are in *strong dissipative warm inflation*.

4.3 Slow-roll WI

Since WI can be well described by a slow-roll approximation, the relevant equations are therefore:

$$H^2 \simeq \frac{V_{eff}}{3M_p^2}\,, \tag{4.11}$$

$$\dot{\phi} \simeq -\frac{V_{eff,\phi}}{3H(1+Q)}\,, \tag{4.12}$$

$$Ts_R \simeq Q\dot{\phi}^2\,. \tag{4.13}$$

Roughly speaking, above set consists of dropping the leading derivatives of eqs. (4.2,4.3,4.7). Besides, the radiative corrections modify the potential and its derivatives, they alter the standard slow-roll parameters, being from $\epsilon_\phi = M_P^2(V_{,\phi}/V)^2/2$ and $\eta_\phi = M_P^2 V_{,\phi\phi}/V$ to:

$$\epsilon_{eff} = \frac{M_p^2}{2}\left(\frac{V_{eff,\phi}}{V_{eff}}\right)^2\,, \qquad \eta_{eff} = M_p^2\frac{V_{eff,\phi\phi}}{V_{eff}}\,, \tag{4.14}$$

where $V_{eff,\phi\phi} = V(\phi)_{,\phi\phi} + V_{T,\phi\phi}$. Moreover, WI has an extra slow-roll parameter in addition to the usual set for CI due to the presence of the damping term:

$$\beta_\phi = M_P^2\frac{\Upsilon_{,\phi}V_{eff,\phi}}{\Upsilon V_{eff}}\,. \tag{4.15}$$

As an example, to set up the WI slow-roll conditions let us start from the eq. (4.11) and taking the time derivative, then using eq. (4.12), and finally dividing by H^2, we have:

$$-\frac{\dot{H}}{H^2} = \frac{M_p^2}{2}\left(\frac{V_{eff,\phi}}{V_{eff}}\right)^2\frac{1}{1+Q} = \frac{\epsilon_{eff}}{1+Q}\,, \tag{4.16}$$

where $\dot{T} \simeq 0$ [c] in the slow-roll regime; in fact this analogous to the estimation $T\dot{s}_R \simeq 0$ from eq. (4.7). Since $\epsilon_H = -\dot{H}/H^2 < 1$ therefore $\epsilon_{eff} < 1+Q$. Thus the full set of warm-inflation slow-roll conditions then reads [70, 71]:

$$\epsilon_{eff} < 1+Q\ , \quad |\eta_{eff}| < 1+Q\ , \quad \beta_\phi < 1+Q\ . \tag{4.17}$$

Recall that inflation happens when $\dot{\phi}^2/2 \ll V_{eff}$ so does $(Ts_RQ^{-1}/2) \ll V_{eff}$, but even if small compared to the inflaton effective potential, it can be larger than the expansion rate with $(Ts_R)^{1/4} \gtrsim H$ [d]; by assuming thermalisation, this translates roughly into

[c] The caveat to be aware here is that the temperature behaves monotonically, however, during the slow-roll regime one can consider that T remains unchanged. Only at the end of inflation T ceases to be constant.

[d] In fact this condition must be $(3Ts_R/4)^{1/4} \gtrsim H$ or $\rho_R^{1/4} \gtrsim H$ in the case when the temperature corrections to the potential are negligible. However, since $(3/4)^{1/4} \simeq 0.93$, it is sufficient to consider

$T \gtrsim H$, so one can obtain a warm inflationary universe consistently with a slow-roll evolution, as long as the radiative corrections are restrained such they do not spoil inflation. This can be quantified into the condition [72]:

$$\delta_\phi = \frac{TV_{eff,\phi T}}{V_{eff,\phi}} < 1\,. \tag{4.18}$$

Once the above condition is fulfilled, the slow-roll conditions in eq. (4.17) ensure that eqs. (4.11-4.13) hold and that radiation is subdominant during inflation. On the other hand, when they are not longer satisfied, either the motion is no longer overdamped and slow-roll ends, or the radiation becomes comparable to the inflaton energy density. Either way, inflation will end shortly afterwards.

Furthermore, one can show that the radiation energy density portrayed by an entropic description can never exceed the inflationary potential in a slow-roll regime, guaranteeing a period of accelerated expansion:

$$\frac{Ts_R}{V_{eff}} \simeq \frac{2}{3}\frac{\epsilon_{eff}}{1+Q}\frac{Q}{1+Q}\,, \tag{4.19}$$

such that consistency of the slow-roll evolution requires $\epsilon_{eff} < 1 + Q$. This in turn also implies that, at the end of the slow-roll regime, when $\epsilon_{eff} \sim 1 + Q$, one may attain $Ts_R \sim V_{eff}$ if a strong dissipative regime $Q \gtrsim 1$ can be achieved. In such cases radiation will smoothly become the dominant component at the end of inflation, providing the necessary "graceful exit" into the SBB cosmic evolution [73]. Although there may be additional particle production at the end of inflation, no reheating is actually necessary in WI when strong dissipation is reached, otherwise such mechanism is needed. Additionally to the smooth exit from inflation, WI exhibits several attractive features that have been explored in recent years. For instance, the dissipative friction damps the inflaton's evolution, making slow-roll easier or, equivalently, alleviating the conditions on the flatness of the inflaton potential, expressed now by the slow-roll conditions $\epsilon_{eff}, |\eta_{eff}| < 1 + Q$. This may potentially provide a solution to the so-called "eta-problem" typically found in string/supergravity inflationary models where generically $\eta_\phi \sim \mathcal{O}(1)$ [29, 72].

4.3.1 Thermal fluctuations. A brief description

Small fluctuations of the inflaton about its homogenous component provide the initial seeds of density perturbation. These density perturbations produced during inflation

that $(Ts_R)^{1/4} \gtrsim H$.

evolve into the classical inhomogeneities observed in the CMB. For WI scenario the fluctuations of the inflaton are thermally induced. As such, these initial seeds of density perturbation already are classical upon definition. Indeed, these thermal fluctuations can be modelled by a stochastic Langevin equation (SLE), where a dissipative term Υ describes the transfer of energy from the inflaton field to the thermal radiation bath, while the back-reaction of the thermal fluctuations in the radiation bath on the inflaton field is described by a stochastic noise term.

On the one hand, the idea of the stochastic inflation scheme was originally proposed by Starobinsky for the CI scenario [74] (see also [75–78]), where the key point is to split the quantum inflaton field in a long-wavelength, super-Hubble modes, and in short-wavelength, sub-Hubble modes. The super-Hubble component effectively behaves like a classical system, and it is influenced by the sub-Hubble quantum modes, which constitute the environment and behave as a stochastic noise term. Thereby, this leads to a stochastic equation, from which the effects of the quantum fluctuations can then be taken into account. Essentially, this represents an effective coarse-graining performed on the quantum inflaton field and on a chosen scale that is at least of the de-Sitter horizon length $1/H$.

On the other hand, in the warm inflation scheme, Ramos and da Silva [79] start by integrating over field degrees of freedom other than the inflaton field, hence the effective equation for the inflaton field turns out to be a Langevin-like equation with dissipation and stochastic noise terms. Then, they perform the coarse-graining on the inflaton field according to the stochastic inflation program. One advantage of their study becomes an equal description of the combined effects of both the inflaton quantum and thermal fluctuations. Finally they compute the inflaton field perturbation power spectrum, obtaining a formula that reproduces the cold and warm inflation results as limiting cases, but that can now also describe the intermediate regimes between the two scenarios. Thus, the amplitude of the primordial spectrum is given by [79]:

$$\Delta^2_{\mathcal{R}} = \left(\frac{H_*}{\dot{\phi}_*}\right)^2 \left(\frac{H_*}{2\pi}\right)^2 \left(1 + 2n_* + \frac{2\sqrt{3}\pi Q_*}{\sqrt{3+4\pi Q_*}}\frac{T}{H}\right) , \tag{4.20}$$

where all quantities are evaluated when the relevant CMB modes become superhorizon 50-60 e-folds before inflation ends; namely at horizon crossing. Then in the expression above, n_* denotes the inflaton phase space distribution at horizon crossing. By the strength of the interactions between the inflaton field and other particles in the thermal bath (including e.g. scattering processes), this might interpolate between the Bunch-Davies vacuum, $n_* = 0$, and the Bose-Einstein distribution at ambient temperature T,

$n_* \simeq \left(e^{H_*/T_*} - 1\right)^{-1}$. We will focus on the latter limiting case in this paper, which we denote as "thermal" inflaton fluctuations. Note that in the zero temperature limit, $T \to 0$, one has to consider the Bunch-Davies vacuum distribution, $n_* = 0$, as well as $\Upsilon \to 0$ ($Q \to 0$) to recover the cold inflation result, eq. (3.42), as expected. On the other hand, in the limit of $Q \gg 1$ and $T/H \gg 1$, one obtains (see Appendix D for the entire derivation):

$$\Delta^2_{\mathcal{R}} \simeq \frac{9H_*^5 T_* Q_*^{5/2}}{4\pi^2 V^2_{eff,\phi *}}\sqrt{3\pi}\,, \tag{4.21}$$

which is the same result, except for a multiplicative factor $\sqrt{3\pi}$, found by Berera and Taylor in [80], also by Hall, Moss and Berera in [70], and by Moss and Xiong in [81].

An additional comment to make about the amplitude of the primordial spectrum is needed. The expression eq. (4.20) neglects the coupling between inflaton and radiation fluctuations associated with the temperature dependence of the dissipation coefficient; in other words, eq. (4.20) was computed considering only that $\Upsilon = \Upsilon(\phi)$. However, an effect that may significantly enhance the perturbation growth for a $\Upsilon = \Upsilon(T)$ as well as a description for strong dissipation, $Q \gtrsim 1$, was realised by Graham and Moss [82]. In this new analysis, they introduce the function $G(Q_*)$, which accounts for the growth of inflaton fluctuations due to the coupling to radiation fluctuations through the temperature dependence of the dissipation coefficient and must be determined numerically. In the subsequent years, more studies were done, for instance see [83]. Thus, the general expression for the amplitude of the primordial spectrum is given by [70, 79–83]:

$$\Delta^2_{\mathcal{R}} = \left(\frac{H_*}{\dot{\phi}_*}\right)^2 \left(\frac{H_*}{2\pi}\right)^2 \left(1 + 2n_* + \frac{2\sqrt{3}\pi Q_*}{\sqrt{3 + 4\pi Q_*}}\frac{T}{H}\right) G(Q_*)\,. \tag{4.22}$$

Typically, $G(Q_*)$ is well approximated by a fraction of polynomials in Q with numerical fitted coefficients for most of the known models [82, 83]; and it reduces to 1 for $Q = 0$. Beside this function also exhibits a mild dependence on the form of the scalar potential. In general, with thermalised inflation fluctuations $1 + 2n_* = \coth\left(H_*/(2T_*)\right)$ and in the slow-roll regime, we have:

$$\Delta^2_{\mathcal{R}} \simeq \left(\frac{3H_*^3(1+Q_*)}{2\pi V_{eff,\phi *}}\right)^2 \left(\frac{2\sqrt{3}\pi Q_*}{\sqrt{3 + 4\pi Q_*}}\frac{T_*}{H_*} + \coth\left(\frac{H_*}{2T_*}\right)\right) G(Q_*)\,. \tag{4.23}$$

Then from the amplitude of the curvature power spectrum, we may determine the scalar spectral index $n_s - 1 \simeq d\ln\Delta^2_{\mathcal{R}}/dN_e$. Since, for $T \ll M_P$, gravitational waves are not significantly affected by thermal effects, the primordial tensor spectrum is given by the

standard inflationary form $\Delta_t^2 = 2H_*^2/(\pi^2 M_P^2)$. The tensor-to-scalar ratio $r = \Delta_t^2/\Delta_{\mathcal{R}}^2$ is nevertheless affected, and as mentioned above typically reduced, by the modifications to the scalar curvature perturbations introduced due to dissipation; which is basically a function of T_*/H_* and Q_*. We illustrate this fact by using the slow-roll dynamics, where the ratio r can be written as:

$$r \simeq \frac{16\epsilon_{eff}}{(1+Q_*)^2 K(T_*/H_*, Q_*)}\,, \tag{4.24}$$

where

$$K(T_*/H_*, Q_*) = \left(\frac{2\sqrt{3}\pi Q_*}{\sqrt{3+4\pi Q_*}}\frac{T_*}{H_*} + \coth\left(\frac{H_*}{2T_*}\right)\right) G(Q_*)\,, \tag{4.25}$$

note that r is suppressed w.r.t. the CI prediction by a factor $(1+Q_*)^2 K(T_*/H_*, Q_*) > 1$. In fact, an inflationary scenario with a chaotic quartic potential, already ruled out by $n_s - r$ constraints in the CI paradigm, is now brought back into agreement with the Planck data [23, 58].

Chapter 5

Dynamical and observational constraints on the Warm Little Inflaton scenario

> "¿Por qué escribo esto? No tengo ideas claras, ni siquiera tengo ideas. Hay jirones, impulsos, bloques, y todo busca una forma, entonces entra en juego el ritmo y yo escribo dentro de ese ritmo, escribo por él, movido por él y no por eso que llaman el pensamiento y que hace la prosa, literaria u otra."
>
> —Julio Cortázar, Rayuela

Realising warm inflation within a consistent quantum field theory framework has, however, proved to be a challenging endeavour. Non-equilibrium dissipative effects are Boltzmann suppressed unless the particles in the radiation bath are relativistic, while the inflaton typically gives a large mass to the fields it couples directly to. In addition, relativistic particles change the form of the inflaton potential at finite temperature, typically inducing large thermal corrections to the inflaton's mass that may prevent slow-roll unless the associated inflaton couplings are very suppressed, therefore rendering dissipative effects ineffective in sustaining a thermal bath during inflation [16, 17]. For several years, the leading solution to these problems was to consider models where the inflaton only couples directly to heavy fields, which in turn decay into light particles in the thermal bath [18]. In these scenarios thermal corrections to the inflaton potential become Boltzmann-suppressed, while dissipative effects can nevertheless be significant if one considers a large number of fields coupled to the

inflaton[a]. While such scenarios may find natural realisations in specific constructions within e.g. string theory [22] where field multiplicities can be large during inflation, they cannot provide a simple and sufficiently generic realisation of warm inflation.

A more promising scenario was proposed recently [23] where the above-mentioned problems were addressed using symmetries rather than large field multiplicities. This *Warm Little Inflaton* (WLI) scenario, so-called due to its similarities with Little Higgs models of electroweak symmetry breaking [24, 25], considers an inflaton field that corresponds to the relative phase between two complex Higgs scalars that collectively break a local U(1) symmetry. Both fields have an equal nonzero vacuum expectation value: $\langle\phi_1\rangle = \langle\phi_2\rangle \equiv M/\sqrt{2}$, where M is the symmetry breaking scale. In the broken phase we can parametrise the fields as follows:

$$\phi_1 = \frac{M}{\sqrt{2}} e^{i\phi/M} , \qquad \phi_2 = \frac{M}{\sqrt{2}} e^{-i\phi/M} , \tag{5.1}$$

where we assume the radial Higgs fields to decouple for $T \lesssim M$. We thus take the inflaton to be the PNGB ϕ. These complex scalars are coupled to left-handed fermions ψ_{1L} and ψ_{2L} with U(1) charge q as well as their right-handed counterparts ψ_{1R} and ψ_{2R}, which we take to be gauge singlets. We consider identical couplings in magnitude and impose the interchange symmetry $\phi_1 \leftrightarrow i\phi_2$, $\psi_{1L,R} \leftrightarrow \psi_{2L,R}$, such that the allowed Yukawa interactions are of the form:

$$\begin{aligned} -\mathcal{L} &= \frac{g}{\sqrt{2}} (\phi_1 + \phi_2)\, \bar{\psi}_{1L}\psi_{1R} - i\frac{g}{\sqrt{2}} (\phi_1 - \phi_2)\, \bar{\psi}_{2L}\psi_{2R} \\ &= gM\cos(\phi/M)\bar{\psi}_1\psi_1 + gM\sin(\phi/M)\bar{\psi}_2\psi_2 \ . \end{aligned} \tag{5.2}$$

where g is a dimensionless coupling. The resulting Dirac fermion masses are:

$$m_{1,2}^2 = g^2M^2\cos^2(\phi/M) + g^2M^2\sin^2(\phi/M) = g^2M^2 \ , \tag{5.3}$$

thus $m_{1,2} \leq gM$, such that they may remain light during inflation for an arbitrary inflaton value, provided that $gM \lesssim T \lesssim M$. Hence, the particular form of this Lagrangian makes the fermion masses bounded from above, such that large inflaton field values do not lead to heavy fermions, and in addition leads to the cancellation of the leading thermal contributions of the fermion fields to the inflaton's mass. To show the last statement, we start by replacing $\phi \to \phi + \delta\phi$ in the interaction Lagrangian (5.2) to determine the interaction between inflaton particles and the fermions $\psi_{1,2}$.

[a] In this case dissipative effects are the result of heavy virtual modes that are not Boltzmann-suppressed [19–21].

Expanding up to quadratic order in $\delta\phi$ we obtain:

$$\mathcal{L} = -\sum_{i=1,2}\left[m_i + g_i\delta\phi + \frac{f_i}{2}\delta\phi^2 + \cdots\right]\bar{\psi}_i\psi_i \ , \tag{5.4}$$

where the effective masses and couplings depend on the background inflaton value ϕ and are given by:

$$\begin{aligned} m_1 &= gM\cos(\phi/M) \ , & m_2 &= gM\sin(\phi/M) \ , \\ g_1 &= -g\sin(\phi/M) \ , & g_2 &= g\cos(\phi/M) \ , \\ f_1 &= -\frac{g}{M}\cos(\phi/M) \ , & m_2 &= -\frac{g}{M}\sin(\phi/M) \ . \end{aligned} \tag{5.5}$$

The leading 1-loop contributions to the inflaton self-energy are given by the diagrams (a) and (b) in the figure 5.1 below. Using the Feynman rules at finite temperature in

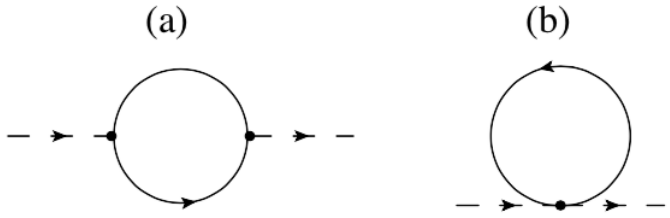

Figure 5.1: Feynman diagrams contributing to the inflaton self-energy. The solid fermion lines in the loops correspond to either ψ_1 or ψ_2. Note that diagram (a) is associated with the g_i vertices, while diagram (b) is associated with the f_i vertices.

the imaginary-time formalism [84, 85], we obtain for the contribution of ψ_i to diagram (a) at vanishing external momentum:

$$\begin{aligned} -i\Pi_i^{(a)}(0) &= (-1)(-ig_i)^2\left(iT\sum_n\int\frac{d^3k}{(2\pi)^3}\right)\mathrm{Tr}\left[\frac{i}{(\not{k}-m_i)}\frac{i}{(\not{k}-m_i)}\right] \\ &= -ig_i^2T\sum_n\int\frac{d^3k}{(2\pi)^3}\frac{\mathrm{Tr}\left[(\not{k}+m_i)^2\right]}{(k^2-m_i^2)^2} \\ &= -4ig_i^2T\sum_n\int\frac{d^3k}{(2\pi)^3}\frac{k^2+m_i^2}{(k^2-m_i^2)^2} \\ &= -4ig_i^2T\sum_n\int\frac{d^3k}{(2\pi)^3}\left[\frac{1}{k^2-m_i^2}+\frac{2m_i^2}{(k^2-m_i^2)^2}\right] \\ &= -4ig_i^2T\sum_n\int\frac{d^3k}{(2\pi)^3}\left[-\frac{1}{\omega_n^2+|\mathbf{k}|^2+m_i^2}+\frac{2m_i^2}{(\omega_n^2+|\mathbf{k}|^2+m_i^2)^2}\right] \end{aligned} \tag{5.6}$$

where $k^2 = (k^0)^2 - |\mathbf{k}|^2 = (i\omega_n)^2 - |\mathbf{k}|^2 = -(\omega_n^2 + |\mathbf{k}|^2)$ is the four-momenta, $\mathbf{k}$ is the three-momenta, and the sum is over the fermionic Matsubara frequencies $\omega_n =$

$(2n+1)\pi T$ [84, 85]. For $m_i \ll T$ or Hard Thermal Loop (HTL) approximation we may neglect the second term within brackets and the masses in the denominator of the propagators [b], such that:

$$\Pi_i^{(a)}(0) \simeq -4g_i^2 T \sum_n \int \frac{d^3k}{(2\pi)^3} \frac{1}{\omega_n^2 + |\mathbf{k}|^2} \ . \tag{5.7}$$

Similarly, for diagram (b) we obtain:

$$\begin{aligned} -i\Pi_i^{(b)}(0) &= (-1)(-if_i) \left(iT \sum_n \int \frac{d^3k}{(2\pi)^3} \right) \mathrm{Tr} \left[\frac{i}{(\not{k} - m_i)} \right] \\ &= -if_i T \sum_n \int \frac{d^3k}{(2\pi)^3} \frac{\mathrm{Tr}\left[\not{k} + m_i\right]}{k^2 - m_i^2} \\ &= -4if_i m_i T \sum_n \int \frac{d^3k}{(2\pi)^3} \frac{1}{k^2 - m_i^2} \ , \end{aligned} \tag{5.8}$$

such that in HTL approximation we get:

$$\Pi_i^{(b)}(0) \simeq -4f_i m_i T \sum_n \int \frac{d^3k}{(2\pi)^3} \frac{1}{\omega_n^2 + |\mathbf{k}|^2} \ . \tag{5.9}$$

Then the total contribution to the inflaton self-energy becomes:

$$\begin{aligned} \Pi_\phi(0) &= \sum_{i=1,2} \left[\Pi_i^{(a)}(0) + \Pi_i^{(b)}(0) \right] = \left[(g_1^2 + m_1 f_1) + (g_2^2 + m_2 f_2) \right] I_T \\ &= g^2 \left[(\sin^2(\phi/M) - \cos^2(\phi/M)) + (\cos^2(\phi/M) - \sin^2(\phi/M)) \right] I_T \\ &= g^2 \left[-\cos(2\phi/M) + \cos(2\phi/M) \right] I_T \\ &= 0 \ , \end{aligned} \tag{5.10}$$

so that the leading contributions of each fermion to the inflaton mass in the high temperature limit cancel. Note that the quantity I_T is given by:

$$I_T = -4T \sum_n \int \frac{d^3k}{(2\pi)^3} \frac{1}{\omega_n^2 + |\mathbf{k}|^2} \ . \tag{5.11}$$

These fermions are also allowed to decay into other light fermions and scalars, not directly coupled to the inflaton, through standard Yukawa interactions parametrised by a dimensionless coupling h with Lagrangian density:

$$\mathcal{L}_{\psi,\sigma} = -h\sigma \sum_{i=1,2} \left(\bar{\psi}_i \psi_\sigma + \bar{\psi}_\sigma \psi_i \right) \ , \tag{5.12}$$

[b] For instance, we have $\omega_n^2 + |\mathbf{k}|^2 + m_i^2 = [(2n+1)^2\pi^2 + (|\mathbf{k}|/T)^2 + (m_i/T)^2]T^2 \simeq [(2n+1)^2\pi^2 + (|\mathbf{k}|/T)^2]T^2 = \omega_n^2 + |\mathbf{k}|^2$ for $m_i \ll T$.

where σ is a scalar singlet and ψ_σ is an additional light fermion. This simple scenario has been shown to lead to a consistent realisation of warm inflation with a small number of fields and parameters. The inflaton is, moreover, a gauge singlet, such that the scenario can accommodate different forms of the scalar potential compatible with the reflection symmetry $\phi/M \to \pi/2 - \phi/M$ inherited from the discrete interchange symmetry mentioned above. Moreover, this scenario leads to observational predictions for chaotic inflation with a quartic potential compatible with the latest Planck data [23, 86], a simple model that is observationally ruled out within the standard "cold inflation" paradigm.

In this work, we extend the analysis done in [23, 86] for different forms of the scalar potential, thoroughly exploring the parametric regimes where the WLI scenario can be consistently implemented and comparing the associated observational predictions with Planck 2015 data [87]. In addition to the quartic monomial potential, we also study a Higgs-like symmetry breaking potential and a non-renormalisable plateau-like potential also considered in [56, 88] in the context of warm inflation. We wish to determine, in particular, the allowed ranges for the dimensionless couplings g and h and the symmetry breaking scale M for which the WLI scenario can be consistently realised with different potentials, as well as characterise the dynamics of warm inflation in the consistent parametric regimes.

5.1 Warm inflation dynamics and primordial perturbation spectrum

Since the leading contributions of each fermion to the inflaton mass in the high temperature limit cancel, in WI the background evolution equations for the inflaton-radiation system are given by:

$$\begin{aligned} \ddot{\phi} + (3H + \Upsilon)\dot{\phi} + V'(\phi) &= 0\,, \\ \dot{\rho}_R + 4H\rho_R &= \Upsilon\dot{\phi}^2\,, \end{aligned} \tag{5.13}$$

where dots correspond to time derivatives, primes denote derivatives with respect to ϕ, Υ is the dissipative coefficient in the leading adiabatic approximation and H is the Hubble parameter, given by the Friedmann equation for a flat FRW universe:

$$3H^2 = \frac{\rho}{M_P^2}\,, \tag{5.14}$$

where $\rho = \rho_\phi + \rho_R$ is the total energy density, with $\rho_\phi = \dot{\phi}^2/2 + V(\phi)$. In the WLI scenario, the dissipation coefficient resulting from the interaction between the inflaton and the fermions ψ_1 and ψ_2 in eq. (5.2) (from a diagram of the form (a) in fig. 5.1) is proportional to the temperature of the radiation bath and given by [23] (see also Appendix A):

$$\Upsilon = C_T T\,, \quad C_T \simeq \frac{3g^2}{h^2(1-0.34\log(h))}\,, \tag{5.15}$$

where C_T is a function of the coupling g and the Yukawa coupling h determining the decay of the $\psi_{1,2}$ fermions into a light σ scalar and a light ψ_σ fermion. Note that $h^2/(4\pi)$ is the true expansion parameter, so one must guarantee that this parameter remains small enough $h^2/(4\pi) < 1$ to yield the leading perturbatively resumed result for the decay width. In this regime, any higher-order corrections are necessarily sub-leading so will not change the results in a significant way. The above dissipation coefficient is valid in the high-temperature regime where the fermions are relativistic. At finite temperature, both fermion obtain thermal masses. These additions are identical for both fields, and they emerge from the contributions of the σ and ψ_σ fields corresponding to $h^2T^2/8$ [89]. Given that, including thermal mass corrections: $m_1^2 = g^2M^2\cos^2(\phi/M) + h^2T^2/8$ and $m_2^2 = g^2M^2\sin^2(\phi/M) + h^2T^2/8$, the fermions remain light during inflation for an arbitrary inflaton value, provided that $gM \lesssim T \lesssim M$. Note that the upper bound on the temperature ensures that the underlying U(1) symmetry is spontaneously broken during inflation. The contribution of the fermions ψ_1 and ψ_2 to the finite temperature effective potential is given by [84, 90]:

$$\begin{aligned} V_T \simeq & \left\{-\frac{28\pi^2}{15} + h^2\left[1 + \frac{3h^2}{32\pi^2}\left[\ln\left(\frac{\mu^2}{T^2}\right) - c_f\right]\right]\right\}\frac{T^4}{48} \\ & + \left\{1 + \frac{3h^2}{16\pi^2}\left[\ln\left(\frac{\mu^2}{T^2}\right) - c_f\right]\right\}\frac{g^2M^2}{12}T^2 \\ & + \frac{g^4M^4}{16\pi^2}\left[\cos^4(\phi/M) + \sin^4(\phi/M)\right]\left[\ln\left(\frac{\mu^2}{T^2}\right) - c_f\right]\,, \end{aligned} \tag{5.16}$$

where μ [c] is the $\overline{\text{MS}}$ renormalisation scale and $c_f = 2.635$. Its derivatives are given by:

$$V_{T,\phi} \simeq -\frac{g^4M^3}{16\pi^2}\sin(4\phi/M)\left[\ln\left(\frac{\mu^2}{T^2}\right) - c_f\right]\,, \tag{5.17}$$

$$V_{T,\phi\phi} \simeq -\frac{g^4M^2}{4\pi^2}\cos(4\phi/M)\left[\ln\left(\frac{\mu^2}{T^2}\right) - c_f\right]\,, \tag{5.18}$$

where the leading thermal inflaton mass corrections from both fermions cancel each other, and the remaining oscillatory corrections vanish, on average, for $\phi \gg M$,

[c] For convenience we select this scale as the symmetry breaking scale M.

although we will include them explicitly in our analysis.

The fermion decay width is given by [23], which at 1-loop corresponds to the diagram below (see fig. 5.2), neglecting the mass of its decay products:

$$\Gamma_{\psi_i} = \frac{h^2}{16\pi}\frac{T^2 m_i^2}{\omega_p^2|\mathbf{p}|}\left[F\left(\frac{k_+}{T},\frac{\omega_p}{T}\right) - F\left(\frac{k_-}{T},\frac{\omega_p}{T}\right)\right], \tag{5.19}$$

where $\omega_p = \sqrt{m_i^2 + |\mathbf{p}|^2}$, $k_\pm = (\omega_p \pm |\mathbf{p}|)/2$ and

$$F(x,y) = xy - \frac{x^2}{2} + (y-x)\ln\left(\frac{1-e^{-x}}{1+e^{x-y}}\right) + \mathrm{Li}_2\left(e^{-x}\right) + \mathrm{Li}_2\left(-e^{x-y}\right), \tag{5.20}$$

where $\mathrm{Li}_2(z)$ is the dilogarithm function. The thermal mass corrections, given by the Yukawa interactions, dominate over the inflaton contribution to the fermion masses for $h \gg g$ and $T \lesssim M$, such that $m_i^2 \simeq h^2T^2/8$. To ensure the validity of the adiabatic approximation in the computation of the dissipation coefficient and that the fermions are in a nearly-thermal equilibrium state, we must then impose $\Gamma_\psi/H > 1$. For practical purposes, we evaluate the decay width at the momentum value $p_{max} \simeq 3.24T$ that yields the largest contribution to the dissipation coefficient [23]. In addition to this requirement, we demand $T > H$, where a flat space approximation can be employed in the computation of the dissipation coefficient [91].

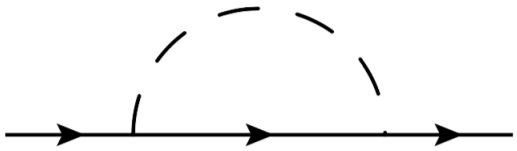

Figure 5.2: Feynman diagram contributing at 1-loop to the fermion self-energy, where the internal lines correspond to the (massless) ψ_σ and σ fermion and scalar fields, respectively.

For thermalised inflation fluctuations, $1 + 2n_* = \coth(H_*/(2T_*))$, and since $T_*/H_* = 3Q_*/C_T$ the resulting dimensionless power spectrum has the form:

$$\Delta^2_{\mathcal{R}} = \frac{5C_T^4}{24\pi^4 g_*}Q_*^{-3}\left(\frac{\sqrt{3}\pi}{\sqrt{3+4\pi Q_*}}\frac{6}{C_T}Q_*^2 + \coth\left(\frac{C_T}{6Q_*}\right)\right)G(Q_*)\,. \tag{5.21}$$

The function $G(Q_*)$ accounts for the growth of inflaton fluctuations due to the coupling to radiation fluctuations through the temperature dependence of the dissipation coefficient and must be determined numerically. This function also exhibits a mild dependence on the form of the scalar potential. An extended analysis in [23, 92], for

the potentials considered in this work, obtained the numerical fit:

$$G(Q_*) \simeq \begin{cases} 1 + 0.0185\, Q_*^{2.315} + 0.335\, Q_*^{1.364} & \text{quartic potential}\,, \\ 1 + 0.01\, Q_*^{1.8} + 0.18\, Q_*^{1.4} & \text{Higgs-like and plateau-like potentials}\,. \end{cases} \tag{5.22}$$

This implies that the measured amplitude of the primordial power spectrum $\Delta^2_{\mathcal{R}} \simeq 2.2 \times 10^{-9}$ [10] constrains the observationally consistent scenarios independently of the form of the scalar potential. In particular, it yields an upper bound $C_T \lesssim 0.02$, which implies that the coupling g must be at least an order of magnitude smaller than the coupling h.

From the amplitude of the curvature power spectrum, we determine the scalar spectral index $n_s - 1 \simeq d \ln \Delta^2_{\mathcal{R}} / dN_e$, which we may write as:

$$n_s = 1 + \frac{Q_*}{3 + 5Q_*} \left(6\epsilon_\phi - 2\eta_\phi\right) \frac{d \ln \Delta^2_{\mathcal{R}}}{dQ_*}\,. \tag{5.23}$$

Since, for $T \ll M_P$, gravitational waves are not significantly affected by thermal effects, the primordial tensor spectrum is given by the standard inflationary form $\Delta^2_t = 2H_*^2/(\pi^2 M_P^2)$. The tensor-to-scalar ratio $r = \Delta^2_t/\Delta^2_{\mathcal{R}}$ is nevertheless affected, and as mentioned above typically reduced, by the modifications to the scalar curvature perturbations introduced by dissipation.

5.2 Analysis of different inflaton potentials

Previous studies of the WLI scenario have shown that it may be consistently implemented and yield observationally viable predictions with a quartic inflaton potential for specific parameter values [23, 86]. In this section, we will perform a full parametric analysis of this case, considering all dynamical consistency conditions, and then extend the study to additional typical forms of the inflaton potential. We will require, in particular, that the fermions remain light during inflation and that they maintain a near-equilibrium distribution, such that dissipative processes also occur in an adiabatic regime. This implies imposing the conditions $\Gamma_\psi/H > 1$, $T/H > 1$ and $gM \lesssim T \lesssim M$ for 50-60 e-folds of inflationary expansion. After determining the regions of parameter space where these conditions are satisfied, we will then compute the corresponding inflationary observables.

In order to scan the parameter space, we implement a numerical method. This is to solve the system of equations (5.13) and (5.14). Now, since the coupling constants

involved in the dynamics differ by several orders of magnitude, for instance $\lambda \sim 10^{-14}$ for the inflaton self-interactions and $h = \mathcal{O}(1)$, it is useful to use rescaled quantities in the numerical procedure to evolve the background field and radiation equations (5.13). In particular, in the numerical code we use $\tilde{C}_T = \tilde{g}^2\lambda^{1/4} f(\tilde{h})$, $f(\tilde{h}) = 3/(\tilde{h}^2(1 - 0.34\log(\tilde{h})))$, and $\tilde{g} = g/\lambda^{1/4}$. This allows us to consider input values g_0 and h_0 for the couplings and a reference input value $\lambda_0 = 10^{-14}$ for the inflaton self-coupling. With these input values we evolve the background equations from initial conditions yielding a large number of e-folds (> 60), and then determine the values of the different dynamical quantities (ϕ, Q) at horizon-crossing 50-60 e-folds before the end of inflation. From this iterative procedure we then determine the physical value of λ yielding the measured amplitude of the scalar curvature power spectrum, and use the rescaled quantities above to compute the physical values of the couplings g and h. As mentioned earlier, for the Yukawa coupling the expansion parameter must satisfy $h^2/(4\pi) < 1$, thus $h \lesssim 3.5$ in order to be perturbative.

For instance, to study a Higgs-like potential:

$$V(\phi) = \frac{\lambda}{4}(\phi^2 - v^2)^2 \ , \tag{5.24}$$

we do the analysis for different values of $v/M_P = 2, 5, 10, 20$, and vary the parameters g, h, and M. We integrate the background EOM for the inflaton field and radiation: (5.13) and (5.14), looking for initial conditions that allow a certain value of N_e e-folds (> 60). Inflation will end when slow-roll conditions are violated, in particular we set the end of inflation at $\epsilon_H = -\dot{H}/H^2 = 1$. A certain N_e e-folds (50-60) before the end of inflation we read the values at horizon crossing, get the amplitude of the spectrum, obtain the value of λ, and the predictions for the spectral index n_s and the tensor-to-scalar ratio r. Numerically, we evolve dimensionless quantities. The "program" variables (denoted by a "tilde") are defined as:

$$\tilde{\phi} = \frac{\phi}{v} \ , \qquad \tilde{\dot{\phi}} = \frac{\dot{\phi}}{v\lambda^{1/2}} \ , \tag{5.25}$$

$$\tilde{H} = \frac{H}{v\lambda^{1/2}} \ , \qquad \tilde{\Upsilon} = \frac{\Upsilon}{v\lambda^{1/2}} \ , \tag{5.26}$$

$$\tilde{\rho}_i = \frac{\rho_i}{v^4\lambda^2} \ , \qquad \tilde{T} = \frac{T}{v\lambda^{1/4}} \ , \tag{5.27}$$

where ρ_i are the energy densities either of the inflaton or radiation: $\rho_\phi = \dot{\phi}^2/2 + V(\phi)$ and $\rho_R = \pi^2 g_* T^4/30 = C_R T^4$. From the rescaling of the dissipative coefficient we also

have:

$$\tilde{\Upsilon} = \tilde{C}_T \tilde{T} \ , \ \tilde{C}_T = \tilde{g}^2 \lambda^{1/4} f(\tilde{h}) \ , \ f(\tilde{h}) = \frac{3}{\tilde{h}^2(1 - 0.34 \log(\tilde{h}))} \ , \ \tilde{g} = \frac{g}{\lambda^{1/4}} \ , \ \tilde{h} = h \ . \quad (5.28)$$

With this rescaling we have that the ratio of scales entering in the thermal potential is independent of λ:

$$\frac{gT}{M} = \frac{\tilde{g}\tilde{T}}{\tilde{M}} \ , \quad (5.29)$$

with $\tilde{M} = M/v$. Therefore, we will use as input the value of $\tilde{g}$, and a reference value for the potential coupling $\lambda_0 = 10^{-14}$, which is of the expected order of magnitude to get the primordial spectrum. For each value of v, we scan over the parameters $g_0 = \lambda_0^{1/4}\tilde{g}$, h_0 and M. This gives the value of

$$\tilde{C}_T(0) = \tilde{g}^2 \lambda_0^{1/4} f(\tilde{h}_0) \ , \quad (5.30)$$

and therefore that of Q for each point in the scan. Once we have obtained the values at horizon crossing (Q_*), in program units, we impose the normalisation of the spectrum (eq. (5.21) $\Delta^2_{\mathcal{R}} \simeq 2.2 \times 10^{-9}$ [10]) to obtain the true value λ. And once we have obtained the true value λ, we can cross-check the different constraints for the model:

- The symmetry breaking scale M should be large enough, but fermions should be light: $gM/T = \tilde{g}\tilde{M}/\tilde{T} < 1$ and $M/T = \tilde{M}/(\lambda^{1/4}\tilde{T}) > 1$.
- For the consistency of the dissipative coefficient calculation, we must have: $T/H = \tilde{T}/(\lambda^{1/4}\tilde{H}) > 1$.
- Light fermions should maintain a near-equilibrium distribution at T, which requires: $\Gamma_\psi/H > 1$.

In order to cross-check the adiabaticity condition $\Gamma_\psi/H > 1$ we need first to get the physical value of h from the equality of $\tilde{C}_T$ and the input value $\tilde{C}_T(0)$ in eq. (5.30); i.e. we need to solve one equation numerically:

$$\lambda_0^{1/4} f(\tilde{h}_0) = \lambda^{1/4} f(\tilde{h}) \ . \quad (5.31)$$

At last the physical value of g is given by $g = (\lambda/\lambda_0)^{1/4} g_0$. This procedure is done only for the Higgs-like potential and Plateau-like potential with sextic power, since the typical value of the potential coupling constant of the chaotic quartic is of the order $\lambda \sim 10^{-14}$ or $\lambda \sim 10^{-15}$, then it is essentially accessible to explore the parameter space varying λ as well.

5.2.1 Chaotic inflation with a quartic potential: $V(\phi) = \frac{\lambda}{4}\phi^4$

For the quartic potential, we show in fig. 5.3 the regions in the $(g, M/M_P)$ plane where all dynamical consistency conditions are satisfied for two different values of the Yukawa coupling, $h = 2$ and $h = 3$ ($h \simeq h_0$ and $g \simeq g_0$ in this case), indicating the regions where each condition fails.

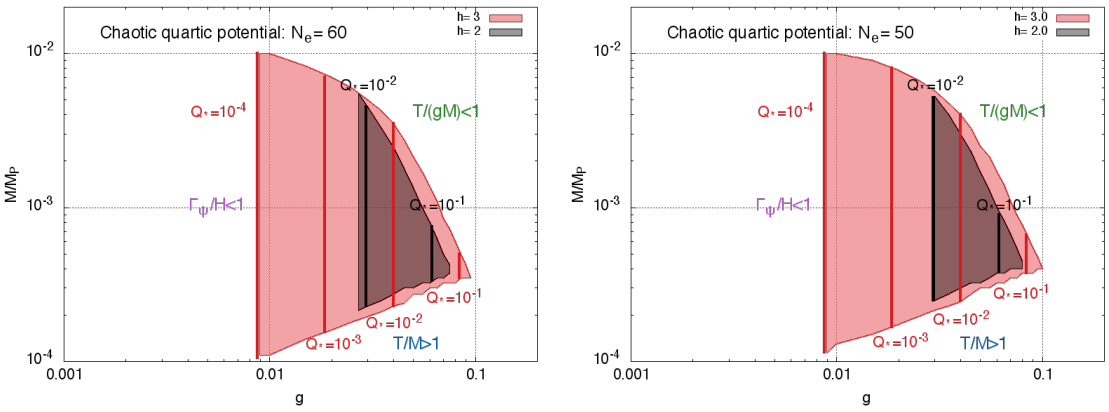

Figure 5.3: *Allowed regions in the plane $(g, M/M_P)$ for the chaotic quartic potential with $h = 2$ (gray) and $h = 3$ (red), for $N_e = 50$ (right) and $N_e = 60$ (left). Notice that there are no allowed regions for $h \simeq 1$. The vertical lines correspond to different values of the dissipative ratio at horizon-crossing, Q_*.*

As one can easily see, the adiabatic condition $\Gamma_\psi > H$ implies a lower bound on $g \gtrsim 0.01$, while the conditions on the temperature limit this coupling from above, $g \lesssim 0.1$. We find no consistent solutions for $h \lesssim 1$ (due to the condition $\Gamma_\psi > H$), with larger values of this coupling increasing the range of the allowed values for g and M. Note, however, that for larger values of the Yukawa coupling perturbation theory may break down. The symmetry breaking scale may take values in the range $10^{-4}M_P - 10^{-2}M_P$. Detailed limits are given in Table 5.1

$N_e = 60$	M_{min}/M_P	M_{max}/M_P	g_{min}	g_{max}	Q_{*min}	Q_{*max}
h=3	1.1×10^{-4}	1×10^{-2}	8.9×10^{-3}	0.095	1×10^{-4}	0.16
h=2	2.15×10^{-4}	5.5×10^{-3}	0.027	0.075	7.7×10^{-3}	0.2
$N_e = 50$	M_{min}/M_P	M_{max}/M_P	g_{min}	g_{max}	Q_{*min}	Q_{*max}
h=3	1.15×10^{-4}	1×10^{-2}	8.9×10^{-3}	0.1	1.1×10^{-4}	0.19
h=2	2.5×10^{-4}	5.25×10^{-3}	0.03	0.08	0.01	0.25

Table 5.1: *Allowed parametric ranges for the WLI scenario with a quartic potential for $N_e = 50, 60$ and $h = 2, 3$.*

We also find that the dissipative ratio at horizon-crossing can consistently take values in the range $10^{-4} \lesssim Q_* \lesssim 10^{-1}$, the lower bound being set by the condition of nearly-

thermalized fermions and the upper bound by the high-temperature approximation. Thus, generically we find that inflation must start in the weak dissipative regime, although Q increases during inflation for the quartic potential so that in a wide region of parameter space one reaches $Q > 1$ before the end of inflation, a necessary condition for radiation to dominate after the slow-roll regime with no further reheating (see Eq. (4.19)). In fig. 5.4 we show the predictions for the scalar spectral index and tensor-to-scalar ratio in the allowed parametric ranges, exhibiting a remarkable consistency with the Planck data. This is particularly relevant given that the quartic potential is already excluded by Planck data within the cold inflation paradigm. The tensor-to-scalar ratio lies in the range $10^{-3} \lesssim r \lesssim 10^{-2}$, with a smaller Yukawa coupling suppressing the amount of tensor modes.

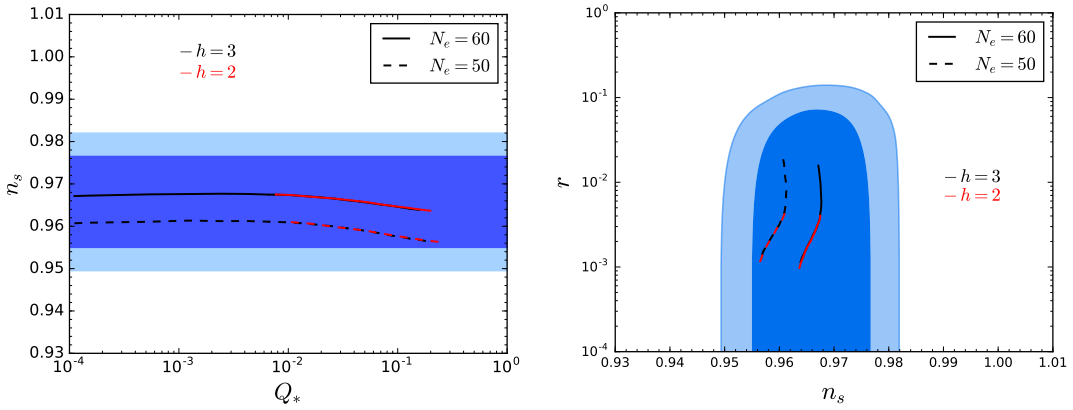

Figure 5.4: Observational predictions of the WLI scenario with a quartic potential for 50-60 e-folds of inflation and two distinct values of the Yukawa coupling $h = 2$ and $h = 3$. The plot on the left shows the spectral index n_s as a function of the dissipative ratio at horizon-crossing, Q_*, while the plot on the right shows the allowed trajectories in the (n_s, r) plane. The blue contours correspond to the 68% and 95% C.L. results from Planck 2015 TT+lowP data [87].

The agreement between the WLI quartic model and the Planck data had already been observed in [23, 86], although without taking into account all the dynamical consistency conditions. Interestingly, these conditions exclude the parametric regimes for which $Q_* \gtrsim 1$, where the growing mode due to the coupling between inflaton and radiation perturbations would render the spectrum more blue-tilted and disfavoured by Planck. Hence, it is truly remarkable that consistency of the analysis leads to a full agreement with Planck and also to a finite range for the tensor-to-scalar ratio within the reach of B-mode polarisation experiments in the near future (see e.g. [51]).

5.2.2 Inflation with a Higgs-like potential: $V(\phi) = \frac{\lambda}{4}(\phi^2 - v^2)^2$

For a Higgs-like "mexican hat" inflaton potential, with inflation occurring in the "hilltop" part of the potential, we show in figs. 5.5 and 5.6 the regions in the $(g, M/M_P)$ plane where all dynamical consistency conditions are satisfied, for different values of the symmetry breaking scale v and two different values of the input Yukawa coupling h_0 (which differs from the physical value of the coupling as discussed below). We present a general analysis of the outcome only when $N_e = 60$, since the results are very similar for $N_e = 50$.

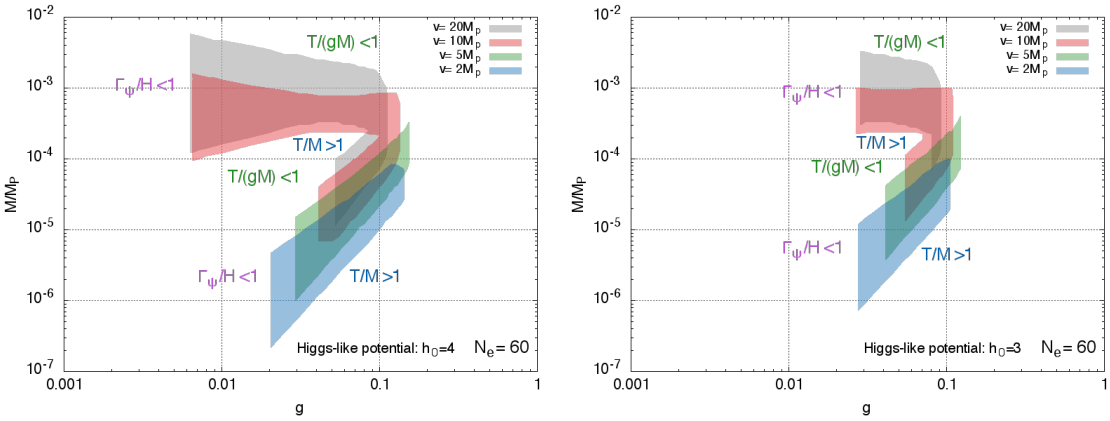

Figure 5.5: *Allowed regions in the $(g, M/M_P)$ plane for the Higgs-like potential with $h_0 = 3$ (right) and $h_0 = 4$ (left), for $N_e = 60$ and different values of the symmetry breaking scale v. Notice that there are no allowed regions for $h_0 \simeq 2$.*

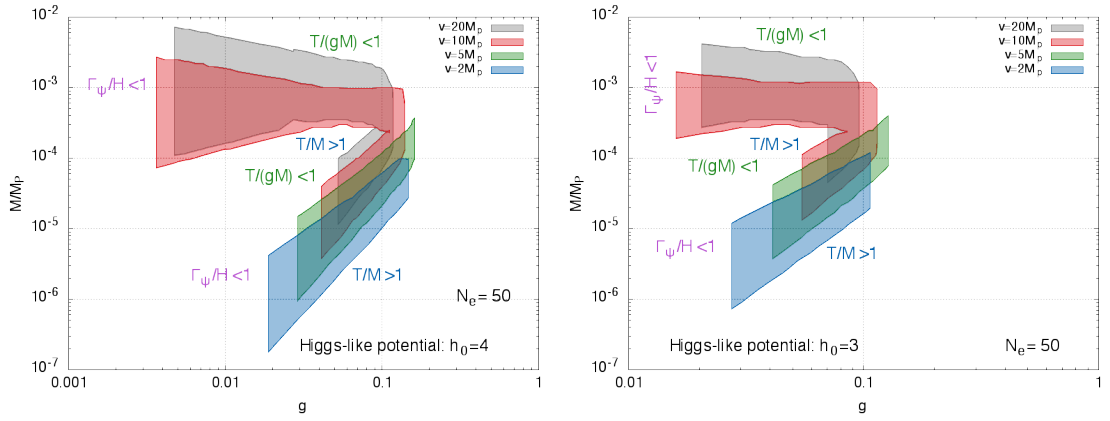

Figure 5.6: *Allowed regions in the $(g, M/M_P)$ plane for the Higgs-like potential with $h_0 = 3$ (right) and $h_0 = 4$ (left), for $N_e = 50$ and different values of the symmetry breaking scale v. Notice that there are no allowed regions for $h_0 \simeq 2$.*

As one can see in fig. 5.5, larger values of v imply larger values of the WLI symmetry breaking scale M, which may lie in a wider range than for the quartic potential studied earlier. As for the latter, the condition $\Gamma_\psi > H$ yields a lower bound on the coupling

$g \gtrsim 0.01$, while the conditions for light fermions and U(1) symmetry breaking yield an upper bound $g \lesssim 0.1$. We also find that the input value for the Yukawa coupling $h_0 \gtrsim 2$ in order to satisfy all consistency conditions, with larger values of h_0 increasing the allowed region in the $(g, M/M_P)$ plane.

Detailed limits on the parameters are given in Table 5.2, where one can see that the WLI scale $10^{-7}M_P \lesssim M \lesssim 10^{-2}M_P$ and that, despite the lower bound on h_0, the physical value of the Yukawa coupling can take values $h \lesssim 1$. In fact, we find that in this regime inflation occurs in the strong dissipation regime already at horizon-crossing, being consistent to have $Q_* \lesssim 10^3$. To better understand the different dynamical regimes at horizon-crossing, we plot in fig. (5.7) the relation between the physical couplings g and h and Q_* for $N_e = 60$.

$N_e = 60$

$h_0 = 4$	M_{min}/M_P	M_{max}/M_P	h_{min}	h_{max}	g_{min}	g_{max}	Q_{*min}	Q_{*max}
$v/M_P = 20$	1.15×10^{-5}	5.75×10^{-3}	0.475	3.559	6.3×10^{-3}	0.112	2.76×10^{-5}	58.237
$v/M_P = 10$	7.0×10^{-6}	1.6×10^{-3}	0.354	3.526	6.54×10^{-3}	0.135	3.135×10^{-5}	186.515
$v/M_P = 5$	1.0×10^{-6}	3.25×10^{-4}	0.243	2.154	0.029	0.153	2.95	704.09
$v/M_P = 2$	2.15×10^{-7}	8.5×10^{-5}	0.167	1.66	0.02	0.143	11.0	2999.9
$h_0 = 3$	M_{min}/M_P	M_{max}/M_P	h_{min}	h_{max}	g_{min}	g_{max}	Q_{*min}	Q_{*max}
$v/M_P = 20$	7.0×10^{-5}	3.25×10^{-3}	0.856	1.99	0.028	0.092	9.11×10^{-3}	7.32
$v/M_P = 10$	1.35×10^{-5}	1.0×10^{-3}	0.499	2.035	0.027	0.106	7.14×10^{-3}	48.4
$v/M_P = 5$	3.75×10^{-6}	4.0×10^{-4}	0.35	1.52	0.041	0.123	4.5	174.75
$v/M_P = 2$	7.25×10^{-7}	1.0×10^{-4}	0.229	1.112	0.028	0.106	20.18	883.8

$N_e = 50$

$h_0 = 4$	M_{min}/M_P	M_{max}/M_P	h_{min}	h_{max}	g_{min}	g_{max}	Q_{*min}	Q_{*max}
$v/M_P = 20$	1.15×10^{-5}	7.25×10^{-3}	0.475	4.04	4.75×10^{-3}	0.117	9.29×10^{-6}	65.55
$v/M_P = 10$	3.75×10^{-6}	2.75×10^{-3}	0.354	4.61	3.62×10^{-3}	0.141	3.19×10^{-6}	209.381
$v/M_P = 5$	9.25×10^{-7}	3.75×10^{-4}	0.241	2.233	0.029	0.162	3.55	805.51
$v/M_P = 2$	1.75×10^{-7}	9.75×10^{-5}	0.154	1.689	0.019	0.147	14.763	3983.59
$h_0 = 3$	M_{min}/M_P	M_{max}/M_P	h_{min}	h_{max}	g_{min}	g_{max}	Q_{*min}	Q_{*max}
$v/M_P = 20$	4.5×10^{-5}	4.25×10^{-3}	0.694	2.272	0.02	0.096	2.46×10^{-3}	14.714
$v/M_P = 10$	1.3×10^{-5}	1.7×10^{-3}	0.5	2.577	0.016	0.115	8.6×10^{-4}	54.289
$v/M_P = 5$	3.75×10^{-6}	4.0×10^{-4}	0.354	1.555	0.041	0.128	5.256	195.866
$v/M_P = 2$	7.25×10^{-7}	1.2×10^{-4}	0.228	1.120	0.027	0.107	24.48	991.673

Table 5.2: Allowed parametric ranges for the WLI scenario with a Higgs-like potential for $N_e = 60$ (top) and $N_e = 50$ (bottom), with $h_0 = 3, 4$ and for different values of the symmetry breaking scale v.

In fig. 5.7 we can clearly identify two distinct allowed parametric regimes. First, a regime where $h \gtrsim 1$ decreases with g that yields weak dissipation at horizon-crossing, much like for the quartic potential. Second, a regime where $h \lesssim 1$ increases with g where dissipation is already strong at horizon-crossing, $Q_* \gtrsim 1$, with Q_* increasing with decreasing values of h. The latter constitutes an allowed parametric window that was absent for the quartic potential.

Despite the larger parametric space found for the Higgs-like potential, in comparison with the quartic potential, we proceed to investigate the observational consistency

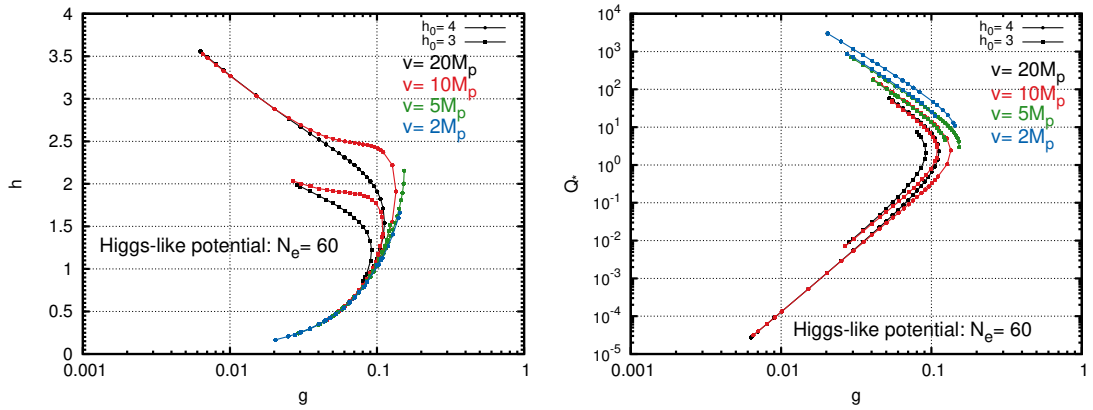

Figure 5.7: Allowed values of the physical couplings g and h (left) in the WLI scenario with a Higgs-like potential for $N_e = 60$ and two different values of the input parameter h_0, for distinct values of the inflaton potential minimum v. The corresponding values of Q_* are also plotted as a function of g (right).

of the allowed parametric ranges, particularly in the regime $Q_* \gtrsim 1$. The obtained inflationary observables are shown in fig. 5.8.

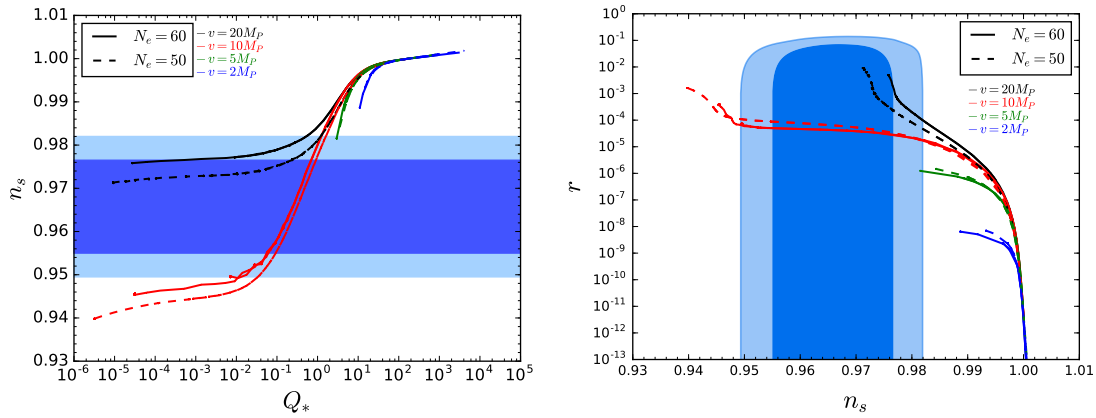

Figure 5.8: Observational predictions of the WLI scenario with a Higgs-like potential for 50-60 e-folds of inflation and different values of the symmetry breaking scale v. The plot on the left shows the spectral index n_s as a function of the dissipative ratio at horizon-crossing, Q_*, while the plot on the right shows the allowed trajectories in the (n_s, r) plane. The blue contours correspond to the 68% and 95% C.L. results from Planck 2015 TT+lowP data [87].

It is clear in fig. 5.8 that the parametric regime where $Q_* \gtrsim 1$ (and $h \lesssim 1$) is disfavoured by the Planck data, essentially due to the growing mode in the spectrum of inflaton perturbations associated with their coupling to radiation perturbations and which makes the spectrum more blue-tilted with increasing Q_*. Hence, in tune with what we found earlier for the quartic model, this scenario is only observationally viable for $Q_* \lesssim 1$ and values of the Yukawa coupling $h \gtrsim 1$, although we emphasise that Q is dynamical and a strong dissipative regime can be attained before the end of inflation. Values for which $Q_* \gtrsim 1$ correspond to the region $M \lesssim 10^{-4} M_P$, and therefore, like for the quartic model, agreement with Planck restricts the symmetry breaking scale

to the range $10^{-4}M_P \lesssim M \lesssim 10^{-2}M_P$. In addition, observations also restrict the Higgs symmetry breaking scale to the range $5M_P \lesssim v \lesssim 20M_P$, which is essentially a restriction on the η_ϕ slow-roll parameter at horizon-crossing [d]. An important difference between the Higgs-like potential and the quartic potential is that the tensor-to-scalar ratio can be much lower in the latter, with $r \gtrsim 10^{-6}$ for the Higgs-like potential in the allowed window.

5.2.3 Inflation with a non-renormalisable plateau-like potential: $V(\phi) = \lambda v^4 \left(1 - 3\frac{\phi^4}{v^4} + 2\frac{\phi^6}{v^6}\right)$.

To complete our discussion of inflationary potentials, we consider a non-renormalisable plateau-like potential with quartic and sextic inflaton monomials. This has a symmetry-breaking shape like the Higgs-like potential studied above, with the important difference that both slow-roll parameters ϵ_ϕ and η_ϕ vanish at the origin, making the resulting inflationary plateau much flatter. This potential is, in fact, very similar to the Coleman-Weinberg potential typically considered in several inflationary models (see e.g. [56]).

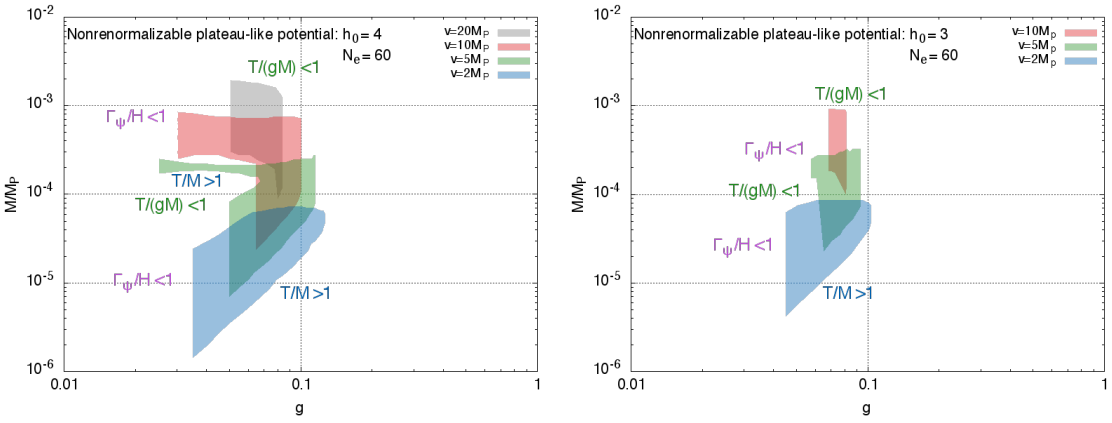

Figure 5.9: Allowed regions in the plane $(g, M/M_P)$ for the non-renormalisable plateau-like potential with $h_0 = 3$ (right) and $h_0 = 4$ (left), for $N_e = 60$ and different values of the symmetry breaking scale v. Notice that there are no allowed regions for $h_0 \simeq 2$.

In figs. 5.9 and 5.10 we show the regions in the $(g, M/M_P)$ plane where all dynamical consistency conditions are satisfied, for different values of the symmetry breaking scale v and two different values of the input Yukawa coupling h_0 (which differs from the physical value of the coupling). As for the Higgs-like potential, we report only the outcome at $N_e = 60$ for clarity of the plots, since the results are very similar for $N_e = 50$.

[d] Given that, without radiative corrections, $\eta_\phi = -4\left(\frac{M_P}{v}\right)^2 \frac{1-3x^2}{(1-x^2)^2}$, where $x = \phi/v$. From this we can see that the potential suffers from an "eta" problem and will not be able to sustain a long period of inflation for $v < 2M_P$.

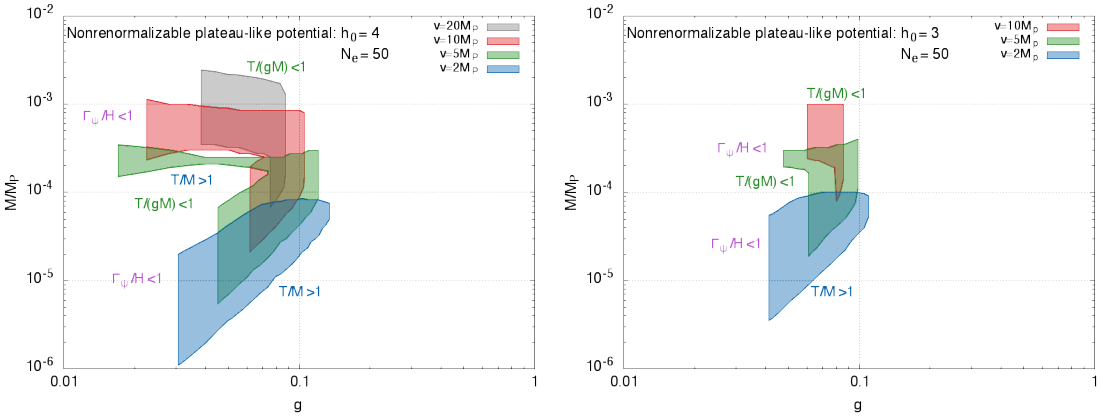

Figure 5.10: Allowed regions in the plane $(g, M/M_P)$ for the non-renormalisable plateau-like potential with $h_0 = 3$ (right) and $h_0 = 4$ (left), for $N_e = 50$ and different values of the symmetry breaking scale v. Notice that there are no allowed regions for $h_0 \simeq 2$.

fig. 5.9 shows that the allowed parametric regions for the non-renormalisable plateau-like potential are very similar to the Higgs-like potential, with larger values of v shifting the allowed window for the symmetry breaking scale M towards larger values, and larger values of h_0 enhancing the allowed parametric window. This window is somewhat narrower than for the Higgs-like potential, but again we find a lower bound $h_0 \gtrsim 2$ on the input value of the Yukawa coupling, and that $0.01 \lesssim g \lesssim 0.1$. In this case the decrease in the allowed parametric region between $h_0 = 4$ and $h_0 = 3$ is more pronounced than for the Higgs-like potential, and in fact the case $v = 20M_P$ is excluded by the dynamical consistency conditions for $h_0 = 3$. Detailed limits on the parameters are given in Table 5.3.

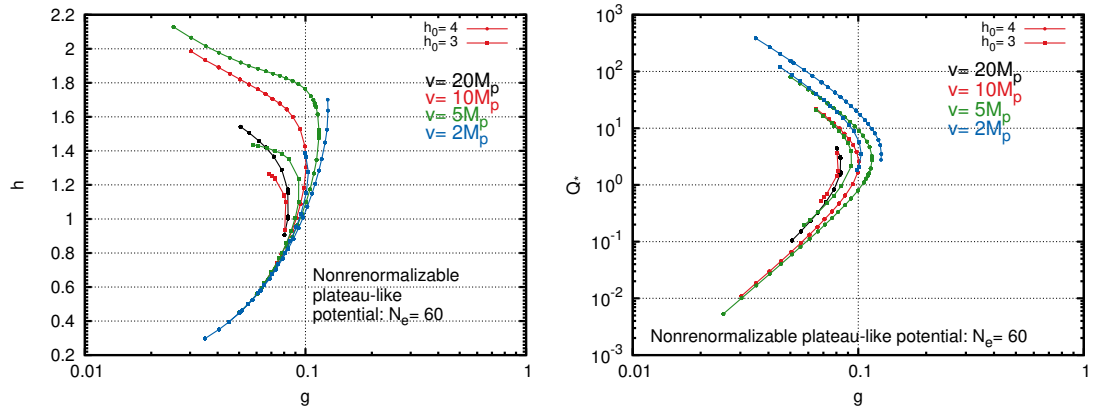

Figure 5.11: Allowed values of the physical couplings g and h (left) in the WLI scenario with a non-renormalisable plateau-like potential for $N_e = 60$ and two different values of the input parameter h_0, for distinct values of the inflaton minimum v. The corresponding values of Q_* are also plotted as a function of g (right).

For the plateau-like potential, we thus find that $10^{-6} \lesssim M/M_P \lesssim 10^{-3}$, and as for

the Higgs-like potential we also obtain an allowed region where $h \lesssim 1$ and $Q_* \gtrsim 1$. The dissipative ratio may also attain values $Q_* \lesssim 10^3$ in this case, although somewhat smaller than for the Higgs-like scenario. The relation between the physical couplings and Q_* is qualitatively analogous to the Higgs-like potential as shown in fig. 5.11.

$N_e = 60$

$h_0 = 4$	M_{min}/M_P	M_{max}/M_P	h_{min}	h_{max}	g_{min}	g_{max}	Q_{*min}	Q_{*max}
$v/M_P = 20$	9.0×10^{-5}	1.95×10^{-3}	0.906	1.542	0.051	0.084	0.105	4.413
$v/M_P = 10$	2.4×10^{-5}	8.5×10^{-4}	0.623	1.986	0.030	0.101	0.011	22.042
$v/M_P = 5$	7.0×10^{-6}	2.75×10^{-4}	0.449	2.129	0.025	0.115	5.33×10^{-3}	79.60
$v/M_P = 2$	1.45×10^{-6}	7.25×10^{-5}	0.298	1.701	0.035	0.127	2.776	385.681
$h_0 = 3$	M_{min}/M_P	M_{max}/M_P	h_{min}	h_{max}	g_{min}	g_{max}	Q_{*min}	Q_{*max}
$v/M_P = 20$	$--$	$--$	$--$	$--$	$--$	$--$	$--$	$--$
$v/M_P = 10$	1.0×10^{-4}	9.25×10^{-4}	0.932	1.266	0.069	0.081	0.526	3.726
$v/M_P = 5$	2.3×10^{-5}	3.25×10^{-4}	0.625	1.436	0.058	0.093	0.196	20.894
$v/M_P = 2$	4.25×10^{-6}	8.5×10^{-5}	0.396	1.389	0.045	0.103	1.799	119.033

$N_e = 50$

$h_0 = 4$	M_{min}/M_P	M_{max}/M_P	h_{min}	h_{max}	g_{min}	g_{max}	Q_{*min}	Q_{*max}
$v/M_P = 20$	6.75×10^{-5}	2.45×10^{-3}	0.786	1.764	0.038	0.088	0.029	7.876
$v/M_P = 10$	2.1×10^{-5}	1.15×10^{-3}	0.584	2.284	0.022	0.105	3.2×10^{-3}	29.013
$v/M_P = 5$	5.5×10^{-6}	3.5×10^{-4}	0.396	2.514	0.017	0.121	1.125×10^{-3}	118.615
$v/M_P = 2$	1.1×10^{-6}	8.5×10^{-5}	0.256	1.771	0.031	0.134	3.409	603.231
$h_0 = 3$	M_{min}/M_P	M_{max}/M_P	h_{min}	h_{max}	g_{min}	g_{max}	Q_{*min}	Q_{*max}
$v/M_P = 20$	$--$	$--$	$--$	$--$	$--$	$--$	$--$	$--$
$v/M_P = 10$	8.0×10^{-5}	1.0×10^{-3}	0.879	1.427	0.060	0.086	0.23	5.404
$v/M_P = 5$	1.9×10^{-5}	4.0×10^{-4}	0.570	1.602	0.048	0.099	0.077	29.578
$v/M_P = 2$	3.5×10^{-6}	1.0×10^{-4}	0.357	1.532	0.041	0.110	1.404	169.071

Table 5.3: Allowed parametric ranges for the WLI scenario with a non-renormalisable plateau-like potential for $N_e = 60$ (top) and $N_e = 50$ (bottom), with $h_0 = 3, 4$ and for different values of the symmetry breaking scale v.

Not surprisingly, scenarios with strong dissipation at horizon-crossing are observationally disfavoured by Planck data, again due to the growing mode in the power spectrum, as shown in fig. 5.12. Nevertheless, we may have viable scenarios with $Q_* \sim 3$ in this case, which is somewhat larger than for the other potentials studied in this work, and also for $v = 2M_P$, which did not occur for the Higgs-like potential. Of the three forms of the potential considered in this work, this flatter plateau is thus the one that allows for stronger dissipation at horizon-crossing and hence larger values of the inflaton mass compared to the Hubble parameter, showing that warm inflation can significantly alleviate the "eta-problem". The non-renormalisable plateau also yields lower allowed values for the tensor-to-scalar ratio, with $r \gtrsim 10^{-8}$ in this case.

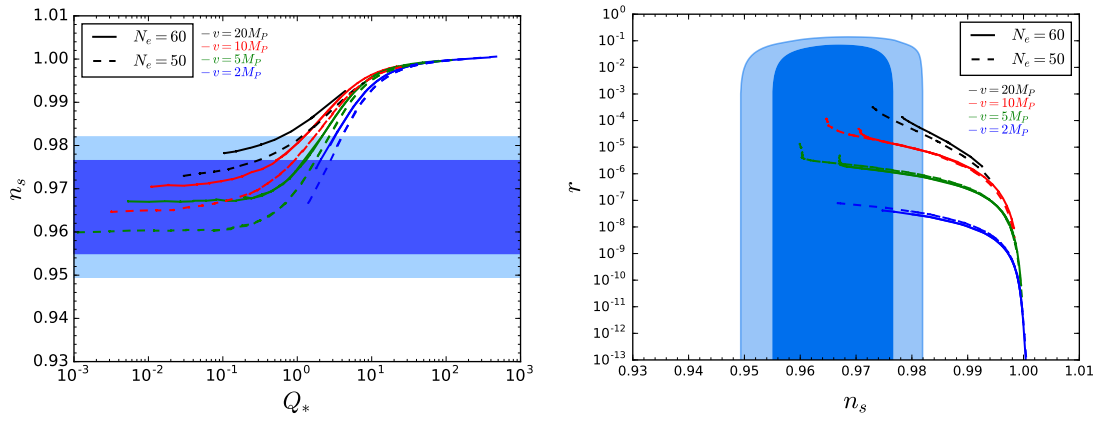

Figure 5.12: Observational predictions of the WLI scenario with a non-renormalisable plateau-like potential for 50-60 e-folds of inflation and different values of the symmetry breaking scale v. The plot on the left shows the spectral index n_s as a function of the dissipative ratio at horizon-crossing, Q_*, while the plot on the right shows the allowed trajectories in the (n_s, r) plane. The blue contours correspond to the 68% and 95% C.L. results from Planck 2015 TT+lowP data [87].

5.3 Final remarks

In this work, we have studied the implementation of the *Warm Little Inflaton* scenario [23] for different forms of the inflaton potential, considering a large-field chaotic model and small-field models like the Higgs-like and non-renormalisable plateau-like potentials. We have scanned the parameter space of the model imposing all the relevant consistency conditions and compared the associated observational predictions with the most recent Planck data. We have included in our analysis all thermal corrections to the effective scalar potential that remain upon cancellation of the leading inflaton thermal mass corrections.

Although results are quantitatively different for the three potentials, we have found several generic features of the WLI model. Consistent realisations require a coupling between the inflaton and fermion fields $0.01 \lesssim g \lesssim 0.1$ and that the latter decay through a Yukawa coupling $h \gtrsim 1$ (although within the perturbative regime $h \lesssim 3.5$). Within these limits, observe in figs. 5.7 and 5.11 the difference in the numerical values of the input parameter h_0 compared to the true physical coupling h. This is particularly pronounced for the Higgs-like and non-renormalisable potentials, for instance, in the plot g vs h of fig. 5.7 when $h_0 = 4$ (circles) its physical values h start at 3.5 and end when $h < 0.5$. As such, this represents a considerable difference between the input h_0 and the physical h. In contrast, the difference between both couplings is negligible for the chaotic quartic potential. Thus, this ensures that the fermions can

remain light throughout inflation ($gM \lesssim T$) for temperatures below the symmetry breaking scale $T \lesssim M$, and that they decay faster than the inflationary expansion. The Yukawa coupling h can reach up to the higher end of the perturbative limit, which arises precisely due to having to enforce the adiabatic condition that ensures the thermal bath is maintained. Imposing these requirements we have found that the condition for a warm inflationary regime, $T \gtrsim H$, is easily satisfied, not imposing any additional constraints. Dynamical consistency also imposes 10^{12} GeV $\lesssim M \lesssim 10^{16}$ GeV, with observations favouring the larger values, thus suggesting a possible connection between the WLI scenario and grand unification theories.

For the quartic chaotic scenario, dynamical consistency imposes $Q_* \lesssim 0.1$ for the dissipative ratio at horizon-crossing, while for the two hilltop potentials dynamical constraints allow for $Q_* \lesssim 10^3$. However, we have found that all scenarios with $Q_* \gtrsim 1$ are disfavoured by the Planck data, essentially due to a growing mode in the curvature power spectrum associated with the coupling between inflaton and radiation fluctuations that is present in all warm inflation scenarios with $\Upsilon \propto T^n$, $n > 0$, and which generically leads to larger n_s values. Nevertheless, in all cases discussed we may reach values of Q_* close or even slightly above unity, and since Q grows throughout inflation for all potentials considered, we have thus obtained scenarios where the dynamics of warm inflation occurs essentially in the strong dissipation regime, $Q > 1$, and for which the "eta-problem" can thus be significantly alleviated.

The dynamical and observational constraints (essentially on the scalar spectral index n_s) also allow us to place lower limits on the tensor-to-scalar ratio ranging from $r \gtrsim 10^{-3}$ for the quartic model down to $r \gtrsim 10^{-8}$ for the plateau-like potential, and in all cases consistent models have $r \lesssim 10^{-2}$. In the chaotic model the dynamical constraints are, in fact, sufficient to limit the values of n_s and r to values within the Planck bounds, with $10^{-3} \lesssim r \lesssim 10^{-2}$ being potentially within the reach of ongoing and planned B-mode polarisation experiments [51].

The remarkable agreement of the quartic potential with Planck data is particularly significant given that such self-interactions should generically be present in the scalar potential, not being forbidden by any symmetries[e], and dominate over a quadratic mass term for sufficiently large field values. This scenario thus yields the most natural renormalisable realisation of chaotic inflation, where slow-roll is a phase-space attractor as opposed to plateau-like models (see e.g. [93]). While in the absence of dissipation its predictions are in severe tension with observational data [87], it is in perfect agreement

[e]The interchange symmetry actually requires the potential to be of the form $V(\phi) = \lambda M^4(\phi/M - \pi/2)^4$, but this is well approximated by a quartic monomial for $\phi \gg M$.

with Planck within the WLI realisation of warm inflation (see also [58]).

Of course that, as in cold inflation models, several scalar potentials will be excluded by observational data within the WLI scenario. We have focused, in this work, on three types of potential for which we find agreement with observations in a broad region of parameter space, thus showing that the WLI scenario can lead to different realisations of warm inflation that are both dynamically and observationally consistent. The modifications to the primordial perturbation spectrum induced by dissipative and thermal effects within the WLI scenario generically lead to a more blue-tilted scalar spectrum and a more suppressed tensor component with respect to cold inflation models with the same potential functions. Hence, scalar potentials that were excluded within the cold inflation paradigm for being too red-tilted and yielding a too large tensor-to-scalar ratio are generically in better agreement with observations within warm inflation.

Chapter 6

DM model

> "Oneness, then, is all that I predicate of the originally created Matter; but I propose to show that this Oneness is a principle abundantly sufficient to account for the constitution, the existing phenomena and the plainly inevitable annihilation of at least the material Universe.
> The willing into being the primordial particle, has completed the act, or more properly the conception, of Creation. We now proceed to the ultimate purpose for which we are to suppose the Particle created-that is to say, the ultimate purpose so far as our considerations yet enable us to see it-the constitution of the Universe from it, the Particle."
>
> —Edgar Allan Poe, Eureka: a prose poem.

In the essential WI scheme, the sole requirement is that radiation energy is produced during inflation and that mechanism of production is due to dissipative effects on the inflaton. Thereby if all microscopic motion is slow relative to the relevant microscopic time scales, the macroscopic dynamics can be treated adiabatically; and if the interactions are weak, perturbation theory is applicable. Hence, in such a thermalised, adiabatic, perturbative regime, a well formulated quantum field theory dissipative dynamics can be formulated. The original idea of a quantum multi-field warm inflation model was proposed in [27–29], called distributed mass (DM) model, built on the context of string theory. The model was intended to illustrate a scheme developed by first principles inspired by string theories exhibiting $\mathcal{N} = 1$ global supersymmetry, with the inflaton coupled to massive modes of the string [32]. Thus the DM model describes how the interaction between the inflaton ϕ and any other light constituents (fermion or scalar fields), establishes a mass scale distribution for such fields, which is determined by the mass parameter M. The key property of the DM

model is that for a given temperature T, only the fields with masses $g^2(\phi - M_i)^2 \lesssim T^2$ will contribute to the dissipation, where g is a coupling constant.

Inflation is assumed to be described by low-energy Effective Field Theory (EFT), although in many models inflation can happen when the inflaton field is super-Planckian, particularly by considering monomial chaotic potentials in cold inflation. Furthermore, an EFT can be ultraviolet (UV) complete if it can be successfully incorporated in a quantum theory of gravity, such as String Theory. This paradigm provides a vast landscape of consistent embeddings of the EFT of gravity into a quantum theory, but this does not imply that any EFT coupled to gravity is consequently included in the landscapes. Those EFT's that are in fact inconsistent with a quantum theory of gravity lie in the surrounding swamplands [94, 95]. Hence, a benchmark is needed to ensure a de Sitter vacuum EFT can live in the desired string landscapes. Recently two swampland criteria relevant for inflationary theories have been proposed [96, 97], $|\Delta\phi|/M_P < \Delta$ and $M_P|V_\phi|/V > c$, provided that $V > 0$, where $\{\Delta, c\} \sim \mathcal{O}(1)$. Nonetheless, these criteria have been noted to pose inherent threats to the basic mechanism of slow-roll in cold inflation [97]. However, as part of the subsequent analysis we evaluate the aforementioned criteria in the warm inflation scenario. We show models of warm inflation that can be very consistent with the swampland criteria. Inherently the dissipative feature in warm inflation makes it amenable for consistency with swampland criteria, as already noted in the literature [98–102].

6.1 Supersymmetric distributed mass model

Let us consider the general form of an effective $\mathcal{N} = 1$ global SUSY theory version of the distributed mass (DM) model with chiral superfields Φ, X_i and Y_i, described by the superpotential [20, 21, 72, 89]:

$$W = \sum_i \left[\frac{g}{2}(\Phi - M_i)X_i^2 + \frac{h}{2} X_i Y_i^2 \right] , \tag{6.1}$$

where g and h are coupling constants. The chiral superfields Φ, X_i and Y_i have (scalar, fermion) components (ϕ,ψ_ϕ), (χ_i,ψ_{χ_i}) and (σ_i,ψ_{σ_i}), respectively. Note that these are complex scalars and Weyl fermions, each with two degrees of freedom. We may use the Majorana representation for the spinors, i.e. use a 4-component Majorana spinor built from the same Weyl fermion. In this case, note that a Majorana fermion is its own anti-particle. The sum in the superpotential is taken over all the states in the tower.

We have taken different Y_i fields coupled to each X_i field in the tower to avoid mass mixing at the level of the thermal masses.

The scalar interaction terms in the theory are obtained from the superpotential using:

$$-\mathcal{L}_S = |\partial_\Phi W|^2 + \sum_i |\partial_{X_i} W|^2 + \sum_i |\partial_{Y_i} W|^2 \,, \tag{6.2}$$

where

$$\partial_\Phi W = \sum_i \frac{g}{2} X_i^2 \,, \tag{6.3}$$

$$\partial_{X_i} W = g(\Phi - M_i) X_i + \frac{h}{2} Y_i^2 \,, \tag{6.4}$$

$$\partial_{Y_i} W = h X_i Y_i \,, \tag{6.5}$$

hence

$$|\partial_\Phi W|^2 = \sum_{i,j} \frac{g^2}{4} X_i^2 (X_j^\dagger)^2 \,, \tag{6.6}$$

$$\begin{aligned} |\partial_{X_i} W|^2 &= g^2 (\Phi - M_i)(\Phi - M_i)^\dagger X_i X_i^\dagger + \frac{h^2}{4} Y_i^2 (Y_i^\dagger)^2 \\ &\quad + \frac{gh}{2}(\Phi - M_i) X_i (Y_i^\dagger)^2 + \frac{gh}{2}(\Phi - M_i)^\dagger X_i^\dagger Y_i^2 \,, \end{aligned} \tag{6.7}$$

$$|\partial_{Y_i} W|^2 = h^2 X_i X_i^\dagger Y_i Y_i^\dagger \,. \tag{6.8}$$

By selecting the boson field components of the chiral superfields Φ, X_i and Y_i, which are ϕ, χ_i and σ_i, respectively. We obtain:

$$\begin{aligned} -\mathcal{L}_S &= g^2 \sum_i |\phi - M_i|^2 |\chi_i|^2 + \frac{gh}{2} \sum_i \left[(\phi - M_i) \chi_i (\sigma_i^\dagger)^2 + (\phi - M_i)^\dagger \chi_i^\dagger \sigma_i^2 \right] \\ &\quad + h^2 \sum_i |\chi_i|^2 |\sigma_i|^2 + \frac{g^2}{4} \sum_{i,j} \chi_i^2 (\chi_j^\dagger)^2 + \frac{h^2}{4} \sum_i |\sigma_i|^4 \,. \end{aligned} \tag{6.9}$$

The fermion Lagrangian can be computed from the general formula:

$$-\mathcal{L}_F = \frac{1}{2} \sum_{n,m} \frac{\partial^2 W}{\partial \xi_n \partial \xi_m} \bar{\psi}_n P_L \psi_m + \frac{1}{2} \sum_{n,m} \frac{\partial^2 W^\dagger}{\partial \xi_n^\dagger \partial \xi_m^\dagger} \bar{\psi}_n P_R \psi_m \,, \tag{6.10}$$

where ξ_n is a superfield and $P_L = 1 - P_R = (1+\gamma_5)/2$ are the chiral projection operators acting on Majorana 4-spinors. Note that $\partial W / \partial X_i \partial Y_i = \partial W / \partial Y_i \partial X_i$ and similarly $\partial W^\dagger / \partial X_i^\dagger \partial Y_i^\dagger = \partial W^\dagger / \partial Y_i^\dagger \partial X_i^\dagger$. Then by selecting the boson field components of the

chiral superfields Φ, X_i and Y_i, which are ϕ, χ_i and σ_i, respectively, we obtain:

$$\begin{aligned}
-\mathcal{L}_F &= \frac{g}{2}\sum_i(\phi - M_i)\bar{\psi}_{\chi_i}P_L\psi_{\chi_i} + \frac{g}{2}\sum_i(\phi - M_i)^\dagger\bar{\psi}_{\chi_i}P_R\psi_{\chi_i} \\
&\quad + g\sum_i \chi_i\bar{\psi}_\phi P_L\psi_{\chi_i} + g\sum_i \chi_i^\dagger\bar{\psi}_\phi P_R\psi_{\chi_i} + \frac{h}{2}\sum_i \chi_i\bar{\psi}_{\sigma_i}P_L\psi_{\sigma_i} \\
&\quad + \frac{h}{2}\sum_i \chi_i^\dagger\bar{\psi}_{\sigma_i}P_R\psi_{\sigma_i} + \frac{h}{2}\sum_i \chi_i\bar{\psi}_{\sigma_i}P_L\psi_{\sigma_i} + \frac{h}{2}\sum_i \chi_i^\dagger\bar{\psi}_{\sigma_i}P_R\psi_{\sigma_i} \\
&\quad + h\sum_i \sigma_i\bar{\psi}_{\sigma_i}P_L\psi_{\chi_i} + h\sum_i \sigma_i^\dagger\bar{\psi}_{\sigma_i}P_R\psi_{\chi_i}\,. \qquad (6.11)
\end{aligned}$$

Note that by decomposing the fields into their real and imaginary part via $\phi = (\phi_R + i\phi_I)/\sqrt{2}$, then the modulus square $|\phi - M_i|^2$ becomes $(\phi_R/\sqrt{2} - M_i)^2 + \phi_I^2/2$, where $\phi_R/\sqrt{2}$ is the expectation value of the inflaton field. So this definition introduces another decay channel, namely:

$$\begin{aligned}
-\mathcal{L}_S &= g^2\sum_i\left(\frac{\phi_R}{\sqrt{2}} - M_i\right)^2|\chi_i|^2 + g^2\sum_i\frac{\phi_I^2}{2}|\chi_i|^2 \\
&\quad + \frac{gh}{2}\sum_i\left(\frac{\phi_R}{\sqrt{2}} - M_i\right)\left[\chi_i(\sigma_i^\dagger)^2 + \chi_i^\dagger\sigma_i^2\right] + \frac{gh}{2}\sum_i\frac{i\phi_I}{\sqrt{2}}\left[\chi_i(\sigma_i^\dagger)^2 - \chi_i^\dagger\sigma_i^2\right] \\
&\quad + h^2\sum_i|\chi_i|^2|\sigma_i|^2 + \frac{g^2}{4}\sum_i|\chi_i|^4 + \frac{h^2}{4}\sum_i|\sigma_i|^4\,, \qquad (6.12) \\
-\mathcal{L}_F &= \frac{g}{2}\sum_i\left(\frac{\phi_R}{\sqrt{2}} - M_i\right)\bar{\psi}_{\chi_i}P_L\psi_{\chi_i} + \frac{g}{2}\sum_i\left(\frac{\phi_R}{\sqrt{2}} - M_i\right)\bar{\psi}_{\chi_i}P_R\psi_{\chi_i} \\
&\quad \frac{g}{2}\sum_i\frac{i\phi_I}{\sqrt{2}}\bar{\psi}_{\chi_i}P_L\psi_{\chi_i} - \frac{g}{2}\sum_i\frac{i\phi_I}{\sqrt{2}}\bar{\psi}_{\chi_i}P_R\psi_{\chi_i} \\
&\quad + g\sum_i \chi_i\bar{\psi}_\phi P_L\psi_{\chi_i} + g\sum_i \chi_i^\dagger\bar{\psi}_\phi P_R\psi_{\chi_i} \\
&\quad + \frac{h}{2}\sum_i \chi_i\bar{\psi}_{\sigma_i}P_L\psi_{\sigma_i} + \frac{h}{2}\sum_i \chi_i^\dagger\bar{\psi}_{\sigma_i}P_R\psi_{\sigma_i} \\
&\quad + h\sum_i \sigma_i\bar{\psi}_{\sigma_i}P_L\psi_{\chi_i} + h\sum_i \sigma_i^\dagger\bar{\psi}_{\sigma_i}P_R\psi_{\chi_i}\,. \qquad (6.13)
\end{aligned}$$

However, as $\phi_R/\sqrt{2}$ is the nonzero vacuum expectation value of ϕ, which will be the only term that will contribute to dissipation in the scalar fields effective equation of motion, then the imaginary part of the inflaton ϕ_I is not relevant for the subsequent analysis. Moreover, in order to be coherent with further calculations, ϕ is going to be considered only as the classical expectation value, without the label R and the factor $1/\sqrt{2}$. Therefore the relevant Lagrangians that may contribute to dissipation in the

scalar fields effective equation of motion are:

$$
\begin{aligned}
-\mathcal{L}_S &= g^2 \sum_i (\phi - M_i)^2 |\chi_i|^2 + \frac{gh}{2} \sum_i (\phi - M_i) \left[\chi_i (\sigma_i^\dagger)^2 + \chi_i^\dagger \sigma_i^2 \right] \\
&\quad + h^2 \sum_i |\chi_i|^2 |\sigma_i|^2 + \frac{g^2}{4} \sum_i |\chi_i|^4 + \frac{h^2}{4} \sum_i |\sigma_i|^4 \,, \qquad (6.14) \\
-\mathcal{L}_F &= \frac{g}{2} \sum_i (\phi - M_i) \, \bar{\psi}_{\chi_i} P_L \psi_{\chi_i} + \frac{g}{2} \sum_i (\phi - M_i) \, \bar{\psi}_{\chi_i} P_R \psi_{\chi_i} \\
&\quad + \frac{h}{2} \sum_i \chi_i \bar{\psi}_{\sigma_i} P_L \psi_{\sigma_i} + \frac{h}{2} \sum_i \chi_i^\dagger \bar{\psi}_{\sigma_i} P_R \psi_{\sigma_i} \\
&\quad + h \sum_i \sigma_i \bar{\psi}_{\sigma_i} P_L \psi_{\chi_i} + h \sum_i \sigma_i^\dagger \bar{\psi}_{\sigma_i} P_R \psi_{\chi_i} \,. \qquad (6.15)
\end{aligned}
$$

Once we decompose the inflaton field, we can identify the bare masses of the χ_i's and ψ_{χ_i}'s as: $m_{\psi_{\chi_i}} = g\,(\varphi - M_i) = m_{\chi_i}$; at zero temperature for unbroken SUSY[a]. This is in agreement with [89] upon rescaling the couplings g and h in the superpotential by 1/2 factors.

At finite temperature, both the χ_i and ψ_{χ_i} receive thermal mass corrections. The contributions of the σ_i and ψ_{σ_i} fields to the latter have been computed in [89] and been shown to be identical for both χ_i and ψ_{χ_i}, corresponding to $h^2T^2/8$ taking into account the coupling normalisation differences. The χ_i scalars also receive thermal corrections from their self-interactions $g^2|\chi_i|^4/4$. Noting that these interactions give a contribution to their tree-level mass $\partial^2 V/\partial\chi_i\partial\chi_i^\dagger = g^2|\chi_i|^2$ and taking into account the contribution of the χ_i fields to the thermal effective potential:

$$
\Delta V_T \subset 2 \times \frac{m_{\chi_i}^2}{24} T^2 = \frac{g^2}{12} T^2 |\chi_i|^2 + \dots \,, \qquad (6.16)
$$

where we have taken into account the two degrees of freedom for complex scalars, this yields a thermal mass correction $g^2T^2/12$ to the χ_i fields. In summary, we obtain:

$$
\Delta m_{\chi_i}^2 = \frac{g^2}{12} T^2 + \frac{h^2}{8} T^2 \,, \qquad \Delta m_{\psi_{\chi_i}}^2 = \frac{h^2}{8} T^2 \,. \qquad (6.17)
$$

We also need to compute the finite temperature decay widths of the χ_i and ψ_{χ_i} fields, however, we only recall such calculations for Dirac fermions [20]; albeit the difference between Majorana and Dirac fermions is only in the overall factors of the decay width. Hence, we can first compute them at zero temperature to set the correct normalisation

[a] Note that in warm inflation SUSY is broken both by the finite temperature and the inflaton energy density. The latter should arise from an additional Φ-dependent term in the superpotential that we have note included above and that will lead to a small splitting of the mass for the real and imaginary components of the χ_i scalar fields.

factors in order to identify these global constants. In general we have for the decay of a particle of mass m at rest into a pair of massless particles:

$$\Gamma = \frac{S}{16\pi m}|\mathcal{M}|^2\,, \tag{6.18}$$

where $S = 1/2$ if the particles are identical and $S = 1$ if they are distinct. The χ_i fields may decay via $\chi_i \to \sigma_i\sigma_i$ and $\chi_i \to \psi_{\sigma_i}\psi_{\sigma_i}$. In the first case, dropping the indices for simplicity, we may decompose the fields into their real and imaginary components via $\chi = (\chi_R + i\chi_I)/\sqrt{2}$ and analogously for σ. This yields the scalar interactions:

$$-\mathcal{L}_{\chi\sigma^2} = \frac{hg}{2\sqrt{2}}(\phi - M_i)\left[\chi_R\sigma_R^2 - \chi_R\sigma_I^2 + 2\chi_I\sigma_R\sigma_I\right]\,. \tag{6.19}$$

Hence, the χ_R scalar may decay into σ_R or σ_I pairs, while the χ_I scalar has only one decay channel $\chi_I \to \sigma_R\sigma_I$. For each of these decay channels, the vertex factor is $-ihg(\phi - M_i)/\sqrt{2}$. Taking into account the $S = 1/2$ factors in the $\chi_R \to \sigma_R\sigma_R$ and $\chi_R \to \sigma_I\sigma_I$ channels, we then find that the decay widths are equal for both χ_R and χ_I, being given by:

$$\Gamma^S_{\chi_i} = \frac{h^2g^2(\phi - M_i)^2}{32\pi m_{\chi_i}}\,. \tag{6.20}$$

The fermionic decay channel comes from the interaction term $\frac{1}{2}h\chi_i\bar{\psi}_{\sigma_i}\psi_{\sigma_i}$, where the vertex factor is simply $-ih$. Since the particles are identical in the final state and computing the matrix element with the usual Feynman rules, this yields:

$$\Gamma^F_{\chi_i} = \frac{h^2}{32\pi}m_{\chi_i}\,. \tag{6.21}$$

Noting that, at zero temperature, $m_{\chi_i} = g(\phi - M_i)$, we see that $\Gamma^S_{\chi_i} = \Gamma^F_{\chi_i}$ in this limit. The fermions ψ_{χ_i} can decay as $\psi_{\chi_i} \to \sigma_i\psi_{\sigma_i}$ via the corresponding Yukawa term above, and this yields simply:

$$\Gamma_{\psi_{\chi_i}} = \frac{h^2}{16\pi}m_{\psi_{\chi_i}}\,. \tag{6.22}$$

Again, note that at zero temperature for unbroken SUSY we have $m_{\chi_i} = m_{\psi_{\chi_i}} = g(\phi - M_i)$, which yields identical total decay widths for the scalars and fermionic superpartners, as it should.

6.1.1 Identifying the vertex factor

From [20] we can identify the vertex factor of the decay of a scalar boson to fermions and the decay of a fermion to a scalar boson and a fermion, by taking the limit $T \to 0$ and comparing with eqs. 6.21 and 6.22, respectively. The first one $\frac{1}{2}h\chi_i\bar{\psi}_{\sigma_i}\psi_{\sigma_i}$, we take

the limit $T \to 0$ and use the pole approximation ($p_0 = \omega_X(p) \simeq m_{\chi_i}$) of eq.(B.12) from [20], it yields:

$$\Gamma^F_{\chi_i} \simeq \frac{g^2_{X1}}{8\pi} m_{\chi_i} \,, \tag{6.23}$$

hence by comparing with eq. 6.21 we have $g^2_{X1} = h^2/4$. Then, for the second process $\psi_{\chi_i} \to \sigma_i \psi_{\sigma_i}$ we use eqs. (B.17-B.20) from [20] having:

$$\Gamma_{\psi_{\chi_i}} = \frac{g^2_{X2}}{16\pi} m_{\psi_{\chi_i}} \,, \tag{6.24}$$

therefore $g^2_{X2} = h^2$. From here we will use above overall factors for the rest of the computations.

6.2 Interactions

The particle physics model considered in this work is inspired by string theory exhibiting $\mathcal{N} = 1$ global supersymmetry, with the inflaton field coupled to massive modes of the string, as discussed in [32]. Several interactions are identified by the shifted couplings $g^2(\phi - M_i)^2\chi_i^2$, and $g(\phi - M_i)\bar{\psi}_{\chi_i}\psi_{\chi_i}$ for bosons χ_i and fermions ψ_{χ_i} respectively, with $\{M_i\}$ ranging over mass scales. This feature yields the name of distributed-mass-model (DM-model). In the subsequent segments we establish the relevant interplay the inflaton field has with the aforementioned fields. We will restrict to interactions such that the leading contribution will come dominantly from one-loop processes, when the decaying field is light. The key property of the DM model is that for a given temperature T, only the fields with masses $g^2(\phi - M_i)^2 \lesssim T^2$ will contribute to the dissipation. Henceforth, we will refer such configuration of states as thermally excited sites. We will consider separately the dissipative processes associated with the excitation of the scalar χ_i fields, which may decay via $\chi_i \to \sigma_i\sigma_i$ or $\chi_i \to \bar{\psi}_{\sigma_i}\psi_{\sigma_i}$, and those associated with the excitation of the fermionic ψ_{χ_i} fields, which decay via $\psi_{\chi_i} \to \sigma_i\psi_{\sigma_i}$, with technical details of the computation given in the following sections.

6.2.1 Bosonic sector

The leading contribution to the dissipative coefficient from scalar χ_i arises at one-loop order, as illustrated in fig. 6.1, and has the following form [20, 21]:

$$\Upsilon^S = \sum_{i=1}^{t.e} \frac{4}{T}\left(\frac{g^2}{2}\right)^2 (\phi - M_i)^2 \int \frac{d^4p}{(2\pi)^4}\rho^2_\chi n_B(1 + n_B) \,, \tag{6.25}$$

where 't.e.' means sum over all thermally excited sites, $n_B = [e^{p_0/T} - 1]^{-1}$ is the Bose-Einstein distribution and ρ_χ is the spectral function for the χ_i field. The spectral function for the χ_i field entering in eq.(6.25) corresponds to the fully dressed propagator, including the effect of their finite decay width into σ and ψ_σ particles:

$$\rho_\chi(p, p_0) = \frac{4\omega_p \Gamma_\chi}{(p_0^2 - \omega_p^2)^2 + 4\omega_p^2 \Gamma_\chi^2}\,, \tag{6.26}$$

where $\omega_p = \sqrt{\tilde{m}_{\chi\, i}^2 + p^2}$ and $\tilde{m}_{\chi\, i}^2 = m_{\chi\, i}^2 + g^2/12 + h^2 T^2/8$. The leading process contribution to the decay width of the χ_i fields is then the two-body decay $\chi_i \to \sigma_i \sigma_i$ and $\chi_i \to \bar{\psi}_{\sigma_i} \psi_{\sigma_i}$; where at finite temperature we include contributions from both decays and inverse decay, as well as thermal scattering off particles in the radiation bath.

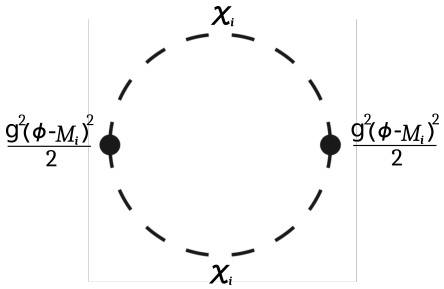

Figure 6.1: Feynman diagram contributing to the bosonic dissipative coefficient at leading order.

In order to compute both decay widths and the resulting dissipative coefficient, let me introduce three different methods to solve eq. (6.25). For simplicity I will omit, in the subsequent segments, the sum in the dissipative coefficient.

Full integral: numerical computation

Expanding all integrals, after solving the angular ones, we have:

$$\Upsilon_i^S = \frac{g^4}{4\pi^3} \frac{(\phi - M_i)^2}{T} \int dp \int dp_0 p^2 \rho_\chi^2 n_B (1 + n_B)\,, \tag{6.27}$$

then, let us define I_B as:

$$I_B = \int dp \int dp_0 p^2 \rho_\chi^2 n_B (1 + n_B)\,. \tag{6.28}$$

To solve numerically I_B, we have to do a conformal mapping in the variables of integration, as follows:

$$p_0 = \frac{x}{1-x}\,, \qquad p = \frac{y}{1-y}\,, \qquad J(x,y) = \frac{1}{(1-x)^2(1-y)^2}\,, \tag{6.29}$$

then the integration interval is only $[0,1]$. Therefore we have:

$$I_B = \int_0^1 dy \int_0^1 dx \frac{y^2}{(1-y)^4}\frac{1}{(1-x)^2}\rho_\chi^2(x,y) n_B(x,y)(1+n_B(x,y))\,. \tag{6.30}$$

Pole contribution: numerical computation

An analysis of Eq.(6.25) indicates that the behaviour of the dissipation coefficient in the different temperature and interaction regimes is determined by an interplay between the spectral function and the thermal occupation numbers. When the temperature is large, the occupation numbers are also large, so in this regime, the poles of the spectral functions will dominate the integral and this will be referred to as the pole approximation. As such, the pole approximation works well in the high-T region. The dissipation coefficient about its pole at $p_0 \simeq \omega_p$ is:

$$\Upsilon^S_{i\,Pole} = \frac{2}{T}\left(\frac{g^2}{2}\right)^2 (\phi - M_i)^2 \int \frac{d^3p}{(2\pi)^3}\frac{1}{\Gamma_\chi \omega_p^2} n_B(1+n_B)\,, \tag{6.31}$$

expanding in the same way as the previous case, after solving the angular integrals, we have:

$$\Upsilon^S_{i\,Pole} = \frac{g^4}{4\pi^3}\frac{(\phi - M_i)^2}{T}\pi \int dp \frac{p^2}{\Gamma_\chi \omega_p^2} n_B(1+n_B)\,. \tag{6.32}$$

let $I_B^{(Pole)}$ as:

$$I_B^{(Pole)} = \pi \int dp \frac{p^2}{\Gamma_\chi \omega_p^2} n_B(1+n_B)\,. \tag{6.33}$$

Making the same kind of conformal transformation, in order to have only the interval of integration $[0,1]$, we have:

$$p = \frac{z}{1-z}\,, \qquad J(z) = \frac{1}{(1-z)^2}\,, \tag{6.34}$$

therefore

$$I_B^{(Pole)} = \pi \int_0^1 dz \frac{z^2}{(1-z)^4}\frac{1}{\Gamma_\chi(z)\omega_p^2(z)} n_B(z)(1+n_B(z))\,. \tag{6.35}$$

Pole contribution: analytical computation

We already have the dissipation coefficient about its pole eq. (6.31), but now let us consider an analytical approximation. The first decay process has been computed in [20, 21] from the imaginary part of the χ_i self energy at one-loop order, as seen in fig. 6.2, yielding:

$$\Gamma_{\chi_i}(\chi_i \to \sigma_i \sigma_i) = \frac{h^2}{32\pi} \frac{m_{\chi i}^2}{\omega_p} F_T^{\sigma_i \sigma_i}(p, p_0)\,, \tag{6.36}$$

where

$$\begin{aligned} F_T^{\sigma_i\sigma_i}(p,p_0) &= \left[\frac{\omega_+^{\sigma_i}-\omega_-^{\sigma_i}}{p} + \frac{T}{p}\ln\left(\frac{1-e^{-\frac{\omega_+^{\sigma_i}}{T}}}{1-e^{-\frac{\omega_-^{\sigma_i}}{T}}}\frac{1-e^{-\frac{p_0-\omega_-^{\sigma_i}}{T}}}{1-e^{-\frac{p_0-\omega_+^{\sigma_i}}{T}}}\right)\right]\theta(p_0^2-p^2-4m_{\sigma_i}^2) \\ &+ \left[\frac{T}{p}\ln\left(\frac{1-e^{-\frac{\omega_+^{\sigma_i}}{T}}}{1-e^{-\frac{\omega_-^{\sigma_i}}{T}}}\frac{1-e^{-\frac{p_0+\omega_-^{\sigma_i}}{T}}}{1-e^{-\frac{p_0+\omega_+^{\sigma_i}}{T}}}\right)\right]\theta(-p_0^2+p^2)\,, \end{aligned} \tag{6.37}$$

with m_{σ_i} denoting the scalar σ_i mass, $\theta(x)$ the Heaviside function and

$$\omega_\pm^{\sigma_i} = \sqrt{(k_\pm^{\sigma_i})^2 + m_{\sigma_i}^2}\,, \qquad k_\pm^{\sigma_i} = \frac{1}{2}\left|p \pm p_0\left(1-\frac{4m_{\sigma_i}^2}{p_0^2-p^2}\right)^{1/2}\right|\,. \tag{6.38}$$

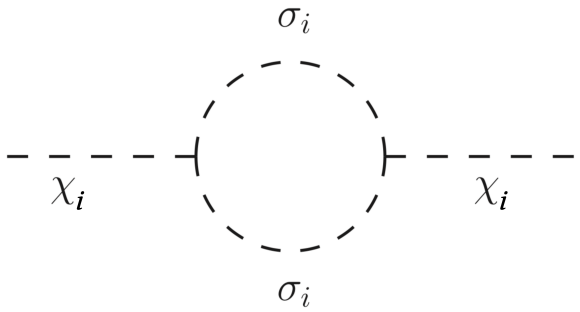

Figure 6.2: Feynman diagram contributing to the self-energy of the χ_i fields to leading order.

The following calculations are done in the low-momentum p approximation and in the limit $m_\sigma \ll T$. First we have that $\omega_\pm^{\sigma_i}/T$ can be expanded as:

$$\begin{aligned} \frac{\omega_\pm^{\sigma_i}}{T} &= \sqrt{\frac{(k_\pm^{\sigma_i})^2}{T^2}+\frac{m_\sigma^2}{T^2}} \simeq \frac{k_\pm^{\sigma_i}}{T} + \underbrace{\frac{1}{2}\frac{m_\sigma^2}{T^2}\frac{T}{k_\pm^{\sigma_i}} - \frac{1}{8}\frac{m_\sigma^4}{T^4}\frac{T^3}{(k_\pm^{\sigma_i})^3} + \cdots}_{\ll 1} \\ &\simeq \frac{k_\pm^{\sigma_i}}{T}\,, \end{aligned} \tag{6.39}$$

then $k_\pm^{\sigma_i} = (p_0 \pm p)/2$, therefore $\omega_\pm^{\sigma_i} = (p_0 \pm p)/2$. Now we have the relations:

$$p_0 - \omega_-^{\sigma_i} = \omega_+^{\sigma_i}\,, \tag{6.40}$$

$$p_0 - \omega_+^{\sigma_i} = \omega_-^{\sigma_i}\,, \tag{6.41}$$

hence the logarithmic function becomes:

$$\ln\left[\frac{1-e^{-\frac{\omega_+^{\sigma_i}}{T}}}{1-e^{-\frac{\omega_-^{\sigma_i}}{T}}}\frac{1-e^{-\frac{p_0-\omega_-^{\sigma_i}}{T}}}{1-e^{-\frac{p_0-\omega_+^{\sigma_i}}{T}}}\right] = \ln\left[\left(\frac{1-e^{-\frac{\omega_+^{\sigma_i}}{T}}}{1-e^{-\frac{\omega_-^{\sigma_i}}{T}}}\right)^2\right] = 2\ln\left[\frac{1-e^{-\frac{\omega_+^{\sigma_i}}{T}}}{1-e^{-\frac{\omega_-^{\sigma_i}}{T}}}\right]. \tag{6.42}$$

Note that the logarithm can be expanded for $x \ll 1$ in the following way:

$$\ln\left(1-e^{-x}\right) = \ln x - \frac{1}{2!}x + \frac{1}{4!}x^2 - \frac{1}{2^2 6!}x^4 + \frac{2}{9!}x^6 + \mathcal{O}(x^8)\,, \tag{6.43}$$

therefore

$$\begin{aligned}
&2\ln\left[\frac{1-e^{-\frac{\omega_+^{\sigma_i}}{T}}}{1-e^{-\frac{\omega_-^{\sigma_i}}{T}}}\right] = 2\left\{\ln\left[1-e^{-\frac{\omega_+^{\sigma_i}}{T}}\right] - \ln\left[1-e^{-\frac{\omega_-^{\sigma_i}}{T}}\right]\right\} \\
\simeq\ & 2\left\{\ln\left(\frac{\omega_+^{\sigma_i}}{\omega_-^{\sigma_i}}\right) - \frac{1}{2!}\frac{\omega_+^{\sigma_i}-\omega_-^{\sigma_i}}{T} + \frac{1}{4!}\frac{(\omega_+^{\sigma_i})^2-(\omega_-^{\sigma_i})^2}{T^2}\right. \\
&\left. -\frac{1}{2^2 6!}\frac{(\omega_+^{\sigma_i})^4-(\omega_-^{\sigma_i})^4}{T^4} + \frac{2}{9!}\frac{(\omega_+^{\sigma_i})^6-(\omega_-^{\sigma_i})^6}{T^6} + \cdots\right\} \\
\simeq\ & 2\ln\left(\frac{p_0+p}{p_0-p}\right) - \frac{p}{T} + \frac{2}{4!}\frac{p_0 p}{T^2} - \frac{1}{2^2 6!}\frac{p_0 p}{T^4}(p_0^2+p^2) \\
&+\frac{1}{2^2 9!}\frac{p_0 p}{T^6}(3p_0^4+10p_0^2p^2+3p^4) + \cdots\,,
\end{aligned} \tag{6.44}$$

where

$$\omega_+^{\sigma_i} - \omega_-^{\sigma_i} = p \tag{6.45}$$

$$(\omega_+^{\sigma_i})^2 - (\omega_-^{\sigma_i})^2 = p_0 p \tag{6.46}$$

$$(\omega_+^{\sigma_i})^4 - (\omega_-^{\sigma_i})^4 = \frac{p_0 p}{2}(p_0^2+p^2) \tag{6.47}$$

$$(\omega_+^{\sigma_i})^6 - (\omega_-^{\sigma_i})^6 = \frac{p_0 p}{16}(3p_0^4+10p_0^2p^2+3p^4)\,, \tag{6.48}$$

then

$$\frac{\omega_+^{\sigma_i}-\omega_-^{\sigma_i}}{p}+\frac{T}{p}\ln\left(\frac{1-e^{-\frac{\omega_+^{\sigma_i}}{T}}}{1-e^{-\frac{\omega_-^{\sigma_i}}{T}}}\frac{1-e^{-\frac{p_0-\omega_-^{\sigma_i}}{T}}}{1-e^{-\frac{p_0-\omega_+^{\sigma_i}}{T}}}\right)\simeq$$

$$1+2\frac{T}{p}\ln\left(\frac{p_0+p}{p_0-p}\right)-1+\frac{2}{4!}\frac{p_0}{T}-\frac{1}{2^26!}\frac{p_0}{T^3}(p_0^2+p^2)+\frac{1}{2^29!}\frac{p_0}{T^5}(3p_0^4+10p_0^2p^2+3p^4)$$

$$\simeq 2\frac{T}{p}\ln\left(\frac{p_0+p}{p_0-p}\right)+\frac{2}{4!}\frac{p_0}{T}-\frac{1}{2^26!}\frac{p_0}{T^3}(p_0^2+p^2)+\frac{1}{2^29!}\frac{p_0}{T^5}(3p_0^4+10p_0^2p^2+3p^4)\,, \quad (6.49)$$

now, since $p_0=\omega_p$ the function $F(p,p_0)$ becomes:

$$F(p,\omega_p)\simeq 2\frac{T}{p}\ln\left(\frac{\omega_p+p}{\omega_p-p}\right)+\frac{2}{4!}\frac{\omega_p}{T}-\frac{1}{2^26!}\frac{\omega_p}{T^3}(\omega_p^2+p^2)+\frac{1}{2^29!}\frac{\omega_p}{T^5}(3\omega_p^4+10\omega_p^2p^2+3p^4)\,. \quad (6.50)$$

We still can simplify even more the above expression, and in particular the logarithm function. Since at low-momentum p the argument of the logarithm goes to 1, we can expand it in the following way:

$$\ln x = x-1-\frac{1}{2}(x-1)^2+\frac{1}{3}(x-1)^3-\frac{1}{4}(x-1)^4+\cdots\,, \quad (6.51)$$

then we have

$$\begin{aligned}\ln\left(\frac{\omega_p+p}{\omega_p-p}\right) &\simeq \left(\frac{\omega_p+p}{\omega_p-p}-1\right)-\frac{1}{2}\left(\frac{\omega_p+p}{\omega_p-p}-1\right)^2+\frac{1}{3}\left(\frac{\omega_p+p}{\omega_p-p}-1\right)^3+\cdots\\ &\simeq \frac{2p}{\omega_p-p}-\frac{2p^2}{(\omega_p-p)^2}+\frac{2^3p^3}{3(\omega_p-p)^3}+\cdots\,. \quad (6.52)\end{aligned}$$

Finally, by taking the limit $p\to 0$, which implies that $\omega_p\simeq\tilde{m}_{\chi_i}$, this yields:

$$F(p\to 0,\tilde{m}_{\chi_i})\simeq\frac{4T}{\tilde{m}_{\chi_i}}+\frac{2}{4!}\frac{\tilde{m}_{\chi_i}}{T}-\frac{1}{2^26!}\frac{\tilde{m}_{\chi_i}^3}{T^3}+\frac{3}{2^29!}\frac{\tilde{m}_{\chi_i}^5}{T^5}+O\left(\left(\frac{\tilde{m}_{\chi_i}}{T}\right)^7\right)\,. \quad (6.53)$$

Therefore, the decay rate for the process $\chi_i\to\sigma_i\sigma_i$ in the pole approximation at low p at leading order is:

$$\Gamma_{\chi_i}(\chi_i\to\sigma_i\sigma_i)=\frac{h^2}{8\pi}\frac{m_{\chi_i}^2}{\tilde{m}_{\chi_i}}\frac{T}{\omega_p}\,, \quad (6.54)$$

On the other hand, the leading contribution to the decay width of the χ_i fields into two fermions $\bar{\psi}_{\sigma_i}\psi_{\sigma_i}$, as seen in fig. 6.3, has been computed in [20] from the imaginary part of the χ_i self energy at one-loop order, yielding:

$$\Gamma_{\chi_i}(\chi_i\to\bar{\psi}_{\sigma_i}\psi_{\sigma_i})=\frac{h^2}{32\pi\omega_p}F_T^{\bar{\psi}_{\sigma_i}\psi_{\sigma_i}}(p,p_0)\,, \quad (6.55)$$

where

$$F_T^{\bar{\psi}_{\sigma_i}\psi_{\sigma_i}}(p,p_0) = (p_0^2-p^2)\left[1-\frac{4m^2_{\psi_{\sigma_i}}}{p_0^2-p^2}\right]\left[\frac{\omega_+^{\psi_{\sigma_i}}-\omega_-^{\psi_{\sigma_i}}}{p}\right.$$
$$\left.+\frac{T}{p}\ln\left(\frac{1+e^{-\frac{\omega_+^{\psi_{\sigma_i}}}{T}}}{1+e^{-\frac{\omega_-^{\psi_{\sigma_i}}}{T}}}\frac{1+e^{-\frac{p_0-\omega_-^{\psi_{\sigma_i}}}{T}}}{1+e^{-\frac{p_0-\omega_+^{\psi_{\sigma_i}}}{T}}}\right)\right]\theta(p_0^2-p^2-4m^2_{\psi_{\sigma_i}})$$
$$+(p_0^2-p^2)\left[1-\frac{4m^2_{\psi_{\sigma_i}}}{p_0^2-p^2}\right]\frac{T}{p}\ln\left(\frac{1+e^{-\frac{\omega_+^{\psi_{\sigma_i}}}{T}}}{1+e^{-\frac{\omega_-^{\psi_{\sigma_i}}}{T}}}\frac{1+e^{-\frac{p_0+\omega_-^{\psi_{\sigma_i}}}{T}}}{1+e^{-\frac{p_0+\omega_+^{\psi_{\sigma_i}}}{T}}}\right)\theta(-p_0^2+p^2)\,, \quad (6.56)$$

then $m_{\psi_{\sigma_i}}$ is the fermionic ψ_{σ_i} mass and

$$\omega_\pm^{\psi_{\sigma_i}} = \sqrt{(k_\pm^{\psi_{\sigma_i}})^2+m^2_{\psi_{\sigma_i}}}\,, \qquad k_\pm^{\psi_{\sigma_i}} = \frac{1}{2}\left|p\pm p_0\left(1-\frac{4m^2_{\psi_{\sigma_i}}}{p_0^2-p^2}\right)^{1/2}\right|. \quad (6.57)$$

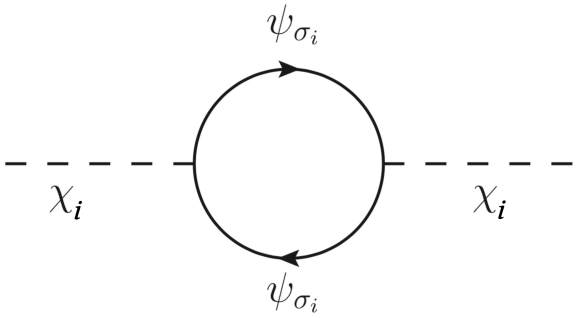

Figure 6.3: Feynman diagram contributing to the self-energy of the χ_i fields to leading order.

We essentially follow the same approach from the case before. Then at low-momentum p, in the limit $m_{\psi_{\sigma_i}} \ll T$, $\omega_\pm^{\psi_{\sigma_i}}/T$ can be expanded as:

$$\frac{\omega_\pm^{\psi_{\sigma_i}}}{T} = \sqrt{\frac{(k_\pm^{\psi_{\sigma_1}})^2}{T^2}+\frac{m^2_{\psi_{\sigma_i}}}{T^2}} \simeq \frac{k_\pm^{\sigma_i}}{T}+\underbrace{\frac{1}{2}\frac{m^2_{\psi_{\sigma_i}}}{T^2}\frac{T}{k_\pm^{\psi_{\sigma_i}}}-\frac{1}{8}\frac{m^4_{\psi_{\sigma_i}}}{T^4}\frac{T^3}{(k_\pm^{\psi_{\sigma_i}})^3}+\cdots}_{\ll 1}$$
$$\simeq \frac{k_\pm^{\psi_{\sigma_i}}}{T}\,, \quad (6.58)$$

then $k_\pm^{\psi_{\sigma_i}} = (p_0 \pm p)/2$, therefore $\omega_\pm = (p_0 \pm p)/2$. This yields:

$$p_0-\omega_-^{\psi_{\sigma_i}} = \omega_+^{\psi_{\sigma_i}}\,, \quad (6.59)$$
$$p_0-\omega_+^{\psi_{\sigma_i}} = \omega_-^{\psi_{\sigma_i}}\,, \quad (6.60)$$

we have in the logarithm:

$$\ln\left[\frac{1+e^{-\frac{\omega_+^{\psi_{\sigma_i}}}{T}}}{1+e^{-\frac{\omega_-^{\psi_{\sigma_i}}}{T}}}\frac{1+e^{-\frac{p_0-\omega_-^{\psi_{\sigma_i}}}{T}}}{1+e^{-\frac{p_0-\omega_+^{\psi_{\sigma_i}}}{T}}}\right]=\ln\left[\left(\frac{1+e^{-\frac{\omega_+^{\psi_{\sigma_i}}}{T}}}{1+e^{-\frac{\omega_-^{\psi_{\sigma_i}}}{T}}}\right)^2\right]=2\ln\left[\frac{1+e^{-\frac{\omega_+^{\psi_{\sigma_i}}}{T}}}{1+e^{-\frac{\omega_-^{\psi_{\sigma_i}}}{T}}}\right]. \tag{6.61}$$

Then, the logarithm can be expanded for $x \ll 1$ in the following way:

$$\ln\left(1+e^{-x}\right)=\ln 2-\frac{1}{2}x+\frac{1}{8}x^2-\frac{1}{192}x^4+\mathcal{O}(x^6)\,, \tag{6.62}$$

hence

$$\begin{aligned}
2\ln\left[\frac{1+e^{-\frac{\omega_+^{\psi_{\sigma_i}}}{T}}}{1+e^{-\frac{\omega_-^{\psi_{\sigma_i}}}{T}}}\right] &= 2\left\{\ln\left[1+e^{-\frac{\omega_+^{\psi_{\sigma_i}}}{T}}\right]-\ln\left[1+e^{-\frac{\omega_-^{\psi_{\sigma_i}}}{T}}\right]\right\}\\
&\simeq 2\left\{-\frac{1}{2}\frac{\omega_+^{\psi_{\sigma_i}}-\omega_-^{\psi_{\sigma_i}}}{T}+\frac{1}{8}\frac{(\omega_+^{\psi_{\sigma_i}})^2-(\omega_-^{\psi_{\sigma_i}})^2}{T^2}-\frac{1}{192}\frac{(\omega_+^{\psi_{\sigma_i}})^4-(\omega_-^{\psi_{\sigma_i}})^4}{T^4}+\cdots\right\}\\
&\simeq -\frac{p}{T}+\frac{1}{4}\frac{p_0 p}{T^2}-\frac{1}{192}\frac{p_0 p}{T^4}(p_0^2+p^2)+\cdots\,,
\end{aligned} \tag{6.63}$$

where

$$\omega_+^{\psi_{\sigma_i}}-\omega_-^{\psi_{\sigma_i}} = p\,, \tag{6.64}$$

$$(\omega_+^{\psi_{\sigma_i}})^2-(\omega_-^{\psi_{\sigma_i}})^2 = p_0 p\,, \tag{6.65}$$

$$(\omega_+^{\psi_{\sigma_i}})^4-(\omega_-^{\psi_{\sigma_i}})^4 = \frac{p_0 p}{2}(p_0^2+p^2)\,, \tag{6.66}$$

then

$$\frac{\omega_+^{\psi_{\sigma_i}}-\omega_-^{\psi_{\sigma_i}}}{p}+\frac{T}{p}\ln\left(\frac{1+e^{-\frac{\omega_+^{\psi_{\sigma_i}}}{T}}}{1+e^{-\frac{\omega_-^{\psi_{\sigma_i}}}{T}}}\frac{1+e^{-\frac{p_0-\omega_-^{\psi_{\sigma_i}}}{T}}}{1+e^{-\frac{p_0-\omega_+^{\psi_{\sigma_i}}}{T}}}\right)\simeq\frac{p_0}{4T}-\frac{p_0(p_0^2+p^2)}{192T^3}\,. \tag{6.67}$$

Recall that in the pole approximation $p_0 \simeq \omega_p$, then by taking the limit $p \to 0$ implies that $\omega_p \simeq \tilde{m}_{\chi_i}$ and $4m^2_{\psi_{\sigma_i}}/\tilde{m}^2_{\chi_i} \ll 1$, as a result we have:

$$F(p\to 0,\tilde{m}_\chi)\simeq\tilde{m}_{\chi_i}^2\left[\frac{\tilde{m}_{\chi_i}}{4T}-\frac{\tilde{m}_{\chi_i}^3}{192T^3}+\mathcal{O}\left(\left(\frac{\tilde{m}_{\chi_i}}{T}\right)^5\right)\right]. \tag{6.68}$$

Therefore, the decay rate for the process $\chi_i \to \bar{\psi}_{\sigma_i}\psi_{\sigma_i}$ in the pole approximation at low p at leading order is:

$$\Gamma_{\chi_i}(\chi_i\to\bar{\psi}_{\sigma_i}\psi_{\sigma_i})=\frac{h^2}{128\pi}\frac{\tilde{m}_{\chi_i}^3}{\omega_p T}\,, \tag{6.69}$$

Consequently the total decay rate for both processes becomes:

$$\Gamma^{S}_{\chi_i} = \Gamma_{\chi_i}(\chi\sigma\sigma) + \Gamma_{\chi_i}(\chi\bar{\psi}_\sigma\psi_\sigma) = \frac{h^2}{128\pi}\frac{T\tilde{m}_{\chi_i}}{\omega_{\chi_i}(p)}\left[16\frac{m^2_{\chi_i}}{\tilde{m}^2_{\chi_i}} + \frac{\tilde{m}^2_{\chi i}}{T^2}\right] . \tag{6.70}$$

Finally we compute the integral in Eq. (6.31), by following the same procedure as in [27], obtaining the total scalar dissipative coefficient:

$$\Upsilon^{S}(\phi, T) = \sum_{i=1}^{t.e}\frac{32g^4}{\pi h^2\left[16\frac{m^2_{\chi_i}}{\tilde{m}^2_{\chi_i}} + \frac{\tilde{m}^2_{\chi i}}{T^2}\right]}\ln\left(\frac{2T}{\tilde{m}_{\chi_i}}\right)\frac{(\phi - M_i)^2}{\tilde{m}_{\chi_i}} . \tag{6.71}$$

The next figs. 6.4 and 6.5 represent the comparison among the three different methods that solve eq. (6.25). However, for the sake of comprehensibility each figure represent only the differentiation between the numeric result, either the full integral or its pole approximation one, and the analytical approximation of an individual dissipation process, namely:

$$I_B^{Analytical}(\chi_i \to \sigma_i\sigma_i) = \frac{8\pi^2}{h^2}\frac{\tilde{m}_\chi T}{m^2_\chi}\ln\left(\frac{2T}{\tilde{m}_\chi}\right) , \tag{6.72}$$

$$I_B^{Analytical}(\chi_i \to \bar{\psi}_{\sigma_i}\psi_{\sigma_i}) = \frac{128\pi^2}{h^2}\frac{T^3}{\tilde{m}^3_\chi}\ln\left(\frac{2T}{\tilde{m}_\chi}\right) . \tag{6.73}$$

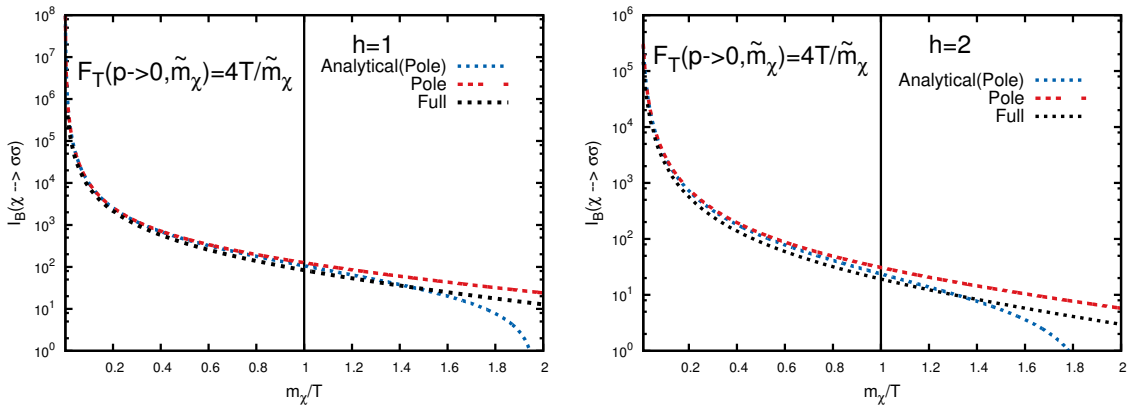

Figure 6.4: Comparison between the solution of the full integral eq. (6.30) (Full), the pole approximation eq. (6.35) (Pole), and the analytical solution eq. (6.72) (Analytical Pole). For both numerical implementations, we consider $m_{\sigma_i}/T = 0$. In addition two different coupling values are employed $h = 2, 1$.

Note that for the decay process $\chi \to \sigma\sigma$ the three distinct methods are contrasted (fig. 6.4); on the other hand, only two approaches are presented for other channel $\chi \to \bar{\psi}_\sigma\psi_\sigma$ (fig. 6.5). This is due to merely simplification, since the pole approximation is a rather good implementation. Moreover, we will see later that the coupling constant $g \ll h$, then for this reason we only stress results with the coupling h.

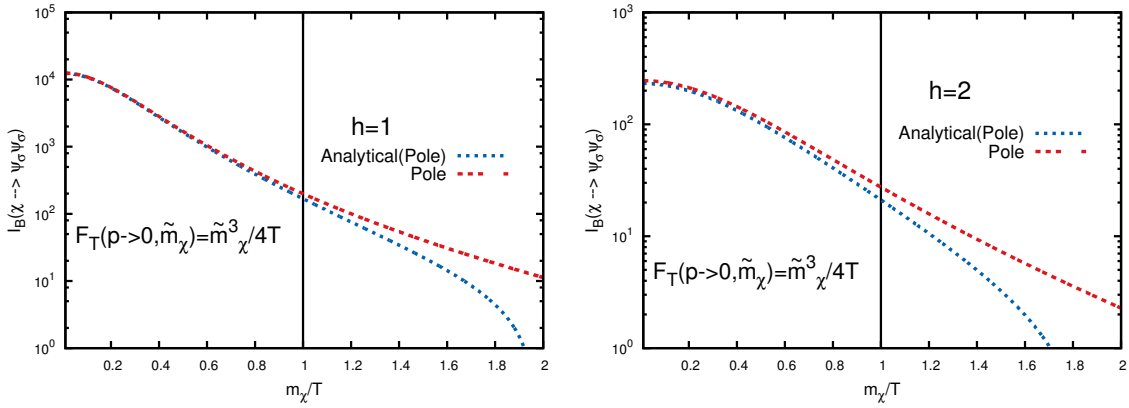

Figure 6.5: Comparison between the pole approximation eq.(6.35) (Pole) and the analytical solution eq.(6.73) (Analytical Pole). For the pole approximation, we consider $m_{\sigma_i}/T = 0$. In addition two different coupling values are employed $h = 2, 1$.

We need to ensure that all light bosons remain in a nearly-thermal state during inflation, so that the above result for the dissipation coefficient is a consistent approximation. For simplicity, we may take the thermal average of the above decay width, such:

$$\bar{\Gamma}^S_{\chi_i} = \frac{1}{n^B}\int \frac{d^3p}{(2\pi)^3}\Gamma^S_{\chi_i} f^B \tag{6.74}$$

where $f^B(\mathbf{p}/T)$ is the Bose-Einstein distribution and $n^B(\tilde{m}_{\chi_i}/T)$ the associated number density. Hence we have:

$$\bar{\Gamma}^S_{\chi_i} = \frac{h^2 T\tilde{m}_{\chi_i}}{128\pi}\left[16\frac{m^2_{\chi_i}}{\tilde{m}^2_{\chi_i}} + \frac{\tilde{m}^2_{\chi i}}{T^2}\right] I(\tilde{m}_{\chi_i}/T)\,, \quad I(\tilde{m}_{\chi_i}/T) = \frac{\int \frac{d^3p}{(2\pi)^3}\frac{f_B}{\omega_{\chi_i}(p)}}{\int \frac{d^3p}{(2\pi)^3} f_B}\,. \tag{6.75}$$

The integral factor $I(\tilde{m}_{\chi_i}/T)$ can be obtained numerically and is well approximated by (see fig. 6.6):

$$I(\tilde{m}_{\chi_i}/T) = \frac{1}{T}\frac{\int \frac{dxx^2}{\sqrt{x^2+a^2}}(e^{\sqrt{x^2+a^2}}-1)^{-1}}{\int dxx^2(e^{\sqrt{x^2+a^2}}-1)^{-1}} \simeq \frac{1}{T}\frac{0.68}{(1+0.77a)}\,, \tag{6.76}$$

where we have defined $x = p/T$ and $a = \tilde{m}_{\chi_i}/T$. Hence the thermal average of the scalar decay width is:

$$\bar{\Gamma}_{\chi_i} \simeq \frac{h^2\tilde{m}_{\chi_i}}{128\pi}\left[16\frac{m^2_{\chi_i}}{\tilde{m}^2_{\chi_i}} + \frac{\tilde{m}^2_{\chi i}}{T^2}\right]\frac{0.68}{(1+0.77f^{1/2})}\,. \tag{6.77}$$

Moreover, in the limit $m_{\chi_i}/T \lesssim 1$ we have that the effective finite thermal mass $\tilde{m}_{\chi_i}$ can be fittingly taken as $\tilde{m}_{\chi_i} \simeq f^{1/2}T$, where $f = f(g,h) = g^2/12 + h^2/8$. Therefore

the average decay width becomes:

$$\bar{\Gamma}_{\chi_i} \simeq \frac{h^2 f^{1/2}}{128\pi}\left[\frac{16}{f}\frac{m_{\chi_i}^2}{T^2}+f\right]\frac{0.68}{(1+0.77f^{1/2})}T\,. \tag{6.78}$$

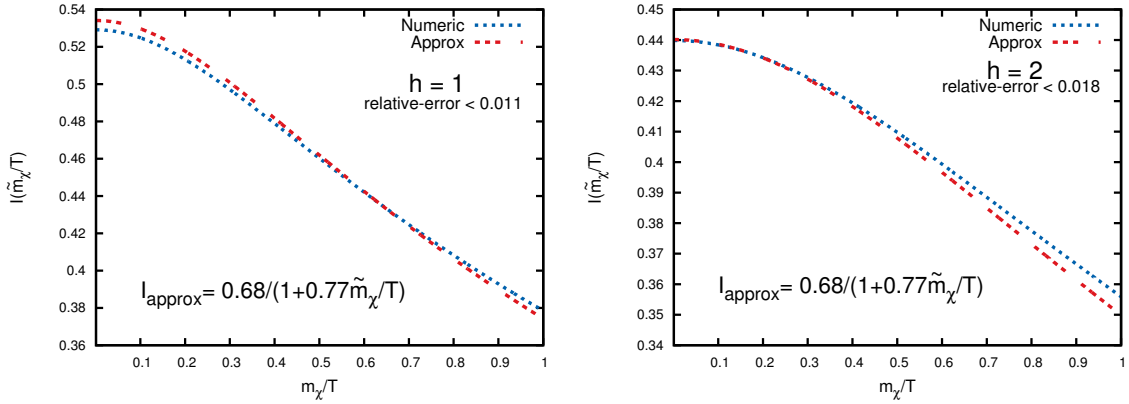

Figure 6.6: Comparison between the full integral $I(\tilde{m}_{\chi_i}/T)$ and the numerical fit, both given by eq.(6.75). Two different coupling values are employed $h = 2, 1$, and $g = 0.1$.

Note that eq. (6.78) is enhanced by the factor m_{χ_i}/T since it determines the position of the system within the tower of states. For instance, when $m_{\chi_i}/T = 0$, the dynamics acts in the central spot of the tower, hence the χ_i fields become massless and they do not contribute to dissipation; on the other hand, at the corner of the tower, $m_{\chi_i}/T \simeq 1$, these fields will yield the highest dissipation. Therefore, we will consider the edge of the tower ($m_{\chi_i}/T \simeq 1$) when computing the whole system numerically.

6.2.2 Fermionic sector

The calculation of the dissipation coefficient can be done following essentially the same steps as in the WLI model [23, 86, 92] (see also Appendix A), yielding:

$$\Upsilon^F = \sum_{i=1}^{N_M} C_T^F T\,, \quad C_T^F \simeq \frac{3g^2}{h^2(1-0.34\log(h))}\,. \tag{6.79}$$

This calculation involves computing the finite temperature decay width of all interaction processes, which is given by

$$\Gamma_\psi^F = \Gamma_\psi(\psi_\chi\sigma\psi_\sigma) = \frac{h^2}{16\pi}\frac{T^2 m_{\psi i}^2}{\omega_{\psi i}^2(p)|\mathbf{p}|}\left[F\left(\frac{k_+}{T},\frac{\omega_{\psi i}(p)}{T}\right)-F\left(\frac{k_-}{T},\frac{\omega_{\psi i}(p)}{T}\right)\right], \tag{6.80}$$

where, neglecting the masses of the decay products σ and ψ_σ, we have $\omega_{\psi i}(p) = \sqrt{\tilde{m}_{\psi i}^2 + |\mathbf{p}|^2}$, $k_\pm = (\omega_{\psi i}(p) \pm |\mathbf{p}|)/2$ and

$$F(x,y) = xy - \frac{x^2}{2} + (y-x)\ln\left(\frac{1-e^{-x}}{1+e^{x-y}}\right) + \mathrm{Li}_2\left(e^{-x}\right) + \mathrm{Li}_2\left(-e^{x-y}\right) , \tag{6.81}$$

where $\mathrm{Li}_2(z)$ is the dilogarithm function. Note that the mass of the light fields is corrected by a factor $h^2T^2/8$ due to their interactions with the thermal bath through ψ_σ and σ, which we will take to be dominant over the inflaton contribution, i.e. we take $\tilde{m}_{\psi i} \simeq h^2T^2/8$ in the above computation of the decay width. We need to ensure that all light fermions remain in a nearly-thermal state during inflation, so that the above result for the dissipation coefficient is a consistent approximation. For simplicity, we may take the thermal average of the above decay width in the high-temperature and ultra-relativistic region:

$$\bar{\Gamma}_\psi^F = \frac{1}{n^F}\int \frac{d^3p}{(2\pi)^3}\Gamma_\psi^F f^F \tag{6.82}$$

where $f^F(\mathbf{p}/T)$ is the Fermi-Dirac distribution and $n^F(\tilde{m}_{\chi_i}/T)$ the associated number density. This yields in the limit $m_{\psi i} \lesssim T$:

$$\bar{\Gamma}_\psi^F \simeq 10^{-3}\left[1 - 0.875\ln\left(\frac{h^2}{8}\right)\right] h^4 T\,. \tag{6.83}$$

6.3 Mass distribution function

In the DM model the dissipative mechanism is well described by the interaction between the inflaton ϕ and the finite number of fermion and boson fields that are light at any given time as the scalar field scans the tower of states. DM models are distinguished by how the mass sites are distributed. Such an idea has a natural realisation with string theory, whereby the inflaton is suggestive of an excited string zero mode, which then interacts with massive string levels. A construction of DM models from string theory was shown in [30]. However, we will envisage a phenomenological approach and look at various types of mass site configurations, so that these will determine what kind of dissipation dynamics lead to. This represent a small first step to test the viability of such models. In this section we develop some basic properties of the mass distribution function.

Recall that any mass state labeled by i is, as discussed previously in 6.1, $m_{\chi i}^2 = m_{\psi_{\chi_i}}^2 = g^2(\phi - M_i)^2$ and so is modulated by the parameter M_i. It is the distribution of these mass sites M_i that the underlying theory should determine, but here we treat them as

phenomenological parameters and examine different types of distributions of M_i over mass sites labelled by i. We want to build the mass sites shifted in such a way that the inflaton value becomes irrelevant with respect to this configuration, but bearing in mind that the whole tower has to be "big enough" so the inflaton can go throughout it entirely, i.e. enough sites has to be provided. Hence, suppose the inflaton field ϕ sat in the middle of some mass sites. Thus for all mass sites $\phi - T/g \leq M_i \leq \phi + T/g$, as shown in Fig. 6.7, the corresponding fields χ_i and ψ_{χ_i} would be thermally excited. The key idea of warm inflation in such models is that the inflaton rolls through a region with many such mass sites, thus thermally exciting for some time given fields and then once ϕ is far enough away, those field again are no longer thermally excited. This implies as the inflaton slow-rolls during inflation, a thermal interval surrounding it moves with it.

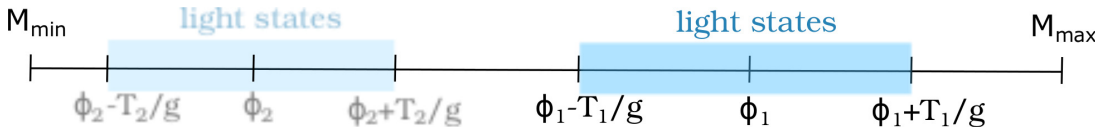

Figure 6.7: Schematic representation of the time evolution in the model assuming that the temperature decreases.

With no underlying theory to dictate such mass distributions, we will simply consider one type of construction to make the idea more tangible. We will assume the mass sites can be written as:

$$M_i = \phi + iK(\phi, T, m, g)\,, \tag{6.84}$$

where K is of mass dimension one and in general is a slowly varying function depending on the value of ϕ, the temperature scale T, some intrinsic mass scale m and the couplings such as g. The inflaton is going to move along the tower of states, influencing only such light fields that are included in the region:

$$M_{min}(i_{min} = 1) = \phi + K = \phi - \frac{T}{g}\,, \qquad M_{max} = \phi + i_{max}K = \phi + \frac{T}{g}\,, \tag{6.85}$$

where we have set simply $i_{min} = 1$. Hence i_{max}, which is maximum number of sites included in the thermal interval $\{M_{min}, M_{max}\}$, becomes:

$$i_{max} = \frac{T}{gK}\,. \tag{6.86}$$

We want that $i_{max} \gg 1$, so the inflaton would have "enough space" to cover for 50-60

e-folds of inflation. Therefore we must satisfy:

$$\frac{T}{g} \gg K\,. \tag{6.87}$$

Note that by considering $\phi - M_i = -iK$, we can compute any sum such as:

$$\begin{aligned}\sum_{i=1}^{i_{max}} g^n(\phi - M_i)^n &= (-1)^n g^n K^n \sum_{i=1}^{i_{max}} i^n \simeq (-1)^n g^n K^n \frac{i_{max}^{n+1}}{n+1} \\ &\simeq \frac{(-1)^n}{n+1}\frac{T^{n+1}}{gK}\,,\end{aligned} \tag{6.88}$$

where we have considered up to the leading order in the sum[b]. Hence we can compute both sources of dissipation (scalar eq. (6.71) and fermions eq. (6.79)) as:

$$\Upsilon^S(\phi,T) = \sum_{i=1}^{i_{max}} \frac{g^2 C_\phi^S}{T}(\phi - M_i)^2 \simeq \frac{C_\phi^S}{3}\frac{T^2}{gK}\,,\ C_\phi^S = \frac{32g^2}{\pi h^2\left[\frac{16}{f}\frac{m_{\chi_i}^2}{T^2} + f\right]}\ln\left(\frac{2}{\sqrt{f}}\right) \tag{6.89}$$

$$\Upsilon^F(\phi,T) = \sum_{i_{min}}^{i=1} C_T^F T \simeq \frac{C_T^F T^2}{gK}\,, \tag{6.90}$$

where we have assumed that $\ln(2T/\tilde{m}_{\chi i}) \simeq \ln\left(2/\sqrt{f}\right)$ since the thermal mass can be approximated as $\tilde{m}_{\chi i}^2 \simeq g^2T^2/12 + h^2T^2/8$ given that the χ_i fields must remain light, i.e. satisfying $m_{\chi i}^2/T^2 < 1$. Note that the above scalar component depends on the factor $m_{\chi_i}/T = g(\phi - M_i)/T$, but it was not considered during the computation of the sum since different fields will decay at different rates; and as previously stated, when analysing the consistency of the model, namely whether the χ_i decay faster than expansion in order to remain close to thermal equilibrium, we will consider the states for which $m_{\chi_i}/T \simeq 1$. Note that both channels can be described as simply one source, namely:

$$\Upsilon(\phi,T) = \Upsilon^S(\phi,T) + \Upsilon^F(\phi,T) \simeq \tilde{C}_\phi \frac{T^2}{gK}\,, \quad \tilde{C}_\phi = \frac{C_\phi^S}{3} + C_T^F \tag{6.91}$$

Since we can provide a general dissipative coefficient (eq (6.91)), we directly select a particular form of K for a suitable shape of Υ. For instance:

$$\Upsilon \sim \phi\,, \qquad K = \frac{T^2}{g\phi}\,, \qquad i_{max} = \frac{\phi}{T} \tag{6.92}$$

$$\Upsilon \sim T\,, \qquad K = Tg\,, \qquad i_{max} = \frac{1}{g^2} \tag{6.93}$$

$$\Upsilon \sim m\,, \qquad K = \frac{T^2}{g^2 m}\,, \qquad i_{max} = \frac{gm}{T} \tag{6.94}$$

[b] Note that $\sum_{i=1}^{i_{max}} i^n = i_{max}^{n+1}/(n+1) + \mathcal{O}(i_{max}^n)$

where m is a fixed intrinsic mass scale. During the course of the observable range of inflation (around 50-60 e-folds), the inflaton will traverse some distance covering many thermal intervals $\Delta\phi$, so we must guarantee the condition $i_{max} \gg 1$ is met throughout all evolution, thus for each of above cases we have the criteria: $\Delta T \ll \Delta\phi$, $g^2 \ll 1$, and $\Delta T \ll gm$. So that the inflaton crosses many mass sites in each thermal interval $\{M_{min}, M_{max}\}$. One expects at least tens of mass sites per thermal interval and hundreds to thousands of thermal intervals crossed during the observable period of inflation. In other words, in each e-fold of inflation one expects tens or few hundred mass sites to be crossed.

6.3.1 Effective potential at finite temperature

We can follow the above prescription in order to evaluate the effective finite temperature potential, where for the sake of simplicity we evaluate only the bare masses of the χ_i's and ψ_{χ_i}'s fields. We start by considering the contribution of the light bosons in the tower to the finite temperature effective potential given by [84, 90, 103]:

$$V_T^{\chi_i} \simeq 2\sum_i \left\{ -\frac{\pi^2}{90}T^4 + \frac{m_{\chi_i}^2 T^2}{24} - \frac{m_{\chi_i}^3 T}{12\pi} - \frac{m_{\chi_i}^4}{64\pi^2}\left[\ln\left(\frac{\mu^2}{T^2}\right) - c_b\right]\right\}, \tag{6.95}$$

where μ denotes the $\overline{\text{MS}}$ renormalisation scale, $c_b = 5.41$. Note the overall factor 2 in front of the sum, which represents the fact that the χ_i's scalars are complex fields. Recall that $m_{\chi_i} = g(\phi - M_i) = -iK$, then we have:

$$\begin{aligned} V_T^{\chi_i} &\simeq -\sum_{i=1}^{i_{max}} \frac{\pi^2}{45}T^4 + \frac{T^2}{12}\sum_{i=1}^{i_{max}} m_{\chi_i}^2 - \frac{T}{6\pi}\sum_{i=1}^{i_{max}} m_{\chi_i}^3 - \frac{1}{32\pi^2}\left[\ln\left(\frac{\mu^2}{T^2}\right) - c_b\right]\sum_{i=1}^{i_{max}} m_{\chi_i}^4 \\ &\simeq -\frac{\pi^2}{45}T^4\frac{T}{gK} + \frac{T^2}{36}\frac{T^3}{gK} + \frac{T}{24\pi}\frac{T^4}{gK} - \frac{1}{160\pi^2}\frac{T^5}{gK}\left[\ln\left(\frac{\mu^2}{T^2}\right) - c_b\right] \\ &\simeq \frac{T^5}{gK}\left\{-\frac{\pi^2}{45} + \frac{1}{36} + \frac{1}{24\pi} - \frac{1}{160\pi^2}\left[\ln\left(\frac{\mu^2}{T^2}\right) - c_b\right]\right\}. \end{aligned} \tag{6.96}$$

Next we examine the contribution of the light fermions in the tower to the finite temperature effective potential, which is given by [84, 90, 103]:

$$V_T^{\psi_{\chi_i}} \simeq \frac{1}{2}\sum_{i=1}^{i_{max}} \left\{ -\frac{7\pi^2}{180}T^4 + \frac{m_{\psi_{\chi_i}}^2 T^2}{12} + \frac{m_{\psi_{\chi_i}}^4}{16\pi^2}\left[\ln\left(\frac{\mu^2}{T^2}\right) - c_f\right]\right\}, \tag{6.97}$$

where $c_f = 2.635$. Note that the overall factor $1/2$ in front of the sum is related to the Majorana nature of the fermions in the SUSY model. Following the same procedure as

for the bosonic contribution, we have for the fermionic sector:

$$V_T^{\psi_{\chi_i}} \simeq \frac{T^5}{gK}\left\{-\frac{7\pi^2}{360}+\frac{1}{24}+\frac{1}{32\pi^2}\left[\ln\left(\frac{\mu^2}{T^2}\right)-c_f\right]\right\}, \tag{6.98}$$

therefore the total effective finite temperature potential becomes:

$$V_T^{\chi_i}+V_T^{\psi_{\chi_i}} \simeq \frac{T^5}{gK}\left[-\pi^2+3+\frac{4}{\pi}+\frac{3}{4\pi^2}(c_b-c_f)\right]. \tag{6.99}$$

Note that adding both finite temperature contributions arises a cancelation of radiatively generated vacuum energy corrections in the effective potential [103, 104], i.e the logarithm term on both finite temperature potentials (eqs. (6.96) and (6.98)) cancel each other. We want to estimate the contribution of these radiative corrections to the total effective potential V_{eff}, so we must compare them with respect to the zero temperature potential. Since the bare potential $V(\phi)$ is only ϕ dependent, we must implement a comparison, for the whole dynamics, between the inflaton value and the temperature T. Since $\Delta T/\Delta\phi \ll 1$ [c], we can estimate that the contribution of the finite temperature effective potential is small compare to the bare one. These estimates show that the DM-models are viable for a range of types of dissipative coefficients.

6.4 Results

Let us now analyse the inflationary dynamics for a quartic scalar potential, $V(\phi) = \lambda\phi^4$, taking into account both scalar and fermionic contributions to the dissipation coefficient. In addition different types of mass distribution functions will be used leading to dissipative coefficients of various forms: $\Upsilon \propto T^2$, $\Upsilon \propto T$, and $\Upsilon \propto \phi$. Finite temperature corrections to the effective potential are computed (if necessary) for each case. These effects can be controlled thus preventing thermal effects from generating large contributions to the inflaton mass that could reintroduce the "η-problem".

Essentially I analyse three distinct models. The first one correspond to a homogeneous distribution of states in the tower, which also corresponds to mass scales evenly spaced. Following this particular choice of the mass splitting scale, M, and by selecting scalar fields as the light components, I was able to compute semi-analytically the dissipative coefficient, yielding $\Upsilon \sim T^2$, and the thermal corrections to the inflation driven potential. Most of the work I put it in the Appendix B. Nonetheless, we could not find the numerical fit $G(Q_*)$ (the growing mode) needed to find the self interacting

[c] This is usually certain for large-field inflaton potentials, such as monomial ones.

coupling λ from the normalisation of the power spectrum Δ_R^2 (eq. 4.23), hence we could not continue with the rest of dynamics and observables. Even though, this scenario is unfinished, this project allowed me to develop the tools needed for the subsequent tasks.

Then by selecting a particular choice of the K function such as eq. (6.92), hence $\Upsilon \propto \phi$. I study analytically the observables in strong dissipative regime, since we expect that this model fits perfectly in it. This facilitates all calculations, so we will use standard analytical tools, i.e. we may implement the standard slow-roll approximation. Moreover, as mentioned before, radiative corrections to the total effective potential do not contribute to the dynamics, hence they basically are neglected. We will see later than this model remains as the most attractive one among the other examples since the observables fall within Planck Legacy; moreover, ϕ_*/M_P can reach sub-Planckian values for fairly reasonable dissipative ratio Q_* (at horizon crossing).

In the last scenario for $\Upsilon \propto T$ we consider the continuum limit, which is well developed in the Appendix C. This last model was studied numerically mainly for two reasons; first due to the function $G(Q_*)$, which accounts for the growth of inflaton fluctuations due to the coupling to radiation fluctuations through the temperature dependence of the dissipation coefficient, and second due to its large parameter space that covers both strong and weak dissipative regimes.

6.4.1 $\Upsilon \propto T^2$

For a homogeneous distribution of states in the tower, with constant mass splitting ΔM, as proposed by [27–29], the resulting scalar coefficients grows with temperature as $\Upsilon \propto T^2$ (see Appendix B for the entire derivation), with fermions contributing only about 20% to the total dissipation as first estimated in [27–29]. However, there is little we discuss about the full dynamics and the observables, since one must find an appropriate numerical fit of the growing mode function $G(Q_*)$, but this might be studied on another occasion. Although, one would expect certain behaviour by investigating related previous works; for instance, see the WLI model [23, 86, 92], where the observational predictions of a bunch of different inflationary potentials exhibit a generic behaviour in the high dissipative regime: the scalar spectral index n_s is rather blue-tilted.

6.4.2 $\Upsilon = \tilde{C}_\phi \phi$ and $V(\phi) = \lambda\phi^4$

We want to study this model within the strong dissipative regime ($Q \gg 1$), since we expect that this model fits perfectly in it. This facilitates all calculations, so we will use standard analytical tools, i.e. we may implement the standard slow-roll parameters $\epsilon_\phi = M_P^2(V_{,\phi}/V)^2/2$ and $\eta_\phi = M_P^2 V_{,\phi\phi}/V$, as well as $\beta_\phi = M_P^2 \Upsilon_{,\phi} V_{,\phi}/(\Upsilon V)$. Besides, the slow-roll conditions are now given by $\epsilon_\phi < Q\,, |\eta_\phi| < Q\,, \beta_\phi < Q$. We use the slow-roll equations, at $Q \gg 1$, in order to find a direct relation between Q and ϕ, yielding:

$$Q = \frac{\tilde{C}_\phi}{\sqrt{3\lambda}} \frac{M_P}{\phi}\,, \tag{6.100}$$

and the slow-roll parameters are:

$$\epsilon_\phi = \frac{8M_P^2}{\phi^2}\,, \quad \eta_\phi = \frac{12M_P^2}{\phi^2}\,, \quad \beta_\phi = \frac{4M_P^2}{\phi^2} \tag{6.101}$$

so in the strong dissipative regime inflation ends at $\epsilon_\phi \simeq Q$, this yields the inflaton value:

$$\phi_{end} = \frac{8\sqrt{3\lambda}}{\tilde{C}_\phi} M_P\,. \tag{6.102}$$

The number of e-folds during inflation in the aforementioned regime is:

$$\begin{aligned} N_e &= -\frac{1}{M_P^2}\int_{\phi_*}^{\phi_{end}} d\phi \frac{QV}{V_\phi} = -\frac{\tilde{C}_\phi}{4\sqrt{3\lambda}M_P}\int_{\phi_*}^{\phi_{end}} d\phi \\ &= \frac{\tilde{C}_\phi}{4\sqrt{3\lambda}}\left[\left(\frac{\phi_*}{M_P}\right) - \left(\frac{\phi_{end}}{M_P}\right)\right]\,, \end{aligned} \tag{6.103}$$

hence the inflaton value at horizon crossing is:

$$\phi_* = \frac{4\sqrt{3\lambda}(N_e+2)}{\tilde{C}_\phi} M_P = 2\sqrt{\frac{N_e+2}{Q_*}} M_P\,. \tag{6.104}$$

Once we have determined ϕ_* we can evaluate the observables at 50-60 e-folds before inflation ends. Before we proceed, one should note that in the strong dissipative regime many parameters and formulas simplify, in fact, one of them is an analytic approximation to the density perturbation amplitude. Recall that for $T > H$, the dominant contribution to the primordial perturbation spectrum are thermal fluctuations of the inflaton field, as opposed to the conventional quantum fluctuations in cold inflation models. Upon exiting the horizon these thermal fluctuations freeze out as classical perturbations and during slow-roll at $Q \gg 1$ the amplitude of the curvature perturbation power spectrum is given by [70, 105] (see Appendix D for a clearer and

understandable derivation of it):

$$\Delta^2_{\mathcal{R}} \simeq \frac{9}{4\pi^2}\frac{H_*^5 T_* Q_*^{5/2}}{V^2_{\phi_*}}\,, \tag{6.105}$$

where all quantities are evaluated at horizon-crossing. Hence the scalar spectral index $n_s - 1 \simeq d\ln\Delta^2_{\mathcal{R}}/dN_e$ is modified as well, becoming [70] (see also see Appendix D):

$$\begin{aligned} n_s &= 1 + \frac{3}{2}\left(\frac{\eta_V}{Q} - \frac{3}{2}\frac{\epsilon_V}{Q} - \frac{3}{2}\frac{\beta_V}{Q}\right) = 1 - \frac{9}{4}\left(\frac{2\sqrt{3\lambda}}{\tilde{C}_\phi}\frac{M_P}{\phi_*}\right) \\ &= 1 - \frac{9}{4}\left(\frac{1}{N_e+2}\right)\,. \end{aligned} \tag{6.106}$$

Remarkably, note that n_s only depend of the number of e-folds: $n_s(N_e = 50) = 0.9567$ and $n_s(N_e = 60) = 0.9637$; where at 60 e-folds this scalar spectral index agrees outstandingly with Planck data [10]. The tensor-to-scalar ratio $r = \Delta^2_t/\Delta^2_{\mathcal{R}}$, as mentioned above, is typically reduced by the modifications to the scalar curvature perturbations introduced due to dissipation, which is basically a function of Q_*. We illustrate this fact by using the slow-roll dynamics, where the ratio r can be written as:

$$r = \frac{2H_*^2}{\pi^2 M_P^2 \Delta^2_{\mathcal{R}}} = \frac{2\lambda}{3\pi^2\Delta^2_{\mathcal{R}}}\frac{\phi_*^4}{M_P^4} = \frac{32\lambda}{3\pi^2\Delta^2_{\mathcal{R}}}\frac{(N_e+2)^2}{Q^2} \tag{6.107}$$

The value of λ is fixed by using the normalisation of amplitude of the primordial spectrum $\Delta^2_R \simeq 2.2\times 10^{-9}$ [10]. Using the slow-roll equations in Eq. (D.7), we have:

$$\lambda = (\Delta^2_{\mathcal{R}})^{4/3}\left(\frac{(12\pi^4 C_R^{1/2})^{2/3}}{(N_e+2)^3}\right)\,, \tag{6.108}$$

where $C_R = \pi^2 g_{eff}/30$, and $g_{eff} = 1 + 15N_M/4$, N_M being the number of bosonic χ_i (fermionic ψ_i) light degrees of freedom at horizon crossing. The tensor-to-scalar ratio is then just a function of Q_* and N_e,

$$r = \frac{64(6\Delta^2_{\mathcal{R}})^{1/3}}{3Q_*^2(N_e+2)}\,. \tag{6.109}$$

As one expected, the tensor-to-scalar ratio is highly suppressed by dissipation. In fact this ratio lies in the region $10^{-9} < r \lesssim 10^{-4}$ at $10 \leq Q_* \leq 1000$, for $N_M = O(10-100)$, having the bigger suppression at the largest Q_*, see fig. 6.8.

We can also look at the ratios ϕ_*/M_P and m_{ϕ_*}/H_*, in order to illustrate that for this model the relevant scales can indeed happen in the sub-Planckian region, as shown in fig. 6.9. This occurs thanks to the high dissipation dynamics, since in WI field

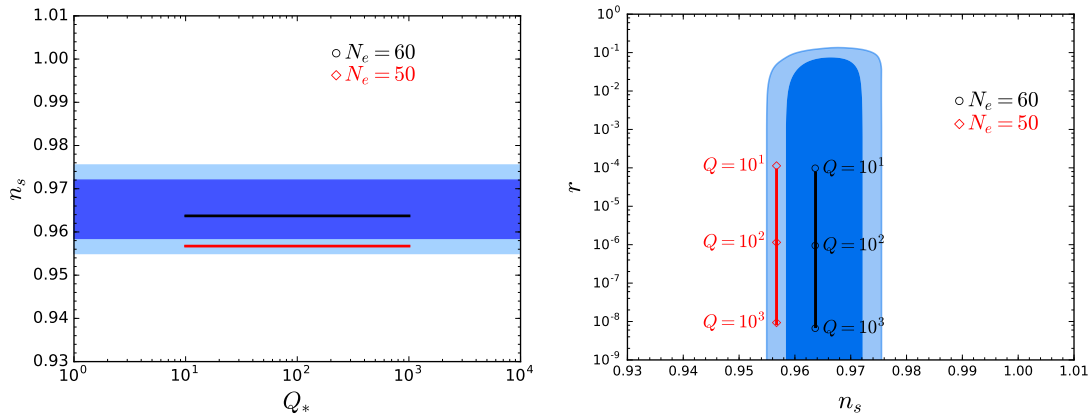

Figure 6.8: Observational predictions of the DM scenario with a quartic potential for 50 (diamonds) and 60 (circles) e-folds of inflation in colours black, and red respectively. Also, a Yukawa coupling $h = 2.5, 1.0$, and fixed number of light states $N_M = 10$. The plot on the left shows the spectral index n_s as a function of the dissipative ratio at horizon-crossing, Q_*, while the plot on the right shows the allowed trajectories in the (n_s, r) plane. The blue contours correspond to the 68% and 95% C.L. results from Planck 2018 TT,TE,EE+lowE+lensing data [10]. Note that $n_s(N_e = 60) = 0.9637$ agrees remarkably with Planck data.

potentials that are not flat enough to allow the standard slow-roll inflaton evolution, i.e. they do not have large enough initial inflaton values so not "sufficient" inflation takes place, can in fact lead to a longer period of inflation due to the extra friction induced by Υ. Hence, for small (even sub-Planckian) ϕ_* inflation can last 50-60 e-folds in the strong dissipative regime.

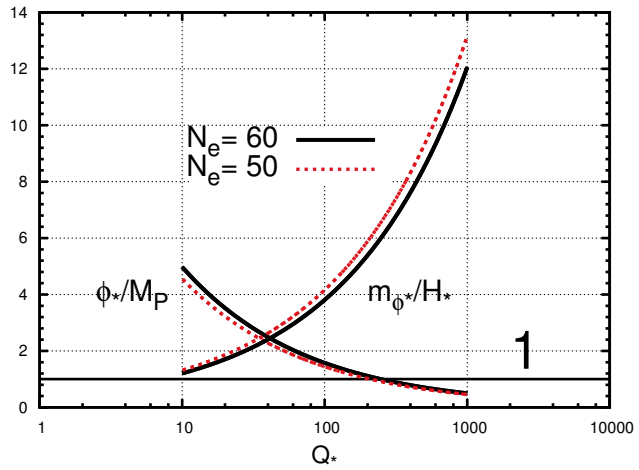

Figure 6.9: Ratios m_{ϕ_*}/H_* and ϕ_*/M_P, as a function of the dissipative ratio Q_*, within a DM scenario with a dissipative coefficient of the form $\Upsilon \propto \phi$ described by a quartic potential for 50 (red dashed-line) and 60 (black solid-line) e-folds of inflation. Note that m_{ϕ_*}/H_* is always larger than 1 for $Q_* > 10$, while $\phi_*/M_P < 1$ (sub-Planckian) at $Q_* \sim 210$.

We can even generalise above results for a dissipative coefficient of the form: $\Upsilon = C_\phi \phi^p m^{1-p}$, where m is a mass scale and p is a free parameter. For this generic case,

the scalar spectral index and the tensor-to-scalar ration become very simple expressions that yield a remarkable agreement with Planck legacy [10] (see Fig. 6.10):

$$n_s = 1 - \frac{9}{4}\left(\frac{p}{pN_e + 2}\right), \qquad r = \frac{32\lambda}{3\pi^2\Delta^2_{\mathcal{R}}}\frac{(pN_e+2)^2}{Q^2} \tag{6.110}$$

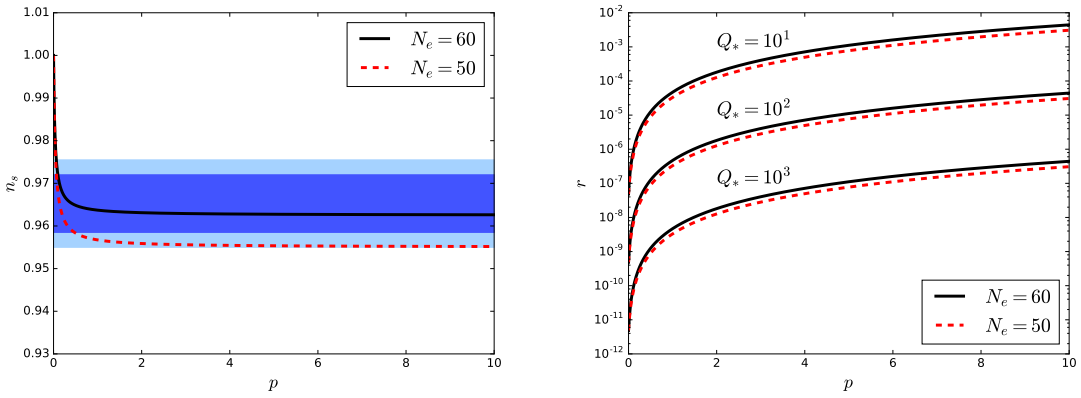

Figure 6.10: Observational predictions of the DM scenario with a dissipative coefficient of the form $\Upsilon \propto \phi^p$ described by a quartic potential for 50 (red dashed-line) and 60 (black solid-line) e-folds of inflation. The plot on the left shows the spectral index n_s as a function the parameter p, while the plot on the right shows the tensor-to-scalar ratio r as a function of p for three values of Q_*. The blue contours correspond to the 68% and 95% C.L. results from Planck 2018 TT,TE,EE+lowE+lensing data [10]. Note that n_s lies well inside the Planck contours at $p \geq 1$. On the other hand, r gets enhanced for larger p.

The good agreement between WI with a dissipative coefficient of the form: $\Upsilon = C_\phi \phi^p m^{1-p}$ described by a chaotic quartic potential has been reported before, for instance [79] analysed the $\Upsilon \propto \phi^2$ case, finding observably favourable region for $Q \gg 1$. On the other hand, the tensor-to-scalar ratio is enhanced by larger p, so for very large p this ratio r can indeed become bigger than 1. The limits on ongoing and planned B-mode polarisation experiments [51] suggest sensitivity down to $r \gtrsim 10^{-3}$. This leaves open the door to access desirable values of r for very large Q_*.

6.4.3 $\Upsilon = C_T T$ and $V(\phi) = \lambda\phi^4$

We can ensure a linear dissipative coefficient by considering a DM model with a constant no. of bosonic (fermionic) light degrees of freedom N_M during the evolution of the inflaton field. This is equivalent at having in the continuum limit a density of states $n(\phi)$ that goes inversely with T, such that $N_M \simeq 2Tn(\phi)/g$ (see Appendix C for the entire derivation). On the other hand the same prescription can be obtained by setting the mass distribution function $K = Tg$ (eq. (6.93). However, for this case we study this scenario in the continuum limit. Using this, and performing the sums in eqs. (6.71) and

(6.79) in the continuum limit (once again see Appendix C for the explicit calculations), we then have:

$$\Upsilon^S(\phi,T) = N_M C_T^S T\,, \quad C_T^S = \frac{2g^2\sqrt{f}}{\pi}\ln\left(\frac{2}{\sqrt{f}}\right)\left[1-\frac{f}{4}\mathrm{ArcTan}\left(\frac{4}{f}\right)\right]\,, \quad (6.111)$$

$$\Upsilon^F(\phi,T) = N_M C_T^F T\,, \quad (6.112)$$

where C_T^F was given in eq. (6.79) and $f = f(g,h) = g^2/12 + h^2/8$. The observational predictions will depend now on the couplings g and h, and the parameter N_M. In our analysis, we have also included the one loop thermal effective potential, computed in Appendix C. The full contribution to the finite temperature effective potential is given by the fermionic and bosonic towers, the inflaton field ϕ and a light fermion-scalar pair $\psi_\sigma\sigma$, hence $V_T^{Full} = V_T^{\phi,\sigma} + V_T^{\psi_\sigma} + V_T^{\psi_i,\bar{\psi}_i} + V_T^{\chi_i}$:

$$V_T^{Full} = -\frac{\pi^2}{24}T^4 + V_T^{\psi_i,\bar{\psi}_i} + V_T^{\chi_i}\,, \quad (6.113)$$

where

$$\begin{aligned} V_T^{\psi_i,\bar{\psi}_i} + V_T^{\chi_i} \;=\; & N_M T^4\left\{-\frac{\pi^2}{24}+\frac{1}{72}+\frac{h^2}{192}+\frac{f}{12}+\frac{f^2}{16\pi}\ln\left(\frac{\sqrt{f}}{\sqrt{1+f}+1}\right)\right. \\ & -\left(\frac{2+5f}{48\pi}\right)\sqrt{1+f}+\frac{1}{32\pi^2}\left[\frac{c_b-c_f}{5}+\left(\frac{2f}{3}+f^2\right)c_b-\left(\frac{h^2}{12}+\frac{h^4}{64}\right)c_f\right] \\ & \left.+\frac{1}{32\pi^2}\left(\frac{h^2}{12}+\frac{h^4}{64}-\frac{2f}{3}-f^2\right)\ln\left(\frac{\mu^2}{T^2}\right)\right\}\,. \end{aligned} \quad (6.114)$$

This correction to the zero temperature potential is due to all relativistic degrees of freedom. Only massless light fields will contribute to the entropy density, yielding:

$$s_R = \frac{2\pi^2}{45}\left(1+\frac{15}{2}N_M\right)T^3\,, \quad (6.115)$$

hence the effective degrees of freedom are:

$$g_{eff} = 1 + 4N_M\left(1+\frac{7}{8}\right)\,. \quad (6.116)$$

For any (or even both) dissipative coefficient(s) eqs. (6.111) and (6.112) we may construct a master formula using the slow-roll equations, yielding:

$$Q^3(1+Q)^2 = \frac{C_T}{4C_R(T)}\left(\frac{C_T}{3}\right)^3\left(\frac{V_{eff,\phi}}{3H^3}\right)^2\,, \quad (6.117)$$

where C_T is either $C_T = N_M C_T^S$, $C_T = N_M C_T^F$ or $C_T = N_M(C_T^S + C_T^F)$. Then we can derive the evolution equation for the ratio $Q = \Upsilon/(3H)$:

$$\left(\frac{3+5Q}{1+Q}\right)\frac{d\ln Q}{dN_e} = -2\frac{\eta_{eff}}{1+Q} + 6\epsilon_H\,, \tag{6.118}$$

where $\epsilon_H = -\dot{H}/H^2 = -d\ln H/dN_e$, $\dot{H} = -(\dot{\phi}^2 + Ts_R)/(2M_p^2)$ being the time derivate of the Hubble parameter. From the amplitude of the curvature power spectrum, we may determine the scalar spectral index $n_s - 1 \simeq d\ln\Delta^2_{\mathcal{R}}/dN_e$, which is given by:

$$\begin{aligned} n_s - 1 &= 2\frac{\eta_{eff}}{1+Q} - 6\epsilon_{H*} + \left[\frac{2Q_*}{1+Q_*} + Q_*\frac{d\ln G(Q)}{dQ}\Big|_*\right]\frac{d\ln Q}{dN_e}\Big|_* \\ &+B(T_*/H_*, Q_*)\left[\frac{12\sqrt{3}\pi Q_*}{\sqrt{3+4\pi Q_*}}\left(\frac{1+\pi Q_*}{3+4\pi Q_*}\right)\frac{T_*}{H_*} - \frac{H_*}{2T_*}\left(1-\coth^2\left(\frac{H_*}{2T_*}\right)\right)\right]\frac{d\ln Q}{dN_e}\Big|_* \end{aligned} \tag{6.119}$$

where

$$B(T_*/H_*, Q_*) = \left[\frac{2\sqrt{3}\pi Q_*}{\sqrt{3+4\pi Q_*}}\frac{T_*}{H_*} + \coth\left(\frac{H_*}{2T_*}\right)\right]^{-1}\,. \tag{6.120}$$

We set the renormalisation scale such as $\mu = \exp(c_f/2)T_*$, where T_* is the temperature at horizon crossing. It is worth to mention that by selecting the renormalisation scale by another prescription, for instance by $\mu = \exp(c_b/2)T_*$, the outcome is not substantially altered. Since the distribution of states is $n \sim T^{-1}$, then the contribution of the finite temperature potential on the derivatives of the effective potential is absent in this model. We want to study both sources of dissipation at once, namely $\Upsilon^{full} = \Upsilon^S + \Upsilon^F$. Then, to satisfy the adiabatic condition we have consider the fermionic and bosonic sectors: $\bar{\Gamma}^S_\chi/H, \bar{\Gamma}^F_\psi/H \gtrsim 1$. Furthermore, note that $\bar{\Gamma}^S_\chi$ can be enhanced by a fixed ratio m_{χ_i}/T, so we will consider $m_{\chi_i}/T = 1$ when computing the whole system numerically, since the scalar fields will yield the highest dissipation at the edge of the tower. It should be noted that since $\Gamma \sim T$, as warm inflation proceeds, thermalisation $T/H \gtrsim 1$ improves. Additionally, we explore various set of parameters determined by N_M and an fixed Yukawa coupling h. In our analysis the growing mode function $G(Q_*)$, given by a chaotic quartic potential, was obtained numerically by [23, 92]:

$$G(Q_*) \simeq 1 + 0.0185\,Q_*^{2.315} + 0.335\,Q_*^{1.364}\,. \tag{6.121}$$

In this segment I will perform a full parametric analysis, requiring that the fermions and scalars maintain a near-equilibrium distribution, such that the dissipative process also occur in an adiabatic regime, this imply imposing the condition $\bar{\Gamma}^S_\chi/H, \bar{\Gamma}^F_\psi/H \gtrsim 1$ for 50-60 e-folds of inflationary expansion. After determining the regions of parameter space

where these conditions are satisfied, I will then compute the corresponding inflationary observables. To inspect the parameter space we compute the coupling λ using the observed amplitude of curvature perturbations, $\Delta_R^2 \simeq 2.2 \times 10^{-9}$ [10], at 50-60 e-folds before inflation ends.

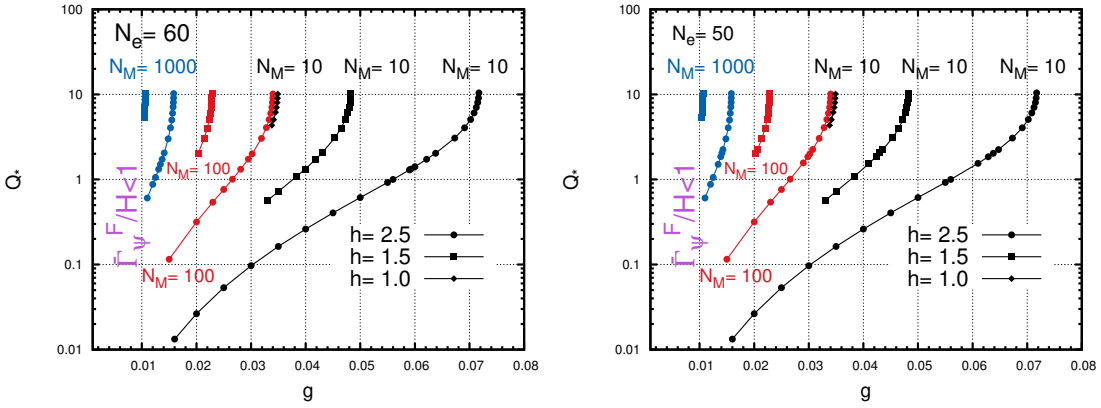

Figure 6.11: Dissipative ratio at horizon-crossing, Q_*, as a function of the coupling g, within a DM scenario with a dissipative coefficient of the form $\Upsilon \propto T$ described by a quartic potential and $N_e = 50$ (right) or $N_e = 60$ (left) e-folds of inflation. We consider different numbers of light states $N_M = 10, 100$ and 1000, shown by the black, red and blue curves, respectively; as well as different values of the Yukawa coupling $h = 2.5$ (circles), $h = 1.5$ (rectangles), and $h = 1.0$ (diamonds). Note that the adiabatic conditions $\bar{\Gamma}_\psi^F/H \gtrsim 1$ is not satisfied for small values of g.

For the quartic potential, we show in fig. 6.11 the obtained values of the dissipative ratio at horizon-crossing, Q_*, as a function of the coupling g, for different numbers of light states and values of the Yukawa coupling h. We note in this figure that the adiabatic condition $\bar{\Gamma}_\psi^F/H \gtrsim 1$ for the fermions is only satisfied for $g \gtrsim 0.01$. We also find a lower bound $Q_* > 0.01$ for the smallest number of fields considered, and that the adiabatic conditions imply generically $h \gtrsim 1$. We only show in this figure values of $Q_* < 11$ since, as we will see below, larger values are incompatible with observational data [10].

This behaviour had been reported before for the WLI model [23, 86, 92] (see also chapter 5). For instance, the analysis in [92] presented a rather similar lower bound on $g \gtrsim 0.01$ and $Q_* \gtrsim 0.001$ due to the adiabatic condition, while the conditions on the temperature limit this coupling from above, $g \lesssim 0.1$ such that $Q_* \lesssim 0.25$. However, the DM model yields a substantially wider consistent parametric range, particularly for the value of the dissipative ratio at horizon-crossing.

Note that for larger values of the number of light states N_M and of the Yukawa coupling h we obtain a much narrower range of consistent values for the coupling g, and the lower bound on Q_* also increases with N_M and h. We thus find scenarios where inflation

can start either in the weak or strong dissipation regimes, noting that Q grows during inflation such that for a wide range of parameters one reaches $Q > 1$ before the end of inflation, a necessary condition for radiation to dominate after the slow-roll regime with no further reheating (see eq. (4.19)).

In figs. 6.12, 6.13 and 6.14 we show the predictions for the scalar spectral index and tensor-to-scalar ratio in the allowed parametric ranges, for different values of h and N_M, exhibiting a remarkable consistency with the Planck legacy results. This is particularly relevant given that the quartic potential is already excluded by such survey within the CI paradigm.

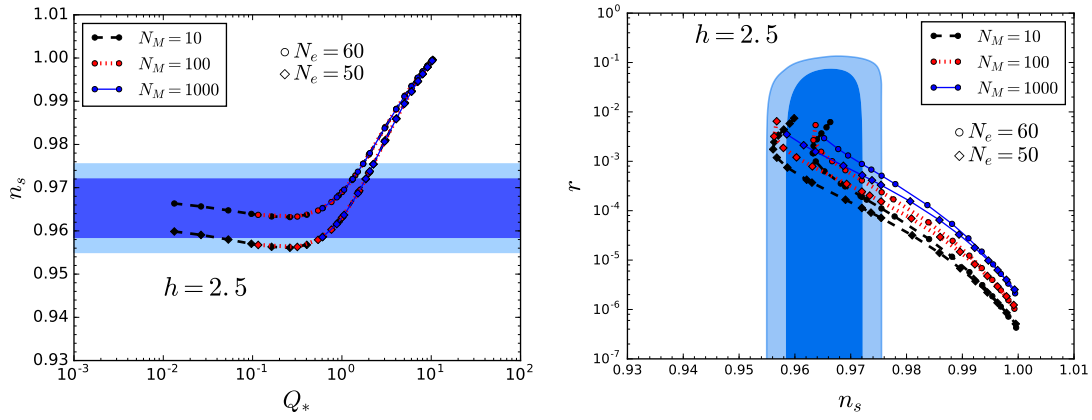

Figure 6.12: Observational predictions of the DM scenario with a dissipative coefficient of the form $\Upsilon \propto T$ described by a quartic potential for 50 (diamonds) and 60 (circles) e-folds of inflation, a Yukawa coupling $h = 2.5$, and three different values of the number of light states $N_M = 10, 100, 100$ in colours (line-style) black (dashed-line), red (pointed-line), and blue (solid-line) respectively. The plot on the left shows the spectral index n_s as a function of the dissipative ratio at horizon-crossing, Q_*, while the plot on the right shows the allowed trajectories in the (n_s, r) plane. The blue contours correspond to the 68% and 95% C.L. results from Planck 2018 TT,TE,EE+lowE+lensing data [10].

We find agreement with the Planck legacy data in the parametric ranges yielding values of $Q_* \lesssim 1$, which is easier to achieve for larger values of the Yukawa coupling, as well as a smaller number of light fields. For instance, we cannot find consistency with the Planck data for $h = 1$, since smaller values of the Yukawa coupling lead to stronger dissipation at horizon-crossing. These results were expected, since the growing mode in the spectrum makes it more blue-tilted with increasing Q_*.

In general, the tensor-to-scalar ratio lies in the range $10^{-4} \lesssim r \lesssim 10^{-2}$, for values of the scalar spectral index within the Planck window, being more suppressed for larger values of Q_* (smaller Yukawa couplings and larger number of light fields N_M). This feature is quite generic, since a similar notable trend was obtained in [23, 58, 72, 86, 92, 106]. Additionally, this significant agreement with Planck data is easily achieved with only

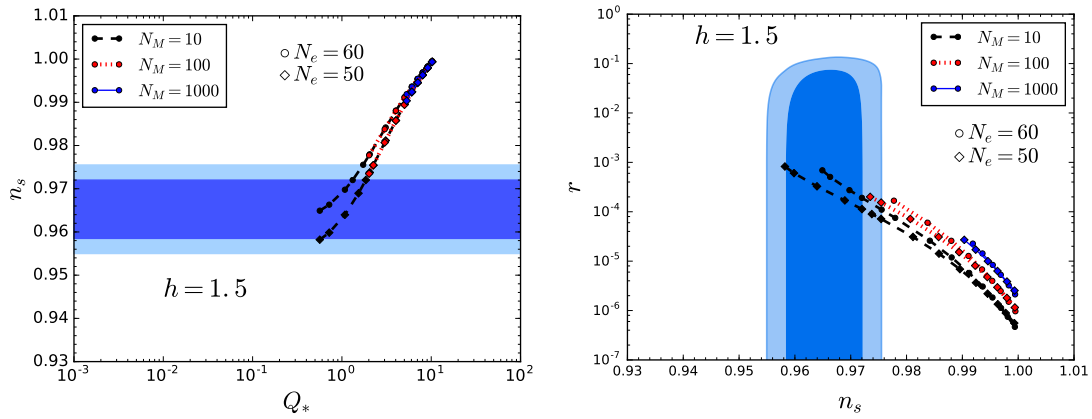

Figure 6.13: Observational predictions of the DM scenario with a dissipative coefficient of the form $\Upsilon \propto T$ described by a quartic potential for 50 (diamonds) and 60 (circles) e-folds of inflation, a Yukawa coupling $h = 1.5$, and three different values of the number of light states $N_M = 10, 100, 100$ in colours (line-style) black (dashed-line), red (pointed-line), and blue (solid-line) respectively. The plot on the left shows the spectral index n_s as a function of the dissipative ratio at horizon-crossing, Q_*, while the plot on the right shows the allowed trajectories in the (n_s, r) plane. The blue contours correspond to the 68% and 95% C.L. results from Planck 2018 TT,TE,EE+lowE+lensing data [10].

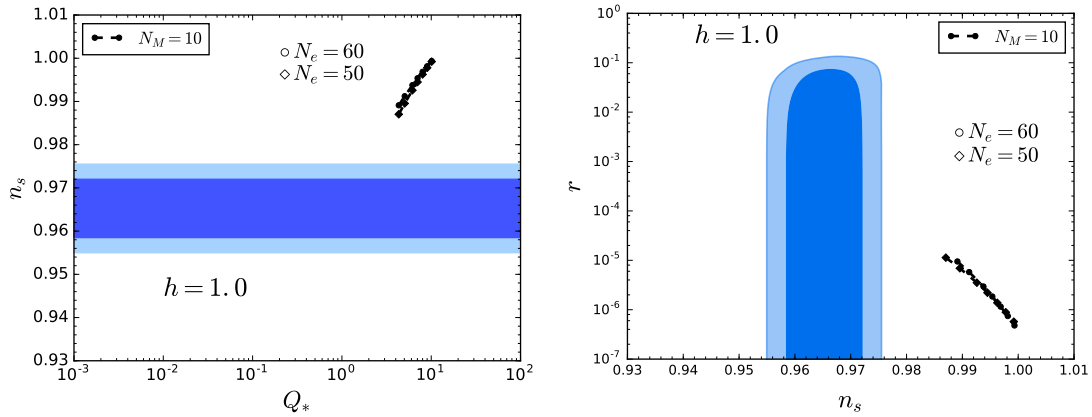

Figure 6.14: Observational predictions of the DM scenario with a dissipative coefficient of the form $\Upsilon \propto T$ described by a quartic potential for 50 (diamonds) and 60 (circles) e-folds of inflation, a Yukawa coupling $h = 1.0$, and three different values of the number of light states $N_M = 10, 100, 100$ in colours (line-style) black (dashed-line), red (pointed-line), and blue (solid-line) respectively. The plot on the left shows the spectral index n_s as a function of the dissipative ratio at horizon-crossing, Q_*, while the plot on the right shows the allowed trajectories in the (n_s, r) plane. The blue contours correspond to the 68% and 95% C.L. results from Planck 2018 TT,TE,EE+lowE+lensing data [10].

a small number of light states N_M.

The remarkable agreement between the DM quartic model and the Planck data is similar to what had been obtained for the WLI quartic model [23, 86, 92] (see also chapter 5), where the dissipation coefficient is also proportional to the temperature. However, while the more constraining conditions of the WLI model limit the consistent

parametric range to $Q_* \lesssim 0.25$, we have found consistent DM scenarios with up to $Q_* \sim 1.85-2.25$ $(1.32-1.73)$ for 50 (60) e-folds of inflation within the contours correspond to the 68% and 95% C.L. results from Planck 2018 TT,TE,EE+lowE+lensing data [10]. In addition, this noteworthy consistency with Planck, which also leads to a finite range for the tensor-to-scalar ratio, might be relevant in the search of primordial gravitational waves via B-mode polarization experiments in the near future (see e.g. [51]).

Finally we evaluate both swampland criteria within the observational window provided by Planck [10], and we find that none is fully satisfied, with $10 \lesssim |\Delta\phi|/M_P \lesssim 21$ and $0.19 \lesssim M_P|V_{eff,\phi}|/V_{eff} \lesssim 0.4$ for 60 e-folds and $7 \lesssim |\Delta\phi|/M_P \lesssim 19$ and $0.2 \lesssim M_P|V_{eff,\phi}|/V_{eff} \lesssim 0.55$ for 50 e-folds. Nevertheless, the scenarios for which $Q_* \sim 1$ are closer to satisfying these criteria than the corresponding cold inflation scenarios, and could in fact satisfied them if they were somewhat relaxed. For instance, it has been discussed in [98, 107] that c could be as small as $\mathcal{O}(10^{-11})$, and it does not object perceiving de Sitter vacua in string landscapes. Moreover, there has been some controversy on the precise values for Δ and c, given that they depend on the specific string model being considered [108]. Basically, if Δ were increased by an order of magnitude, and c were decreasing by around $c \sim 0.4$ both swampland criteria could be easily fulfilled for $Q_* \gtrsim 1$.

6.5 Final remarks

The distributed mass (DM) model of warm inflation studied in this work fits naturally with the string landscape picture with different mass distributions in the model ultimately arising from different possible string vacua. We found for example for the $\Upsilon \sim \phi$ model with $\lambda\phi^4$ potential, full consistency with the conditions in [110] and therefore also consistency with the swampland criteria. As the $\lambda\phi^4$ potential in many respects is the benchmark inflation model, this consistency is a very promising result both for warm inflation and the DM implementation of landscape phenomenology. We also examined other types of mass distribution functions with varied level of success. Overall this shows these models have a robust range of possibility. These results encourage further understanding of DM models in particular in the context of string theory building on the ideas developed in [30].

If one accepts string theory and thus its landscape property as the fundamental description of nature, then it forces a rethink on the relevance of simplicity for an inflation model. Any point on the landscape that leads to a consistent effective field

theory model which agrees with observational data is just as good as any other. We refrain from calling this what it is, but that is the path this line of reasoning evidently takes us down. From the present vantage point with so many possible vacua, it would seem easy to argue that any working low-energy effective model leading to observationally consistent inflation can be found somewhere in this vast landscape. Alternatively said, it is hard to argue that simple low-energy models are the only ones that could arise from this landscape. It is possible that future work in string theory will reduce the number of viable vacua, but given the starting point, that seems a difficult task. From another viewpoint, the loss of predictivity that comes with the landscape property, equally encourages objective thinking whether string theory is the best way to approach the ultraviolet completion problem.

In a certain way of looking at it, DM models are rather complicated in that there are many fields and several conditions to examine and calculate. However from another perspective they are also simple in that they are renormalizable models, with canonical kinetic terms and require no assumptions of the coupling of gravity. Due to these properties, they are very amenable to be part of an extension of the Standard Model. All said, from the landscape perspective, DM models are viable models that are interesting to further explore.

Chapter 7

Conclusions

“ That there That’s not me
I go
Where I please
I walk through walls
I float down the Liffey
I’m not here
This isn’t happening
I’m not here
I’m not here
In a little while
I’ll be gone
The moment’s already passed
Yeah it’s gone
And I’m not here
This isn’t happening
I’m not here
I’m not here
Strobe lights and blown speakers
Fireworks and hurricanes
I’m not here
I’m not here
This isn’t happening
I’m not here
I’m not here ”

Head of a skeleton with a burning cigarette.
Vincent van Gogh (1853 - 1890).

—Radiohead, How to Disappear Completely

Within this thesis we have examined the consequences of dissipative dynamics in the early universe. In the context of a quasi-exponential expansion, this dynamics can yield a period of warm inflation where dissipation can sustain a radiation bath despite such abrupt growth. Moreover, the objective of early universe cosmology is to quantify the observed features of the universe and to develop a physical model to account for them. Then hopefully I described the state of the art, with respect to both warm inflation model building and the confrontation of theory with observation.

Warm inflation might be considered a landmark within the early universe cosmology. It is a precedent of an inflationary dynamics in which the state of the universe during inflation is not the vacuum state, but rather an excited statistical thermal state. It introduces dissipation into the inflationary dynamics which can be well explained by first principles of a quantum multi-field theory. Besides, this approach has several attractive features. For instance, the additional friction may ease the required flatness of the inflaton potential alleviating one of the swampland criterion. Also, even if radiation is subdominant during inflation, may smoothly become the leading component if $Q \gtrsim 1$ at the end of inflation ($\epsilon_{eff} \sim 1 + Q$), with no need for a separate reheating period. It also may explain the nature of the classical inhomogeneities observed in the CMB, since for WI the fluctuations of the inflaton are thermally induced; hence there is no need to explain the troublesome quantum-to-classical transition problem of CI, due to the purely quantum origin of the CI density perturbations. Furthermore, one well established key aspect, forecasted before by [58, 72, 106], was the prediction for a low tensor-to-scalar ratio, which now we see is consistent with data [10]. These observational predictions for warm inflation were most recently tested in [109] with good agreement with Planck data.

Taking into account above encouraging WI characteristics, we examined thoroughly two basic models: The *Warm Little Inflaton* (WLI) scenario [23] and the distributed mass (DM) model [27–29].

The WLI scenario [23] is currently the most promising realisation of warm inflation within a quantum field theory model, involving only a handful of fields and employing symmetries to cancel the troublesome thermal corrections to the inflaton potential that have frustrated earlier attempts to construct a simple warm inflation model in the high-temperature regime. Despite this crucial cancellation, a consistent inflationary dynamics requires that several conditions are satisfied throughout inflation, in particular that the fermions coupled directly to the inflaton remain light and in a near-thermal equilibrium state, ensuring also that the dissipation coefficient can be computed in the adiabatic approximation and neglecting spacetime curvature

corrections. We have focused on three types of potential for which we find agreement with observations in a broad region of parameter space, hence showing that the WLI scenario can lead to different realisations of warm inflation that are both dynamically and observationally consistent. Remarkably, WLI realisation "resurrects" the chaotic quartic potential, already ruled out by observational data within CI. Furthermore, the results of the upcoming experiments will be exciting, since in the chaotic model the dynamical constraints are, in fact, sufficient to limit the values of n_s and r to values within the Planck bounds, with $10^{-3} \lesssim r \lesssim 10^{-2}$ being potentially within the reach of ongoing and planned B-mode polarisation experiments [51].

The key outcome of this model is that sufficiently strong dissipative effects are attained, within the observational window, hence sustaining a radiation bath during inflation that becomes dominant at the end of the slow-roll regime, which in turn gives rise to a smooth transition to post-inflationary epochs. We thus hope that this work motivates further studies of the WLI scenario and of other simple realisations of warm inflation, both from the model-building and from the observational perspectives, considering also its impact on the subsequent cosmic history, towards building a complete and testable particle physics description of the early universe.

On the other hand, the ultimate goal in building inflation models is to have them consistent with observational data and also be theoretically consistent. The latter has many levels of criteria. In [110], based on general properties of quantum field theory, conditions were listed for theoretically consistent warm inflation models. In fact a subset of those conditions would also apply to cold inflation models. Amongst the criteria stated were that $\phi < M_P$ and $m_\phi > H$. The former was based on general consideration of low-energy effective field theory. The latter is so that inflaton particles remained sub-Hubble scale and is basically the η-condition. However, in contrast to cold inflation, where this condition is something one needs to model build around, in warm inflation due to the presence of dissipation this condition can hold and inflation can still occur. In Sect. (6.4) explicit examples of warm inflation models are shown where $\phi < M_p$ and $m_\phi > H$, such as in fig. 6.9. These are very stringent requirements for an inflation model and no cold inflation models can achieve both of them. The swampland criteria are basically contained within these criteria. In this work we have found warm inflation models which are consistent with all the criteria stated in [110] and so in turn are also consistent with the swampland criteria.

In a certain way of looking at it, DM models are rather complicated in that there are many fields and several conditions to examine and calculate. However from another perspective they are also simple in that they are renormalisable models, with canonical

kinetic terms and require no assumptions of the coupling of gravity. Due to these properties, they are very amenable to be part of an extension of the Standard Model. All said, from the landscape perspective, DM models are viable models that are interesting to further explore.

Modestly, I hope this attempt to describe a scenario of an early universe confronted with observational data, has allowed us a bit further our understanding of the earliest moments of the cosmos. However, perhaps the upcoming experiments would yield novel observational signatures at the end.

Appendix A

Warm Little Inflaton notes

In this appendix I copy the notes from Mar Bastero-Gil, Arjun Berera, Rudnei O. Ramos and João G. Rosa (February 27, 2016), where they computed all relevant formulas I used in chapters 5 and 6. Hence I acknowledge that I did not contribute in any of the following notes. Also, to my knowledge, all the details described in this appendix have not never been released, so I recognise that this material eventually would be potentially published in a particular journal; although, the main results are already issued in Phys. Rev. Lett. **117**, no. 15, 151301 (2016) [23].

A.1 Fermion decay width

In this appendix we compute the decay width of a fermion ψ into a boson-fermion pair, $\psi \to \sigma\psi_\sigma$, which is required for the computation of the dissipation coefficient. Since in the high-temperature regime the main contribution to the dissipation coefficient comes from on-shell fermion modes (i.e. the poles in the corresponding spectral function), we will focus on the on-shell case, where $p_0 = \omega_p = \sqrt{\mathbf{p}^2 + m^2}$, where $m \ll T$ denotes the fermion mass. In this case there are no contributions from Landau damping (thermal scatterings) to the imaginary part of the fermion self-energy, since these are kinematically forbidden and only decays and inverse decays contribute to the total decay width. Considering a standard Yukawa interaction with coupling h, the imaginary part of the fermion self-energy, which at 1-loop corresponds to the diagram below (see fig. A.1), is given by [20]:

$$\mathrm{Im}\Sigma_\psi(p_0, \mathbf{p}) = h^2 \left(1 + e^{p_0/T}\right) \int \frac{d^4k}{(2\pi)^4} n_F(p_0 - k_0)\rho_F(p - k)n_B(k_0)\rho_F(k) \ , \qquad \text{(A.1)}$$

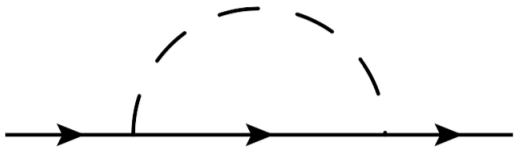

Figure A.1: Feynman diagram contributing at 1-loop to the fermion self-energy, where the internal lines correspond to the (massless) ψ_σ and σ fermion and scalar fields, respectively.

where $n_B(\omega) = (e^{\omega/T} - 1)^{-1}$ and $n_F(\omega) = (e^{\omega/T} + 1)^{-1}$ are the Bose-Einstein and Fermi-Dirac distributions, respectively. Neglecting the masses of the decay products, the corresponding spectral functions are given by:

$$\rho_B(k) = 2\pi\delta(k_0^2 - |\mathbf{k}|^2) \ , \qquad \rho_F(k) = -2\pi \not{k}\delta(k_0^2 - |\mathbf{k}|^2) \ . \tag{A.2}$$

This allows us to perform the k_0 integral in the imaginary part of the fermion self-energy, yielding:

$$\mathrm{Im}\Sigma_\psi(p_0, \mathbf{p}) = 2\pi h^2 \left(1 + e^{p_0/T}\right) \int \frac{d^3k}{(2\pi)^3} \frac{n_B(|\mathbf{k}|) n_F(|\mathbf{p} - \mathbf{k}|)}{4|\mathbf{k}||\mathbf{p} - \mathbf{k}|} (\not{k} - \not{p})\delta(p_0 - |\mathbf{k}| - |\mathbf{p} - \mathbf{k}|) \ , \tag{A.3}$$

now, one can show that:

$$1 + n_B(k_0) - n_F(p_0 - k_0) = (1 + e^{p_0/T}) n_B(k_0) n_F(p_0 - k_0) \ , \tag{A.4}$$

so that

$$\mathrm{Im}\Sigma_\psi(p_0, \mathbf{p}) = 2\pi h^2 \int \frac{d^3k}{(2\pi)^3} \frac{(1 + n_B(|\mathbf{k}|) - n_F(|\mathbf{p} - \mathbf{k}|))}{4|\mathbf{k}||\mathbf{p} - \mathbf{k}|} (\not{k} - \not{p})\delta(p_0 - |\mathbf{k}| - |\mathbf{p} - \mathbf{k}|) \ . \tag{A.5}$$

The energy conservation equation, enforced by the delta-function in the above integral, allows one to determine the angle between the $\mathbf{p}$ and $\mathbf{k}$ vectors as a function of their norms, yielding:

$$\begin{aligned} p_0 - \mathbf{k} &= \sqrt{|\mathbf{p}|^2 + |\mathbf{k}|^2 - 2|\mathbf{p}||\mathbf{k}|\cos\theta} \Leftrightarrow \\ p_0^2 + |\mathbf{k}|^2 - 2p_0|\mathbf{k}| &= |\mathbf{p}|^2 + |\mathbf{k}|^2 - 2|\mathbf{p}||\mathbf{k}|\cos\theta \Leftrightarrow \\ \cos\theta &= \frac{p_0}{|\mathbf{k}|} + \frac{|\mathbf{p}|^2 - p_0^2}{2|\mathbf{p}||\mathbf{k}|} \equiv \cos\theta_* \ . \end{aligned} \tag{A.6}$$

Using that $\delta(f(x)) = \sum_i \delta(x - x_i)/|f'(x_i)|$ where $f(x_i) = 0$, we may then write:

$$\delta(p_0 - |\mathbf{k}| - |\mathbf{p} - \mathbf{k}|) = \frac{|\mathbf{p} - \mathbf{k}|}{|\mathbf{p}||\mathbf{k}|}\delta(\cos\theta - \cos\theta_*) \ . \tag{A.7}$$

Notice that for an on-shell massless fermion we have $p_0 = |\mathbf{p}|$, such that $\cos\theta_* = 1$ independently of $|\mathbf{k}|$, which would lead us to (wrongly) conclude that the energy conservation delta-function does not impose any restrictions on the integration over $|\mathbf{k}|$. However, for any non-vanishing mass, we must ensure that $-1 \leq \cos\theta_* \leq 1$, which imposes $k_- \leq |\mathbf{k}| \leq k_+$, where

$$k_\pm = \frac{1}{2}(p_0 \pm p) \ . \tag{A.8}$$

We may then write the imaginary part of the self-energy as:

$$\mathrm{Im}\Sigma_\psi(p_0,\mathbf{p}) = \frac{h^2}{8\pi|\mathbf{p}|}\int_{k_-}^{k_+} d|\mathbf{k}|\,(1+n_B(|\mathbf{k}|)-n_F(p_0-|\mathbf{k}|))\,(\not{k}-\not{p}) \ , \tag{A.9}$$

Now, if we multiply this by $\not{p}$ and take the trace over Dirac indices, we obtain

$$\mathrm{Tr}(\not{p}\mathrm{Im}\Sigma_\psi(p_0,\mathbf{p})) = \frac{h^2}{8\pi|\mathbf{p}|}\int_{k_-}^{k_+} d|\mathbf{k}|\,(1+n_B(|\mathbf{k}|)-n_F(p_0-|\mathbf{k}|))\,(4p\cdot(k-p)) \ , \tag{A.10}$$

Using conservation of energy and momentum, we have that:

$$\begin{aligned} (p+k-p)^2 = k^2 &= 0 \Leftrightarrow \\ p^2 + 2p\cdot(k-p) + (k-p)^2 &= 0 \Leftrightarrow \\ 2p\cdot(k-p) &= -p^2 \ , \end{aligned} \tag{A.11}$$

which implies:

$$\mathrm{Tr}(\not{p}\mathrm{Im}\Sigma_\psi(p_0,\mathbf{p})) = -2p^2\frac{h^2}{8\pi|\mathbf{p}|}\int_{k_-}^{k_+} d|\mathbf{k}|\,(1+n_B(|\mathbf{k}|)-n_F(p_0-|\mathbf{k}|)) \ . \tag{A.12}$$

From this we conclude that $\mathrm{Im}\Sigma_\psi(p_0,\mathbf{p})) = \hat{\Gamma}(p_0,\mathbf{p}))\not{p}$, where

$$\begin{aligned} \hat{\Gamma}(p_0,\mathbf{p}) &= -\frac{h^2}{8\pi|\mathbf{p}|p_0}\int_{k_-}^{k_+} d|\mathbf{k}|\,(1+n_B(|\mathbf{k}|)-n_F(p_0-|\mathbf{k}|))\,(p_0-|\mathbf{k}|) \\ &= -\frac{h^2T^2}{8\pi|\mathbf{p}|p_0}\int_{x_-}^{x_+} dx\left(1+\frac{1}{e^x-1}-\frac{1}{e^{y-x}+1}\right)(y-x) \ , \end{aligned} \tag{A.13}$$

where in the last line we defined the dimensionless quantities $x = |\mathbf{k}|/T$, $x_\pm = k_\pm/T$, and $y = p_0/T$. As mentioned above, the kinematic constraints of the value of $|\mathbf{k}|$ are not apparent if one sets $m = 0$, i.e. $p_0 = |\mathbf{p}|$. In the limit $p_0 \ll T$, we would then use:

$$\int_0^\infty dx\left(1+\frac{1}{e^x-1}-\frac{1}{e^{-x}+1}\right)(-x) = -\frac{\pi^2}{4} \ , \tag{A.14}$$

to obtain $\hat{\Gamma} = h^2T^2/(32\pi|\mathbf{p}|^2)$, which is the result obtained in [31] (up to a factor of 2!). It is not, however, consistent with conservation of energy to extend the integration up to arbitrarily large momentum values for the decay products, and we must instead use:

$$\begin{aligned} f(x,y) &= \int dx \left(1 + \frac{1}{e^x - 1} - \frac{1}{e^{y-x}+1}\right)(y-x) \\ &= yx - \frac{x^2}{2} + (y-x)\log\left(\frac{1-e^{-x}}{1+e^{-(y-x)}}\right) + \mathrm{Li}_2(e^{-x}) + \mathrm{Li}_2(-e^{-(y-x)}) \ , \end{aligned} \quad \text{(A.15)}$$

where $\mathrm{Li}_2(z)$ is the dilogarithm function. It is easy to see that this exhibits a logarithmic divergence for $m \to 0$, since $x_- \to 0$ in this limit for on-shell fermions, in contrast with the result in [31]. We may write for on-shell fermions ($p_0 = \omega_p$):

$$\hat{\Gamma}(\omega_p, |\mathbf{p}|) = -\frac{h^2}{8\pi|\mathbf{p}|\omega_p} F\left(\frac{|\mathbf{p}|}{T}, \frac{m}{T}\right) \quad \text{(A.16)}$$

where $F\left(|\mathbf{p}|/T, m/T\right) = f(x_+, y) - f(x_-, y)$ for $y = \omega_p/T$. For $|\mathbf{p}| \gtrsim m$ and $m \ll T$, we have approximately:

$$F\left(\frac{|\mathbf{p}|}{T}, \frac{m}{T}\right) \simeq -\frac{|\mathbf{p}|^2}{2T^2} + \frac{|\mathbf{p}|}{T}\log\left[\frac{4|\mathbf{p}|T}{m^2}\left(1 + e^{|\mathbf{p}|/T}\right)\right] - \frac{\pi^2}{4} + \mathrm{Li}_2(e^{-|\mathbf{p}|/T}) - \mathrm{Li}_2(-e^{-|\mathbf{p}|/T}) \quad \text{(A.17)}$$

This exhibits considerable deviations from the value $-\pi^2/4$ used in [31] and, in particular, it exhibits the opposite sign as illustrated in the figure below (see fig. A.2). One should note that, despite the sign difference, the magnitude of $\hat{\Gamma}$ for $|\mathbf{P}| \sim T$ is

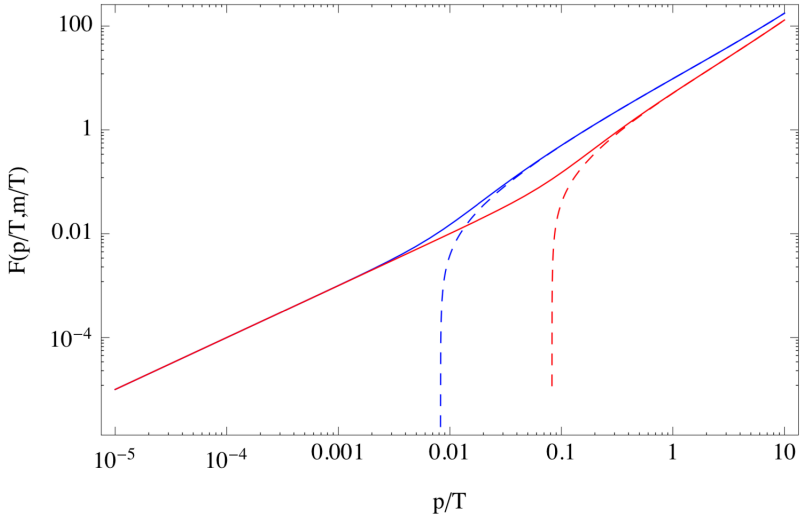

Figure A.2: Function $F\left(|\mathbf{p}|/T, m/T\right)$ for $m/T = 0.01$ (blue) and $m/T = 0.1$ (red). The corresponding dashed curves represent the approximation in eq. (A.17).

similar to the estimate of Yokoyama and Linde in [31], although there are numerical

differences that must be taken into account when computing the dissipation coefficient as we explain in the next section of this appendix. To compute the fermion decay width from the imaginary part of the self-energy, we must consider the dressed fermion propagator:

$$\begin{aligned} S_\psi(p) &= \frac{i}{\not{p} - m - i\mathrm{Im}\Sigma_\psi} = \frac{i}{(1 - i\hat{\Gamma})\not{p} - m} \\ &= \frac{i\left((1 - i\hat{\Gamma})\not{p} + m\right)}{(1 - 2i\hat{\Gamma})p^2 - m^2} \ , \end{aligned} \tag{A.18}$$

where we absorbed the real part of the fermion self-energy in the renormalised mass m and kept the lowest order terms n $\hat{\Gamma}$. The poles in the propagator then occur for:

$$\begin{aligned} (1 - 2i\hat{\Gamma})(p_0^2 - |\mathbf{p}|^2) - m^2 = 0 \quad &\Leftrightarrow \\ p_0^2 - |\mathbf{p}|^2 = m^2(1 + 2i\hat{\Gamma}) \quad &\Leftrightarrow \\ p_0^2 = \omega_p^2 + 2im^2\hat{\Gamma} \quad &\Leftrightarrow \\ p_0 = \omega_p + i\frac{m^2}{\omega_p}\hat{\Gamma} \ , \end{aligned} \tag{A.19}$$

so that the fermion decay width is given by:

$$\Gamma = \frac{m^2}{\omega_p}|\hat{\Gamma}| \ . \tag{A.20}$$

A.2 Dissipation coefficient

In this section we compute the dissipation coefficient for a Yukawa-like interaction between the inflaton and a fermion ψ in the high-temperature regime, where $m \ll T$. The 1-loop dissipation coefficient computed in the adiabatic approximation (from a diagram of the form (a) in fig. 5.1) can be written as [20]:

$$\Upsilon = \frac{g^2}{2T}\int \frac{d^4p}{(2\pi)^4}\mathrm{Tr}[\rho_F^2]n_F(p_0)(1 - n_F(p_0)) \ , \tag{A.21}$$

where the trace is taken over Dirac indices and the fermionic spectral function is given by:

$$\begin{aligned} \rho_F(p_0) &= \frac{i}{(1 - i\hat{\Gamma})\not{p} - m} - \frac{i}{(1 + i\hat{\Gamma})\not{p} - m} \\ &= -\frac{2\hat{\Gamma}}{(p^2 - m^2)^2 + 4\hat{\Gamma}^2p^4}\left[\not{p}(p^2 + m^2) + 2mp^2\right] \ . \end{aligned} \tag{A.22}$$

At high temperatures, $m \ll T$, the leading contribution to the dissipation coefficient

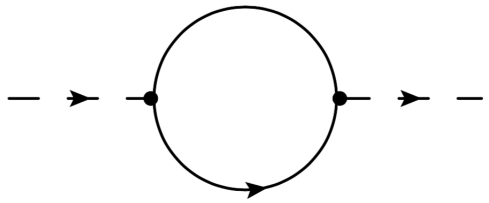

Figure A.3: Feynman diagram contributing at 1-loop to the fermion self-energy, where the internal lines correspond to the (massless) ψ_i and ϕ fermion and scalar fields, respectively. This diagram yields a nonlocal contribution, with external legs corresponding to different times t and t'.

comes from the poles in the spectral function, i.e. from real fermion modes in the thermal bath. We may then write the spectral function near the poles as [85]:

$$\rho_F(p) = -(\not{p} + m)\rho_B \ , \quad \rho_B = \frac{4\omega_p \Gamma}{(p_0^2 - \omega_p^2)^2 + 4\omega_p^2 \Gamma^2} \ , \tag{A.23}$$

where ρ_B is the bosonic spectral function with the well-known Breit-Wigner form, and we have used the result in eq. (A.20) for the fermion decay width. In the narrow width limit, $\Gamma \ll m$, the bosonic spectral function becomes:

$$\rho_B = 2\pi\delta(p_0^2 - \omega_p^2) = 2\pi \left(\frac{\delta(p_0 - \omega_p)}{2\omega_p} + \frac{\delta(p_0 + \omega_p)}{2\omega_p} \right) \ , \tag{A.24}$$

while the product of two bosonic spectral functions becomes:

$$\rho_B^2 = \frac{\rho_B}{2} \times 2\pi\delta(p_0^2 - \omega_p^2) = \frac{\pi}{2\omega_p^2 \Gamma} \left[\delta(p_0 - \omega_p) + \delta(p_0 + \omega_p) \right] \ . \tag{A.25}$$

Using that $\mathrm{Tr}[(\not{p} + m)^2] = 4(p^2 + m^2) = 8m^2$ for on-shell particles, we can perform the p_0 integral to yield for the dissipation coefficient:

$$\Upsilon = \frac{2g^2}{T} \int \frac{d^3p}{(2\pi)^3} \frac{m^2}{\omega_p^2 \Gamma} n_F(\omega_p)(1 - n_F(\omega_p)) \ . \tag{A.26}$$

We may then use the results obtained in the previous section for the fermion decay width, assuming that $g \ll h$ so that the coupling between the inflaton and the fermion gives a sub-dominant contribution to the latter. This then gives:

$$\Upsilon = \frac{8}{\pi} \frac{g^2}{h^2} T \int_0^\infty dx x^3 \frac{n_F(1 - n_F)}{F(x, \tilde{m})} \ , \tag{A.27}$$

where we have defined $x = |\mathbf{p}|/T$ and $\tilde{m} = m/T$. Note that the Fermi-Dirac distribution is evaluated at $\omega_p/T = \sqrt{x^2 + \tilde{m}^2}$. The dissipation coefficient is thus of the form:

$$\Upsilon = C_T T \ , \quad C_T = \alpha(\tilde{m}) \frac{g^2}{h^2} \ , \tag{A.28}$$

where the parameter $\alpha(\tilde{m})$ can be obtained numerically and is illustrated in the fig. A.4 below. As one can see in fig. A.4, the parameter α is about one order of magnitude lower

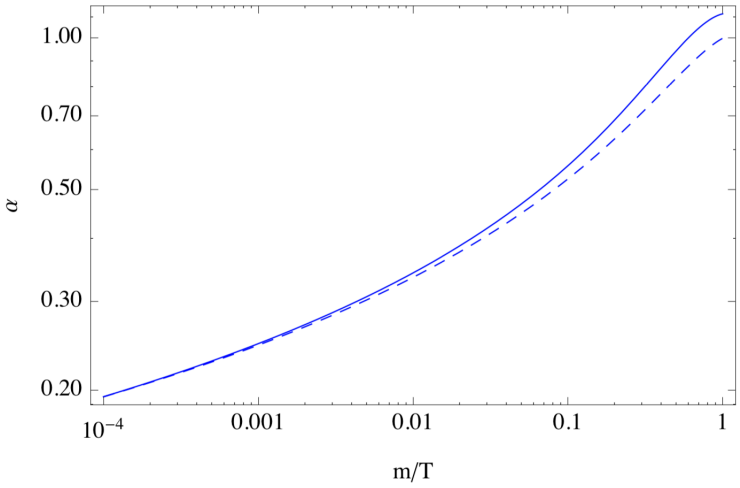

Figure A.4: The parameter $\alpha = \Upsilon h^2/(g^2 T)$ as a function of the fermion mass, obtained numerically (solid blue curve). The dashed blue curve yields the result obtained by replacing $F(x, \tilde{m}) \simeq F(p_{max}/T, m/T)$.

than the estimate made by Yokoyama and Linde of ~ 11.2, which is associated with their underestimation of the fermion decay width. As shown by the dashed curve in the figure above, one can obtain a good approximation to the parameter α by evaluating the width function $F(|\mathbf{p}|/T, m/T)$ at $p_{max}/T \simeq 3.24$, which corresponds to the momentum value where the integrand function $|\mathbf{p}|^3 n_F(1 - n_F)$ is peaked, i.e. the momentum value which gives the dominant contribution to the dissipation coefficient. Note that Yokoyama and Linde had used their estimate of the fermion decay width for $p \ll T$, which explains part of the discrepancy. We then have:

$$F\left(\frac{p_{max}}{T}, \frac{m}{T}\right) \simeq 3 + p_{max} \log\left(\frac{4 p_{max}}{m^2/T^2}\right) \ , \tag{A.29}$$

which takes values $\mathcal{O}(10 - 100)$ for $m/T = 10^{-6} - 1$ and

$$\alpha(\tilde{m}) \simeq \frac{3}{(1 - 0.34 \log(h))} \ . \tag{A.30}$$

The fermion decay width at this momentum value is then given by:

$$\Gamma\left(\frac{p_{max}}{T},\frac{m}{T}\right)\simeq\frac{h^2}{8\pi}\frac{m^2T^2}{p_{max}\omega_{p_{max}}^2}F\left(\frac{p_{max}}{T},\frac{m}{T}\right)\ . \tag{A.31}$$

Taking the fermion mass to be dominated by the thermal contribution $m^2\simeq h^2T^2/8$, we may estimate the decay width at the maximum momentum value, which is the value which one must compare with the Hubble expansion rate during inflation to ensure that the dominant momentum modes are nearly thermalised. This is illustrated in the fig. A.5 below as a function of the Yukawa coupling h. It is curious to note that, as illustrated in this figure, the value of the decay width is quite similar to the one estimated by Yokoyama and Linde for $p\sim T$, despite their approximation overestimating the dissipation coefficient by roughly an order of magnitude.

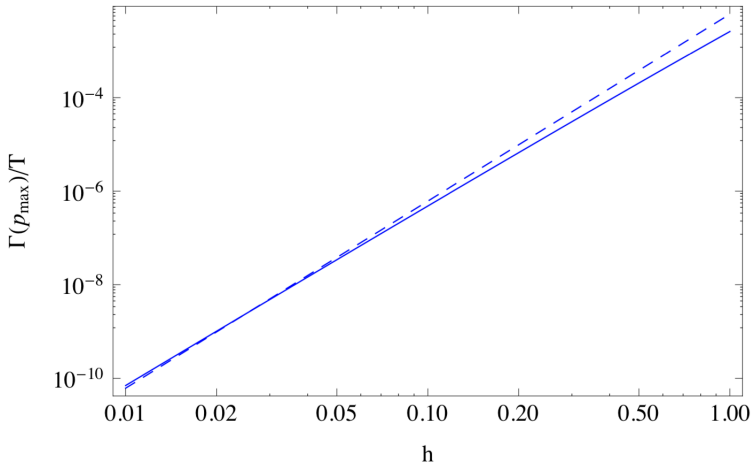

Figure A.5: Fermion decay width evaluated at the dominant momentum p_{max} as a function of the coupling h (solid curve). The dashed curve corresponds to the estimate obtained by Yokoyama and Linde for $p\sim T$ [31].

Once again I repeat: I did not contribute at all in the elaboration of above notes.

Appendix B

Homogeneous DM Scalars

The key feature of the model is that the inflaton field couples to a tower of scalar particles with effective masses $\tilde{m}^2_{\chi i} = m^2_{\chi i} + m^2_T$ that depend on the inflaton field:

$$\tilde{m}^2_{\chi i} = g^2(\phi - M_i)^2 + fT^2\,, \qquad f = \frac{g^2}{12} + \frac{h^2}{8}\,. \tag{B.1}$$

These scalars can be classified as light or heavy states according to their bare masses $m_{\chi i}$. We relate as light states to those whose masses are smaller than the temperature $m_{\chi i}/T < 1$, whilst heavy states correspond to $m_{\chi i}/T > 1$. We may also refer as high or low temperature regime, respectively. The tower of scalars is sufficiently large such that the number of light fields at both sides of the inflaton remains the same during all the inflationary evolution. The dissipative coefficient arising from the pattern of interactions among the scalar component and the light states is given by [27–29] (see also 6.2.1):

$$\Upsilon^S(\phi, T) = \sum_{i=1}^{t.e} \frac{32g^4}{\pi h^2 \left[16\frac{m^2_{\chi i}}{\tilde{m}^2_{\chi i}} + \frac{\tilde{m}^2_{\chi i}}{T^2}\right]} \ln\left(\frac{2T}{\tilde{m}_{\chi i}}\right) \frac{(\phi - M_i)^2}{\tilde{m}_{\chi i}}\,. \tag{B.2}$$

where "t.e." means sum over all thermally excited sites. In the computation of the dissipative coefficient, the thermal corrections to χ_i masses induced by the self interactions are already taken into account through the couplings g and h. Also the total decay rate for all processes is [27–29] (see also 6.2.1):

$$\Gamma^S_{\chi_i} = \Gamma_{\chi_i}(\chi\sigma\sigma) + \Gamma_{\chi_i}(\chi\bar{\psi}_\sigma\psi_\sigma) = \frac{h^2}{128\pi}\frac{T\tilde{m}_{\chi_i}}{\omega_{\chi_i}(p)}\left[16\frac{m^2_{\chi i}}{\tilde{m}^2_{\chi i}} + \frac{\tilde{m}^2_{\chi i}}{T^2}\right]\,. \tag{B.3}$$

We are interested in developing an approach capable of adding the contributions from only the light fields. Moreover, this model is based on a discrete tower of states, then let $M_b = M_{max} - b\Delta m$, $M_{max} = \phi + T/g$ and $\Delta m = 2T/(g n_\chi(T))$, where $n_\chi(T)$ represents the no. of effective light degrees of freedom. So that we fix the initial value of $n_\chi(T_0)$ and that sets the mass splitting in the tower Δm. Hence let us define z_b in the following way:

$$z_b = \frac{m_{\chi b}}{T} = \frac{g}{T}(M_b - \phi) = \left(1 - \frac{2b}{n_\chi}\right), \tag{B.4}$$

now in order to have symmetric sums we set $b' = b - n_\chi/2$, then we have:

$$z_{b'} = \frac{m_{\chi b'}}{T} = -\frac{2b'}{n_\chi}, -\frac{n_\chi}{2} \leq b' \leq \frac{n_\chi}{2}. \tag{B.5}$$

We already have a suitable prescription on how to perform the sums adequately; but before, to approximate the dissipative coefficient eq. (B.2), we may write it as:

$$\Upsilon^S = \frac{32 g^2}{\pi h^2} T \sum_{b'=-n_\chi/2}^{n_\chi/2} \frac{z_{b'}^2 \sqrt{z_{b'}^2 + f}}{\left[16 z_{b'}^2 + (z_{b'}^2 + f)^2\right]} \ln\left(\frac{2}{\sqrt{z_{b'}^2 + f}}\right), \tag{B.6}$$

where we made use of $\tilde{m}_\chi^2$ (eq. (B.1)). Since $-1 \leq z_{b'} \leq 1$ we can approximate above function by a Taylor expansion:

$$\frac{z_{b'}^2 \sqrt{z_{b'}^2 + f}}{\left[16 z_{b'}^2 + (z_{b'}^2 + f)^2\right]} \ln\left(\frac{2}{\sqrt{z_{b'}^2 + f}}\right) \simeq A_0 + A_1(z_{b'} - 1) + A_2(z_{b'} - 1)^2, \tag{B.7}$$

where the expansion was performed only at $z_{b'} = +1$, since the function is even, and coefficients A_i are:

$$A_0 = \frac{\sqrt{f+1}(\ln(4) - \ln(f+1))}{2f(f+2) + 34} \tag{B.8}$$

$$\begin{aligned} A_1 = \frac{1}{2\sqrt{f+1}(f(f+2)+17)^2} \big[& -\left((2f+3)f^2 + 15\right)\ln(f+1) \\ & + f(f(f\ln(16) - 2 + \ln(64)) - 4) - 34 + 30\ln(2)\big] \end{aligned} \tag{B.9}$$

$$\begin{aligned} A_2 = \frac{2}{4(f+1)^{3/2}(f(f+2)+17)^3} \big\{ \big[& f\left(f\left(f\left(f\left(f^2\ln(4) - f(5+\ln(8)) - 17 - 126\ln(2)\right)\right.\right.\right. \\ & \left.\left.\left. -2(57 + 73\ln(2))\right) - 6(27 + \ln(32))\right) - 281 + 157\ln(2)\right) - 221 - 94\ln(2)\big] \\ & + (f(f(f(f((3-2f)f + 126) + 146) + 30) - 157) + 94)\ln(f+1)\big\} \end{aligned} \tag{B.10}$$

Moreover, given that at both limits $z_b = \pm 1$ the coefficients A_i are symmetric, certainly due to the argument of the sum eq. (B.7) being an even function, we compute half of

the sum and multiply by a factor of 2, then we have:

$$
\begin{aligned}
2\sum_{b'=-\frac{n_\chi}{2}}^{0}&\left\{A_0+A_1\left(-\frac{2b'}{n_\chi}-1\right)+A_2\left(-\frac{2b'}{n_\chi}-1\right)^2\right\}\\
&=2A_0-A_1+A_2+\left(A_0-\frac{A_1}{2}+\frac{A_2}{3}\right)n_\chi+\frac{2A_2}{2n_\chi}\\
&\simeq\left(A_0-\frac{A_1}{2}+\frac{A_2}{3}\right)n_\chi
\end{aligned}
\tag{B.11}
$$

where the final result comes by taken only the leading n_χ. Although the series eq. (B.7) is a good estimation, it does not fit well at $z_{b'}=0$, and being that this contribution is null in the sum, we subtract that value (at $z_{b'}=0$) from eq. (B.7) once to improve such approximation. We have the following factor that takes into account this adjustment:

$$
\hat{S}=A_0-\frac{A_1}{2}+\frac{A_2}{3}-(A_0-A_1+A_2)=\frac{A_1}{2}-\frac{2A_2}{3}\,. \tag{B.12}
$$

Once we identify the general mass scale $M=g\Delta m$, we have $n_\chi(T)/T=n_\chi(T_0)/T_0=2/(g\Delta m)$, then numerically we set the initial value of $n_\chi(T_0)$ or else Δm. Therefore the dissipative coefficient can be approximated as:

$$
\Upsilon^S\simeq\frac{48Ng^2\hat{S}}{\pi}n_\chi(T)T\simeq\hat{C}T^2\,,\quad \hat{C}=\frac{48Ng^2\hat{S}}{\pi}\frac{n_\chi(T_0)}{T_0}=\frac{48Ng^2\hat{S}}{\pi}\frac{2}{g\Delta m}\,. \tag{B.13}
$$

To compute the radiative corrections to the potential we implement the same above prescription. The thermal correction for light bosons can be approximated by the expression [104]:

$$
V_T^S=-\sum_i^{t.e.}\frac{\pi^2}{90}T^4+\frac{1}{24}\sum_i^{t.e.}m_{\chi i}^2T^2-\frac{1}{12\pi}\sum_i^{t.e.}m_{\chi i}^3T-\frac{1}{64\pi^2}\sum_i^{t.e.}m_{\chi i}^4\ln\frac{m_{\chi i}^2}{c_BT^2}\,, \tag{B.14}
$$

where $\ln c_B=\frac{3}{2}+2\ln 4\pi-2\gamma\simeq 5.41$ [104]. The semi-analytical approximation for the radiative corrections, only for the light degrees of freedom coming from the scalar

tower of states, are:

$$\frac{V_T^S(z)}{T^4} \simeq \sum_{b'=-n_\chi/2}^{n_\chi/2} \left[-\frac{\pi^2}{90} + \frac{z_{b'}^2}{24} - \frac{z_{b'}^3}{12\pi} - \frac{z_{b'}^4}{64\pi^2} \ln\left(\frac{z_{b'}^2}{c_b}\right) \right]$$
$$\simeq -\frac{\pi^2(1+n_\chi)}{90} + \frac{(1+n_\chi)(2+n_\chi)}{72 n_\chi} - \frac{(1+n_\chi)(n_\chi+2)(3n_\chi(n_\chi+2)-4)}{960\pi^2 n_\chi^3} \ln\left(\frac{4}{c_b n_\chi^2}\right)$$
$$+\frac{3\zeta(5) - 4\pi^4 \zeta^{(1,0)}\left(-4, 1+\frac{n_\chi}{2}\right)}{4\pi^6 n_\chi^4} \tag{B.15}$$

$$\frac{\partial}{\partial z_b}\left(\frac{V_T^S(z)}{T^4}\right) \simeq \sum_{b'=-n_\chi/2}^{n_\chi/2} \left[\frac{z_{b'}}{12} - \frac{3}{12\pi} z_{b'}^2 - \frac{z_{b'}^3}{16\pi^2}\left[\ln\left(\frac{z_{b'}^2}{c_b}\right) + \frac{1}{2} \right] \right]$$
$$= -\frac{(1+n_\chi)(2+n_\chi)}{12\pi n_\chi} \tag{B.16}$$

where $\zeta^{(1,0)}(a,x) = \partial\zeta(y,x)/\partial y \mid_{y=a}$, it is the first partial derivative of the Hurwitz Zeta function evaluated at some integer a, and $\zeta(a)$ is the Riemann Zeta function. The first partial derivative of the Hurwitz Zeta function can be evaluated as [111]:

$$\zeta^{(1,0)}(1-n,a) = \frac{1}{n}\left(\ln a - \frac{1}{n}\right) B_n(a) - \frac{a^{n-1}}{2n} - \frac{1}{n}\sum_{k=2}^{n} B_k \sum_{j=0}^{k-1} \binom{n}{j} \frac{(-1)^j}{k-j} a^{n-k}$$
$$+(-1)^{n-1}(n-1)! \sum_{k=n+1}^{\infty} \frac{B_k}{k(k-1)\cdots(k-n)} a^{n-k}\,, \tag{B.17}$$

where $B_n(a)$ and B_k are the Bernoulli polynomial of degree n and Bernoulli number respectively. For the second derivative we approximate $\ln z_{b'}^2$ using a Taylor expansion around $z_{b'}^2 = 1$, as follows: $\ln z_{b'}^2 \simeq -z_{b'}^4/2 + 2z_{b'}^2 - 3/2$; therefore the second derivative is:

$$\frac{\partial^2}{\partial z_b^2}\left(\frac{V_T^S(z)}{T^4}\right) \simeq \sum_{b'=-n_\chi/2}^{n_\chi/2} \left[\frac{1}{12} - \frac{z_{b'}}{2\pi} + \left(\frac{3}{2} + \ln c_b\right) \frac{3z_{b'}^2}{16\pi^2} - \frac{15 z_{b'}^4}{16\pi^2} + \frac{7 z_{b'}^6}{16\pi^2} \right]$$
$$\simeq \frac{1+n_\chi}{12} + \left(\frac{3}{2} + \ln c_b\right) \frac{(1+n_\chi)(2+n_\chi)}{16\pi^2 n_\chi} - \frac{(1+n_\chi)(2+n_\chi)(-4+6n_\chi+3n_\chi^2)}{16\pi^2 n_\chi^3}$$
$$+\frac{(1+n_\chi)(2+n_\chi)(16-24n_\chi+12n_\chi^3+3n_\chi^4)}{48\pi^2 n_\chi^5}\,. \tag{B.18}$$

With above eqs. (B.15-B.18) we construct the following temperature and field derivatives:

$$V^S_{T,T} = 4T^3\frac{V^S_T}{T^4} - m_\chi T^2\frac{\partial}{\partial z_{b'}}\left(\frac{V^S_T}{T^4}\right) \simeq T^3\sum_{b'=-n_\chi/2}^{n_\chi/2}\left[-\frac{4\pi^2}{90}+\frac{z^2_{b'}}{12}-\frac{z^3_{b'}}{12\pi}+\frac{z^4_{b'}}{32\pi^2}\right]$$
$$\simeq T^3\left\{-\frac{2\pi^2(1+n_\chi)}{45}+\frac{(1+n_\chi)(2+n_\chi)}{36n_\chi}\right.$$
$$\left.+\frac{(1+n_\chi)(2+n_\chi)(-4+6n_\chi+3n^2_\chi)}{480\pi^2 n^3_\chi}\right\} \tag{B.19}$$

$$V_{T,TT} = m^2_\chi\frac{\partial^2}{\partial z^2_{b'}}\left(\frac{V^S_T}{T^4}\right) - 6m_\chi T\frac{\partial}{\partial z_{b'}}\left(\frac{V^S_T}{T^4}\right) + 12T^2\frac{V^S_T}{T^4}$$
$$\simeq T^2\sum_{b'=-n_\chi/2}^{n_\chi/2}\left[-\frac{12\pi^2}{90}+\frac{z^2_{b'}}{12}-\frac{z^4_{b'}}{32\pi^2}\right]$$
$$\simeq T^2\left\{-\frac{2\pi^2(1+n_\chi)}{15}+\frac{(1+n_\chi)(2+n_\chi)}{36n_\chi}\right.$$
$$\left.-\frac{(1+n_\chi)(2+n_\chi)(-4+6n_\chi+3n^2_\chi)}{480\pi^2 n^3_\chi}\right\} \tag{B.20}$$

$$V^S_{T,T\phi} = -gm_\chi T\frac{\partial^2}{\partial z^2_{b'}}\left(\frac{V^S_T}{T^4}\right) + 3gT^2\frac{\partial}{\partial z_{b'}}\left(\frac{V^S_T}{T^4}\right) \simeq gT^2\sum_{b'=-n_\chi/2}^{n_\chi/2}\left[\frac{z_{b'}}{6}-\frac{z^2_{b'}}{4\pi}+\frac{z^3_{b'}}{8\pi^2}\right]$$
$$\simeq -gT^2\frac{(1+n_\chi)(2+n_\chi)}{12\pi n_\chi} \tag{B.21}$$

Note that all eqs. (B.19-B.21) result after having done the sum. By considering the mass scales to be evenly spaced and implementing a semi-analytical approximation, we were able to compute both the radiative corrections and the dissipative coefficient, yielding non-zero contributions of the effective finite temperature potential and its derivatives and a quadratic dissipative coefficient. Furthermore, we may have a linear dissipative coefficient by keeping $n_\chi(T) =$ constant; wherein such temperature dependancy was studied before within the WLI scenario [23, 86, 92], having remarkable agreement with Planck data 2015 [87]. Then we must guarantee that all light scalars remain in a nearly-thermal state during inflation, so that the above result for the dissipation coefficient is a consistent approximation. Such requirement refers to the adiabatic condition $\Gamma^S_\chi/H \gtrsim 1$, which can be written in terms of $z_{b'}$ as:

$$\frac{\Gamma^S_\chi}{H} = \frac{1}{128\pi}\left[16\frac{z^2_{b'}}{z^2_{b'}+f}+z^2_{b'}+f\right]\frac{T}{H} \gtrsim 1\,, \tag{B.22}$$

where essentially one evaluates such constriction at any spot on the tower of states, for instance, the edges at $z_{b'} = \pm 1$; as well as when $z_{b'} = 0$ ($\phi = M_{b'}$), where at this

location the sole contribution in the adiabatic condition becomes the massless χ's fields (recall the bare masses $m^2_{\chi b'} = g^2(\phi - M'_b)^2$). For the dissipation coefficient eq. (B.13) we can construct a master formula using the slow-roll equations, yielding:

$$Q(1+Q)^2 = \frac{\hat{C}^2}{12C_R(T)}\left(\frac{V_{eff,\phi}}{3H^2}\right)^2 , \tag{B.23}$$

Then from eq. (B.23) we can derive the evolution equation for the ratio $Q = \Upsilon/(3H)$:

$$\left(\frac{1+3Q}{1+Q} - A_T\right)\frac{d\ln Q}{dN_e} = -2\frac{\eta_{eff}}{1+Q} + (4 - A_T)\,\epsilon_H \,, \tag{B.24}$$

where $\epsilon_H = -\dot{H}/H^2 = -d\ln H/dN_e$, $\dot{H} = -(\dot{\phi}^2 + Ts_R)/(2M_p^2)$ being the time derivate of the Hubble parameter; and we have defined A_T as:

$$A_T = T\left(\frac{\partial \ln V_{eff,\phi}}{\partial T} - \frac{1}{2}\frac{d\ln g_{eff}(T)}{dT}\right) , \tag{B.25}$$

note the second term needs $g_{eff} = g_{eff}(T)$, otherwise this term is null. From the amplitude of the curvature power spectrum eq. (4.23), we may determine the scalar spectral index $n_s - 1 \simeq d\ln\Delta^2_{\mathcal{R}}/dN_e$, which is given by:

$$\begin{aligned} n_s - 1 = {} & 2\frac{\eta_{eff}}{1+Q} - \left(\frac{11}{2} - T_*\frac{\partial \ln V_{eff,\phi}}{\partial T}\Big|_*\right)\epsilon_{H*} \\ & + \left[\frac{2Q_*}{1+Q_*} + Q_*\frac{d\ln G(Q)}{dQ}\Big|_* - T_*\frac{\partial \ln V_{eff,\phi}}{\partial T}\Big|_*\right]\frac{d\ln Q}{dN_e}\Big|_* \\ & + \left[2\frac{T_*}{H_*}\left(\frac{\sqrt{3}\pi Q_*}{\sqrt{3+4\pi Q_*}} + 1\right) + 1\right]^{-1} \times \\ & \times \left\{\left(\frac{T_*}{H_*}\right)\left[\frac{\sqrt{3}\pi Q_*}{\sqrt{3+4\pi Q_*}}\left(\frac{9+8\pi Q_*}{3+4\pi Q_*}\right) + 1\right]\frac{d\ln Q}{dN_e}\Big|_* - \frac{\epsilon_{H*}}{2}\right\} . \end{aligned} \tag{B.26}$$

Although tensor perturbations are not affected by dissipation, the ratio r of the tensor-to-scalar perturbations will change due to the modified amplitude of the primordial scalar spectrum. Hence r results in:

$$r \simeq \frac{16\epsilon_{eff}}{(1+Q_*)^2 K(T_*/H_*, Q_*)} , \tag{B.27}$$

where

$$K(T_*/H_*, Q_*) = \left(\frac{2\sqrt{3}\pi Q_*}{\sqrt{3+4\pi Q_*}}\frac{T_*}{H_*} + \coth\left(\frac{H_*}{2T_*}\right)\right) G(Q_*) \,, \tag{B.28}$$

note that r is suppressed w.r.t. the CI prediction by a factor $(1+Q_*)^2 K(T_*/H_*, Q_*) > 1$. On the other hand, little can be said about the scalar spectral index, since one must find an appropriate numerical fit of the growing mode function $G(Q_*)$, but this

might be studied on another occasion; although, one would expect certain behaviour by investigating related previous works; for instance see the WLI model [23, 86, 92], where the observational predictions of a bunch of different inflationary potentials exhibit a generic behaviour in the high dissipative regime: the scalar spectral index n_s is rather blue-tilted.

Furthermore, in the original idea of DMS model [27–29] authors found that in order to have 60 e-folds of inflation was needed to introduce at least $10^2 \sim 10^5$ mass sites N_M or equivalent number of scalar fields. This proposal was highly criticised at that time, for instance in [31] authors remarked how difficult is to realise the idea of WI in realistic models of elementary particles. Nevertheless, the model was intended to illustrate a scheme developed by first principles inspired by string theories exhibiting $\mathcal{N} = 1$ global supersymmetry, with the inflaton coupled to massive modes of the string [32]. Within this context, as a natural consequence of the modification of short-distance physics, required by string theory, a large number of fields is necessary to accomplish sufficient inflation [27–29]. Although, this model may be regarded discouraging from any realistic inflation physics, such methodology is a good constructive tool for studying WI dynamics. Moreover, this scheme is evidence that combining theoretical implementation with observations, inflation paradigm can be examined as multi-field problem.

Appendix C

DM in the continuum limit

Even though we developed a very simple methodology in order to compute the finite sums in both dissipative coefficients and radiative contribution to finite temperature potential (see 6.3 for the entire description), we also explore the continuum limit of such mass states distribution. We restrict ourselves to a straightforward first attempt: constant number of mass sites. Moreover, we compute the contributions to the effective potential considering even the effective mass of both channels: fermions and scalars. Indeed, in most of the calculation we consider the thermal mass the dominant component, as such our results constitute a different approach that the one we examined before.

C.1 Dissipative coefficients in the continuum limit

For given values of ϕ and T, the light states in the tower have bare masses between $M_- = \phi - T/g$ and $M_+ = \phi + T/g$. Let us consider the continuum limit, where the mass gap $\Delta M_i = M_i + 1 - M_i \ll M_i$. The total number of light states is then given by:

$$N_M = \int_{M_-}^{M_+} dM n(M)\,, \tag{C.1}$$

where $n(M)$ is the density of states, i.e. the number of states with masses between M and $M + dM$. Let $n_\pm = n(M_\pm)$, and for $g\phi \ll T$, we may consider a local approximation:

$$n_\pm = n(\phi) \pm \frac{T}{g} n'(\phi) + \cdots\,, \tag{C.2}$$

where $n'(\phi) = dn/dM|_{M=\phi}$. Let $x = \phi - M$, integrating eq.(C.1) using x as the integration variable and the local approximation eq.(C.2), we have:

$$\begin{aligned} N_M &= \int_{M_-}^{M_+} dM n(M) = \int_{-T/g}^{T/g} dx n(\phi - x) = \int_{-T/g}^{T/g} dx \left[n(\phi) - x n'(\phi) + \cdots \right] \\ &= \frac{2T}{g} n(\phi) + \frac{T^3}{3g^3} n''(\phi) + \cdots . \end{aligned} \tag{C.3}$$

Note that the field dependancy of $n(\phi)$ is not explicitly evident, it may be obtained by solving the background dynamics given an inflationary potential. Once we have established a method to obtain the total number of mass sites crossed by the inflaton ϕ during warm inflation, we can transform the sums of both dissipative coefficients eqs. (6.71) and (6.79) to integrals. Having for the scalar one at leading order:

$$\begin{aligned} \Upsilon^S(\phi, T) &= \frac{32 g^4}{\pi T \sqrt{f}} \ln\left(\frac{2}{\sqrt{f}}\right) \int_{-T/g}^{T/g} dx \left[n(\phi) - x n'(\phi) + \cdots \right] \frac{x^2}{\left[\frac{16 g^2}{f} \frac{x^2}{T^2} + f \right]} \\ &\simeq \frac{2 C_T^S}{g} n(\phi) T^2 , \quad C_T^S = \frac{2 g^2 \sqrt{f}}{\pi} \ln\left(\frac{2}{\sqrt{f}}\right) \left[1 - \frac{f}{4} \mathrm{ArcTan}\left(\frac{4}{f}\right) \right] , \end{aligned} \tag{C.4}$$

where we have assumed that $\ln(2T/\tilde{m}_{\chi i}) \simeq \ln\left(2/\sqrt{f}\right)$ since the thermal mass can be approximated as $\tilde{m}_{\chi i}^2 \simeq g^2 T^2/12 + h^2 T^2/8$ given that the χ_i fields must remain light, i.e. satisfying $m_{\chi i}^2/T^2 < 1$. By using the same prescription, we have for the fermionic dissipative coefficient:

$$\Upsilon^F(\phi, T) \simeq \frac{2 C_T^F}{g} n(\phi) T^2 . \tag{C.5}$$

The explicit field dependancy of $n(\phi)$ will be determined by the distribution of the mass states. We will see later how this field dependancy indeed affects the behaviour of the dissipative coefficient.

C.2 Constant number of mass sites

The number of states satisfying $g^2(\phi - M_i)^2 \lesssim T^2$ indeed depends on the mass spectrum in the tower and the evolution of both the inflaton field value and the temperature. Naturally, the higher the temperature the larger the range of masses of light states satisfying this condition, but at the same time the inflaton field value will be slowly scanning different portions of the tower as inflation proceeds. Typically, the temperature decreases during warm inflation, such that if the light states are evenly distributed in mass the number of light states contributing to the inflationary dynamics (dissipation, thermal corrections to the potential) will decrease as inflation

proceeds. We will assume the existence of a tower such that the number of light states remains approximately constant at a value $N_M = N_\chi$ $(= N_\psi)$ for scalar (fermions) during inflation. We thus take N_M to be a free model parameter characterising the bosonic and fermionic mass spectrums. Under this assumption all light states contribute equally to the dissipation coefficient, and we discard the contribution from heavy fields $(g^2(\phi - M_i)^2 \gtrsim T^2)$. By differentiating with respect to time eq.(C.3), noting that $\phi = \phi(t)$ and $T = T(t)$, we obtain:

$$\dot{N}_M = \frac{2}{g}\left[n'(\phi)\dot{\phi}T + n(\phi)\dot{T}\right] + \cdots . \tag{C.6}$$

In general at leading order, we may determine the distribution of states in the tower by requiring $\dot{N}_M = 0$, yielding:

$$\frac{1}{n(\phi)}\frac{dn(\phi)}{d\phi} = -\frac{\dot{T}}{T\dot{\phi}} = -\frac{1}{T}\frac{dT}{d\phi}\,, \tag{C.7}$$

which solution is $n = C_\phi T^{-1}$. Such field dependancy of $n(\phi)$ is not explicitly evident, it may be obtained by solving the background dynamics given an inflationary potential. However, having that $n \sim T^{-1}$, at leading order, could be highly convenient because that would suggest that the density of states depends of the ambient temperature T, whichever is, and explicitly is independent of the field. Hence, this implies that the DM scenario with a constant number of sites will not depend too much on the inflationary model behind, otherwise this function $n(\phi)$ may be conditioned on the inflationary driven potential. Hence, in the local approximation the density of states could be taken only as temperature T dependent, and independent of the field; therefore $n'(\phi) = n''(\phi) = 0$. Thus we have $N_M \simeq 2Tn/g$ (see eq. (C.3)), hence $n \simeq gN_M/(2T)$. In this regime both dissipative coefficients become:

$$\Upsilon^S(T) \simeq N_M C_T^S T\,, \tag{C.8}$$

$$\Upsilon^F(T) \simeq N_M C_T^F T\,. \tag{C.9}$$

We implement the results above to evaluate the contribution of the light fermions and light scalars in the tower of the finite temperature effective potential. We start by considering the contribution of the light fermions in the tower to the finite temperature effective potential given by [84, 90, 103]:

$$V_T^{\psi_{\chi_i}} \simeq \frac{1}{2}\sum_i \left\{ -\frac{7\pi^2}{180}T^4 + \frac{\tilde{m}^2_{\psi_{\chi_i}}T^2}{12} + \frac{\tilde{m}^4_{\psi_{\chi_i}}}{16\pi^2}\left[\ln\left(\frac{\mu^2}{T^2}\right) - c_f\right]\right\}, \tag{C.10}$$

where μ is the $\overline{\rm MS}$ renormalisation scale, $c_f = 2.635$, and the effective thermal fermion masses $\tilde{m}^2_{\psi i} = g^2(\phi - M_i)^2 + h^2T^2/8$. Note that the overall factor $1/2$ in front of the sum is related to the Majorana nature of the fermions in the SUSY model. In the continuum limit we may write this in the form:

$$\begin{aligned}
V_T^{\psi_i} &\simeq \frac{T^4}{2}\sum_i \left\{ -\frac{7\pi^2}{180} + \left[\frac{g^2(\phi-M_i)^2}{T^2} + \frac{h^2}{8}\right]\frac{1}{12} \right. \\
&\qquad \left. + \left[\frac{g^4(\phi-M_i)^4}{T^4} + \frac{h^2}{4}\frac{g^2(\phi-M_i)^2}{T^2} + \frac{h^4}{64}\right]\frac{1}{16\pi^2}\left[\ln\left(\frac{\mu^2}{T^2}\right) - c_f\right]\right\} \\
&\simeq \frac{T^4}{2}\left\{\left[-\frac{7\pi^2}{180} + \frac{h^2}{96} + \frac{h^4}{1024\pi^2}\left[\ln\left(\frac{\mu^2}{T^2}\right) - c_f\right]\right]\int_{M_-}^{M_+} dMn(M) \right. \\
&\qquad + \frac{g^2}{T^2}\left[\frac{1}{12} + \frac{h^2}{64\pi^2}\left[\ln\left(\frac{\mu^2}{T^2}\right) - c_f\right]\right]\int_{M_-}^{M_+} dMn(M)(\phi - M)^2 \\
&\qquad \left. + \frac{1}{16\pi^2}\frac{g^4}{T^4}\left[\ln\left(\frac{\mu^2}{T^2}\right) - c_f\right]\int_{M_-}^{M_+} dMn(M)(\phi - M)^4\right\} \\
&\simeq \frac{T^4}{2}\left\{\left[-\frac{7\pi^2}{180} + \frac{h^2}{96} + \frac{h^4}{1024\pi^2}\left[\ln\left(\frac{\mu^2}{T^2}\right) - c_f\right]\right]\left[\frac{2T}{g}n(\phi) + \cdots\right] \right. \\
&\qquad + \frac{g^2}{T^2}\left[\frac{1}{12} + \frac{h^2}{64\pi^2}\left[\ln\left(\frac{\mu^2}{T^2}\right) - c_f\right]\right]\left[\frac{2}{3}\frac{T^3}{g^3}n(\phi) + \cdots\right] \\
&\qquad \left. + \frac{1}{16\pi^2}\frac{g^4}{T^4}\left[\ln\left(\frac{\mu^2}{T^2}\right) - c_f\right]\left[\frac{2}{5}\frac{T^5}{g^5}n(\phi) + \cdots\right]\right\} \\
&\simeq \frac{T^5}{2g}n(\phi)\left\{-\frac{7\pi^2}{90} + \frac{1}{18} + \frac{h^2}{48} + \frac{1}{16\pi^2}\left(\frac{2}{5} + \frac{h^2}{6} + \frac{h^4}{32}\right)\left[\ln\left(\frac{\mu^2}{T^2}\right) - c_f\right]\right\} + \cdots
\end{aligned} \tag{C.11}$$

where the integrals are in general

$$\begin{aligned}
&\int_{M_-}^{M_+} dMn(M)(\phi - M)^n = \int_{-T/g}^{T/g} dx\left[n(\phi) - xn'(\phi) + \frac{x^2}{2!}n''(\phi) + \cdots\right]x^n \\
&= n(\phi)\frac{x^{n+1}}{n+1} - n'(\phi)\frac{x^{n+2}}{n+2} + n''(\phi)\frac{x^{n+3}}{n+3} + \cdots\Big|_{-T/g}^{T/g} \\
&= \begin{cases} \frac{2}{n+1}\left(\frac{T}{g}\right)^{n+1} n(\phi) + \cdots & , n = 0, 2, 4, \ldots \\ -\frac{2}{n+2}\left(\frac{T}{g}\right)^{n+2} n'(\phi) + \cdots & , n = 1, 3, 5, \ldots \end{cases}
\end{aligned} \tag{C.12}$$

We have considered the local approximation, i.e. that only states in the vicinity of $M = \phi(t)$ are light at any given time. Note that to obtain the derivatives of this potential correction with respect to the field, one needs to take into account that both the integrand and the integration limits are ϕ-dependent, the end result corresponding

to differentiating eq. (C.11), such that:

$$V^{\psi_i}_{T,\phi} \simeq \frac{T^5}{2g} n'(\phi) \left\{ -\frac{7\pi^2}{90} + \frac{1}{18} + \frac{h^2}{48} + \frac{1}{16\pi^2}\left(\frac{2}{5} + \frac{h^2}{6} + \frac{h^4}{32}\right)\left[\ln\left(\frac{\mu^2}{T^2}\right) - c_f\right]\right\} + \cdots \tag{C.13}$$

$$V^{\psi_i}_{T,\phi\phi} \simeq \frac{T^5}{2g} n''(\phi) \left\{ -\frac{7\pi^2}{90} + \frac{1}{18} + \frac{h^2}{48} + \frac{1}{16\pi^2}\left(\frac{2}{5} + \frac{h^2}{6} + \frac{h^4}{32}\right)\left[\ln\left(\frac{\mu^2}{T^2}\right) - c_f\right]\right\} + \cdots \tag{C.14}$$

Nevertheless, in the local approximation the density of states could be taken only as temperature-dependent $n \sim T^{-1}$ and independent of the field, since $n \simeq gN_M/(2T)$; hence $n'(\phi) = n''(\phi) = 0$; but most importantly $V^{\psi_{\chi_i}}_{T,\phi} = V^{\psi_i}_{T,\phi\phi} \simeq 0$. Finally the finite temperature corrections to the effective potential due to the fermionic tower, in the local approximation at leading order, can be written as:

$$V^{\psi_i}_T \simeq \frac{N_M}{4} T^4 \left\{ -\frac{7\pi^2}{90} + \frac{1}{18} + \frac{h^2}{48} + \frac{1}{16\pi^2}\left(\frac{2}{5} + \frac{h^2}{6} + \frac{h^4}{32}\right)\left[\ln\left(\frac{\mu^2}{T^2}\right) - c_f\right]\right\} . \tag{C.15}$$

Next we examine the contribution of the light bosons in the tower to the finite temperature effective potential given by [84, 90, 103]:

$$V^{\chi_i}_T \simeq 2\sum_i \left\{ -\frac{\pi^2}{90} T^4 + \frac{\tilde{m}^2_{\chi_i} T^2}{24} - \frac{\tilde{m}^3_{\chi_i} T}{12\pi} - \frac{\tilde{m}^4_{\chi_i}}{64\pi^2}\left[\ln\left(\frac{\mu^2}{T^2}\right) - c_b\right]\right\} , \tag{C.16}$$

where again μ denotes the $\overline{\text{MS}}$ renormalisation scale, $c_b = 5.41$, and the effective thermal boson masses $\tilde{m}^2_{\chi_i} = g^2(\phi - M_i)^2 + g^2T^2/12 + h^2T^2/8$. Note the overall factor 2 in front of the sum, which represents the fact that the χ_i's scalars are complex fields. Following the same procedure as for the fermionic tower, we have for the bosonic sector:

$$\begin{aligned} V^{\chi_i}_T \simeq \frac{2T^5}{g} n(\phi) \Bigg\{ & -\frac{\pi^2}{45} + \frac{f^2(g,h)}{16\pi} \ln\left(\frac{\sqrt{f(g,h)}}{\sqrt{1+f(g,h)}+1}\right) + \frac{f(g,h)}{12} \\ & - \frac{(2+5f(g,h))}{48\pi}\sqrt{1+f(g,h)} \\ & - \frac{1}{16\pi^2}\left(\frac{1}{10} + \frac{f(g,h)}{3} + \frac{f^2(g,h)}{2}\right)\left[\ln\left(\frac{\mu^2}{T^2}\right) - c_b\right]\Bigg\} + \cdots \end{aligned} \tag{C.17}$$

where $f(g,h) = g^2/12 + h^2/8$. Once again $n(\phi) \sim T^{-1}$, hence the inflaton ϕ derivatives are zero: $V^{\chi_i}_{T,\phi} = V^{\chi_i}_{T,\phi\phi} \simeq 0$. Finally the finite temperature corrections to the effective potential due to the bosonic tower, in the local approximation at leading order, can be

written in the form:

$$V_T^{\chi_i} \simeq N_M T^4 \left\{ -\frac{\pi^2}{45} + \frac{f^2(g,h)}{16\pi} \ln\left(\frac{\sqrt{f(g,h)}}{\sqrt{1+f(g,h)}+1} \right) + \frac{f(g,h)}{12} \right.$$
$$- \frac{(2+5f(g,h))}{48\pi} \sqrt{1+f(g,h)}$$
$$\left. - \frac{1}{16\pi^2} \left(\frac{1}{10} + \frac{f(g,h)}{3} + \frac{f^2(g,h)}{2} \right) \left[\ln\left(\frac{\mu^2}{T^2} \right) - c_b \right] \right\} . \quad \text{(C.18)}$$

By implementing, as first attempt, the continuum limit we could compute the relevant contributions to dissipation. Moreover, as a outstanding consequence of having $n \sim T^{-1}$, then manifestly $n \neq n(\phi)$, the derivatives of the finite temperature effective potential, with respect to the inflaton, are null $V_{T,\phi}^{\psi_i,\bar{\psi}_i} = V_{T,\phi\phi}^{\psi_i,\bar{\psi}_i} = V_{T,\phi}^{\chi_i} = V_{T,\phi\phi}^{\chi} \simeq 0$. This results indeed facilitates the entire evolution of the inflaton.

In summary, we require that $N_M = N_\psi = N_\chi$ since it must be an equal number of Bose and Fermi degrees of freedom at each mass site. Furthermore, this relation on the degrees of freedom along with the assumption that $g \ll h$, hence $f \simeq h^2/8$, implies a cancelation of radiatively generated vacuum energy corrections in the effective potential [103, 104], which is the last term of eq. (C.20). This is a remarkable outcome also noted before in 6.3, where we only considered the bare masses of the light fields. Indeed, both channels due to SUSY conspire in such a way that the radiative corrections vanish at $T = 0$. Hence, by having a regime when $g \ll h$ either radiatively generated vacuum energy or finite temperature corrections are equivalent removed.

Finally, the full contribution to the finite temperature effective potential is given by the fermionic and bosonic towers, the inflaton field ϕ and a light fermion-scalar pair $\psi_\sigma \sigma$, hence $V_T^{Full} = V_T^{\phi,\sigma} + V_T^{\psi_\sigma} + V_T^{\psi_i,\bar{\psi}_i} + V_T^{\chi_i}$:

$$V_T^{Full} = -\frac{\pi^2}{24} T^4 + V_T^{\psi_i,\bar{\psi}_i} + V_T^{\chi_i} , \quad \text{(C.19)}$$

where

$$V_T^{\psi_i,\bar{\psi}_i} + V_T^{\chi_i} = N_M T^4 \left\{ -\frac{\pi^2}{24} + \frac{1}{72} + \frac{h^2}{192} + \frac{f}{12} + \frac{f^2}{16\pi} \ln\left(\frac{\sqrt{f}}{\sqrt{1+f}+1} \right) \right.$$
$$- \left(\frac{2+5f}{48\pi} \right) \sqrt{1+f} + \frac{1}{32\pi^2} \left[\frac{c_b - c_f}{5} + \left(\frac{2f}{3} + f^2 \right) c_b - \left(\frac{h^2}{12} + \frac{h^4}{64} \right) c_f \right]$$
$$\left. + \frac{1}{32\pi^2} \left(\frac{h^2}{12} + \frac{h^4}{64} - \frac{2f}{3} - f^2 \right) \ln\left(\frac{\mu^2}{T^2} \right) \right\} . \quad \text{(C.20)}$$

This correction to the zero temperature potential is due to all relativistic degrees of

freedom. Only massless light fields will contribute to the entropy density, yielding:

$$s_R = \frac{2\pi^2}{45}\left(1+\frac{15}{2}N_M\right)T^3\,, \tag{C.21}$$

hence the effective degrees of freedom are:

$$g_{eff} = 1+4N_M\left(1+\frac{7}{8}\right)\,. \tag{C.22}$$

For any (or even both) dissipative coefficient(s) eqs. (C.8) and (C.9) we may construct a master formula using the slow-roll equations, yielding:

$$Q^3(1+Q)^2 = \frac{C_T}{4C_R(T)}\left(\frac{C_T}{3}\right)^3\left(\frac{V_{eff,\phi}}{3H^3}\right)^2\,, \tag{C.23}$$

where C_T is either $C_T = N_M C_T^S$, $C_T = N_M C_T^F$ or $C_T = N_M(C_T^S + C_T^F)$. Then we can derive the evolution equation for the ratio $Q = \Upsilon/(3H)$:

$$\left(\frac{3+5Q}{1+Q}\right)\frac{d\ln Q}{dN_e} = -2\frac{\eta_{eff}}{1+Q} + 6\epsilon_H\,, \tag{C.24}$$

where $\epsilon_H = -\dot{H}/H^2 = -d\ln H/dN_e$, $\dot{H} = -(\dot{\phi}^2 + Ts_R)/(2M_p^2)$ being the time derivate of the Hubble parameter. From the amplitude of the curvature power spectrum, we may determine the scalar spectral index $n_s - 1 \simeq d\ln\Delta^2_{\mathcal{R}}/dN_e$, which is given by:

$$\begin{aligned} n_s - 1 = {} & 2\frac{\eta_{eff}}{1+Q} - 6\epsilon_{H*} + \left[\frac{2Q_*}{1+Q_*} + Q_*\frac{d\ln G(Q)}{dQ}\Big|_*\right]\frac{d\ln Q}{dN_e}\Big|_* \\ & + B(T_*/H_*, Q_*)\left[\frac{12\sqrt{3}\pi Q_*}{\sqrt{3+4\pi Q_*}}\left(\frac{1+\pi Q_*}{3+4\pi Q_*}\right)\frac{T_*}{H_*} - \frac{H_*}{2T_*}\left(1-\coth^2\left(\frac{H_*}{2T_*}\right)\right)\right]\frac{d\ln Q}{dN_e}\Big|_* \end{aligned} \tag{C.25}$$

where

$$B(T_*/H_*, Q_*) = \left[\frac{2\sqrt{3}\pi Q_*}{\sqrt{3+4\pi Q_*}}\frac{T_*}{H_*} + \coth\left(\frac{H_*}{2T_*}\right)\right]^{-1}\,. \tag{C.26}$$

Appendix D

Observables in the strong dissipative regime exclusively for $\Upsilon = \Upsilon(\phi)$ and $V = V(\phi)$

The general expression for the amplitude of the primordial spectrum with thermalised inflation fluctuations $1 + 2n_* = \coth\left(H_*/(2T_*)\right)$, is given by [12, 70, 79, 81, 83]:

$$\Delta^2_{\mathcal{R}} \simeq \left(\frac{3H_*^3(1+Q_*)}{2\pi V_{,\phi_*}}\right)^2 \left(\frac{2\sqrt{3}\pi Q_*}{\sqrt{3+4\pi Q_*}}\frac{T_*}{H_*} + \coth\left(\frac{H_*}{2T_*}\right)\right) G(Q_*)\,. \tag{D.1}$$

When $\Upsilon = \Upsilon(\phi)$ the growing mode function $G(Q_*)$ is absent, since such field dependancy on the dissipative coefficient does not enhance the primordial power spectrum at large $Q_* \gg 1$. Moreover, for large values of T_*/H_* or $H_*/T_* \ll 1$, we have:

$$\coth\left(\frac{H_*}{2T_*}\right) \simeq 2\frac{T_*}{H_*} + \frac{H_*}{6T_*} + \mathcal{O}\left(\frac{H_*}{T_*}\right)^2\,, \tag{D.2}$$

hence

$$\Delta^2_{\mathcal{R}} \simeq \frac{9H_*^6Q_*^2}{4\pi^2V_{,\phi_*}^2}2\frac{T_*}{H_*}\left(\frac{\sqrt{3}\pi Q_*}{\sqrt{3+4\pi Q_*}} + 1\right)\,, \tag{D.3}$$

then we may approximate, at $Q_* \gg 1$, the term inside the brackets as:

$$\frac{\sqrt{3}\pi Q_*}{\sqrt{3+4\pi Q_*}} + 1 = \frac{\pi Q_*}{\sqrt{1+\frac{4\pi}{3}Q_*}} + 1 \simeq \frac{\sqrt{3\pi}}{2}Q_*^{1/2} + 1 + \mathcal{O}\left(\frac{1}{Q_*}\right)^{1/2}\,, \tag{D.4}$$

hence

$$\Delta^2_{\mathcal{R}} \simeq \frac{9H_*^6Q_*^2}{4\pi^2V^2_{,\phi_*}}2\frac{T_*}{H_*}\left(\frac{\sqrt{3\pi}}{2}Q_*^{1/2}+1\right) \simeq \frac{9H_*^6Q_*^2}{4\pi^2V^2_{,\phi_*}}2\frac{T_*}{H_*}\frac{\sqrt{3\pi}}{2}Q_*^{1/2}\left(1+\frac{2}{\sqrt{3\pi Q_*}}\right), \quad \text{(D.5)}$$

note that the last second term inside the brackets is much smaller than 1, therefore the scalar power spectrum at the limit $Q_* \gg 1$ becomes:

$$\Delta^2_{\mathcal{R}} \simeq \frac{9H_*^5T_*Q_*^{5/2}}{4\pi^2V^2_{,\phi_*}}\sqrt{3\pi}\,. \quad \text{(D.6)}$$

Above result is quite similar to [70, 80, 105]:

$$\Delta^2_{\mathcal{R}} = \frac{9}{4\pi^2}\frac{H_*^5T_*Q_*^{5/2}}{V^2_{\phi_*}}\,, \quad \text{(D.7)}$$

except for a multiplicative factor $\sqrt{3\pi}$. To compute the scalar spectral index n_s, we need the following expression. The energy density of the radiation field during slow-roll becomes:

$$\rho_R = C_RT^4 = \frac{1}{12Q}\frac{V_\phi^2}{H^2}\,. \quad \text{(D.8)}$$

Using above relation and $Q = \Upsilon/3H$, the evolution of the dynamical quantities can be written in terms of the slow-roll parameters:

$$\frac{d\ln H}{dN_e} = -\epsilon_H = -\frac{\epsilon_\phi}{Q} \quad \text{(D.9)}$$

$$\frac{d\ln Q}{dN_e} = -\frac{\beta_\phi}{Q}+\frac{\epsilon_\phi}{Q} \quad \text{(D.10)}$$

$$\frac{d\ln \Upsilon}{dN_e} = -\frac{\beta_\phi}{Q} \quad \text{(D.11)}$$

$$\frac{d\ln V_\phi}{dN_e} = -\frac{\eta_\phi}{Q} \quad \text{(D.12)}$$

$$\frac{d\ln T}{dN_e} = \frac{\beta_\phi}{4Q}+\frac{\epsilon_\phi}{4Q}-\frac{\eta_\phi}{2Q}\,, \quad \text{(D.13)}$$

then from the amplitude of the curvature power spectrum, we may determine the scalar spectral index n_s, which is exactly the same for any of above prescription $\Delta^2_{\mathcal{R}}$; yielding:

$$\begin{aligned} n_s-1 &\simeq \frac{d\ln\Delta^2_{\mathcal{R}}}{dN_e}\,|_* = \frac{\partial\Delta^2_{\mathcal{R}}}{\partial Q}\frac{dQ}{dN_e}\,|_* + \frac{\partial\Delta^2_{\mathcal{R}}}{\partial T}\frac{dT}{dN_e}\,|_* + \frac{\partial\Delta^2_{\mathcal{R}}}{\partial H}\frac{dH}{dN_e}\,|_* + \frac{\partial\Delta^2_{\mathcal{R}}}{\partial V_\phi}\frac{dV_\phi}{dN_e}\,|_* \\ &\simeq \frac{3}{2}\frac{\eta_{\phi_*}}{Q_*}-\frac{9}{4}\frac{\epsilon_{\phi_*}}{Q_*}-\frac{9}{4}\frac{\beta_{\phi_*}}{Q_*}\,. \end{aligned} \quad \text{(D.14)}$$

Bibliography

[1] G. J. Holton, S. G. Brush, *Physics, the Human Adventure: From Copernicus to Einstein and Beyond*, Piscataway, NJ: Rutgers University Press. (2009).

[2] T. Kuhn, *The Copernican Revolution: Planetary Astronomy in the Development of Western Thought*, Harvard University Press (1957).

[3] B. Clegg, *Before the Big Bang: The Prehistory of Our Universe*, St. Martin's Press (2009).

[4] S. Weinberg, *Gravitation and cosmology: principles and applications of the general theory of relativity*, John Wiley & Sons, Inc. New York London Sydney Toronto (1972).

[5] J. N. Islam, *An introduction to mathematical cosmology*, second edition, Cambridge University Press (2002).

[6] A. A. Starobinsky, Phys. Lett. B **91**, 99 (1980); K. Sato, Mon. Not. Roy. Astron. Soc. **195**, 467 (1981); A. H. Guth, Phys. Rev. **D23**, 347 (1981); A. Albrecht, P. J. Steinhardt, Phys. Rev. Lett. **48**, 1220 (1982); A. D. Linde, Phys. Lett. **B108**, 389 (1982).

[7] S. Perlemutter et al., *Astrophys. J.* **483** 565 (1997);
S. Perlemutter et al., *Nature* **391** 51 (1998);
P. M. Garnavich et al., *Astrophys. J.* **493** L53 (1998).

[8] L. Amendola y D. Tochini-Valentini, *Phys. Rev.* **D66**, 043528 (2002);
L. Amendola, *Phys. Rev.* **D62**, 043511 (2000).

[9] Edmund J. Copeland, M. Sami, Shinji Tsujikawa, Int. J. Mod. Phys. D **15**, 1753 (2006).

[10] P. A. R. Ade et al. (Planck Collaboration), *Planck* 2018 results. I. Overview and the cosmological legacy of Planck, [arXiv:1807.06205 [astro-ph.CO]].

[11] A. Albrecht, P. J. Steinhardt, M. S. Turner and F. Wilczek, Phys. Rev. Lett. **48**, 1437 (1982); L. F. Abbott, E. Farhi and M. B. Wise, Phys. Lett. **117B**, 29 (1982); L. Kofman, A. D. Linde and A. A. Starobinsky, Phys. Rev. D **56**, 3258 (1997); P. B. Greene, L. Kofman, A. D. Linde and A. A. Starobinsky, Phys. Rev. D **56**, 6175 (1997).

[12] I. G. Moss and C. M. Graham, Phys. Rev. D **78**, 123526 (2008) [arXiv:0810.2039 [hep-ph]].

[13] A. Berera and L. -Z. Fang, Phys. Rev. Lett. **74**, 1912 (1995) [astro-ph/9501024].

[14] A. Berera, Phys. Rev. Lett. **75**, 3218 (1995) [astro-ph/9509049].

[15] L. Z. Fang, Phys. Lett. **95B**, 154 (1980); I. G. Moss, Phys. Lett. **154B**, 120 (1985); J. Yokoyama and K. i. Maeda, Phys. Lett. B **207**, 31 (1988);

[16] A. Berera, M. Gleiser and R. O. Ramos, Phys. Rev. D **58**, 123508 (1998) [hep-ph/9803394].

[17] J. Yokoyama and A. D. Linde, Phys. Rev. D **60**, 083509 (1999) [hep-ph/9809409].

[18] A. Berera and R. O. Ramos, Phys. Lett. B **567**, 294 (2003) [hep-ph/0210301].

[19] I. G. Moss and C. Xiong, hep-ph/0603266.

[20] M. Bastero-Gil, A. Berera and R. O. Ramos, JCAP **1109**, 033 (2011) [arXiv:1008.1929 [hep-ph]].
[21]

[21] M. Bastero-Gil, A. Berera, R. O. Ramos and J. G. Rosa, JCAP **1301**, 016 (2013) [arXiv:1207.0445 [hep-ph]].

[22] M. Bastero-Gil, A. Berera and J. G. Rosa, Phys. Rev. D **84**, 103503 (2011) [arXiv:1103.5623 [hep-th]].

[23] M. Bastero-Gil, A. Berera, R. O. Ramos and J. G. Rosa, Phys. Rev. Lett. **117**, no. 15, 151301 (2016) [arXiv:1604.08838 [hep-ph]].

[24] N. Arkani-Hamed, A. G. Cohen and H. Georgi, Phys. Lett. B **513**, 232 (2001) [hep-ph/0105239].

[25] M. Schmaltz and D. Tucker-Smith, Ann. Rev. Nucl. Part. Sci. **55**, 229 (2005) [hep-ph/0502182].

[26] A. Berera, Phys. Rev. D **54**, 2519 (1996) doi:10.1103/PhysRevD.54.2519 [hep-th/9601134].

[27] A. Berera, M. Gleiser and R. O. Ramos, Phys. Rev. D **58** (1998) 123508 [hep-ph/9803394].

[28] A. Berera, M. Gleiser and R. O. Ramos, Phys. Rev. Lett. **83** (1999) 264 [hep-ph/9809583].

[29] A. Berera, Nucl. Phys. B **585** (2000) 666 [hep-ph/9904409].

[30] A. Berera and T. W. Kephart, Phys. Rev. Lett. **83**, 1084 (1999) doi:10.1103/PhysRevLett.83.1084 [hep-ph/9904410].

[31] J. Yokoyama and A. D. Linde, Phys. Rev. D **60**, 083509 (1999) doi:10.1103/PhysRevD.60.083509 [hep-ph/9809409].

[32] A. Berera and T. W. Kephart, Phys. Lett. B **456**, 135 (1999) doi:10.1016/S0370-2693(99)00515-8 [hep-ph/9811295].

[33] P. Coles y F. Lucchin, *Cosmology. The origin and evolution of cosmic structure*, Second edition, John Wiley & Sons, LTD (2002).

[34] M. Lpez-Corredoira, Recent. Res. Devel. Astronomy & Astrophys. **1**, 561 (2003).

[35] http://www.oarval.org/cosmyardsp.htm.

[36] E. Hubble, *Proceedings of the National Academy of Sciences of USA*, **15-23**, 168-173 (1929): http://www.pnas.org/cgi/reprint/15/3/168.

[37] G. Lemaitre, Nature **127**, 706 (1931) [Gen. Rel. Grav. **43**, 2929 (2011)]. doi:10.1007/s10714-011-1214-6, 10.1038/127706b0

[38] P. J. E. Peebles and B. Ratra, Rev. Mod. Phys. **75**, 559 (2003) doi:10.1103/RevModPhys.75.559 [astro-ph/0207347].

[39] A. H. Guth, *The Inflationary Universe: The Quest for a New Theory of Cosmic Origins*, Vintage (1997).

[40] M. Kowalski *et al.* [Supernova Cosmology Project Collaboration], Astrophys. J. **686**, 749 (2008) doi:10.1086/589937 [arXiv:0804.4142 [astro-ph]].

[41] A. D. Linde, Contemp. Concepts Phys. **5**, 1 (1990) [hep-th/0503203].

[42] D. Baumann, arXiv:0907.5424 [hep-th].

[43] D. Baumann and H. V. Peiris, Adv. Sci. Lett. **2**, 105 (2009) doi:10.1166/asl.2009.1019 [arXiv:0810.3022 [astro-ph]].

[44] Dodelson S., Modern Cosmology, Academic Press, Amsterdam, Netherlands (2003).

[45] D. J. Fixsen, Astrophys. J. **707**, 916 (2009) doi:10.1088/0004-637X/707/2/916 [arXiv:0911.1955 [astro-ph.CO]].

[46] H. Georgi and S. L. Glashow, Phys. Rev. Lett. **32**, 438 (1974). doi:10.1103/PhysRevLett.32.438

[47] R. Brout, F. Englert and E. Gunzig, *Ann. Phys.* **115**, 78 (1978); *Gen. Rel. Grav.* **10**, 1 (1979).

[48] A. Guth, *Phys. Rev. D* **23**, 347 (1981).

[49] A. R. Liddle, *An introduction of cosmological inflation*, arXiv:astro-ph/9901124v1 (1999).

[50] Andrew R. Liddle, Paul Parsons and John D. Barrow, *Phys. Rev. D* **50**, 7222 (1994).

[51] M. Kamionkowski and E. D. Kovetz, Ann. Rev. Astron. Astrophys. **54**, 227 (2016) [arXiv:1510.06042 [astro-ph.CO]].

[52] Liddle A. R., and Lyth D. H., The primordial density perturbation, Cambridge University Press, Cambridge, UK (2009).

[53] J. c. Hwang and H. Noh, Class. Quant. Grav. **19**, 527 (2002) doi:10.1088/0264-9381/19/3/308 [astro-ph/0103244].

[54] A. D. Linde, Phys. Lett. **108B**, 389 (1982) [Adv. Ser. Astrophys. Cosmol. **3**, 149 (1987)]. doi:10.1016/0370-2693(82)91219-9

[55] A. Albrecht and P. J. Steinhardt, Phys. Rev. Lett. **48**, 1220 (1982) [Adv. Ser. Astrophys. Cosmol. **3**, 158 (1987)]. doi:10.1103/PhysRevLett.48.1220

[56] M. Bastero-Gil, A. Berera, R. Brandenberger, I. G. Moss, R. O. Ramos and J. G. Rosa, JCAP **1801**, no. 01, 002 (2018) [arXiv:1612.04726 [astro-ph.CO]].

[57] Y. Akrami *et al.* [Planck Collaboration], arXiv:1807.06205 [astro-ph.CO].

[58] S. Bartrum, M. Bastero-Gil, A. Berera, R. Cerezo, R. O. Ramos and J. G. Rosa, Phys. Lett. B **732**, 116 (2014) doi:10.1016/j.physletb.2014.03.029 [arXiv:1307.5868 [hep-ph]].

[59] A. D. Linde, Particle Physics and Inflationary Cosmology, Harwood, Chur, Switzerland, (1990).

[60] L. Kofman, A. D. Linde and A. A. Starobinsky, Phys. Rev. Lett. **73**, 3195 (1994) doi:10.1103/PhysRevLett.73.3195 [hep-th/9405187].

[61] A. D. Dolgov and A. D. Linde, Phys. Lett. **116B**, 329 (1982). doi:10.1016/0370-2693(82)90292-1

[62] L. F. Abbott, E. Farhi and M. B. Wise, Phys. Lett. **117B**, 29 (1982). doi:10.1016/0370-2693(82)90867-X

[63] L. Kofman, A. D. Linde and A. A. Starobinsky, Phys. Rev. D **56**, 3258 (1997) doi:10.1103/PhysRevD.56.3258 [hep-ph/9704452].

[64] L. A. Kofman, astro-ph/9605155.

[65] R. Allahverdi, R. Brandenberger, F. Y. Cyr-Racine and A. Mazumdar, Ann. Rev. Nucl. Part. Sci. **60**, 27 (2010) doi:10.1146/annurev.nucl.012809.104511 [arXiv:1001.2600 [hep-th]].

[66] J. C. Bueno Sanchez, M. Bastero-Gil, A. Berera, K. Dimopoulos and K. Kohri, JCAP **1103**, 020 (2011) doi:10.1088/1475-7516/2011/03/020 [arXiv:1011.2398 [hep-ph]].

[67] S. Bartrum, A. Berera and J. G. Rosa, Phys. Rev. D **86**, 123525 (2012) doi:10.1103/PhysRevD.86.123525 [arXiv:1208.4276 [hep-ph]].

[68] A. Berera, Contemp. Phys. **47**, 33 (2006) doi:10.1080/00107510500392030 [arXiv:0809.4198 [hep-ph]].

[69] A. Berera, I. G. Moss and R. O. Ramos, Rept. Prog. Phys. **72**, 026901 (2009) [arXiv:0808.1855 [hep-ph]].

[70] L. M. Hall, I. G. Moss and A. Berera, Phys. Rev. D **69**, 083525 (2004) [astro-ph/0305015].

[71] I. G. Moss and C. Xiong, JCAP **0811**, 023 (2008) doi:10.1088/1475-7516/2008/11/023 [arXiv:0808.0261 [astro-ph]].

[72] M. Bastero-Gil and A. Berera, Int. J. Mod. Phys. A **24**, 2207 (2009) [arXiv:0902.0521 [hep-ph]].

[73] A. Berera, Phys. Rev. D **55**, 3346 (1997) [hep-ph/9612239].

[74] A. A. Starobinsky, Lect. Notes Phys. **246**, 107 (1986).

[75] S. J. Rey, Nucl. Phys. B **284**, 706 (1987). doi:10.1016/0550-3213(87)90058-7

[76] A. S. Goncharov, A. D. Linde and V. F. Mukhanov, Int. J. Mod. Phys. A **2**, 561 (1987). doi:10.1142/S0217751X87000211

[77] M. Sasaki, Y. Nambu and K. i. Nakao, Nucl. Phys. B **308**, 868 (1988). doi:10.1016/0550-3213(88)90132-0

[78] A. A. Starobinsky and J. Yokoyama, Phys. Rev. D **50**, 6357 (1994) doi:10.1103/PhysRevD.50.6357 [astro-ph/9407016].

[79] R. O. Ramos and L. A. da Silva, JCAP **1303**, 032 (2013) [arXiv:1302.3544 [astro-ph.CO]].

[80] A. N. Taylor and A. Berera, Phys. Rev. D **62**, 083517 (2000) doi:10.1103/PhysRevD.62.083517 [astro-ph/0006077].

[81] I. G. Moss and C. Xiong, JCAP **0704**, 007 (2007) [astro-ph/0701302].

[82] C. Graham and I. G. Moss, JCAP **0907**, 013 (2009) [arXiv:0905.3500 [astro-ph.CO]].

[83] M. Bastero-Gil, A. Berera and R. O. Ramos, JCAP **1107**, 030 (2011) [arXiv:1106.0701 [astro-ph.CO]].

[84] J. I. Kapusta and C. Gale, *Finite-Temperature Field Theory: Principles and Applications*, (Cambridge University Press, Cambridge, England, 2006).

[85] M. L. Bellac, "Thermal Field Theory," doi:10.1017/CBO9780511721700

[86] M. Bastero-Gil, S. Bhattacharya, K. Dutta and M. R. Gangopadhyay, JCAP **1802**, no. 02, 054 (2018) [arXiv:1710.10008 [astro-ph.CO]].

[87] P. A. R. Ade *et al.* [Planck Collaboration], Astron. Astrophys. **594**, A20 (2016) oi:10.1051/0004-6361/201525898 [arXiv:1502.02114 [astro-ph.CO]].

[88] M. Benetti and R. O. Ramos, Phys. Rev. D **95**, no. 2, 023517 (2017) [arXiv:1610.08758 [astro-ph.CO]].

[89] L. M. H. Hall and I. G. Moss, Phys. Rev. D **71**, 023514 (2005) doi:10.1103/PhysRevD.71.023514 [hep-ph/0408323].

[90] J. M. Cline and P. A. Lemieux, Phys. Rev. D **55**, 3873 (1997) [hep-ph/9609240].

[91] N. P. Landsman and C. van Weert, Phys. Rep. **145**, 141 (1987); J. I. Kapusta, *Finite Temperature Field Theory*, Cambridge Univ. Press (Cambridge 1989); M. Le Bellac, *Thermal Field Theory*, Cambridge Univ. Press (Cambridge 1996).

[92] M. Bastero-Gil, A. Berera, R. Hernández-Jiménez and J. G. Rosa, Phys. Rev. D **98**, no. 8, 083502 (2018) doi:10.1103/PhysRevD.98.083502 [arXiv:1805.07186 [astro-ph.CO]].

[93] R. Brandenberger, Int. J. Mod. Phys. D **26**, no. 01, 1740002 (2016) [arXiv:1601.01918 [hep-th]].

[94] C. Vafa, hep-th/0509212.

[95] H. Ooguri and C. Vafa, Nucl. Phys. B **766**, 21 (2007) doi:10.1016/j.nuclphysb.2006.10.033 [hep-th/0605264].

[96] G. Obied, H. Ooguri, L. Spodyneiko and C. Vafa, arXiv:1806.08362 [hep-th].

[97] P. Agrawal, G. Obied, P. J. Steinhardt and C. Vafa, Phys. Lett. B **784**, 271 (2018) doi:10.1016/j.physletb.2018.07.040 [arXiv:1806.09718 [hep-th]].

[98] S. Das, arXiv:1809.03962 [hep-th].

[99] S. Das, arXiv:1810.05038 [hep-th].

[100] M. Motaharfar, V. Kamali and R. O. Ramos, arXiv:1810.02816 [astro-ph.CO].

[101] Z. Yi and Y. Gong, arXiv:1811.01625 [gr-qc].

[102] W. C. Lin and W. H. Kinney, arXiv:1812.04447 [astro-ph.CO].

[103] L. Dolan and R. Jackiw, Phys. Rev. D **9**, 3320 (1974). doi:10.1103/PhysRevD.9.3320

[104] G. W. Anderson and L. J. Hall, Phys. Rev. D **45** (1992) 2685.

[105] S. Bartrum, A. Berera and J. G. Rosa, JCAP **1306**, 025 (2013) doi:10.1088/1475-7516/2013/06/025 [arXiv:1303.3508 [astro-ph.CO]].

[106] Y. F. Cai, J. B. Dent and D. A. Easson, Phys. Rev. D **83**, 101301 (2011) [arXiv:1011.4074 [hep-th]].

[107] A. Kehagias and A. Riotto, arXiv:1807.05445 [hep-th].

[108] Y. Akrami, R. Kallosh, A. Linde and V. Vardanyan, arXiv:1808.09440 [hep-th].

[109] R. Arya and R. Rangarajan, arXiv:1812.03107 [astro-ph.CO].

[110] A. Berera, PoS AHEP **2003**, 069 (2003) doi:10.22323/1.010.0069 [hep-ph/0401139].

[111] E. Elizalde., A. D. Odintsov and A. Romeo, *Zeta Regularization Techniques with Applications*. River Edge, NJ: World Scientific, (1994).